Multiparametric assessment of apical versus septal pacing study using Cardiac Magnetic Imaging

A thesis submitted for the degree of Doctor of Philosophy (PhD) in the Faculty of Medical and Human Sciences at the University of Manchester

2015

Dr Mark Peter Ainslie

BSc (hons) MBChB (hons) MRCP PGDipMedEd

School of Medicine, University of Manchester

Contents

List of Figures

List of tables

Abbreviations

6MWT- 6 minute walk testing

ACC- American College of Cardiology

AF- Atrial fibrillation

AHA- American Heart Association

American Thoracic Society (ATS)

Ao SAX- Aortic short axis

Ao- Aorta

AV- Atrioventricular

AVC- Aortic valve closure (AVC)

AVN- Atrioventricular node

BNP- Brain natriuretic peptide

bSSFP- Balanced steady state free precession

CMR- Cardiac magnetic resonance

CMR-FT- CMR Feature tracking

CMR-TSI- CMR-Tissue Resynchronisation Index

CMRI- Cardiac magnetic resonance imaging

CO- Cardiac output

CPEX- Cardiopulmonary exercise test

CPEX- Cardiopulmonary exercise testing

CRT- Cardiac resynchronisation therapy

CSPAMM- Complimentary SPAMM

Cu_2SO_{4-} Copper Sulphate pentahydrate

CURE- Circumferential uniformity ratio estimate

CVP- Central venous pressure

ECG- Electrocardiogram

EDV- End diastolic volume

EF- Ejection fraction

ENRA- equilibrium radionucleotide-gated blood pool angiography

ESC- European Society of Cardiology

HARP- Harmonic phase analysis

HLA- Horizontal long axis

ICC- Intraclass correlation coefficient

ICD- internal cardioverter defibrillator

IHD- Ischaemic heart disease

IPG- implantable pulse generator

IVMD- Inter-ventricular mechanical delay

LA- Left atrium

LAO- Left anterior oblique

LBBB- Left bundle branch block

LGE- Late gadolinium enhancement

LV- Left ventricle

LVdP/dtmax- maximal rate of rise of left ventricular pressure)

LVdP/dtmin- minimum rate of LV pressure increase

LVEDV- Left ventricular end diastolic volume

LVESV- Left ventricular end-systolic volumes

LVIDd- Left ventricular internal diameter diastole

LVIDs- Left ventricular internal diameter systole

LVMD- Left ventricular mechanical delay

LVOT- Left ventricular outflow tract

LVSD- Left ventricular systolic dysfunction

MA- Mark Ainslie

MAP- Mean arterial blood pressure

MMP- Matrix metalloproteinases

MOLLI- Modified Look-Locker Inversion-recovery

MRI- magnetic resonance imaging

MRI- Magnetic resonance imaging

MS- Matthias Schmitt

PA- Postero-anterior

PA- Pulmonary artery

PPM- Permanent pacemaker

PV- Pulmonary vein

QOL- Quality of life

QOL- Quality of life questionnaire

RAO- Right anterior oblique

ROIs- Regions of interest

RQ- Respiratory quotient

RT3DE- Real time 3 dimensional echo

RV- Right ventricle

RVA- Right ventricular apex

RVOT- Right ventricular outflow tract

RVS- Right ventricular septum

SA- Short axis

SA- Sinoatrial node

SAE- Serious adverse events

SAR- Specific absorption rate

SBP- Systolic blood pressure

SDI- The systolic dyssynchrony index

Short T1 inversion recovery (STIR)

SNR- Signal to noise

SPAMM- Spatial modulation of magnetisation

SpGr- Spoiled gradient

SSFP- Steady state free precession

SVR- Systemic vascular resistance

T1 BB TSE- T1 Black blood turbo spin echo

T2 BB TSE- T2 Black blood turbo spin echo

T2PLS- Time to peak longitudinal strain

T2PLSR- Time to peak longitudinal strain rate

TAPSE- Tricuspid annular systolic plane excursion

TDI- Tissue doppler imaging

TIeff- Effective inversion time

TOE- Transoesophageal echocardiography

TSE- Turbo spin-echo

TTE- Transthoracic echocardiogram

VENC- Velocity-phase encoding gradient

VLA- Vertical long axis

VTI- Velocity time integral

W/Kg- Watts/Kg

Abstract

Dr Mark P Ainslie, submission for the Degree of Doctor of Philosophy (PhD), University of Manchester.

Thesis title: Multiparametric assessment of apical versus septal pacing study using Cardiac Magnetic Imaging. 2015.

The optimal site at which to pace the right ventricle (RV) is still unclear. This study aimed to answer this question utilising cardiac magnetic resonance imaging, which up until recently was contraindicated in pacemaker patient cohorts. The objective was to determine the effect of apical and outflow tract septal pacing on cardiac function and remodeling as assessed by MRI. In addition, physcial and psychological functional parameters were assessed.

A series of sub-studies were performed as part of the research. Study 1 validated the velocity phase encoding used to determine flow measurements. This found measurements were reproducible.

Study 2 and 3 focused on the method of CPEX testing in pacing dependent patients and whether a training effect was observed with the CPEX testing. It found that treadmill testing resulted in a greater heart rate response and higher VO2 max results. No significant training effect was observed.

Study 4 used phantom models to determine the effect of metal susceptibility artefact on mapping and velocity encoded MR sequences. An inverse relationship between artefact and distance from the pacemaker was observed. At approximinately 10 cm from the device, artefact is negligible.

Study 5 determined the best methods of image optimization in the presence of the pacemaker. T1 weighted imaging along with spoiled gradient imaging was less affected by artefact compared to late gadolinium and bSSFP imaging.

Study 6 evaluated in-house developed software to measure torsion using data derived from commercial available tagging and feature tracking software. At low heart rates measures were comparable but tagging became less accurate with heart rates over 100 bpm.

The main study comprised of the baseline data of 50 patients from the ongoing MAPS trial and some intermediate data after 9 months for a smaller cohort. There was not a significant difference in left ventricular volumes or ejection fraction at baseline but differences were observed in deformational indices including longitudinal strain, strain rate, twist and torsion. At 9 months a difference in ejection fraction was observed between the pacing modes along with differences in deformational parameters. Clinically significant differences were not seen between pacing positions at baseline or 9 months but the outflow tract septal position was superior based on deformational data.

Declaration

The candidate confirms that no portion of the work referred to in this work referred to in this thesis has been submitted in support of an application for another degree or qualification of this or any other university or institute of learning.

Copyright

i. The author of this thesis (including any appendices and/or schedules to this thesis) owns certain copyright or related rights in it (the "Copyright") and s/he has given The University of Manchester certain rights to use such Copyright, including for administrative purposes.
ii. Copies of this thesis, either in full or in extracts and whether in hard or electronic copy, may be made only in accordance with the Copyright, Designs and Patents Act 1988 (as amended) and regulations issued under it or, where appropriate, in accordance with licensing agreements which the University has from time to time. This page must form part of any such copies made.
iii. The ownership of certain Copyright, patents, designs, trade marks and other intellectual property (the "Intellectual Property") and any reproductions of copyright works in the thesis, for example graphs and tables ("Reproductions"), which may be described in this thesis, may not be owned by the author and may be owned by third parties. Such Intellectual Property and Reproductions cannot and must not be made available for use without the prior written permission of the owner(s) of the relevant Intellectual Property and/or Reproductions.
iv. Further information on the conditions under which disclosure, publication and commercialisation of this thesis, the Copyright and any Intellectual Property University IP Policy (see http://documents.manchester.ac.uk/display.aspx?DocID=24420), in any relevant Thesis restriction declarations deposited in the University Library, The University Library's regulations (see http://www.library.manchester.ac.uk/about/regulations/) and in The University's policy on Presentation of Theses

My contribution to the work

I developed the research project following an idea proposed originally by Dr Neil Davidson. Together with Dr Matthias Schmitt and Dr Neil Davidson I designed all aspects of the project. This included the design of pacing and scanning protocols, patient information sheets, and other documents required to obtain ethical approval. I obtained ethical approval and was awarded a British Heart Foundation, research fellowship.

I recruited all the patients, supervised all investigations and did all the post processing analysis.

The supervising team included Dr Matthias Schmitt, Professor Andrew Trafford, Dr Neil Davidson, Dr Ben Brown and Dr Chris Miller.

Glyn Coutts helped design the software to measure ventricular twist, expanding on work done by Dr Alex Borg a previous research registrar.

Publications related to this thesis

Papers

Cardiac MRI of patients with implanted electrical cardiac devices.
Ainslie M, Miller C, Brown B, Schmitt M. Heart. 2014 Mar; 100(5): 363-9.

Abstracts

Evaluation of left ventricular torsion using cardiac MRI. Validation of feature tracking.
Ainslie MP, Reid A, Miller C, Clark D, Francis L, Schmitt M. Journal of cardiovascular magnetic resonance. 2015. 17 (suppl 1): O47.

MAPS; acute safety data of the St Jude accent- tendril IPG system during prolonged max power CMR scanning.
Ainslie M, Reid A, Miller C, Clark D, Brown B, Fox D, Davidson N, Trafford A, Schmitt M. Journal of cardiovascular magnetic resonance. 2015. 17 (Suppl 1): M6.

Multiparametric CMR Assessment of RV apical versus septal pacing study (MAPS)- Preliminary acute hemodynamic findings.
Ainslie M, Miller C, Brown B, Fox D, Davidson N, Trafford A, Schmitt M.
Heart 2013; 99: suppl 2 A50.

Multiparametric CMR assessment of RV apical versus septal Pacing Study (MAPS) - preliminary acute hemodynamic findings.
Ainslie M, Miller CA, Brown B, Davidson N, Fox DJ, Schmitt M.
Journal of Cardiovascular Magnetic Resonance. 2013; 15(suppl 1):O85.

Dedication

I would like to thank the many people who contributed or assisted me in this work.

In particular my main supervisor Dr Matthias Schmitt who went to great lengths to get this project going and supported me throughout out the PhD. Without this I would not have been able to get to this point. My co-supervisors also gave invaluable teaching and guidance and included Dr Neil Davidson, Dr Christopher Miller, Dr Ben Brown and Professor Andrew Trafford.

The Electrophysiology and Pacing team; Dr Fox, Dr Simon Williams, Dr Chris Skene, Dr Muhammad Boatiwrat were essential in recruiting patients for the study and offered support throughout the study.

David Clark and colleagues in the CMR unit provided fantastic support for the research scans. David provided excellent tutoring and was always at hand to help in what was a busy unit.

Glyn Coutts provided invaluable physics support, which I am grateful for.

Colleagues Dr Martin Stout, Keith Pearce and Dr Anna Reid provided imaging support and I was grateful for their expertise. Joanne Riley helped me analyse the echo data and taught me how to use the post-processing software.

Dr James Fildes and Lab members at Wythenshawe hospital helped me greatly with use of their equipment and expertise.

The research nurses aided me greatly and continue to follow up the trial patients.

The catheter lab staff, radiographers and in particular all the cardiac physiologists assisted me greatly though out the study.

My parents have been fantastic throughout the years offering guidance, emotional and most helpfully financial support throughout my undergraduate and postgraduate career. Lastly and most importantly I would like to thank Ellie, my wife, who has been a constant rock throughout the PhD and had to endure my stresses as well as her own while looking after our wonderful, but cheeky little boys Benjamin and James.

Chapter 1
Introduction

Chapter 1: Introduction

1.1 Normal Cardiac Conduction system

The heart contains highly specialized conducting tissue that allows both the generation and propagation of an electrical impulse. This tissue is arranged to ensure the depolarizing wave is conducted in a rapid and orderly fashion over the heart to ensure a synchronous contraction. The electrical system helps ensure efficient co-ordination of apical and ventricular contraction and thus when diseased can lead to abnormal cardiac output. It is important to understand normal electrical physiology in order to understand the challenges of artificial cardiac pacing. The normal cardiac conduction tissue is divided into multiple parts as illustrated in Figure 1.

The Sinoatrial node (SA) is the physiological pacemaker and contains cells that spontaneously depolarize to generate the cardiac impulse. These impulses travel across the atria to reach the Atrioventricular node (AVN). The atria and ventricles are electrically isolated and it is only across the AVN that electrical impulses can reach the ventricles in normal circumstances. From here impulses travel through the HIS bundle down the interventricular septum and split into two branches, the left and right bundle branches. Further subdivisions occur into a vast network of purkinje fibres that encompass both ventricles.

Figure 1. The cardiac conduction system

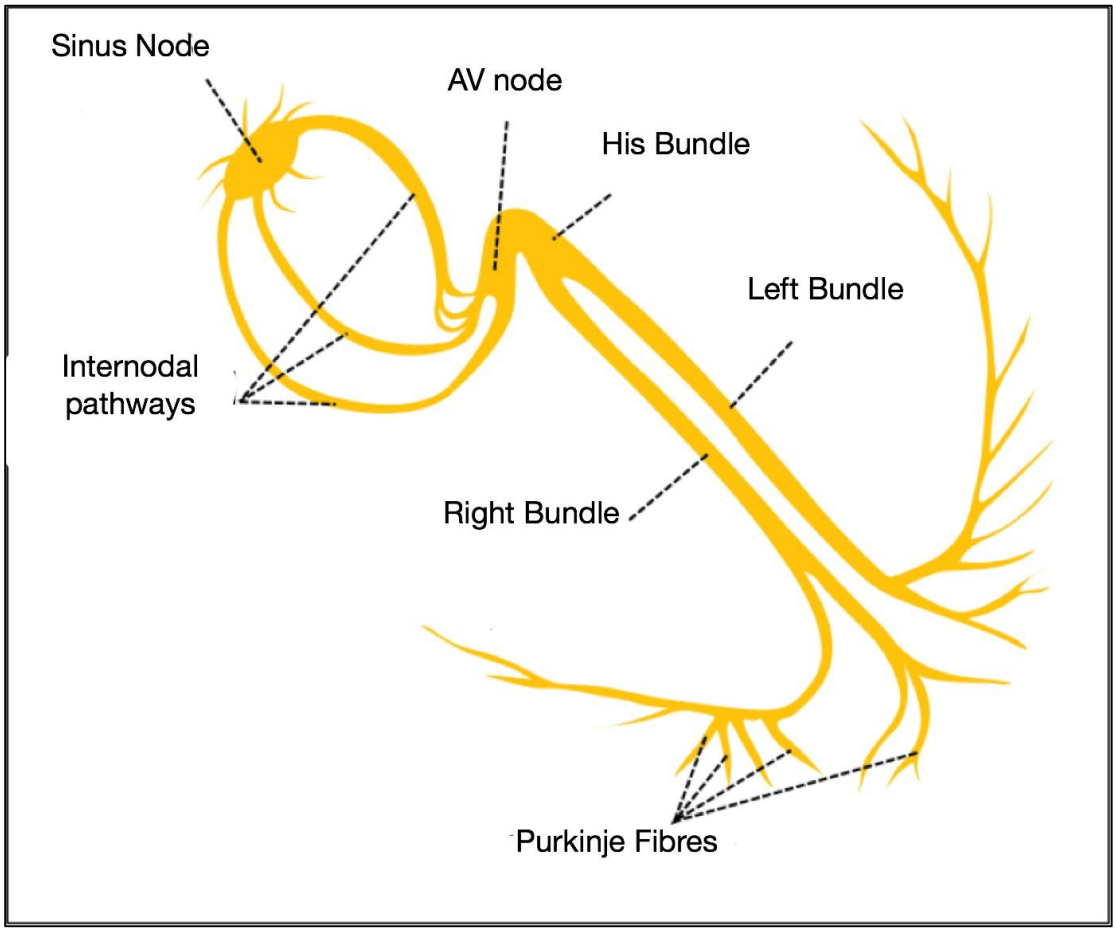

The cardiac conduction system is designed to promote efficient contraction of the myocardium to achieve an effective cardiac output. It does this by the following mechanisms:

1. An electrical delay between the atria and ventricles.
    - The electrical impulse is delayed at the AV node just enough to allow the atria to empty fully. Simultaneous atrial and ventricular contraction would lead to inefficient filling and reduced cardiac output.

2. Very rapid conduction through the HIS-purkinje network.
    - Myocardial cells are effectively stimulated and contract simultaneously.

3. Coordinated activation of myocardium.
    - Ventricular contraction begins at the ventricular apex and forces blood into the outflow tracts.
    - The heart is a functional syncytium where the electrical impulse freely propagates between myocardial cells in all directions. The myocardium acts as a single unit making the contraction more effective.

There are many conditions that can lead to disturbances in the hearts normal electrical conduction. These can be clinically silent with only changes seen on the electrocardiogram (ECG) or the patient can be symptomatic.

Electrical disturbances disrupt the mechanical efficiency of the myocardium and ultimately lead to a fall in stroke volume that leads to a cascade of events that ultimately results in symptoms. Non-reversible causes of conduction disturbance that result in symptoms are always an indication for the implantation of an artificial cardiac pacemaker (PPM).

1.2.1 Atrial Fibrillation

Atrial Fibrillation (AF) is an abnormal cardiac rhythm characterized by an irregular pulse and a loss of p waves on the ECG. During AF the regulation of the heart rate by the sinus node is lost and the ventricular rate is regulated by the conduction ability of the AV node. It is very common and the prevalence of AF is around 2% for the total population. (1) The prevalence increases with age with estimates between 5-15% in those aged over 80 years. (2,3)

1.2.2 Type of AF

AF is often categorized into 3 forms. **Paroxysmal AF** which terminates spontaneously within 7 days of onset, **persistent AF** which either terminates spontaneously after 7 days or requires cardioversion, and finally **permanent AF** which remains despite interventions.

1.2.3 Clinical presentation of AF

There are a number of symptoms that occur with AF. Of these, rapid palpitations, shortness of breath and chest pain are the most common. Symptoms can range from being mild to very severe. The loss of atrial contraction in AF can lead to atrial stasis. This predisposes to clot formation, particularly within the left atrial appendage. One of the most serious consequences of AF is the increased risk of stroke. AF gives a 4-5 fold increase in the risk of an ischaemic stroke. (4) Quality of life and exercise capacity can both be impaired in individuals with AF. LV function is often impaired due to electromechanical dysfunction, with a loss of atrial contraction and irregular

ventricular contraction. Diastolic filling time is also reduced and leads to a reduction in cardiac output. If the rapidly conducted AF is uncontrolled, permanent LV remodelling can occur, leading to heart failure. (5)

AF is also an independent risk factor for death, with death rates found to be double compared to the rest of the population. (6,7)

1.2.3 Pathophysiology

The aetiology of AF is complex and there are several factors that contribute to the initiation and maintenance of AF. It is generally accepted that focal ectopic activity occurs at the entry sites of the 4 pulmonary veins entering the left atrium (LA). AF episodes are often seen to originate from these areas and these ectopics act as a trigger. (8)

Once in AF, atrial remodelling at a cellular level is seen to occur which increases the susceptibility to further AF and promotes the persistence of AF. (9)

AF is associated with many clinical conditions and these are summarized below (Table 1).

Table 1. Associated conditions with atrial fibrillation

- **Hypertension**
- **Heart failure**
- **Valvular heart disease e.g. mitral valve disease**
- **Cardiomyopathies**
- **Congenital heart disease**
- **Coronary artery disease**
- **Thyroid dysfunction**
- **Sleep apnoea**
- **Diabetes mellitus**
- **Chronic obstructive pulmonary disease**
- **Chronic renal disease**

1.2.4 Treatment of AF

AF treatment focuses on two areas. Firstly what is the risk of stroke for the patient and the therapies used to reduce this? Secondly should a rate or rhythm control approach be adopted for the patient?

To assess the risk of stroke in patients with any form of AF, risk calculators such as the $CHADS_2Vasc$ score are used. (10) A score of 2 equates to an annual stroke risk of 2.2% and is viewed as an indication for full anticoagulation. (11) A score of 0 does not usually require full anticoagulation.

A rate control approach adopts therapy that controls the ventricular rate whilst a rhythm control approach adopts therapies to maintain sinus rhythm.

Several randomized studies have compared the effect of rate control versus rhythm control on patient outcomes. The majority of studies have shown that rate control is not inferior to rhythm control. (12,13) This is in part due poor long-term efficacy and adverse effects of many of the drugs used for rhythm control and thus negating any potential benefits of being in sinus rhythm. (14)

Drugs that can be used for AF are given in the following table.

Table 2. Drug therapy for AF.

Rate Control	**Rhythm control**
Beta blocker	Flecainide
Calcium Channel blocker	Propafenone
Digoxin	Sotalol
	Amiodarone
	Dronedarone

1.2.5 Catheter ablation

The use of catheter ablation for the treatment of AF has rapidly increased in the past decade. Multiple catheter delivery systems and strategies have been developed in this progressing field. The most common approach practiced today is to electrically isolate the pulmonary veins and thus disconnect them from the LA. (15) Success rates in appropriate patients are over 70%. (16,17)

1.2.6 AV node ablation and Pacing

It is possible to ablate the AV node and thus prevent the rapid conduction of AF to the ventricles. Although the specialized conduction system distal to the AV node can spontaneously depolarize, it is both unreliable and is at a rate too slow for efficient myocardial contraction. In order to facilitate an AV node ablation an artificial PPM is implanted. This approach is known as a **pace and ablate** strategy and has been shown to improve exercise tolerance, cardiac function and quality of life. (18)

1.2.7 Pacemakers and AF

Cardiac pacing may lead to an increased incidence of AF, but interestingly also offers the potential for preventing it in patients with sinus rhythm and AV block. Physiological pacing where AV synchrony is maintained can prevent the development of mitral regurgitation and ventricular-atrial conduction, both of which could lead to atrial remodelling and an increased risk of AF. Atrial or dual chamber pacing, whereby AV synchrony is maintained, have been shown in numerous studies to have fewer AF episodes compared to ventricular pacing alone. (19–21) In a meta-

analysis, atrial-based pacing was shown to have a 20% reduction in AF episodes. (22) It is hypothesized that right ventricular (RV) pacing itself can lead to increased AF even if AV synchrony is maintained in a dual chamber system. The beneficial effect of AV synchrony is negated by the increased burden of AF that RV pacing confers. (23)

In studies where pacing algorithms have reduced the percentage of RV pacing, a reduction in AF is seen compared to conventional dual chamber pacing. The SAVE PACE trial used such algorithms and a 40% reduction in AF was observed. (24)

Atrial pacing theoretically could reduce AF by preventing potential triggers such as sinus pauses, bradycardia and atrial ectopics. These triggers alter atrial refractoriness and increase inter-atrial conduction times, both of which can result in AF. (25) Alternative sites to pace the right atrium (RA), including Bachmann's bundle, high and low atrial septum and ostium of the coronary sinus have been investigated. Sites which shorten atrial activation times may reduce the susceptibility of AF. (25) Multisite atrial pacing has been investigated and works on the principle that if total atrial activation time is reduced, so is the susceptibility to AF. Two methods exist; biatrial pacing (LA and RA) and dual-site RA pacing. Both pacing models decrease atrial activation time,(26) however the only randomized trial of dual-site versus single RA site pacing did not show a statistically significant benefit. (27)

1.3.1 Cardiac Pacing

An artificial PPM is a medical device that delivers an electrical impulse directly to the heart to cause depolarization of the myocardium and propagate the depolarization to the rest of the myocardium.

The primary purpose of a pacemaker is to maintain an adequate heart rate, because there is dysfunction within the SA node, AV node or highly specialised conduction system. There are many indications for cardiac pacing and both the American and European Cardiac societies have published guidelines. (28,29)

The pacing system consists of a generator that produces the electrical impulse and a set of leads that enable this to be delivered to the heart. The generator itself is a hermetically sealed device that consists of a battery, a sensing amplifier, a microprocessor and output circuitry. Modern pacing leads are delivered transvenously, but epicardial systems still can be used.

Modern PPMs have the ability to sense the heart's intrinsic electrical rhythm and will only deliver a pacing stimulus if they do not detect an atrial or ventricular depolarization. In this way, the PPM can respond appropriately on a beat-to-beat basis, pacing only when required.

With many different manufacturers and models of PPM a generic code has been implemented giving the basic information about how the cardiac PPM functions. This NASPE/BPEG code is shown in table 3 and will be referred to throughout the thesis. The most common pacing modes used in medical practice are DDDR and VVIR.

Table 3. NASPE code for pacing

Table 3. NASPE code for pacing.

I	II	III	IV	V
Chamber (s) paced	Chamber(s) sensed	Response to sensing	Rate modulation	Multisite pacing
O = None	O = None	O = None	O = None	O = None
A = Atrium	A = Atrium	T = Triggered	R = Rate modulation	A = Atrium
V = Ventricle	V = Ventricle	I = Inhibited		V = Ventricle
D = Dual (A+V)	D = Dual (A+V)	D = Dual (T+I)		D = Dual (A+V)

I = First letter of code

V = Fifth letter of code

1.3.2 Right ventricular pacing

Despite over 250,000 bradycardia devices being implanted across Europe each year, (30) the ideal site at which to pace the right ventricle (RV) is not clear. Accordingly, the current ESC/EHRA guidelines do not comment on ventricular lead position.

The most common practice is to place the lead in the right ventricular apical (RVA) position, where it is generally straightforward to implant, safe and effective at pacing. (31) This practice is mainly for historic reasons with original pacing leads having no active fixation method. (32) The next generation of passive fixation pacing leads also relied on tissue ingrowth for true fixation and thus also needed to be placed apically to prevent displacement. The latest generation of active fixation leads have a helical screw, which can be deployed directly into the endocardium. This allows unrestricted positioning of the lead. (33) Initial concerns of the increased risk of lead displacement with other sites has been disproven and specifically pacing on the RV septum is safe, efficacious, with no increases in displacement rates. (34)

1.3.3 Early clinical trials and RV pacing

The DAVID trial was the first multi-centre trial to demonstrate the detrimental effects of RV pacing and raise concerns over its long-term effects. (23) Patients who required an implantable cardioverter defibrillator (ICD) were randomized to be programmed to either VVI at 40bpm (a backup pacing mode) or DDDR at 70bpm. It showed that the 1-year survival free from death or heart failure hospitalization was 83.9% for the VVI 40 and 73.3% for the DDDR 70 group. When a sub-group analysis was performed those patients with >40% ventricular pacing had the worst outcome.

In the MADIT II trial, patients who had a previous myocardial infarction and an ejection fraction (EF) <30% were randomized to receive an ICD or to remain on optimal medical therapy. (35) The ICD group showed greater survival, but patients had an increased incidence of heart failure hospitalization. When a sub-study analysis was performed, those with a high frequency of pacing had a significantly increased risk of new or deterioration of pre-existing heart failure (hazard ratio 1.93, p 0.002) and increased episodes of sustained ventricular arrhythmias requiring therapy only. (36)

In the MOST trial, in patients with sinus node disease, it was shown that cumulative RV pacing was a strong predictor of heart failure hospitalization in both DDDR and VVIR groups and that the risk of developing AF increased linearly with increased cumulative pacing. (37)

The patients in all 3 trials had underlying LV dysfunction and were paced from the right ventricular apex (RVA).

1.3.4 Animal models of pacing

Several pacing models in animals have been published, detailing changes in LV function associated with RV pacing. Mammalian hearts do all contain a His-Purkinje system for rapid electrical conduction but significant inter-species differences in their relative size and distribution exist. (38)

Much of the understanding of normal electrical activation of the ventricles in humans comes from animal models. Impulse conduction in the purkinje system occurs quickly from base to apex and exits in the lower fourth of the RV and lower third of the LV wall in a canine heart. (39) This site corresponds to the earliest activation of ventricular myocardium in the heart. The activation of the myocardial septum, LV and

RV occurs mainly from apex to base, and from the endocardium to epicardium. The electrical impulse is approximately four times slower (0.3-1m/s) in normal myocardial tissue compared to the purkinje system. The QRS complex on an ECG corresponds to total ventricular activation, in humans this is 70-80ms, in canines it is 40-50ms. (40)

Myerburg et al demonstrated in a canine model that electrical impulses coming from the myocardium only enters the purkinje system at the apex, the exit point during normal conduction. (39) Therefore the sequence of activation during ventricular pacing is via slow conduction though the myocardium from the pacing site. (40)

Mapping of mechanical activation in canines paced from the RV apex (RVA), demonstrated that the septum is activated quickly, but there was a delay in activation of the LV free wall. When paced from the LV lateral wall, the opposite pattern is seen to RVA pacing. (41) Ventricular pacing usually results in a doubling of QRS duration of the surface ECG. In two studies it was shown that RVA pacing resulted in a shorter QRS than pacing from the LV at both the lateral and posterior basal walls. (40,42)

Pacing closer to the specialized conducting tissue has been successfully attempted and indeed the QRS duration is shortened when the pacing site is located in the high ventricular septum. (43–45) Pacing the HIS bundle itself has also been achieved in animal studies and unsurprisingly results in the shortest QRS duration and a near normal QRS morphology on ECG. (46)

The effect of altered electrical activation on LV mechanics has also been extensively modelled. Whilst two studies suggested global parameters such as torsion were minimally effected by ventricular pacing,(47,48) multiple studies have shown dramatic derangements at the regional level. In the dog heart when regional strain was measured proximally and distally from the pacing site, two distinct patterns were

seen. Proximal segments, which were activated early, had rapid early systolic shortening of muscle fibres (negative strain) with overall premature relaxation. Those fibres distal showed early pre-stretch (upto 15%) before systolic shortening and had overall delayed relaxation. (49–51) The time to delayed activation leads to regional differences in preload and this may account for the abnormal LV contraction pattern observed. Mechanical workload has been shown to dramatically differ between early and late activated myocardial segments,(49,52) with reduced workload in early segments and increased workload in late segments. Oxygen consumption and glucose uptake also have been shown to follow the same pattern. (50,52)

It has been demonstrated that ventricular performance is influenced by both AV synchrony and ventricular synchrony. In sinus rhythm, the maintenance of AV synchrony improves cardiac output significantly in both animal and human models. (53,54) Both ventricular systolic and diastolic function are seen to be impaired during ventricular pacing. Indeed LVdP/dtmax and LVdP/dtmin, sensitive markers of contractility and relaxation respectively are both reduced in ventricular pacing. (42) The long-term effect of ventricular pacing and the asynchronous activation of the ventricles have been shown to result in adverse ventricular remodelling. Van Oosterhout et al showed in 8 dogs that after 6 months of asynchronous pacing from the LV base, the LV cavity dilated and the site of early-activated myocardium became thinner, whilst the late-activated myocardium became thicker. The hypertrophy was both as a result of myocyte growth and increased collagen. (55) Studies in dogs of pacing in the right ventricular outflow tract (RVOT) have shown better segmental activation and ventricular performance when compared to pacing from the RVA. (45,56) Interestingly the QRS duration on the ECG did not differ significantly between the two sites.

LV pacing, in particular the LV apex consistently results in better ventricular performance when compared to RV pacing, in particular RVA pacing in normal

animal hearts. With the use of magnetic resonance imaging (MRI), MRI tagged sequences in a canine model showed less hypocontractile segments in LV pacing compared to RVA pacing. (49) The combination of LV apical and RV pacing appears to confer additional improved haemodynamic performance compared to LV pacing alone. (57)

1.3.5 Acute RV pacing in humans

Several studies in humans have shown that acute RV pacing, in particular at the RVA may lead to mechanical dyssynchrony and a reduction in global cardiac performance.

Delgado et al studied the acute response of RVA pacing in 25 patients undergoing an electrophysiology study using speckle-tracking strain imaging. (58) A significant decrease in LV end-diastolic diameter and volume was observed (49±5ml sinus rhythm, 45±6, p=<0.001), with no change in LV end-systolic diameter or volume. Subsequently the EF (decreased from 56±8% to 48±9% (p=0.001). During apical pacing the time difference between the earliest and latest activated segments increased significantly from 21ms to 91ms (p<0.001) and in 9 patients a time difference of greater than 130ms was observed, signifying LV mechanical dyssynchrony. LV global longitudinal strain decreased during pacing from -18.3±3.5% to 11.8±3.6% (p<0.001) and so did LV twist (12.4±3.7° to 9.7±2.6°, p=0.001).

Using 3D-echocardiography, Liu et al also demonstrated a reduction in LV EF during apical pacing (54.4±7.7% compared to 56.7±7.9%, p=0.13) and increased septal to posterior wall motion delay (91.9±52.5ms vs 38.6±28.9ms, p<0.0001) in 35 patients undergoing a DDD PPM for sick sinus syndrome. (59)

In a study of 12 patients undergoing DDD implantation, gated cardiac blood pool imaging was performed using a radioactive tracer (technetium 99m) to measure global LV function. This showed not only that acute RVA pacing reduced LV EF (66.5±4.5% to 60.3±5.2%, $p<0.0002$), but also after 1 week the EF was further reduced to 52.9±8.3%. Interestingly, when the pacing was stopped, LV EF did recover over a period of 32 hours to an EF of 62.9±7.6%. This suggested that despite immediate normalization of electrical activity within the heart, the myocardium retained electrical memory for the previous activation sequence or that cardiac remodelling had started to occur. (60)

Acute RV apical pacing in the above studies showed intra-ventricular dyssynchrony (i.e. septal to lateral wall delay). In a study by Bank et al, in a group of 25 patients undergoing an EP study, they found that between-wall dyssynchrony (septal to lateral delay) was not significant in RVA pacing even when compared to biventricular and LV free wall pacing. RVA pacing however did lead to basal to apical dyssynchrony. (61) This is known as intramural dyssynchrony. The characteristic systolic pattern of contraction in the longitudinal direction is displacement base to apex. This motion contributes to around 60% of stroke volume in humans (62) and is required for the normal septal contribution to the EF. (63) In both RV apical and biventricular pacing it was observed that the apical segments of the septum and lateral wall were displaced in the wrong direction initially during contraction. LV free wall pacing in this study showed minimal intramural dyssynchrony.

The pre-pacing LV function is likely to play a role in the subsequent development of pacing related LV dysfunction as demonstrated by Pastore et al. They studied 153 patients paced for 24 hours. In those patients with a normal pre-pacing ejection fraction, 45% developed LV dyssynchrony, in those with moderate pre-pacing LV systolic dysfunction, 93% developed LV dyssynchrony, and in those with severe pre-pacing LV dysfunction, 100% developed LV dyssynchrony. (64)

1.3.6 Longer-term effects of RV pacing in humans

From the large pacing-mode selection trials described previously and observation studies, it became apparent that there was a deleterious effect of long-term RV apical pacing. (65)

However, with such a heterogeneous population that receive a PPM, it is perhaps unsurprising that there are wide variations in the degree of adverse events reported long-term. Certainly not all patients experience adverse events. (66)

In one retrospective study involving 286 patients undergoing a pace and ablate strategy, only 9% of patients had a significant reduction in LV EF during follow-up.(67) Conversely in another retrospective study, this time in patients with high grade AV block, 26% of patients from a total of 304 developed new onset heart failure after a mean of 6.5 years. It is clear that humans are not all effected equally when paced. (68)

It has been shown that ventricular dyssynchrony may be evident in up-to 50% of patients after long-term RV apical pacing. (69,70)

In 58 patients treated with an AV node ablation, Tops et al showed with speckle tracking that after around 4 years of RVA pacing, speckle tracking revealed a difference of greater than 130ms between anterior and posterior wall segments in 57% of patients. In those patients who developed LV dyssynchrony, time to peak radial strain was shorter in the anteroseptal segments and longer in the posterolateral segments compared to baseline. In those without LV dyssynchrony no significant difference was observed. (69)

Fang et al found that in those that had developed significant mechanical dyssynchrony, ventricular size had increased and EF had decreased (64.2±4% vs 52.6±6%) compared to those patients who had not developed dyssynchrony. (71)

Cumulative pacing from the RVA of greater than 40% over 6 months, a low normal EF (50%) and pre-existing LV hypertrophy were found to be predictors of developing dyssynchrony. Thambo et al found in 23 congenital heart block patients that after 10 years of RV pacing, patients had higher values for intra-ventricular delay and septal to posterior wall motion delay and impaired longitudinal contraction compared to a control group. The cardiac output was reduced (3.8±0.6 vs 4.9±0.8 L/min, $p<0.05$) and lower exercise capacity was noted. (70)

Whilst the presence of mechanical dyssynchrony has been shown consistently in several long-term studies, the form that this takes has been shown to vary. Top et al showed radial dyssynchrony was present, whilst Ng et al and Bank et al found no difference between RV paced patients and volunteers. (61,72) Bank et al did show that intramural septal dyssynchrony was characteristic of patients chronically paced from the RV apex. Interestingly when those patients with pacing-induced heart failure are compared to matched heart failure patients with a similar EF, the pattern of dyssynchrony differs. Those paced patients had a smaller LV volume and significantly greater septal intramural dyssynchrony. This suggests the mechanism of LV dysfunction and remodelling is distinct from other causes of heart failure e.g. ischaemic heart disease. (73)

The normal basal and apical twisting motion of the myocardium serves as an important component in the LV ejection of blood. In normal circumstances the base and apex rotate in opposite directions with a differential twist of about 18 degrees. In patients with chronic RVA pacing, both basal and apical twists are reduced, as is the differential twist. In approximately 1/3 of patients apical rotation was in the opposite direction to normal and in the same direction as the base. (74)

Tse et al have evaluated the effect on long-term pacing on myocardial perfusion in 43 patients with complete heart block. After 35 to 42 months of DDDR pacing from

the RVA, patients underwent thallium-201 exercise tests and radionuclide ventriculography studies. Perfusion defects were seen in 65% of patients, most frequently at the RV apex and regional wall abnormalities were seen in 65% of patients. Interestingly on coronary angiography only 19% of patients had epicardial coronary artery disease, suggesting the pacing itself was causing regional flow heterogeneity. This has also been seen in animal models and offers another potential mechanism for the development of abnormal contraction and LV remodelling. (75)

Long-term RVA pacing has also been shown to result in asymmetrical changes in LV wall thickness. This is likely due to an altered dispersion of mechanical workload throughout the cardiac cycle. (70) Histologically, it has been shown that chronic RVA pacing results in changes in myofibre length, fat deposition, fibrosis, sclerosis and mitochondrial morphological changes. (76)

1.3.7 Alternative pacing sites

A growing number of studies have investigated the effect of alternative sites to pace the RV because there is now strong evidence that RVA pacing adversely affects cardiac function. This work forms the rationale for this study. It contributes to worsening heart failure in individuals with pre-existing structural heart disease and LV dysfunction (32,77,78) and also causes ventricular remodelling and a reduction in ejection fractions in those with structurally normal hearts. (70)

The inevitable consequence of RVA pacing is left bundle branch block which in itself is an independent predictor of mortality and morbidity. (79) Accordingly RVA pacing induces electrical and mechanical dyssynchrony. (80,81) Collectively these insights have led to the investigation of alternative pacing sites – most notably the RV septum (RVS) or outflow tract (RVOT), as well as biventricular pacing.

1.3.8 Biventricular pacing versus RV apical pacing

A number of studies have investigated whether biventricular pacing (also known as cardiac resynchronization therapy- CRT) has benefits over standard RVA pacing for non-heart failure patients. Currently CRT is recommended only for those patients with significant LV dysfunction, a QRS complex on the surface ECG of greater than 120ms, whom remain in class II-IV heart failure despite optimal medical therapy. In the HOBIPACE trial, a randomized crossover study of 30 patients with AV block and LV dysfunction compared CRT to DDD pacing. CRT after only 3 months was superior in terms of LV EF and the patients functional status. (82) In the BLOCK-HF trial, 691 patients with an EF of less than 50% were randomized to CRT or RVA pacing. In this cohort, the primary outcome of death from any cause, heart failure admission requiring intravenous therapy or a greater than 15% increase in left ventricular end-systolic volumes (LVESV) were lower in the CRT group. (83)

Yu et al followed 177 patients with normal LV systolic function after being randomized to RVA or CRT pacing. Although, EF was better preserved after one year of pacing, no difference in functional status, nor heart failure was observed, even when the follow-up was extended for another one year. (84,85)

Five clinical trials randomizing a total of 641 patients with permanent AF to RVA pacing or CRT have been carried out (PAVE, MUSTIC AF, OPSITE, Brignole et al group and PREVENT-HF). (86–90) The first three did show some functional patient benefit in favour of CRT with respect of improved six-minute walking distances, and the PAVE study did show the EF to be significantly greater after 6 months in the CRT arm of the study (46%vs 40.7%). Brignole et al showed heart failure hospitalization and death were significantly greater in the RVA group. (89) However in the PREVENT-HF study, after 12 months of pacing no significant volume changes were

seen between the pacing sites, nor were there significant differences in heart failure events.(90)

Whilst CRT appears beneficial in those with reduced baseline function, in those with normal function the evidence is not as strong requiring further work in this area and/or implying a small effect size.

1.3.9 Alternative right ventricular sites

With the increasing evidence that RV apical pacing leads to electrical and mechanical dyssynchrony with the resultant reduction in ventricular function and increased risk of developing heart failure, alternative pacing lead locations have been studied. A summary of the pertinent literature is shown in table 4.

His pacing

Para-hisian pacing whereby the specialized conduction tissue is in part stimulated, perhaps produces ventricular activation most analogous to normal physiology. It appears feasible and has been shown to produce near normal LV activation patterns (91) and in the acute setting result in less dyssynchrony and superior LV function compared to RVA pacing. (92) A 3 month cross-over study comparing HIS and RVA pacing did show reduced LV dyssynchrony using tissue doppler imaging (TDI) and less mitral regurgitation in the HIS group. (93) Over a longer follow up, HIS pacing was shown to improve LV EF and reduce LV end-diastolic diameter in patients with severe LV systolic impairment. (94)

Both intra-ventricular and inter-ventricular dyssynchrony have been shown to be reduced with Para-hisian pacing. (93,95) HIS bundle pacing is technically and logistically challenging requiring a specialized electrophysiology lab setup to achieve it. Practically it is not an option for the majority of PPM implants.

Right ventricular outflow tract

The RVOT is a common alternative site to RVA pacing and several studies have investigated its effect on ventricular function. Initial concerns over lead stability have proved unfounded and RVOT leads perform as well as RV apical leads in the short, intermediate and long term in terms of safety and feasibility. (96–98)

Studies have demonstrated in acute pacing models, improvements in LV function and dyssynchrony when compared to RVA pacing. Using speckle tracking echo, one study in 20 patients showed that RVOT pacing resulted in less radial dyssynchrony than RVA pacing. Coronary perfusion was also less affected. (99) Giudici showed that RVOT increased cardiac output by over 18% compared to RVA pacing, using Doppler echocardiography. (100) Longer-term studies have also shown a favourable outcome. Longitudinal function was shown to be superior in RVOT group in 58 patient followed up over 2 ½ years. (101) An 18 month crossover study in 24 patients who were 100% paced, showed that no changes in perfusion or dyssynchrony could be detected between RVOT and RVA pacing after 6 months. However after 18 months there were significant changes, with more perfusion defects and regional dyssynchrony in the RVA group. (102)

Whilst these studies demonstrated a positive outcome for RVOT pacing, others have failed to show any benefit in terms of LV function and patients functional capacity. Victor et al in a small study of 16 patients, showed no difference in LV function, QRS

duration, or exercise capacity over a 3-month period. (34) Similarly in a larger multi-centre randomized trial, it found no significant difference in EF or exercise capacity between RVA and RVOT sites. (103) Conflicting evidence exists regarding the mortality benefit, one study showing no difference,(104) a second showing improved mortality for the RVOT group. (105)

RV septal pacing

Septal pacing is another alternative site that has been investigated to determine if it offers superior outcomes to RVA pacing. Like RVOT pacing, pacing thresholds and lead stability are good, so this is a feasible method of pacing. (106) Acute studies have demonstrated, less ventricular dyssynchrony is present compared to RVA pacing (107,108) and the QRS duration is shorter and the EF is greater. (109) In the longer term, after 12 months one study showed upto 48% of RVA paced patients (n=46) had intraventricular dyssynchrony compared to only 19.4% of RVS patients (n=47). (110) Like RVOT pacing studies have been conflicting. One acute study showed no significant difference in dyssynchrony between the pacing sites, or LV EF. (111) In one randomized study with 98 patients (53 RVS, 45RVA) no differences were found in EF or exercise capacity after 18 months. (112) The most recently published study by Molina et al, randomized 142 patients with advanced AV block, to RV mid septal or RVA pacing. (113) 50% of the patients during the 1 year follow up were excluded on the basis of less than 98% pacing, leaving 34 patients in the RVA arm and 37 in the RVS arm. At 1 year the 6-minute walk test improved significantly in both groups, but was greatest in the RVS group (15% vs 24% improvement), whilst the EF significantly improved in the RVS group (57 to 61%, p= 0.008) but not the RVA group (52 to 54%, NS). This was due to a reduction in the Left ventricular end

diastolic volume (LVEDD) in the apical group (70.6 to 61.9mls) compared to the slight increase in the RVS group (66.2 to 67.6mls).

Conflicting results between alternate pacing sites

There are several potential reasons why conflicting results have been found. Studies to date have been invariably small and therefore underpowered to detect small differences in cardiac output (which may nonetheless be clinically significant e.g. 5%). Furthermore the methodology to assess ventricular function has varied widely including echocardiography, radionucleotide techniques, and also thermodilution. The cohorts studied have also been disparate with some having individuals with normal LV function, some reduced LV function, some with ischaemic heart disease (IHD), some with no evidence of IHD. As important is a lack of consistency in the definition of both RVS and RVOT pacing sites and the additional variation this can introduce. (97) Mond, an expert in RVOT pacing suggests that it is RVOT septal pacing that is superior rather than just RVOT pacing and that many studies have not used this precise location. (114) The length of studies is clearly important, and at present there is a paucity of good quality long-term trials.

The majority of studies attempting to answer this important clinical question have employed echocardiography to determine LV function. Such studies have shown only a small difference between ejection fractions between pacing sites, in the order of 10%. (34,97,115) Due to the significant test-retest variability paired with mediocre inter- and intra- observer variability of echocardiography it is not possible to robustly measure change of this magnitude. Estimates of the ability of echo to reliably detect inter-study change, are in the order of 13.2% for EF. (116) Given the small sample sizes, the small magnitude in EF changes (< 10% in most positive trials) and its

variability between studies, combined with the sensitivity of echocardiography to detect relatively small change, the reliability of such observations can be reasonably called into question. Conversely, cardiac magnetic resonance imaging (CMR or CMRI) enables the most accurate assessment of ventricular function with an ability to reliably detect a change in EF in the magnitude of 6% or more. (117,118) It is only now that MRI can be performed in those with cardiac devices and this will be discussed later.

The use of measures of dyssynchrony is also challenging since there are over 19 measures described in the literature. This makes comparing one study to another difficult if they have used differing indices.

Table 4. Studies comparing alternative site pacing.

Study	Pacing sites	Design	Duration of follow up	Summary of findings
Benchimol et al 1966 (119)	RVOT, RV inflow, RV septum	6 pts Observational Invasive haemodynamics	Acute	No difference in cardiac index, stoke index, mean arterial pressure.
Barold et al 1969 (120)	RVOT, RV inflow	52 pts Observational Invasive haemodynamics	Acute	No difference seen.
Cowell et al 1994 (121)	RVA RVS	15 pts Observational Invasive haemodynamics	Acute	Increased CO in RVS.

Giudici et al 1997 (100)	RVA RVOT	89 pts Randomised Echocardiography	Acute	CO increased 18% with RVOT.
Buckingham et al 1997 (115)	RVA RVOT	11 pts Randomised, Echocardiography	Acute	Trend towards higher CO with RVOT.
Karpawick and Mital 1997 (122)	RA RVA RVS	22 pts Randomised Invasive haemodynamics	Acute	Significant decrease in LV dp/dt with RVA.
Buckingham et al 1998 (123)	RVOT RVA	14 pts, EF <40% Randomised Invasive haemodynamics Echocardiography	Acute	Diastolic and systolic function small improvement with RVOT.

De Cock et al 1998 (124)	RVA RVOT	17 pts Randomised Invasive haemodynamics Echocardiography	Acute	RVOT pacing higher cardiac index than RVA.
Alboni et al 1998 (125)	RVA RVS RVOT	21 pts Observational	Acute	
Mera et al 1999 (126)	RVS RVA	12 pts Randomized crossover Chronic AF and AVN ablation Mild to moderate LVSD Echocardiography Radionuclide ventriculography	2 months each arm.	Increased LVEF and fractional shortening in RVS

Victor et al 1999 (34)	RVA RVOT	16 pts Prospective randomized crossover Chronic atrial tachycardia and complete AV block EF >40% in 10 pts Echocardiography	4 months then 3 months	No difference in LVEF or CO.
Schwaab et al 1999 (109)	RVA RVS	14 pts Randomized Radionucleotide ventriculography	Acute	Narrower QRS with RVS and better CO.
Kolettis et al 2000 (127)	RVA RVOT	20 pts, randomized Invasive haemodynamics Echocardiography	Acute (5 mins)	No significant difference in systolic function. Diastolic function improved with RVOT but not significant

Tse et al, 2002 (102)	RVA RVOT	24 pts Randomized (12 each) Myocardial scintigraphy Radionuclide ventriculography	6 m and 18m	Increased regional myocardial perfusion defects in RVA group. Increased Regional wall abnormalities in RVA and lower EF.
Stambler et al (the ROVA2003) (103)	RVA RVOT, dual site	103 pts. LVEF<40% Chronic AF Crossover at 6 months Echocardiography 6MWT	12m	No significant difference in 6MWT, EF or QOL

Deshmunkh et al 2004 (128)	RVA His	54 pts EF 23% Invasive haemodynamics, Echocardiography CPEX	6m to 9yrs	Increased EF and Cardiopulmonary fitness in His group.
Occhetta et al 2006 (95)	RVA Par-Hisian	16 pts Chronic AF and AVN ablation Crossover- 6 months each Echocardiography	1 year	Improved 6MWT and less inter-ventricular delay with His. Increased LVEF with HIS but not significant.
Victor et al (129) **2006**	RVS vs RVA	28 pts Chronic AF Crossover 3 months		No difference in pts with baseline LVEF > 45%. Significant difference in those with baseline EF <45%

Res et al, 2007 (96)	RVA vs bifocal RVA/RVOT	42 pts, EF <35% Blind, randomized crossover, 3 months each arm Echocardiography 6MWT QOL	7 m	Bifocal pacing superior EF, 6MWT and QOL.
Ten Cate et al, 2008 (130)	RVA RVOT	14 pts (7 RVOT, 7 RVA) Normal EF Echocardiography	Acute	No difference between sites with respect to longitudinal strain and wall motion score.
Vanerio et al, 2008 (105)	RVA RVOT	150 pts randomized AF and complete heart block (spontaneous or ablation) Compare all cause mortality	Mean 3 years	RVOT improves medium and long-term survival

Molina et al, 2014 (113)	RVA RVS	34 RVA, 37RVS Randomized Echocardiography 6MWT	Acute and 1 year	RVS had significant improvement in EF (57 to 61%, p= 0.008) 6MWT increased in both groups but NS.
Protect PACE 2015 (131)	RVA High RVS	240 pts. 120 each arm. High degree AV block EF >50%	2 years	RVA LVEF reduced from 56±9 to 55±9% RVHS 56±10 to 54±10%. No significant difference in heart failure, AF burden, mortality or BNP levels. No significant difference in intra-patient change in LVEF between pacing groups.

1.4 RVOT anatomy

The RVOT has been historically poorly defined, with the term being used to describe the true outflow tract, the mid septum and the anterior portion superior to the apex.(132)

Attempts have been made to standardize the nomenclature but defining the region is challenging. Anatomists, device implanters and electrophysiologists perhaps all have differing point of view with respect to this region.

Giudici, Karpawich and Lieberman have described the anatomical basis of the non-apical pacing sites including the RVOT, with Mond et al elaborating further on this. (132–134) In 2007, Mond et al published a review of the RVOT in terms of anatomy, radiographic views and the 12 lead ECG appearances, related to lead positioning. Table 5 gives the classification suggested by the 3 authors above, figures 2 and 3 illustrating the anatomy.

Table 5. Anatomy of the RVOT- Differing definitions.

Giudici and Karpawich 1999(133)	**Lieberman et al 2004**(134)	**Mond et al 2007**(132)
RV inlet septal:	**Lower RVOT border:**	**RVOT:**
Above, on or below the annulus of the septal/anterior tricuspid valve leaflet. Normal QRS morphology and axis.	Line extending from the tricuspid valve apex to the border of the RV.	Pulmonary valve superiorly and the superior aspect of the tricuspid apparatus inferiorly. Mond describes 4 components, septum, anterior wall, free wall and posterior wall.
RV infundibular septal pacing:	**Upper RVOT border:**	**RVOT septum:**
Proximal to pulmonary valve, distal to crista supraventricularis. LBBB with Left axis deviation.	Pulmonary valve	Inferior portion below the crista supraventricularis and left of septomarginal trabeculation lies true septum.
RV outflow septal:	**High Septal:**	**RVOT anterior**
Near the septal/moderator band insertion at mid-position of the RV septum.	Above a line mid way between PV and lower RVOT border	

LBBB with left axis deviation.	To the left of a vertical line between PV and RVOT lower border	
RV apical septal:	**Low septal:**	**RVOT posterior wall**
Proximal to septal moderator band. LBBB with left/right/normal axis	Below a line mid way between PV and lower RVOT border To the left of a vertical line between PV and RVOT lower border	
	High free wall:	**RVOT free wall**
	Above a line mid way between PV and lower RVOT border. To the right of a vertical line between PV and RVOT lower border	
	Low free wall:	
	Below a line mid way between PV and lower RVOT border To the right of a vertical line between PV and RVOT lower border	

Figure 2. RVOT anatomy

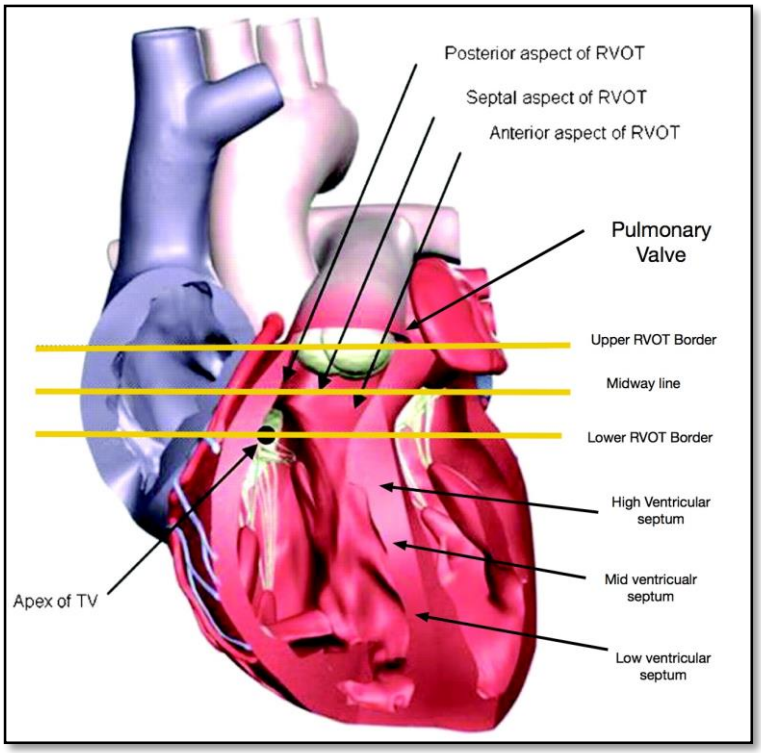

Figure 3. Cross sectional anatomy of the RVOT.

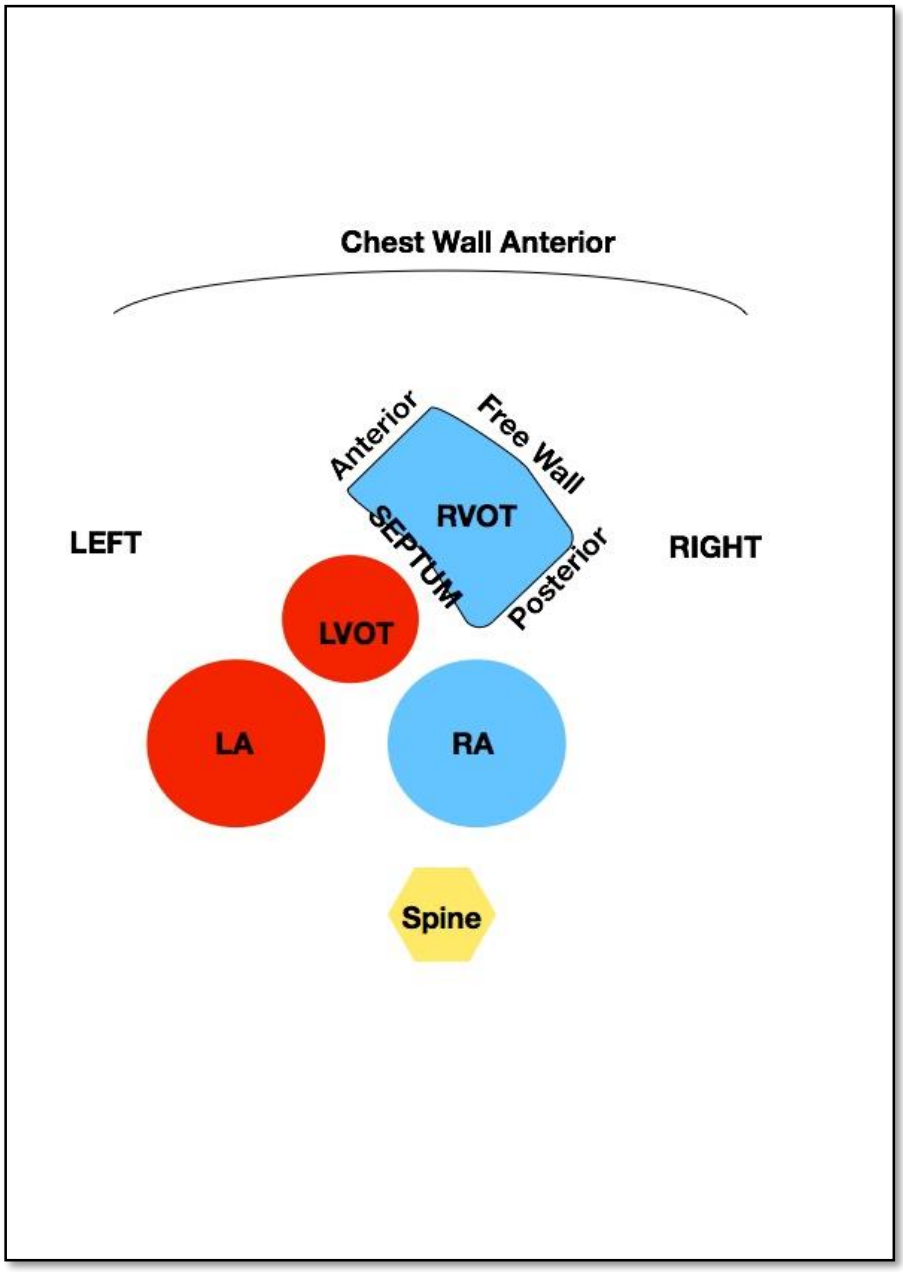

LA- Left atrium

RA-Right atrium

LVOT- Left ventricular outflow tract

RVOT- Right ventricular outflow tract

1.5.1 Cardiac dyssynchrony and imaging methods to measure it.

Cardiac dyssynchrony is described in one of three forms. Inter-ventricular dyssynchrony is a delay between RV and LV systolic contraction, intra-ventricular dyssynchrony is a delay between individual segments of the LV and atrio-ventricular (AV) dyssynchrony is a discordance of the normal sequential AV filling.

AV sequential filling is maintained in dual chamber pacing and atrial-based single chamber pacing and is often referred to as physiological pacing when correctly programmed. The cohort of patients in this thesis all have permanent AF and thus AV synchrony is not present. Therefore only methods of measuring inter-ventricular and intra-ventricular dyssynchrony are described.

1.5.2 Inter-ventricular dyssynchrony

1.5.2.1 Echocardiography

The majority of studies of inter-ventricular dyssynchrony have utilized echocardiography-based measurements. Visual assessment by the human eye alone cannot reliably detect differences of less than 70milliseconds and so predefined measurements and the protocols to achieve them are required. (135)

Measurements using Doppler and TDI echo techniques have been described in the literature.

Pulsed wave Doppler

Pulsed wave Doppler in the pulmonary and aortic outflow tracts can be used to measure pre-ejection times. The time is taken from the start of the QRS complex taken from the surface ECG, to the start of both pulmonary and aortic flow. A delay in the time to pulmonary or aortic flows are called right and left ventricular pre-ejection delays respectively. A difference between left and right pre-ejection times gives us the inter-ventricular mechanical delay (IVMD). A value of greater than 40milliseconds is considered abnormal and was used as one of the selection criteria for the CARE-HF trial. The larger the IVMD, the more likely dyssynchrony is present. This measure of dyssynchrony has shown to be one of the most reproducible measures. (136)

Tissue Doppler Imaging

TDI is a modification of conventional colour Doppler imaging, whereby the velocity of the myocardium is measured. TDI velocities can be displayed as a spectral pulse, m-mode or colour coded in a 2D image. TDI allows the measurement of peak systolic velocities of the myocardium, providing an assessment of longitudinal function throughout the cardiac cycle. Peak systolic velocity of the myocardium can be assessed in relation to the surface ECG. TDI can be used to measure inter-ventricular dyssynchrony by PW Doppler obtained in 2 segments, at the level of the tricuspid wall annulus and LV free wall.

TDI does have some disadvantages. It can only measure one aspect of myocardial function, longitudinal function. It cannot accurately assess either radial or circumferential deformation. Whilst TDI has good temporal resolution it does suffer from a poor signal to noise (SNR) ratio. The spatial resolution is low, and if the heart is off axis, then both longitudinal and radial velocities are included, making interpretation difficult. Another limitation is that it cannot differentiate active and passive myocardial movement. Due to the effect of tethering an infarcted area of

myocardium may have velocity resulting from it being passively pulled by the adjacent healthy segment. Finally TDI appears highly operator dependent and suffers from poor reproducibility, even in experienced technicians hands. (137)

1.5.3 Intra-ventricular dyssynchrony

There are multiple measures of intraventricular dyssynchrony that have been described in the literature and several imaging modalities can be used.

1.5.3.1 Echocardiography

Echocardiography is the most widely described modality for measuring intra-ventricular dyssynchrony.

The simplest measure is the aortic pre-ejection time, measured from onset of the QRS complex to the start of Doppler flow within the aortic outflow tract. A time of greater than 140milliseconds indicates intra-ventricular dyssynchrony is likely to be present. (138) M-mode echocardiography can be used to measure septal to posterior wall delay in the parasternal short axis at the level of the papillary muscles. (139) It has been shown to have some use in predicting response to cardiac resynchronization therapy (139,140) but it is difficult to measure and has high inter-observer variability. (141) One group found that in 38% of patients it could not be accurately measured. (142)

Pulsed wave TDI obtained in the basal lateral and basal septum of the LV 4 chamber can be used to give a septal to lateral delay. A delay of greater than 60 milliseconds is considered to be significant and represent intra-ventricular dyssynchrony. (143)

This is a two-segment model, but with more advanced imaging systems multiple segment models can be utilized so all the LV myocardium can be assessed. A 12-segment model was used by Yu and colleagues to create a dyssynchrony index. Using colour coded TDI, the time to peak systolic velocity in 12 segments obtained in 2, 3 and 4 chamber views are measured and the standard deviation between the segments is calculated. A value less than 34 milliseconds suggests absence of dyssynchrony, whilst the higher the SD, the greater the likelihood of underlying dyssynchrony. (144)

As previously mentioned TDI cannot distinguish between active and passive movement, so it will be less reliable when scar tissue is present. Strain imaging can potentially get around this by assessing the active myocardial deformation. Both the timing and amount of myocardial movement can be measured, with measurement expressed as a percentage change from the original length. Strain and strain rate obtained by TDI, however can be difficult to obtain and analyse. In particular, increased angle between the US beam and the myocardium can lead to an underestimation of strain. (145)

Speckle tracking is another technique that can measure myocardial strain that can be measured offline on conventional 2D echo images. It is not angle dependent like tissue Doppler, but does deliver high frame rates and can produce more noise. Myocardial strain, myocardial strain rate and time to peak strain can all be used to measure dyssynchrony.

Real-time 3-dimentional echo (RT3DE), allows multiple myocardial segments to be viewed at once and potentially allows longitudinal, radial and circumferential deformation to be measured. Although images are quick to acquire, temporal resolution is low. RT3DE allows the generation of volume time curves for the ventricle and it is a change in volume for each myocardial segment that can be used

to determine intra-ventricular dyssynchrony. The standard deviation of the time from QRS onset to minimum systolic volume can be been used for 6, 12 and 16 segment LV models.(146) Studies have shown concordance rates between RT3DE and TDI 56% and 76% for detecting left ventricular mechanical delay (LVMD). (147)

Figure 4. Schematic representations of Inter-ventricular (A) and Intra-ventricular (B) dyssynchrony during RV apical pacing assessed by doppler echocardiography.

A- Both the RV and LV electromechanical delays are measured from the onset of the QRS complex (dashed line). The RV electromechanical delay is the time from the onset of QRS interval to the onset of pulmonary systolic flow (blue arrow). The LV electromechanical delay is the time from the onset of QRS complex to the onset of aortic systolic flow (red arrow). The inter-ventricular dyssynchrony can be calculated as the difference between the RV and the LV electromechanical delays (black arrow).

B- Intra-ventricular dyssynchrony is represented by the delay in mechanical activation between different segments within the LV. The time from onset of the QRS complex to peak systolic strain for the septum (green arrow) and the posterior or lateral wall (red arrow) is indicated. The difference in time-to-peak strain for the various segments is the delay in mechanical activation, or LV intra-ventricular dyssynchrony (indicated by the black arrow).

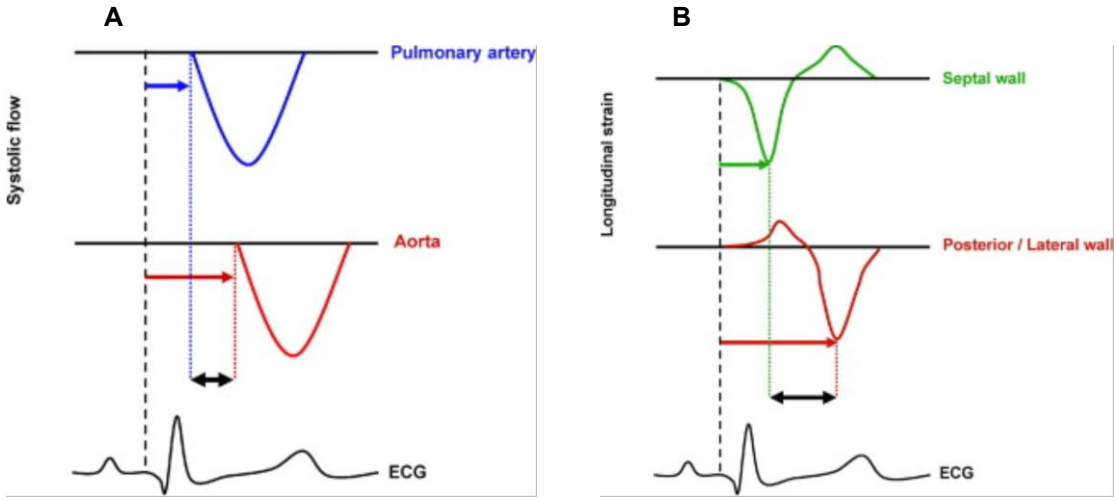

Reprinted from J Am Coll Cardiol, 54(9), Tops LF, Schalij MJ, Bax JJ. The effects of right ventricular apical pacing on ventricular function and dyssynchrony implications for therapy, 764-76, copyright 2009, with permission from Elsevier.

1.5.3.2 Nuclear Imaging

Inter-ventricular and intra-ventricular dyssynchrony can be measured using equilibrium radionucleotide-gated blood pool angiography (ERNA). This technique showed good correspondence between the morphology of the QRS complex and detectable inter and intra-ventricular dyssynchrony. (148)

1.5.3.3 Cardiovascular Magnetic Resonance Imaging

CMRI is the gold standard for ventricular volumetric analysis and assessment of global LV function. This is due to its good spatial resolution, high test-retest reproducibility and the lack of geometric volume assumptions compared to standard echocardiography. (149) MRI cine is also excellent for regional assessment of myocardial function. Several MRI techniques have been developed for the assessment of LV mechanical dyssynchrony. These included myocardial tagging, Vector-velocity-encoding, radial segmentation and feature tracking.

Myocardial tagging is a process whereby non-physical markers (lines or grids) are placed inside the myocardium using magnetizing pulses with a gradient. These markers, called Tags, have had their longitudinal magnetisation altered and appear in the acquired images as dark lines. They act as points of reference that deform with the myocardium to which they are linked. Analysis of the movement of these tags throughout the cardiac cycle can be used to calculate myocardial deformation and strain. The magnetisation pattern is called spatial modulation of magnetisation (SPAMM), which has subsequently been improved with complimentary SPAMM (CSPAMM).

SPAMM uses 2 radiofrequency pulses, separated by a gradient to generate the tag lines. (Figure 5) The tag lines gradually fade due to T1 relaxation of the tissue. Since the T1 relaxation approximates the length of an average cardiac cycle at 1.5 Tesla, the tag lines can fade towards the end of the cardiac cycle and information on myocardial deformation is incomplete in the later phases. (150) CSPAMM acquires two tagged lines that are 180 degrees out of phase with each other and then subtracts them. The tags last much longer throughout both systole and diastole, but acquisition time is increased.

Figure 5. Tagging of the left ventricle in short axis in diastole and systole.

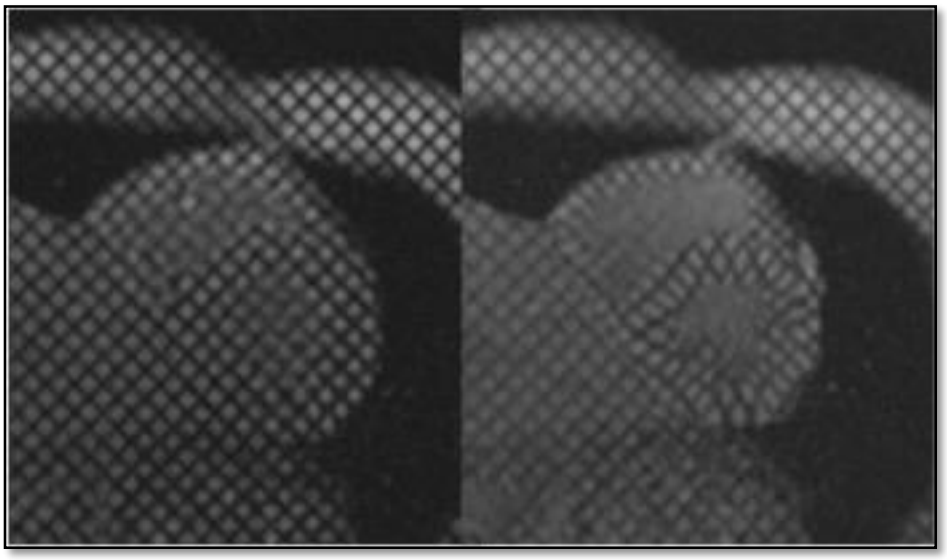

There are several methods for analysing the tagged MR images to obtain deformational data.

Harmonic phase analysis (HARP) measures the movement from tagged images by filtering certain regions in the frequency domain of the images called harmonic peaks.(151) This image is then decomposed into a magnitude and a harmonic phase. The magnitude relates to the underlying anatomy of the heart and the harmonic phase relates to the tag deformation. If one considers a segment of

myocardium with a vertical tag pattern, the number of tags per unit length of this segment is the frequency. When the myocardium contracts, the segment shortens and the tag lines become closer, so the tag frequency increases.

In a study by Rutz et al, post processing using HARP allowed three different dyssynchrony measures to be compared between controls and patients with LBBB and post myocardial infarction. These were the standard deviation of the maximum time to mid wall contraction, the CURE index and the SDI. All three showed a significant difference in dyssynchrony between the control and the patients, with the CURE and SDI in particular having excellent correlation with each other r=0.93 p=0.0001. (152)

The Circumferential uniformity ratio estimate (CURE) index is a number between 1 and 0 generated using fourier transformed circumferential strain data from 24 points around the short axis. Synchronous contraction gives a score of 1 and dyssynchronous gives a score of 0. (153)

The systolic dyssynchrony index (SDI) gives a global estimate of dyssynchrony using data derived from mid wall circumferential shortening. (152)

Velocity-encoded MRI assesses LV dyssynchrony by measuring differences in regional time to peak myocardial velocities, similar to TDI in echocardiography. The time difference between the peak systolic velocity of the septum and the lateral walls is used, with a bigger delay indicating dyssynchrony. (154)

Figure 6. Example of LV dyssynchrony assessment in a patient

(A) The color-coded tissue Doppler images four-chamber view. The velocity graphs are presented in the right panel of A. There is extensive LV dyssynchrony with a septal-to-lateral delay in peak systolic velocities of 115 ms (arrows). The accompanying velocity encoded magnetic resonance imaging and velocity graphs are presented in panels B and C, respectively, confirming extensive LV dyssynchrony with a septal-to-lateral delay of 116 ms.

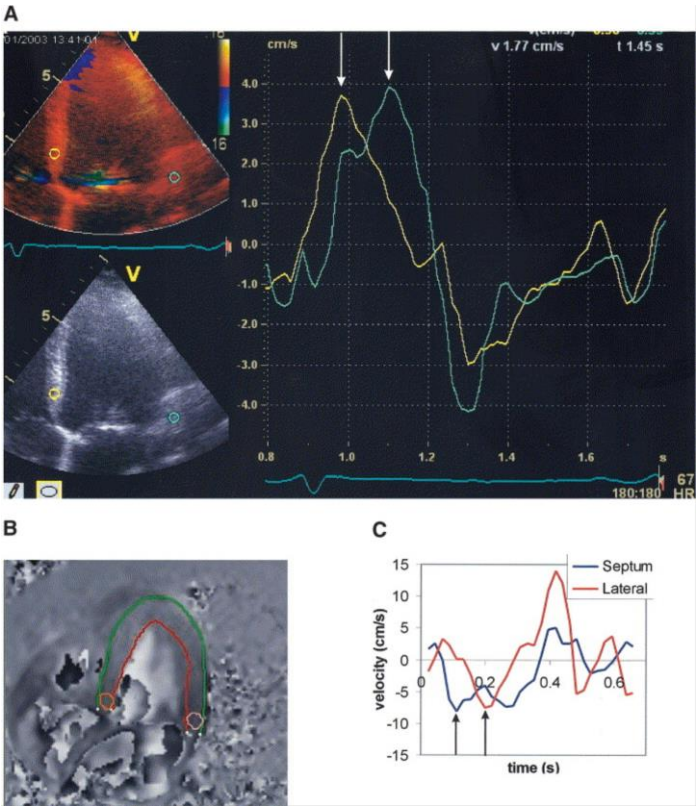

Reprinted from J Am Coll Cardiol, 47(10), Westenberg J, Lamb H, Van der Geest et al. Assessment of left ventricular dyssynchrony with conduction delay and idiopathic dilated cardiomyopathy: head to head comparison between tissue doppler imaging and velocity-encoded magnetic resonance imaging, 2042-2048, copyright 2006, with permission from Elsevier.

Radial motion and radial thickness of the myocardium can be used to measure dyssynchrony. The standard deviation of the time to peak radial motion and thickness in 16 or more LV segments can be used as a marker of mechanical dyssynchrony. (155)

Another novel method of assessing dyssynchrony using radial motion is the CMR-Tissue Resynchronisation Index (CMR-TSI). This assesses the dispersion of time to peak radial motion and has been shown to be an independent risk factor for cardiovascular mortality in heart failure patients. (156)

Diogenes® CMR Feature tracking (CMR-FT) software (TomTec Imaging Systems, Munich, Germany) is a vector-based analysis tool based on a hierarchical algorithm that operates at multiple levels using a combination of 1-dimensional and 2-dimensional FT techniques. A contour is drawn around the LV endocardial border in one frame and the software automatically propagates the contour and follows its features throughout the remainder of the cardiac cycle. Features tracked in each voxel by the software include brightness gradient at the tissue-cavity interface, dishomogeneities of the tissue and geometrical “roughness” of the tissue edges. The information produced allows the software to derive circumferential, longitudinal, and radial tissue velocity, displacement and strain/strain rate. It has been validated in phantom models and patients. (157)

Onishi et al used CMR-FT to measure radial dyssynchrony, defined as a difference between the anteroseptal and posterior wall segmental peak strain and the standard deviation of time to peak strain. This did show agreement with speckle tracking echocardiography for those hearts with electrical dyssynchrony. The advantage CMR-FT has over tagging is that it does not require any extra acquisitions, only standard cine sequences are required. (158)

1.6 Cardiac MRI and pacemakers

Recent (EnRhythm) and on-going safety and image quality studies (ADVISA) in MR conditional PPM patients undergoing MRI (including CMR) have demonstrated the excellent safety profile of the devices. (159)

I have published a review article on the use of CMR imaging (CMRI) and implantable devices and will form the basis of this chapter. (160)

1.6.1 Implantable pulse generators in the MR environment

Implantable pulse generators (IPGs) and defibrillators have traditionally been considered contraindications to MRI However, recent data has challenged this paradigm and demonstrated that patients with newer generation devices can safely undergo MRI, including cardiac MRI, provided basic precautions are taken.

Reflecting its unparalleled soft tissue contrast and absence of ionising radiation, MRI has seen a substantial expansion over the last 15 years, with more than 60 million MRI scans currently performed annually worldwide. (159) CMRI has emerged as a cost effective cardiac imaging modality that provides important diagnostic, and increasingly prognostic information that significantly impacts on patient management. (161) Whilst CMR currently represents only a small proportion of all MRI scans, the number of CMR scans being performed is increasingly rapidly. (162)

An estimated 250,000 patients have implantable pulse generators (IPGs) and implantable cardioverter defibrillators (ICDs) in the UK, with 50,000 patients undergoing implantation in 2011. (163) The probability that a patient with an IPG will

require MRI over the lifetime of their device is estimated at 50-75% and with most hospitals now offering MRI, including some 60 providing CMR in the UK, the issue of MRI in patients with IPGs will be encountered with increasing frequency. (164) Serious adverse events during MRI of patients with cardiac devices, including asystole and ventricular fibrillation, have been reported, albeit rarely, and as such an awareness of the safety issues, the different types of IPGs (MR conditional versus non-MR conditional) and measures to facilitate safe scanning in these patients group. (164–166)

1.6.2 MRI safety terminology

The 2005 MRI task group of the American Society for Testing and Materials defined the following terminology with regards to implants and devices relative to the MRI environment:

MR safe: An item that poses no known hazards in all MRI environments e.g. non-conducting, non-magnetic items such as plastic cannula.

MR conditional: An item that has been demonstrated to pose no known hazards in a specified MRI environment with specified conditions of use. Conditions include static magnetic field strength, spatial gradient, dB/dt (RF) fields, and specific absorption rate (SAR). Additional conditions may be required, including specific configurations of the item.

MR unsafe: An item that is known to pose hazards in all MRI environments. MR unsafe items include magnetic items such as a pair of ferromagnetic scissors or oxygen cylinders. (167)

1.6.3 Safety issues concerning IPGs and ICDs in the MRI environment

Whilst MRI is an inherently safe imaging modality, the MRI environment harbours the potential for even fatal accidents, particularly in patients with cardiac devices. Indeed of the small number of reported MRI-related fatalities, the majority relate to patients with IPGs in-situ (10 out of 15 deaths). (168–170) Risks associated with MRI in patients with IPGs generally arise from the static magnetic field, gradient magnetic fields and radiofrequency energy, which can act in isolation or in combination to adversely affect IPG function (Table 6). Complications may include lead tip and tissue heating, mechanical pull, inappropriate therapies (pacing and device discharge) and failure to pace. (171–176)

Table 6. Theoretical effects of static magnetic field, gradient magnetic filed and radiofrequency energy.

	Static	Gradient	Radiofrequency
Case heating		✓	✓
Force and Torque	✓		
Vibration	✓	✓	
Device Interactions	✓	✓	✓
Lead Heating			✓
Stimulation		✓	✓

1.6.3.1 Tissue heating

Pacing leads can act as antennae, concentrating electromagnetic energy at the un-insulated points of the lead cathode, anode or active fixation helix, which can lead to heating of the surrounding tissue where the energy is dissipated and potentially cause localised oedema and/or fibrosis. Theoretically this could result in increased in pacing thresholds, loss of pacing capture and cardiac perforation. (176–180) The potential for heating depends on the resonant frequency of the lead (dependent on lead length and diameter), the trajectory of the pacing leads, presence of lead loops, lead or insulation fractures, patient size and position within the scanner. (181–185)

In-vitro studies without lead tip irrigation, have demonstrated lead temperature increases in excess of 60^{o}C during MRI scanning although such extreme temperature variations have not been observed in more sophisticated models with

lead tip irrigation. One in-vivo study in pigs found an increase of 20.4^{o}C at the electrode tip in the setting of a SAR approaching 3.8W/kg, considerably higher than that in routine clinical scanning. (186) In another study a small rise in serum troponin was seen following 4 out of 114 scans performed at 1.5T in patients implanted with a variety of conventional (i.e. MR-unsafe) IPGs, which the authors hypothesised likely reflected tissue necrosis secondary to lead tip heating. (187)

1.6.3.2 Force and Torque

IPGs contain ferromagnetic materials, which are subject to force and torque induced by the static and gradient magnetic fields. (176,177,187) This can lead to movement and vibration of the device and leads. These forces are directly related to mass of ferromagnetic material, the strength of the magnetic field and the positioning within the static magnetic field. (188) Whilst there are anecdotal reports of pull/drag, modern (i.e. post 2000) IPGs appear safe with regards to force and torque at 1.5T beyond the first 6 weeks following implantation, after which time healing around the device and leads is thought to provide sufficient anchorage. (188–190)

1.6.3.3 Inappropriate pacing, shocks, inhibition of therapies

Radiofrequency energy pulses can lead to asynchronous pacing, programming changes or battery depletion or be wrongly interpreted as underlying electrical activity or arrhythmias and thus lead to inhibition of demand pacing or delivery of ICD therapy respectively. (187,190–193) In an Ex-vivo study by Erlebacher on 3 IPGs no longer in use, radiofrequency interference caused total inhibition of atrial and ventricular output or resulted in atrial pacing at a high rate. (173) No ICD induced defibrillation therapies in the MR environment have so far been reported, although

this may relate to the inability of the capacitor to sufficiently charge in the static magnetic field. Nevertheless, repeated attempts by a defibrillator to charge itself could lead to battery depletion. (194)

1.6.3.4 Electrical reset

'Electrical reset', 'power on reset' and 'factory reset' are interchangeable terms for the emergency/backup mode that a device reverts to when its battery nears depletion. It is conventionally a VVI pacing mode at the lower rate limit with all advanced functions turned off. (178) For ICDs, power on reset is a safety mechanism, which prevents inappropriate shocks from a damaged device. It is a VVI back up mode with no therapies. It cannot be reprogrammed and the device has to be changed. It should not be confused with the normal magnet response of ICDs. This is fixed rate pacing with therapies disabled, but functions return on removal of the magnet. Publications have quoted an MRI-related incidence of electrical reset as high as 6.1% in conventional (i.e. MR unsafe) IPGs. (188) The conversion of asynchronous or fixed-rate pacing to VVI mode in a IPG-dependent patient without an underlying ventricular rhythm, in combination with radiofrequency energy pulses being wrongly interpreted as intrinsic electric activity is potentially life-threatening and several MRI-related deaths in IPG patients have been attributed to this mechanism.

1.6.3.5 Reed switches

Magnetic-operated reed switches were originally incorporated into IPGs to allow device interrogation. Magnet application activates the reed switch which inhibits demand functions and most commonly, but not consistently, sets an IPG to an asynchronous mode. (165,187) The position of the reed switch has been shown to

be inconsistent within the MRI environment leading to potential malfunction. (190) Variable reed switch responses to MRI have been demonstrated across different IPG models including asynchronous pacing, transient loss of pacing or continuous loss of pacing. (187,190,195) Loss of pacing in a pacing-dependent patient could have significant consequences, whilst asynchronous pacing in individuals with a underlying rhythm could heighten the theoretical risk of R on T phenomenon and induce ventricular arrhythmias. In ICDs, activation of the reed switch commonly leads to deactivation of therapies whilst not affecting backup pacing. (196)

1.6.4 MRI in conventional (i.e. MR unsafe) systems

Whilst the majority of older studies assessing non-thoracic MRI in patients with MR-unsafe IPGs have reported no adverse events, isolated incidents of asystole, ventricular fibrillation and death have been described, (194) although such work is limited by small study size and lack of consistency in reporting type of IPG and leads.

More recently Nazarian et al performed 555 MRI scans (40% brain, 22% spine, 16% heart, 13% abdominal, 9% extremities) on 438 patients with either a IPG (54%) or ICD (46%) of various manufacturers. (197) Three patients experienced electrical reset during scanning but there was no device dysfunction on long-term (up to 5 years) follow up. Minor changes in ventricular and atrial lead impedances (<0.5% acute change) were noted, but no significant differences in threshold occurred. Specifically thoracic imaging was noted to be associated with decreased acute and chronic (> 3months) R wave amplitudes and battery voltage compared to non-thoracic scans suggesting that whilst non-thoracic MRI can be performed safely, thoracic scans may present a higher risk.

Whilst on a smaller scale Junttila et al performed 3 MR scans on each of 10 patients over a period of 12 months. (198) Reassuringly no adverse patient events occurred with a variety of non-MR conditional ICDs and no significant changes were reported in lead threshold, lead impedance or battery voltage. This suggests serial scans may pose no greater risk than single scans.

The Magnasafe registry is a multi-centre prospective study investigating the frequency of major adverse clinical events and device parameter changes for patients with conventional (MR-unsafe) IPGs who undergo clinically indicated non-thoracic MRI at 1.5T. (199) So far over 600 scans across 12 sites have been performed without the occurrence of loss of pacing capture, device failure or death. Decreases in battery voltage, R and P wave amplitudes did occur and the frequency of one or more clinically relevant device changes occurred in 13% of IPGs and 31% of ICDS. This implies that whilst technically safe it is essential to perform a full device interrogation pre and post scan. (200)

1.6.5 MR conditional devices

In recent years the device industry has invested significant effort into developing MR-conditional systems to address the discussed safety issues. Many new design features of both hardware and software have been incorporated into these devices to allow them to perform more reliably in a specified MRI environment (i.e. 1.5T field strength).

Hardware modifications have been made to both the generator and leads whereby some of these changes are manufacturer-specific. (Tables 7 and 8),

Software changes include the incorporation of a dedicated MRI pacing mode that can be activated for the duration of the scan. In most instances this requires a trained

individual, commonly a pacing technician or electrophysiologist, to activate and deactivate this mode. There are novel alternatives, with St Jude providing a hand held activator to perform this task before and after the scan, and Boston Scientific's Ingenio and Advantio devices having an MRI time-out mode negating the need to deactivate the safe mode manually post-scanning. Nevertheless current recommendations are that a full IPG interrogation is carried out pre- and post-MRI. (197)

Table 7. Common design features of MR conditional devices

Generator design
• Ferromagnetic content reduced • Replacement of reed switch with solid state technology e.g. Hall sensor • Bandstop filter (64Mhz) in casing to shield circuitry
Lead design
• Lead pitch of the inner coil redesigned to alter resonant frequency of the lead • Lead diameter altered • Bandstop filter (64Mhz) at lead tip (St Jude Tendril lead)

Table 8. Current MR conditional IPGs on the market.

	St Jude	Medtronic	Boston Scientific	Biotronik	Sorin
Device	Accent MRI	Advisa MRI Enrhythm MRI Ensura MRI	Ingenio MRI Advantio MRI	Evia MRI Estella MRI	Reply MRI
Leads	Tendril MRI	CapsureFix MRI Capsure sense	Fineline II	Safio/Solia	Filtrea
Lead fixation	Active	Active and passive	Active and passive	Active and passive	Active
Lead diameter	6.6F	5.4F	5.1F	5.6F	6.5F
Thorax exclusion	No	No	No	Yes	No
Scan time limit	No	No	No	Yes	No
SAR limit (w/kg)	4	2	2	2	4
Manual programming required post MRI	(activator operated)	Yes	No (automatic timer)	Yes	No

Activation of the “MR Safe” mode switches off advanced functions and the IPG paces in an asynchronous fashion (i.e. no sensing) to reduce the risk of electromagnetic interference being misinterpreted as an intrinsic rhythm with the potential of supressed pacing. In some models the pulse amplitude and pulse duration are also both increased (e.g. 5V and 1mS in the St Jude Accent), which increases the pacing stimulus and minimises the risk of loss of capture.

In the original EnRhythm trial with the Medtronic Surescan pacing system®, 258 implanted patients underwent 14 non-clinically indicated brain and lumbar spine sequences 9-12 weeks post implant in a 1.5T scanner. Pacing parameters were compared with a control group (206 implants) immediately, 1 week and 1 month post MRI. No MRI related complications occurred and changes to pacing parameters were minimal. (181) Thoracic scans were excluded in this trial, but in the more recently published ADVISA study, a prospective randomised non-blinded multi-centre trial in 263 patients, thoracic/cardiac sequences were included. The ADVISA MRI IPG and Capsure-fix safety lead system when scanned in a 1.5T environment with a SAR limit of 2W/Kg resulted in no power on reset, electrical stimulation or pacing threshold changes. (201) The removal of scan area restriction is highly desirable as excluding the thoracic region may negate the performance of up to clinically indicated 40% of MRI scans, including thoracic spinal cord imaging and CMR. To facilitate the recognition of MR-conditional devices on a plain film radiograph, radiopaque markers are found on both the generator and lead, although these are neither standardised nor intuitive and their identification can be a challenge in clinical practice (Figures 7).

Figure 7. Radiopaque markers on a St Jude Medical, Medtronic and Boston Scientific MR conditional pacemakers and leads.

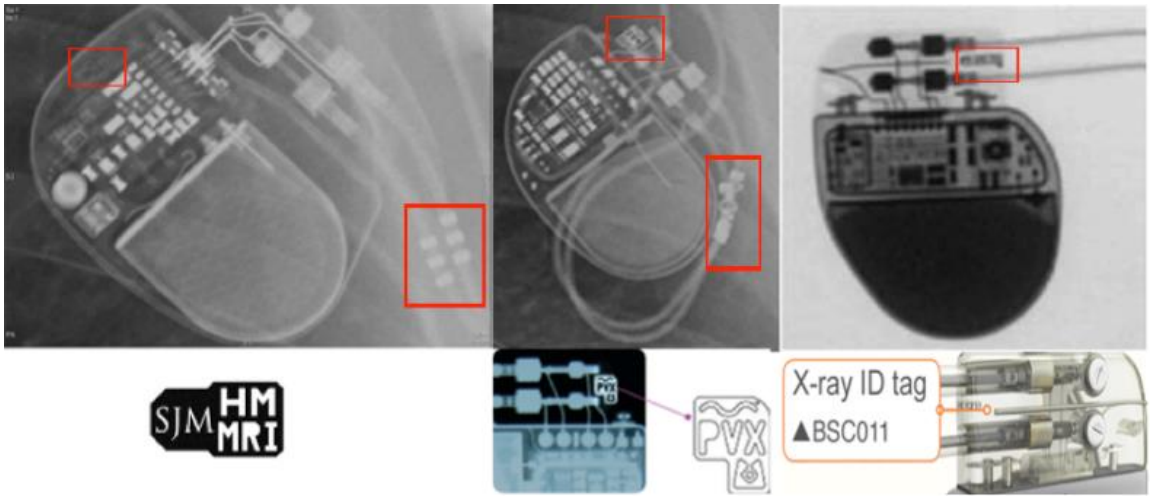

1.6.6 Scanning an IPG patient

When presented with a patient with an IPG in-situ a number of considerations are pertinent (Table 9).

Table 9. Safety considerations pre-scan

Is there an alternative image modality that can answer the clinical question posed?
Duration of device implant.
Manufacturer and model of device.
What is the MR safety label?
What are restrictions associated with device (zonal, SAR)?
Has device been used in safety studies?
Presence of lead loops or lead fractures.
Proximity of the device to region being scanned (thoracic versus extra-thoracic).
What is the likelihood of a non-diagnostic scan 2nd to susceptibility artefacts (left versus right sided implant, device position over thorax?).
Presence of additional hardware e.g. abandoned leads, adapters.
Risk/benefit ratio for specific patient circumstances (e.g. is patient pacing dependent versus good underlying rhythm).
Is diagnosis likely to impact significantly on patient management and/or QOL or outcome?

Established clinical protocols and algorithms have been proposed with physician led scans and pacing support readily available. (177,194) It is good clinical practice to perform device interrogation before and after scanning to assess for battery depletion, programming changes or electrical reset. Patient monitoring throughout the scan period should include monitoring of pulse oximetry, ECG, blood pressure and verbal responsiveness. (197) A suggested algorithm is given in figure 8.

6 weeks is the recommended interval between implant and MR scan from published studies. Lead dislodgment is more frequent in the first 6 weeks following an implant, and thus studies did not want to subject patients to MR scans and the theoretical risk of force and torque on the leads, whilst tissue encapsulation is not fully established. No studies exist that address scanning at shorter time intervals. In emergencies, particular spinal cord lesions, the benefit of an MR scan even within a week of implant may outweigh potential risks.

Figure 8. Algorithm for safe scanning of an IPG patient.

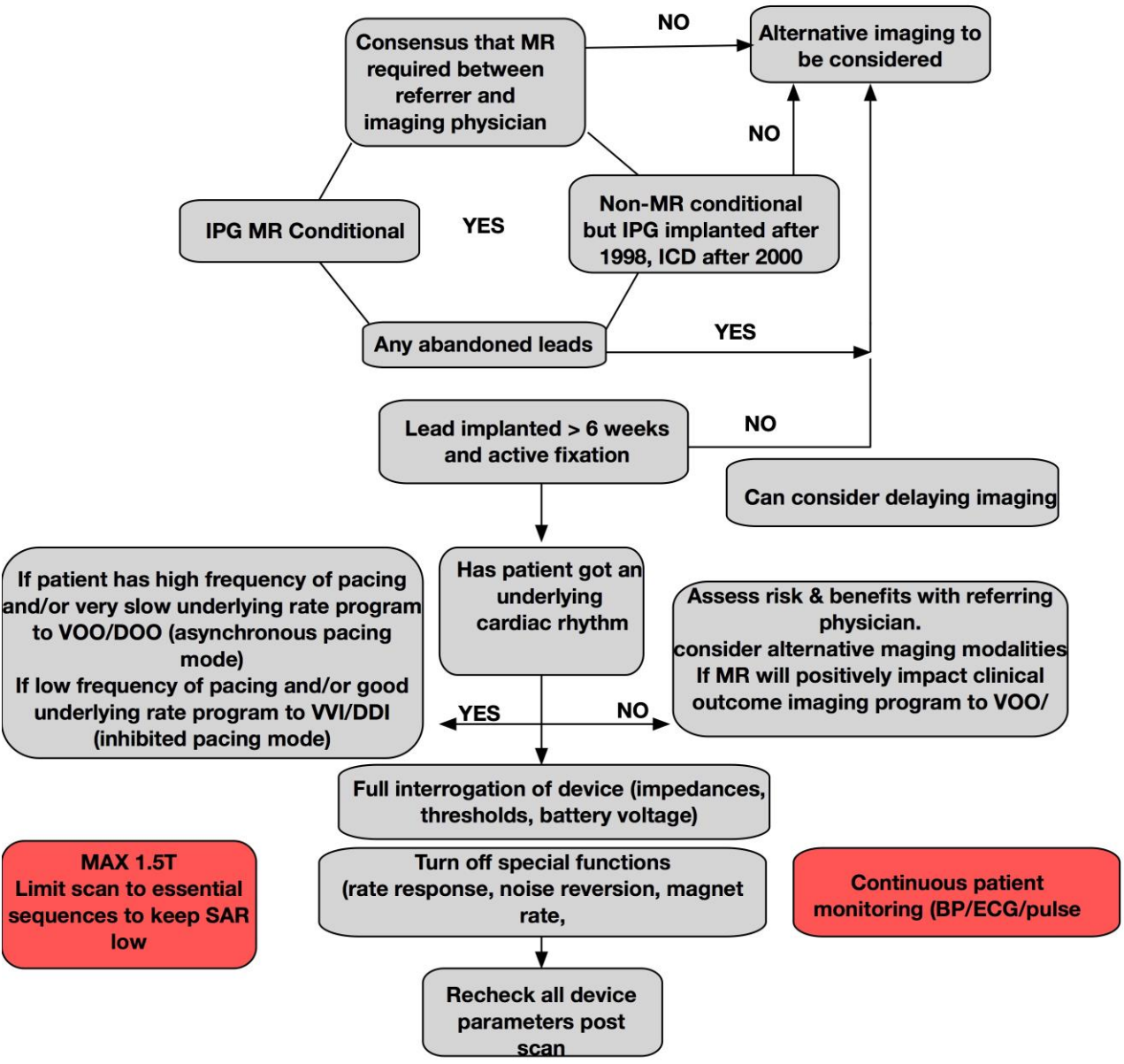

1.6.7 CMR Imaging

The development of MR conditional devices allows this previously excluded cohort to benefit from CMR imaging, however device-related artefacts can impact significantly on image quality. Image distortion appears dependent on the size of the device (larger devices are associated with more artefact), position of the implant, the imaging plane and the scanning protocol. (202) The major field distortion is often limited to an area of approximately 15cm around the device. Artefacts are often more pronounced in the ventricular short axis plane compared to long axis planes, and more so in anterior LV segments. (202) Steady state free precession (SSFP) cine imaging is associated with more susceptibility artefact than spoiled gradient echo imaging (Figure 9 a, b). In the study by Sasaki et al susceptibility artefacts were more pronounced on Late Gadolinium contrast acquisitions than other imaging sequences and were particularly common in the anterior segments. Strategies to optimise imaging sequences and post processing are currently being researched.(203) Despite the presence of artefacts, one study with conventional (MR-unsafe) devices showed that 100% of SSFP cine images in 15 PPM patients and 86% in 56 ICD patients remained diagnostic for LV assessment. (202) In the recent Advisa image quality sub-study, good quality SSFP CMR images assessing cardiac anatomy and biventricular function were obtained in over 90% of patients. Quality was assessed for the LV and RV on a 7 and 5 point scale respectively, whereby grade 1 (excellent image quality) required the absence of both lead and IPG artefacts preventing the interpretation of regional wall motion as defined by systolic wall thickening and endocardial inward movement.

The experience of my research unit is that MR conditional pacing systems still exhibit significant artefacts around the generator (figure 9 c, d), although commonly this

does not prevent LV and RV wall motion assessment, especially when being able to switch to spoiled gradient cine imaging. In our experience lead related artefacts are minimal and do not impact significantly on wall motion assessment and do not prevent of the computations of strain and strain derived indices from tagged images or endocardial feature tracking software packages (e.g. Diogenes®, TomTec) (figure 9 f). It is important to recognise that cardiac devices equally affect CT imaging, whereby lead related artefacts can be particularly prominent. It has been suggested that MRI is superior to assessing the myocardial interface, particularly relevant in ruling out myocardial perforation.(202)

Figure 9. Images of CMR in a patient with a cardiac device.

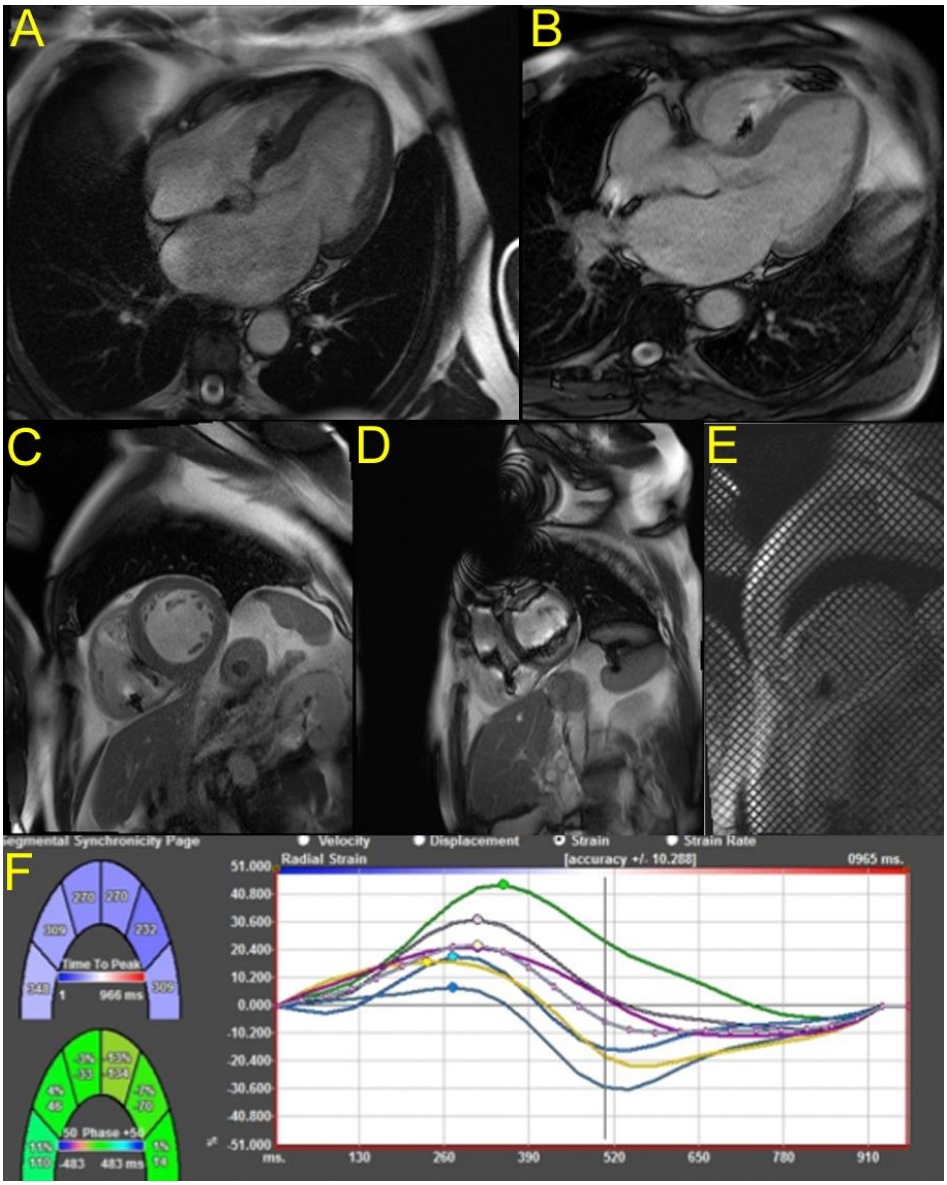

A) The SSFP sequence in 4ch view (B) SpGr sequence in 4ch view (C) SSFP sequence in Short axis view with nor artefact (D) Significant IPG related artefact of short axis slice of SSFP sequence (E) Tagging in the short axis vie (F) Feature tracking of 4 ch view using Tomtec software.

1.6.8 Issues concerning patient selection

Whilst it has been demonstrated that MRI of non-MR conditional IPGs can be performed safely when certain logistic, safety and monitoring requirements are adhered to, concerns remain not only about the unpredictable nature of malfunctioning of such devices in the MR environment (especially in pacing dependent patients), but possibly more so about what potential effects the lowering of the acceptance threshold for scanning IPGs would have in real world clinical practice in the long term. The greatest concern would possibly be that the minimum required standards for proceeding “safely” with such exceptional scans could subsequently become eroded, exposing patients to avoidable risk.

Chapter 2

Methods

CHAPTER 2: Methods

2.0 Methods

This thesis is based upon the MAPS trial- Effect of Septal versus Apical Pacing- a comparative study using Cardiac MRI. ClinicalTrials.gov Identifier: NCT01842243

The methodology described in this chapter is that for the trial with the exception of the biomarker and echocardiography components, which do not form part of this thesis.

2.1 Patient Selection

The study, along with all the methodology described was approved by the South Manchester Local Research Ethics Committee (Manchester REC) and Research and Development department within University Hospital of South Manchester and University Hospital of Central Manchester.

All the patients gave written informed consent prior to enrolment in the study.

50 patients were recruited from the Northwest Cardiac Centre and the Manchester Heart Centre between February 2012 and May 2014

2.1.1 Inclusion Criteria

Inclusion criteria Identified subjects aged 18 years and above who could give informed consent, that were in permanent AF, whom required a PPM to facilitate an AV node ablation or optimization of drug therapy.

Left ventricular function of ≥ 40% on previous echocardiography within 12 months of study enrolment was required.

2.1.2 Exclusion Criteria

1) Patients with known EF <40%.
2) Any contraindication to Magnetic Resonance imaging (see appendix for Contraindications for MRI).
3) Patients indicated for an implantable cardioverter defibrillator or cardiac resynchronization therapy.
4) Patients with a myocardial infarction within three months prior to enrollment.
5) Patients that received bypass surgery within three months prior to enrollment or patients with a mechanical right heart valve.
6) Patients where a RV lead cannot be placed e.g. complex congenital heart disease.
7) Patients with hypertrophic obstructive cardiomyopathy.
8) Patients with acute coronary syndrome, unstable angina, severe mitral regurgitation and/or haemodynamically significant aortic stenosis.

9) Previous implanted PPM or cardioverter defibrillator.
10) Terminal conditions with a life expectancy less than 2 years.
11) Participation in any other study that would confound the results of this study.
12) Psychological or emotional problems that may interfere with the volunteer's ability to provide full consent or fully understand the purposes of the study.
13) Pregnant patients or patients who may become pregnant during the time-scale of the study.

All the patients were deemed to require a PPM as part of their routine clinical care by the treating physicians and referred to myself for further evaluation. All patients received a detailed information sheet either in clinic or the post and a verbal explanation of the study over the phone or in person. All patients were given a period of at least 24 hours to decide if they would participate in the study. Full written informed consent was obtained prior to patient enrolment.

2.2. Study Outline

2.2.1. Study design

The MAPS trial is a prospective longitudinal cohort crossover study of patients with AF undergoing implantation of a PPM with 2 ventricular leads. PPM implantation is followed by an AV node ablation a minimum of 6 weeks after the initial procedure.

Patients are randomly selected to have apical or septal pacing for a period of 9 months following implantation. A baseline CMR scan, transthoracic echocardiogram (TTE), cardiopulmonary exercise test (CPEX), quality of life questionnaire (QOL) and blood sample were performed. At 9 months these investigations are repeated and the pacing mode is switched to the other modality. After a further 9 months these investigations are repeated once more and the study comes to an end. Table 10 gives the investigations as part of the MAPS trial and Figure 10 gives the study timeline.

Table 10. Investigations in the MAPS trial

	0 months	9 months	18 months
Cardiac MRI	✓	✓	✓
Echocardiogram	✓	✓	✓
Quality of life questionnaire	✓	✓	✓
Blood sample (8mls)	✓	✓	✓
Cardiopulmonary exercise test	✓	✓	✓
6 minute walk test	✓	✓	✓
ECG	✓	✓	✓

Figure 10. Study timeline for MAPS trial.

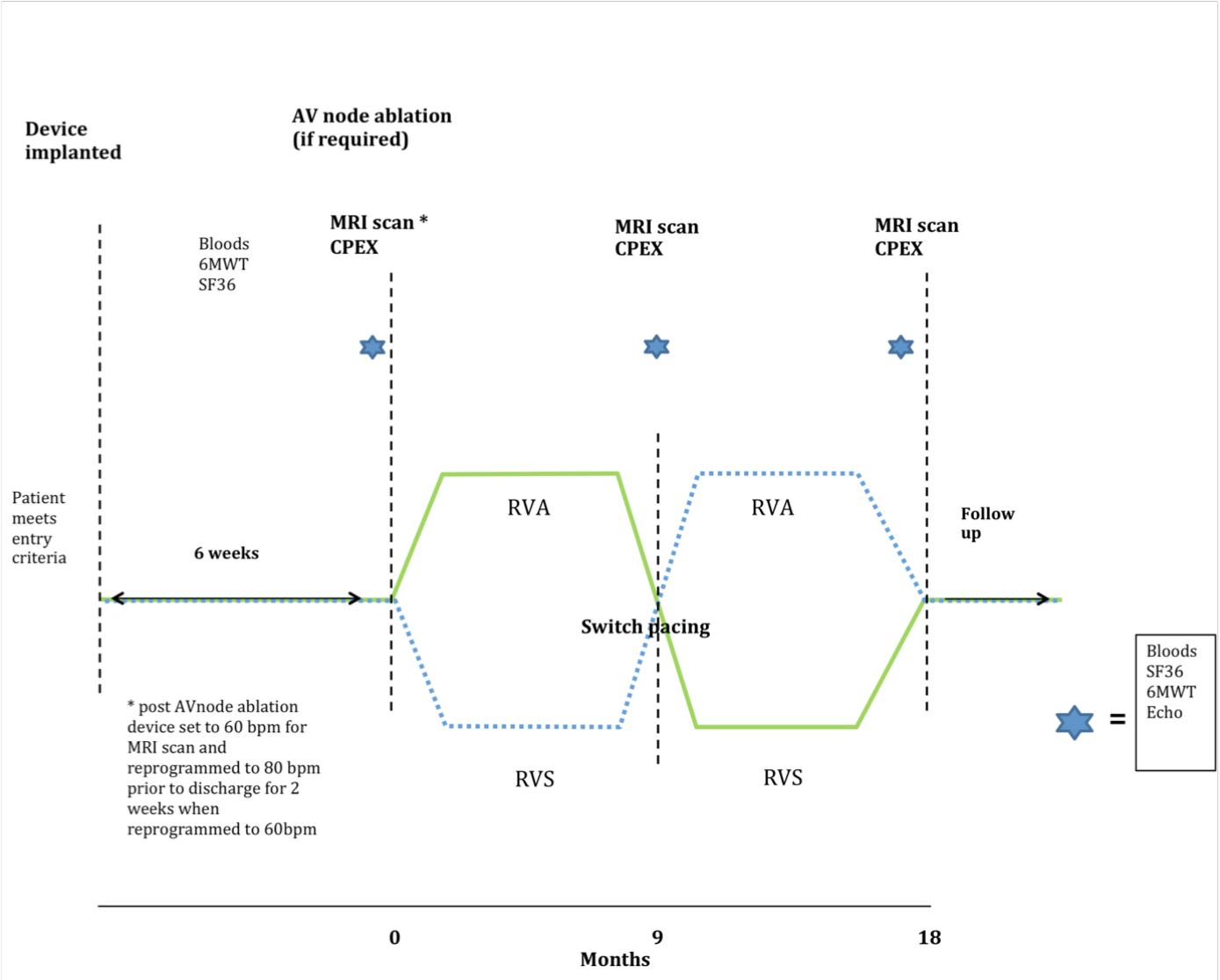

2.2.2 Consent procedures

Patients who were attending the electrophysiology clinics were identified by the medical team as requiring a PPM as part of the management of AF. This was to facilitate an AVN ablation. Patients were given a study pack, which included an official invite letter, a stamp addressed reply slip and information leaflet in clinic. Following this they had the opportunity to discuss the trial. Full consent for the study was obtained on the day of PPM implantation. Copies of the consent form were kept in the research file onsite, patient case notes and also by the patient. (Appendix)

2.2.3 Withdrawal of patients

Patients were given the option to withdraw at anytime from the study.

This did not affect future medical treatment. This was explicitly explained in the oral and written information provided.

2.2.4 Sample size

A cross over study with 50 patients will have 80% power to detect effect sizes of 0.4 or more, and 90% power to detect effect sizes of 0.47 or more between treatment regimes.

Effect size = mean difference between regimes/standard deviation of differences.

2.2.5 Potential risks to patient

PPM implantation ± AVN ablation were part of standard care, and as such the procedural risks were not considered to be different for the study. The addition of a second ventricular lead was not felt to increase the risk of complications significantly. (126) The risks to the patient for a PPM implantation were quoted as 1%, including vascular damage, bleeding, pneumothorax and cardiac perforation. The Medical Physics department at Christie Hospital, Manchester, also carried out a radiation risk assessment. (Appendix)

2.2.6. Adverse event and Serious Adverse Event reporting

All adverse events were reported and recorded in the site file on case report forms.

Serious adverse events (SAE) were considered to be:

- Death during the study.
- Hospitalization due to a cardiovascular cause.

SAE's were reported to the Research and Development office at UHSM within 24 hours of the research team being notified. Report forms were completed and filed in the research file onsite.

2.2.7 Data Collection and record keeping

All data was collected and retained in accordance with the data protection Act. Paper files were kept in a locked filing cabinet in a room with a key code. All computer data was stored on encrypted memory sticks or password protected trust computers. Patient details were anonymised by giving each patient a unique identification number.

2.3 Pacemaker implantation

2.3.1 Pacemaker implantation

Every study patient was implanted with a ST Jude MRI conditional pacing system. This consisted of an St Jude Accent MR conditional PPM and two ST Jude Tendril MR leads.

PPM implantation techniques are well described in the literature and standard practice protocols were adhered to. (33,204)

All procedures were undertaken in a dedicated catheter lab under strict aseptic conditions, with full monitoring of the patients blood pressure, oxygen saturations and ECG. As part of the standard pre-procedure protocol, each patient received a single dose of intravenous antibiotic. This was 1g Flucloxacillin or 400mg Teicoplanin if penicillin allergic as per hospital policy.

To assess venous anatomy including the presence of subclavian stenosis or a persistent left sided subclavian vein, a venogram was performed in each case. This was performed via a large vein in the ipsilateral antecubital fossa.

Subclavian, axillary and cephalic approaches were all utilized for venous access during the study. This was dependent on venous anatomy observed following the venogram and the increasing experience of the primary implanter, including myself. A standard technique was employed in creating a pre-pectoral pocket for the PPM, using both blunt dissection and or/diathermy.

Once venous access was obtained, two 8 French sheaths were inserted to facilitate delivery of the PPM leads to the RV.

Two 58cm active fixation tendril MR leads were deployed in the RV, one at the RVA and the other on the RVOT septum. The leads were tested and secured in position with non-absorbable sutures, before generator implantation. Following implantation a standard PA chest x-ray was performed to confirm final lead positions and check for pneumothoracies.

2.3.2 Lead positioning

In order to get consistent lead positioning at the RVA and RVOT septum, a series of images were acquired on fluoroscopy.

The RVA position was determined using a postero-anterior (PA) and right anterior-oblique view (RAO). RVOT and septal lead positioning has been discussed in detail by Mond and this study used the protocol outlined in Mond's review of septal pacing.(132)

The pacing lead is placed in the pulmonary artery and a Mond stylet (figure 11) introduced to the lead under fluoroscopy. The lead is slowly pulled back into the RVOT until it is seen to jump onto the septum or point towards the septum. The left anterior oblique (LAO) view is used to determine a septal position, with the lead pointing towards the spine. Figures 11-15 demonstrate the views used to determine lead positioning.

Figure 11. Mond stylet. A secondary curve is posteriorly directed to get onto the RVOT septum.

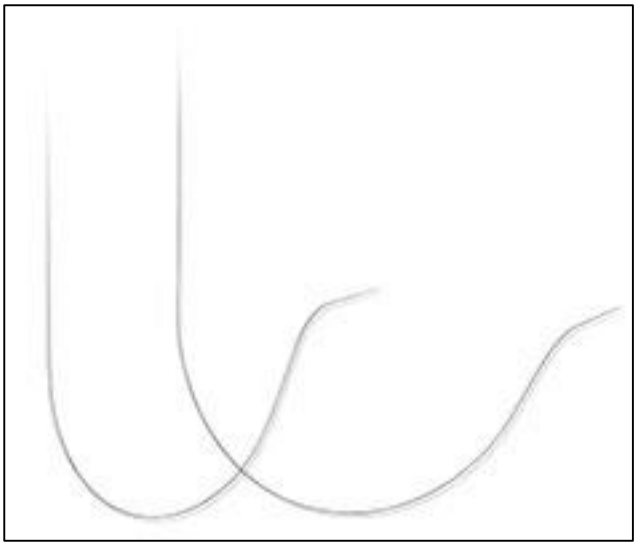

Figure 12. Fluoroscopy PA view- Lower RVOT border marked. Lead is placed within the RVOT in the PA view.

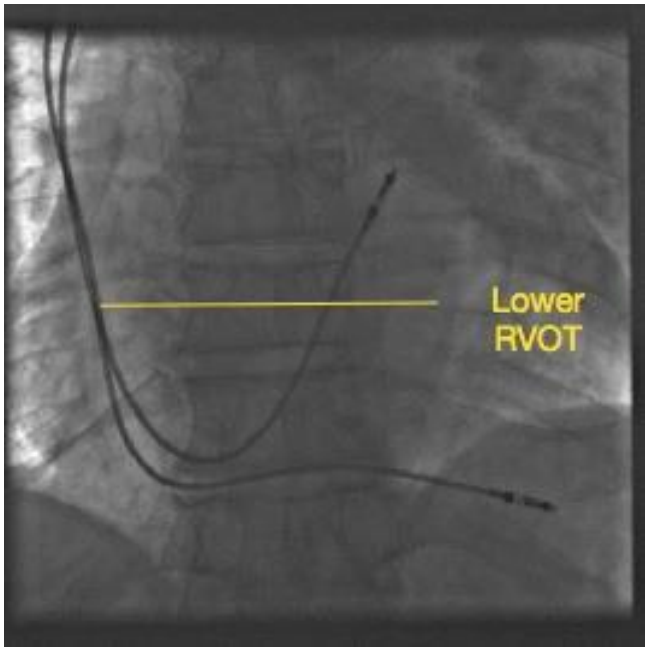

Figure 13. LAO 40-degree view. The Septum and Pulmonary valve are marked. Using the Mond stylet the RVOT lead is pulled down into a suitable septal position

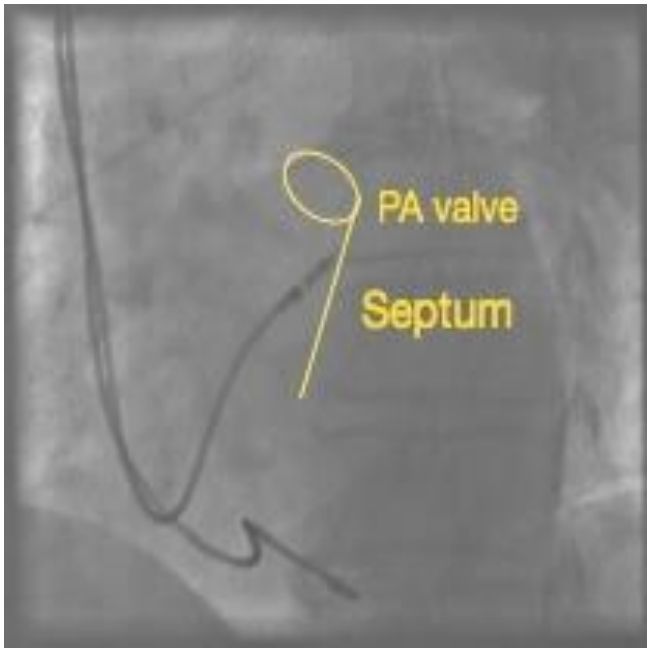

Figure 14. RAO 40 degree view. This is used to confirm apical lead position.

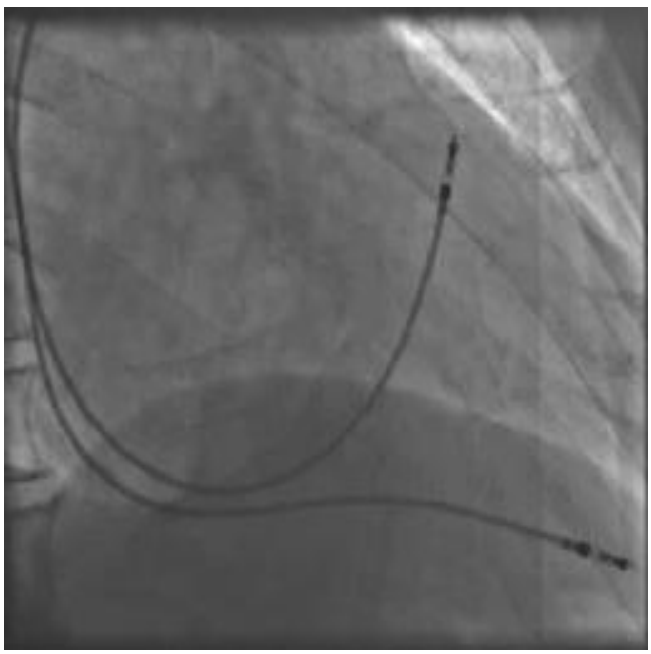

Figure 15. Pacemaker generator at fluoroscopy in PA projection.

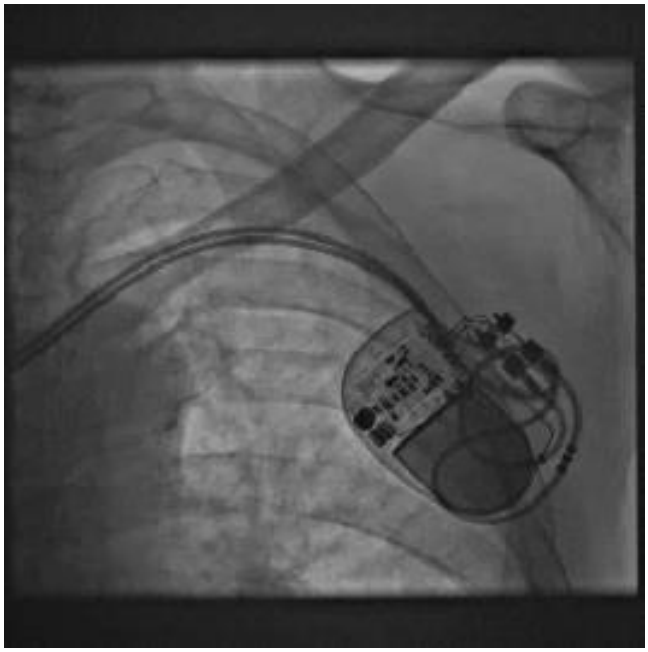

Figure 16. PA CXR illustrating RVOT and Apical lead positions in a study patient.

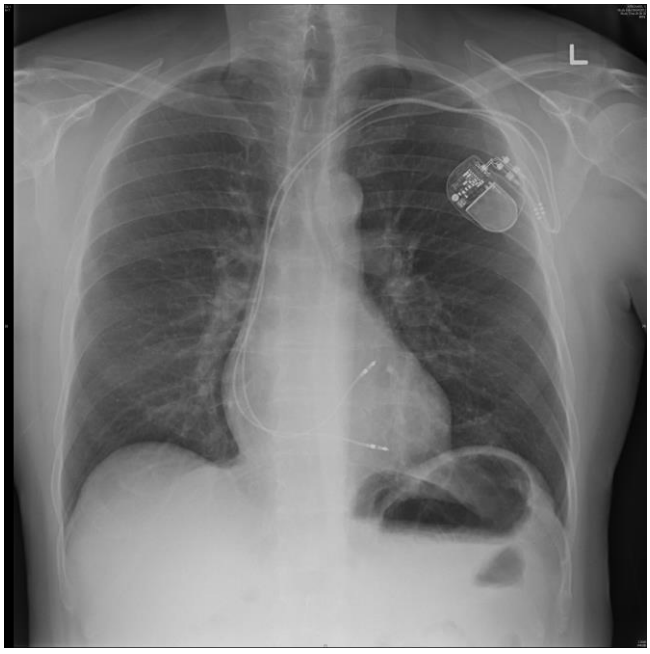

2.4 AV node ablation

The AV node ablation was performed 6 weeks following PPM implantation. This was to ensure an adequate safety margin for any possible lead complications. The AV node ablation was performed in a dedicated electrophysiology lab. A right femoral approach was used in all procedures.

The AV node ablation was performed under conscious sedation in all patients using midazolam and fentanyl individually titrated.

The majority of procedures employed an antegrade approach via the right femoral vein. A retrograde approach via the right femoral artery was used only if repeated attempts at ablation on the right side failed to achieve complete AV block.

2.4.1 Antegrade approach (Right-sided approach)

A single 7F sheath was inserted into the femoral vein using a Seldinger technique.

A coolflow steerable 4mm tip ablation catheter was introduced via the sheath and positioned across the superior tricuspid annulus. The catheter was slowly withdrawn until a clear His signal was visible. The atrial signal should be ideally a similar size to the ventricular signal with a clear and early HIS signal that is stable (Figure 17). This should correspond to the apex of the triangle of Koch where the compact AV node is located (Figure 18). Once located energy was delivered for 30-60 seconds at a temperature of 60-70^{o}C (controlled by thermistor).

Signs of successful ablation were an initial acceleration of the nodal rhythm followed by AV block. If after a period of 20 minutes complete AV block was still present, the procedure was deemed successful.

If unsuccessful a repeat attempt was made both in an inferior or anterior position.

If AV block was still difficult to achieve then a retrograde approach (left sided) approach was used.

2.4.2 Retrograde (Left sided) approach

The position of the His bundle is located via the right sided approach first.

The femoral artery is cannulated with a seldinger technique and a 6F sheath inserted. A 4mm tip ablation catheter is passed across the aortic valve and positioned close to the septum to obtain both a large His signal and the largest possible atrial signal. The energies used for ablation were similar to the right-sided approach.

Figure 17. Intracardiac signals seen on the Map distal catheter when planning an AVN ablation

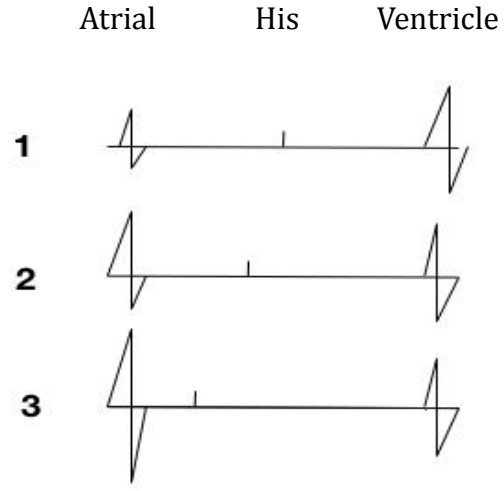

Figure 18. Triangle of Koch with compact AV node at apex.

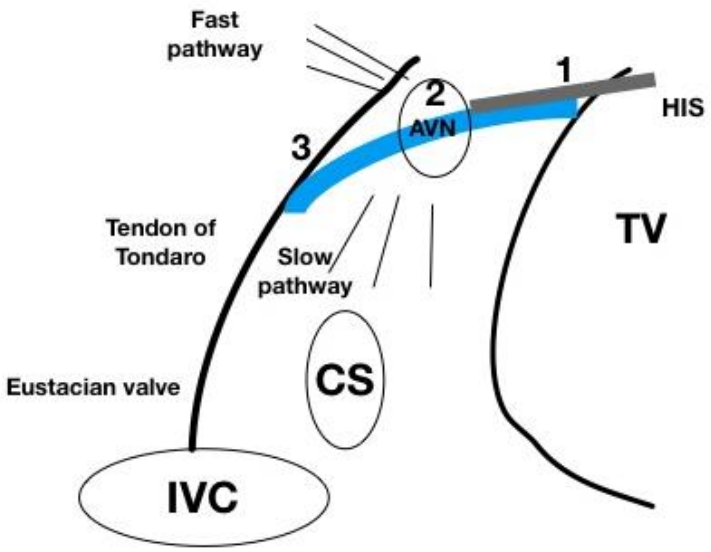

IVC- Inferior vena cava CS- Coronary Sinus AVN- Atrioventricular node

Areas 1, 2 and 3 are shown with the corresponding intracardic electrical trace.

Area 2 is the usual starting point for Av nodal ablation.

2.5. Medical outcomes study Short Form 36 (SF36) health survey

The SF36 is a measure of the extent to which an individual is affected by disease, symptoms and disability in the performance of usual and desired functions and activities. (205) It is a 36-item questionnaire that measures multiple dimensions of health, including physical, social and mental functioning, general health perception, pain and vitality. It has been widely used in cardiovascular patients including those in clinical trials. (4) It is reliable, valid and responsive to small changes. (205,207) For each dimension, scores are summated and transformed onto a scale from 0 to 100, with zero being worst and one hundred being the best. Two component sub-scales, physical (PCS) and mental (MCS), incorporate the 8 health concepts in the survey.

It was given to the patients at baseline, following AV node ablation and every 4.5 months throughout the study. It is both quick and simple to use and patients were able to complete it within 15 minutes. The SF36 used is given in the appendix.

2.6. Cardiac Magnetic resonance

Patients were scanned using a 1.5 Tesla scanner (Avanto, Siemens, Germany) using a 32-channel phased array coil system. Each patient has three CMR scans during the study and scans were performed in each pacing mode on each occasion. The protocol used is outline in appendix.

Multiple measures were used to assess morphology and function of the left and right ventricle. These included:

- LV volume indices and ejection fractions
- LV strain and strain rate
- LV twist, normalised twist and torsion
- RV tricuspid annular systolic plane excursion (TAPSE)
- LV dyssynchrony indices
- Generalised and localised LV myocardial fibrosis
    - T1 mapping, late gadolinium
- Aortic and Pulmonary flow assessment

2.6.1. LV Volumes and function

Analysis was made using CMR tools® off-line. The epicardial border is manually traced at end-diastole in successive short-axis slices. A second contour is placed within the myocardium on the short-axis slices at end-diastole and systole allowing the signal intensity between the two contours (i.e. the signal intensity of myocardium) to be automatically determined. Detailed, semi-automated tracing of the endocardium at end-diastole and end-systole is then performed using a signal intensity 'thresh-holding' tool, such that papillary muscles and trabeculae are included in mass and excluded from volumetric measurements. The mitral and aortic valve positions at end-diastole and systole are manually identified on the 3 long-axis images, allowing the valve planes to be tracked through the cardiac cycle. This is integrated into the SA stack analysis allowing automated identification of the LV base and outflow tract. Finally, end-systole is automatically determined as being the frame with the smallest cavity volume, by calculating cavity volume at each frame.

2.6.2. LV Strain and strain rate

Myocardial strain assessments were used with Tomtec Diogenes® software (based on feature tracking) and InTag® software (based on tagged sequences), applied as a plug in using OsiriX®.

Diogenes® CMR Feature tracking (FT) software (TomTec Imaging Systems, Munich, Germany) is a vector-based analysis tool based on a hierarchical algorithm that operates at multiple levels using a combination of 1-dimensional and 2-dimensional FT techniques. A contour is drawn around the LV endocardial border in one frame and the software automatically propagates the contour and follows its features throughout the remainder of the cardiac cycle. Features tracked in each voxel by the software include brightness gradient at the tissue-cavity interface, dishomogeneities of the tissue and geometrical “roughness” of the tissue edges. The information produced allows the software to derive circumferential, longitudinal, and radial tissue velocity; displacement; and strain/strain rate. It has been validated in phantom models and patients. (157)

InTag® software uses CMR images with a tagging pattern to calculate myocardial strains and mechanics. Motion estimation is based on sine wave modelling, with detection of local spatial phase shift and spatial frequency in images. InTag was used within the open source image processing software OsiriX. Using this, concentric circles of the inner and outer contours of the left ventricle at end-systole were drawn and the software automatically plots the area of the ventricle, producing a colour coded strain map. InTag compares well with the current gold standard of deformation analysis HARP. (208)

2.6.3. LV twist, normalised twist and torsion

Torsion is a fundamental part of LV mechanics and its assessment provides important information on myocardial performance. (209)

In the normal heart, the base rotates clockwise though its axis whilst the apex rotates anti-clockwise during systole. (210) This is due to the oppositely orientated oblique fibres within the myocardial wall. (211) This torsion builds up a lot off elastic energy, which when the ventricle relaxes in early diastole is released and facilitates rapid diastolic filling at the start of diastole. (212) The analogy of wringing out a wet cloth is often made.

Torsion is very sensitive to changes in myocardial contraction and LV remodelling processes, which is reflected by it change in a number of cardiovascular pathologies. (213,214) There appears to be a direct correlation between torsion and LV EF. (215)

Different definitions of LV torsion exist within the literature and at times twist, torsion and shear are used incorrectly.

Twist is defined as the difference in rotation between the base and apex. (213)

Normalised twist or twist per unit length, is the twist angle divided by the distance between the base and apex. (216) This is a more robust measure than twist but is not comparable between different size hearts.

Left ventricular torsion is the shear deformation of the myocardium and is related to the sheer torsional angle created by circumferential and longitudinal contraction. A 2D approximation of torsion is given by the formula below: (217)

$$T = \frac{(\Theta apex - \Theta base) \times (rapex + rbase)}{2D}$$

r= radius

D= distance between base and apex

Θ= angle

Figure 19. LV torsion. Circumferential shear angle.

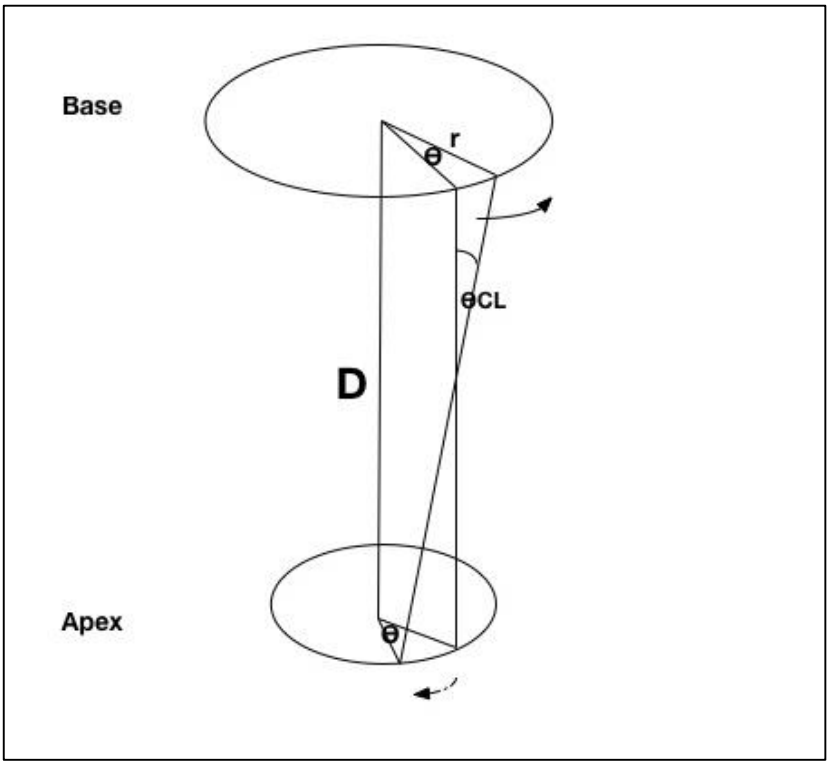

In order to calculate torsion a number of methods were utilized. Two excel in-house developed programs were used to generate data from different programs. One used data generated from tagged images using an OsiriX plugin (Intag®) and the other SSFP cine images using FT software (Tomtec) analysis tools. Both SSFP and tagged images of the LV short axis stack were used to generate data regarding twist angle, radius and distance between base and apex. More details regarding the program are given in the sub-study chapter.

2.7.4. RV TAPSE

The RV free wall on a 4-chamber cine was used to assess TASPE in a similar fashion to the method used in echocardiography and has been precisely validated by our group. (218)

2.7.5. Dyssynchrony indices

A number of measures were used to determine left ventricular dyssynchrony.

These were:

- CMR-adapted Yu index
- Opposing wall delay in long axis views
- Time to peak radial motion
- Time to peak longitudinal strain

The Yu index was originally used in echocardiography. (140) It is the standard deviation of 12 time to peak velocities. The 12 points are of the opposing basal and mid segments of the three long axis views (4Ch/3Ch/2Ch).

Septal to lateral wall delay in peak systolic velocity is a marker of dyssynchrony used originally in echocardiography. (219) It has been shown to predict LV reverse remodelling in cardiac resynchronisation therapy. (219)

From the SSFP short axis stack, basal, mid-ventricular, and apical slices were analysed. Epicardial and endocardial contours, excluding trabeculations and papillary muscles were drawn for all phases, using Diogenes® CMR FT software. A standard AHA 16-segment model was used to divide the basal and mid-ventricular slice into 6 segments and the apex into 4 segments. For each segment, a radial wall thickness curve was automatically plotted and the time to peak strain was determined. The standard deviation of 16 segments was calculated as a marker of global LV dyssynchrony.

In the 4ch view, epicardial and endocardial contours were drawn for all phases using the CMR FT software. The time to peak strain was calculated in all basal, mid and apical segments for both the septal and lateral walls.

2.7.6. LV myocardial fibrosis

A wide number of cardiovascular disease processes result in myocardial fibrosis. (220) In animal and human studies it is associated with worsening left ventricular systolic function and abnormal ventricular remodelling. (221,222)

Two methods were used to estimate the presence and extent of fibrosis in the study cohort.

Both methods used the unique property of the contrast agent gadolinium, which distributes itself in the increased extracellular matrix associated with fibrotic tissue. (220) Gadolinium shortens the T1 relaxation time of adjacent myocardium and allows tissue characterization by virtue of altering signal intensity in a T1 weighted image. The gadolinium contrast agent used was dotarem at a dose of 0.2mmol/kg (double dose). Dotarem has an excellent safety profile and is regarded as safe down to eGFRs of 30mls/min/1.73m^2.

Dotarem behaves like magnevist (perhaps the most widely used agent worldwide) with a similar relaxivity, but is considered safer with no reported cases of nephrogenic systemic sclerosis.

The first method used a conventional inversion-recovery gradient echo sequence, with a TI scout prior to Late Gadolinium enhancement (LGE) imaging at 15 minutes post contrast was used. LGE was performed on a LV short axis stack.

Gadolinium enhancement was assessed visually as being present or absent and its distribution recorded. A semi-quantitative method was employed using

Standard LGE analysis as it is widely used in clinical practice since it provides excellent qualitative assessment of myocardial fibrosis, however it does have limitations. Signal intensity is measured on an arbitrary scale and thus directs signal quantification between studies is difficult. In addition LGE requires the image contrast to be generated by having both normal and fibrotic tissue and correctly setting the inversion time to correct for this. (223) Different methods have been described to define what late enhancement is and there is no clear consensus on parameters such as intensity settings for the detection of myocardial fibrosis. (220) LGE is also

difficult in the setting of diffuse fibrosis where a difference between normal and fibrotic tissue is not seen.

Some of LGEs shortcomings can be addressed by using T1 mapping and this method was also used for determining the presence of diffuse myocardial fibrosis. T1 mapping allows the direct measurement of the T1 relaxation time of the underlying tissue. This allows the signal intensity to be quantified on a standardized scale. A T1 map of the myocardial tissue is a reconstructed image, using multiple inversion times and sampling the intensity of signal for each individual voxel. We used the most widely described T1 mapping sequence, the Modified Look-Locker Inversion-recovery (MOLLI) sequence described by Messroghli et al. (224) The Siemens wip version 448 was used with 3 inversions pulses and a 3, 3, 5 sequence of acquisitions.

T1 mapping was performed using the MOLLI sequence pre-contrast, 10 and 20 minutes post contrast in the 4 chamber and mid short-axis views. Analysis was made using Siemens diagnostic software.

2.7.7. Aortic and Pulmonary flow

Blood flow was measured using phase contrast velocity mapping. This uses the principle that the flowing nuclei in blood will acquire a phase shift when travelling along a gradient magnetic field. The phase shift in a linear gradient is proportional to the velocity of the moving spin i.e. velocity of blood. Phase shift of stationary tissue i.e. vessel wall, connective tissue is compensated by using a bipolar gradient. (225) By repeating measurements with an inverted bipolar gradient and subtracting this from the first data set, the phase shift remaining is used to calculate voxel wise velocities.

Velocity encoding (V_{enc}) is given in centimetres per second and determines the maximum and minimum velocities that can be encoded by pulse contrast. Velocities greater then these will produce aliasing. The initial Venc was set at 150 and if aliasing occurred it was increased to a non-aliasing velocity in 50 cm/sec increments. The data acquisition gives signal magnitude and phase of each voxel. The signal intensities are processed to produce a magnitude image, which corresponds to the anatomical image. The phase information is used to produce a velocity image. (Figure 20)

The sequences are performed during free breathing and retrospective gating.

Flow measurements were repeated both 3 times across the aorta and pulmonary artery. The imaging plane was through plane for both the aorta (AO) and pulmonary artery (PA). The planes were for the aorta at the level of the pulmonary bifurcation and for the PA half way between the pulmonary vein (PV) and the pulmonary bifurcation.

The images were optimized to give the most circular AO and PA, since ovoid measurements are less accurate and indicate incorrect cuts. For each patient, care was taken to reproduce the same imaging planes between the MR scans.

Analysis of flow velocities was made using Argus tools (Siemens). The vessel was manually traced to define the region of interest and this contour was propagated throughout the entire data series. (Figure 21) These were then corrected by using a combination of semi-automatic software algorithms and operator selection. Flow quantification in millilitres and mean and peak flow velocities were generated.

Results of phase contrast methods do correspond well to Doppler derived from echocardiography and invasive measurements based on thermodilution. (226,227)

Figure 20. Magnitude (left) and phase encoded (right) maps of aorta.

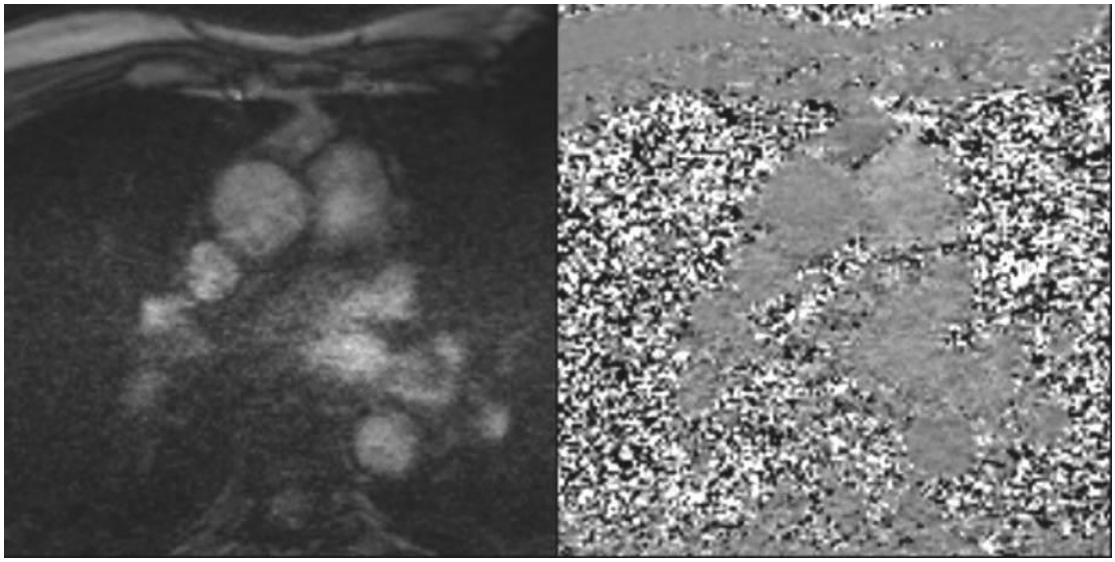

Figure 21. Contour drawn around aorta for analysis.

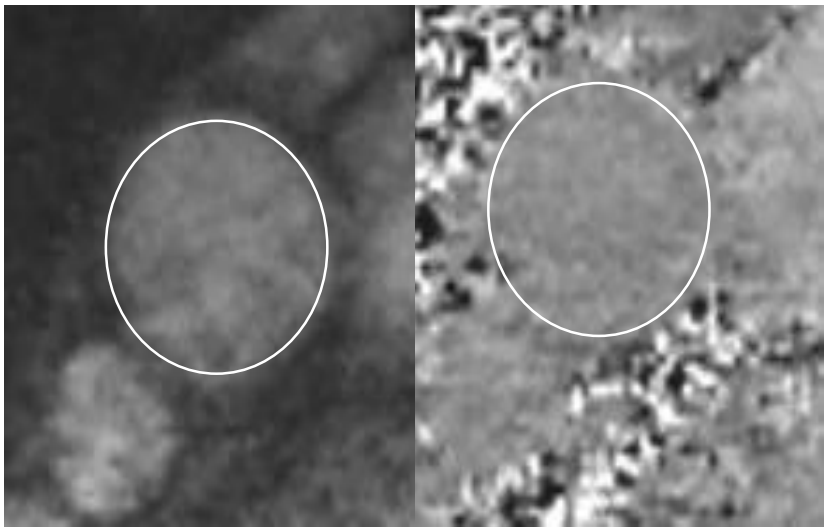

2.8. Cardiopulmonary exercise testing (CPEX)

All the tests were carried out using the same cardiopulmonary exercise system in the Respiratory department at Wythenshawe Hospital, Manchester, UK. Initially the exercise tests were going to use a bicycle ergometer CPEX system with respiratory gas exchange, as it is recognized that it is easier to manipulate the workload. (228) Due to issues relating to the rate response of the IPG, preliminary work was carried out comparing a bicycle and treadmill CPEX. This is described in the next chapter, but following this the study used a treadmill-based protocol.

All patients were familiarised with the technique required to carry out the CPEX test before each test.

A valid test is defined as increasing the ventilator exchange ratio (VCO_2/VO_2) by at least 0.15 or to an absolute value of >1 during exercise.

All tests were to be carried out in the morning with the patients fasted to minimise any diurnal variation. Every test will be performed using the same equipment to ensure reproducibility.

A breath-by-breath technique was used to analyse volume and gas concentrations. Carbon dioxide was measured with an infrared analyser and Oxygen was measured using a paramagnetic analyser. Oxygen and Carbon dioxide analysers were calibrated using a two-point calibration with gas supplied by the same manufacturer (British Oxygen Company- BOC gases)

2.8.1. Bicycle CPEX

The exercise protocol involved the patient's undergoing a three-minute warm up phase at 20 Watts followed by an incremental increase in workload of 10 watts per minute using a ramp protocol. The ECG was monitored throughout the test. The CPEX was performed until the patient had limiting shortness of breath or fatigue.

2.8.2. Treadmill CPEX

The exercise protocol used was the modified Bruce protocol. This has 2 warm-up stages, each lasting 3 minutes. The first is 1.7mph at 0% grade and the second is at 1.7mph at 5% grade. Stage 3 is the same as stage 1 of the Bruce at 1.7mph at 10% grade. The modified Bruce protocol was chosen since the cohort of patients in the study included elderly and all had cardiovascular disease. The 7 stages are shown in the figure below.

Figure 22. Modified Bruce protocol for CPEX testing.

Stage	Speed (mph)	Grade (%)	Duration (min)
0	1.7	0	3
0.5	1.7	5	3
1	1.7	10	3
2	2.5	12	3
3	3.4	14	3
4	4.2	16	3
5	5.0	18	3
6	5.5	20	3
7	6.0	22	3

2.8.3. Indications for termination of exercise testing

The American College of Cardiology (ACC)/American Heart Association (AHA) guidelines specify indications for termination of exercise testing.

Absolute indications for termination of testing included the following:

- Subject's desire to stop
- Drop in systolic blood pressure (SBP) of more than 10 mm Hg from baseline, despite an increase in workload, when accompanied by other evidence of ischemia
- Moderate-to-severe angina
- Increasing nervous system symptoms (e.g., ataxia, dizziness, near-syncope)
- Signs of poor perfusion (cyanosis or pallor)
- Technical difficulties in monitoring ECG tracings or SBP
- Sustained ventricular tachycardia
- ST elevation (> 1 mm) in leads without diagnostic Q waves (other than V_1 or aVR)

2.9. Six minute walk testing

The Six minute walk test (6MWT) is an objective measurement of functional capacity in individuals, which is easy to perform and better tolerated than formal exercise testing such as cardiopulmonary exercise testing.(229)

It is a measure of submaximal exercise tolerance, rather than maximal exercise tolerance but it probably better reflects the functional level for activities of daily living because of this.(229)

It has been most extensively used in measuring the response to medical intervention in cardio-respiratory patients and can act as a predictor of morbidity and mortality. (229)

A 20 m corridor with a flat hard surface marked out with two cones was used to perform the test. Patients were instructed to have appropriate foot wear and wear comfortable clothing for the test. No vigorous activity 2 hours prior to the test was to be performed.

The pre-test period consisted of the patient sitting on a chair for 10 minutes, whilst pulse and Blood pressure were checked and instructions regarding the test were given. Patients were advised how to report their rating of perceived exertion using the Borg scale. (Appendix) A baseline dyspnoea was recorded prior to testing.

The following instructions were given:

" The aim of the test is to see how far you can walk in 6 minutes to give an indication of your base fitness level. You will be required to walk along this corridor between the two cones. You should turn briskly around the cone and continue back along the corridor, repeating the same action at the other end without pausing. 6 minutes is a long time to walk, so you will be exerting yourself and may become short of breath. You can slow down, stop and even rest if necessary but as soon as you can you should resume walking. The timer continues even if you stop. Let me demonstrate a lap. If you are ready please begin."

A lap counter was used to record each lap and a stopwatch was used for timing. Tone encouragement was given as suggested in American Thoracic Society (ATS) guidelines. (229) The end-point was reached when the timer struck zero, upon which the patient was able to rest on a chair. The post-walk Borg scale was determined and pulse and blood pressure was recorded. The number of laps and total distance were recorded on a worksheet (Appendix) and then the data was inputted into a database.

Chapter 3

Sub-Studies

Chapter 3. Sub-Studies

Study 1

Aortic and Pulmonary flow measurements validation

Study 2

Mode of exercise testing in pacing cohort

Study 3

Any training effect of exercise testing

Study 4

Phantom studies

Study 5

Strain and torsion validation in normal volunteers

Study 1. Aortic and pulmonary flow measurements validation

3.1 Aortic and pulmonary flow measurements validation

3.1.2 Aim

To validate the method of velocity phase encoding used and the analysis software, which would be used in the main trial.

3.1.3 Introduction

It was important to determine the reproducibility of the measuring aortic and pulmonary flow and the inter- and intra-observer variability. This was important for the trial analysis as at the time of designing the trial there was no published literature on the potential effects of IPG related susceptibility artefacts on phase coded velocity mapping measures. For this reason we decided to assess aortic and pulmonic flows in those without an IPG first.

3.1.4 Method

20 patients which had flows performed were analysed by the reporting physician and myself.

The images generated were analysed using Argus software, Siemens. A contour was drawn around the phase contrast image of the aorta or pulmonary artery and propagated in slice throughout all images. Careful attention was paid to keep the contour within the vessel wall and this could be manually manipulated for each slice. The flows were analysed by myself on two separate occasions.

3.1.5 Results

The mean age of the patients was 51 ± 7 years. The mean aortic flow measured for rater A was 71.4 ± 16mls and for rater B it was 71.7 ± 16.3mls and 71.1 ± 16mls. The mean pulmonary flow measured was 74.8 ± 17.8mls for rater 1 and for rater 2, 76.5 ± 18mls and 77.4 ± 18mls.

To assess both inter-observer and intra-observer variability, Bland Altman plots were used. (Figures 23-26)

The 95% confidence interval of plus and minus 5 mls is clinically acceptable and the majority of the values fell between these when comparing inter and intra-rater measurements.

The intraclass correlation coefficient (ICC) between raters was 0.989 for aortic flows and 0.92 for pulmonary flows. The ICC for intra-observer measurements was 0.989 for aortic flow measurements and 0.989 for pulmonary measurements.

Figure 23. Bland Altman plot comparing rater A and B for aortic flow measurements.

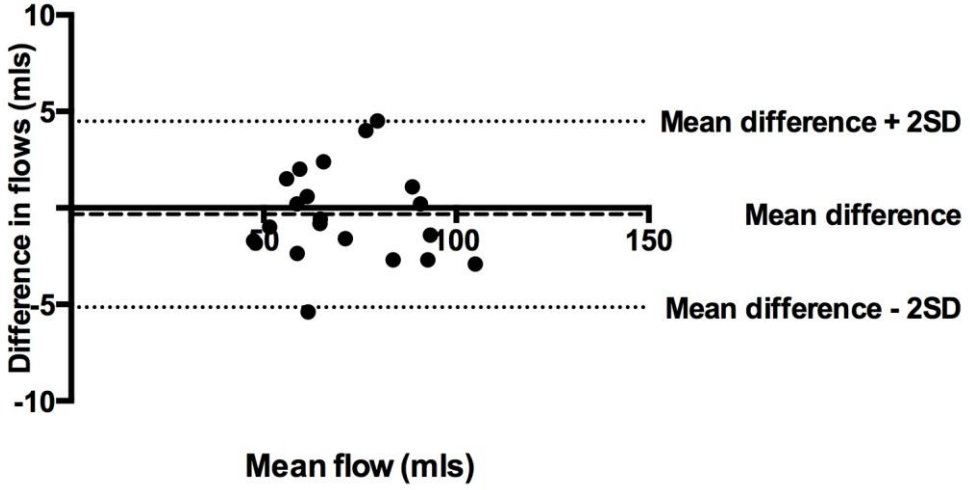

Figure 24. Bland Altman plot comparing rater A and B for pulmonary flow measurements.

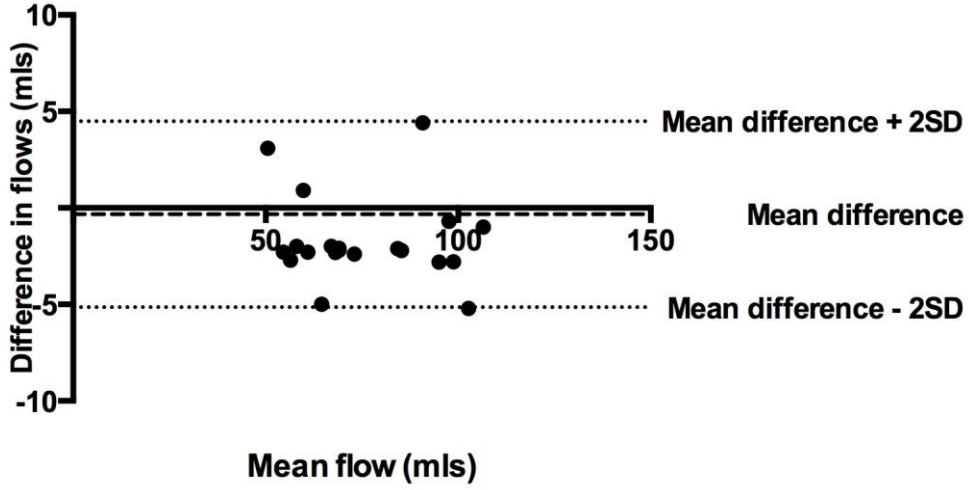

Figure 25. Bland Altman plot comparing rater B on two occasions for aortic flow measurements.

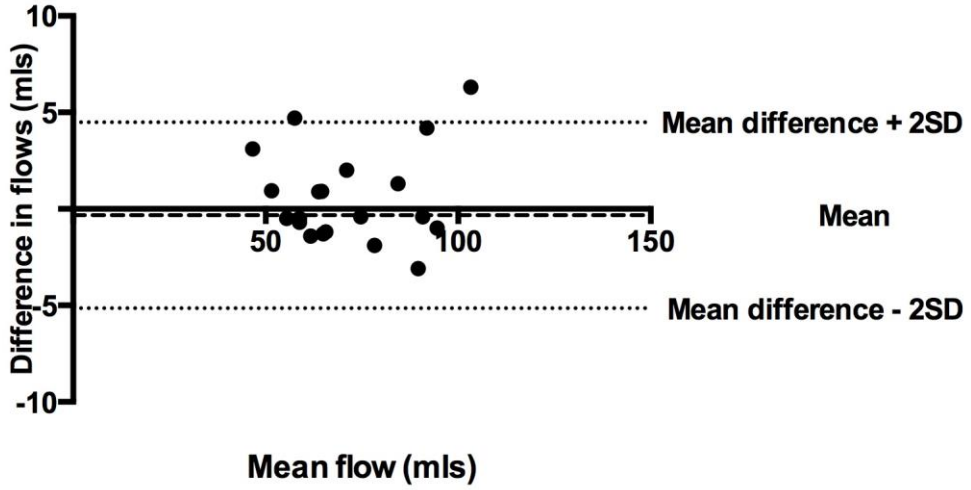

Figure 26. Bland Altman plot comparing rater B on two occasions for pulmonary flow measurements.

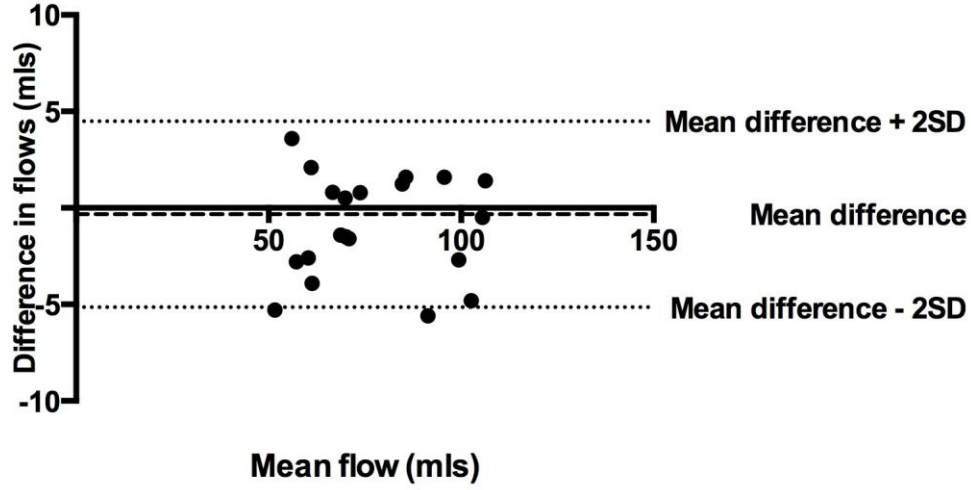

3.1.6 Discussion

This small validation study confirmed that the methodology employed for measuring flows had excellent reproducibility, with both good inter- and intra-observer correlations. The 95% confidence interval of only 5 mls is relatively small and is clinically acceptable difference.

A more detailed discussion regarding CMR derived flow measurements is covered in the phantom study.

Study 2. Which is the most suitable method for CPEX testing in a pacing dependent patient?

3.2 Which is the most suitable method for CPEX testing in a pacing dependent patient?

3.2.1 Aim

To determine which form of exercise testing was most suitable for patients who were pacing dependent and rely on the rate response function of the PPM.

3.2.2 Introduction

It was observed during the initial CPEX test performed using the bicycle ergometer that the patient's heart rate increased much less than predicted. This cohort of patients, following the AVN ablation were dependent on the PPM for a chronotropic response. A nominal setting (factory setting) for rate response had been set for each patient following the PPM implantation and these were maintained during initial testing.

The St Jude Accent PPM uses an accelerometer to detect movement of the patient and this leads to an increase in the paced heart rate. Whilst cycling, the thorax usually remains fixed and certainly on a static bike it will move very little. It was proposed that a bicycle test would not produce a significant heart rate response,

compared to that of a treadmill and as a result may not be the most effective way to measure VO_2 max in this cohort.

3.2.3 Hypothesis

The heart rate will rise significantly more during a treadmill CPEX compared to a bicycle CPEX. This will lead to a higher VO_2 max being measured in the treadmill group.

3.2.4 Method

Five patients enrolled into the MAPS trial were recruited to take part in this sub-study. Each patient undertook a bicycle and treadmill CPEX test on the same day. One test was in the morning and the second was in the afternoon, with a minimum of 3 hours rest period between. The order in which the tests were performed, were randomized to reduce the influence of a training bias and diurnal variation. The clinical study protocol was performed as described in the methods chapter.

3.2.5 Results

The average age of the five patients was 65±7 years. Of the five patients, 3 were male and 2 female.

The mean VO_2 max on the bike was 13.8±3.2ml/min/kg and on the treadmill 15.5±4.2ml/min/kg, p=0.035. The average increase in VO_2 max on the treadmill was

11%. The mean increase in heart rate on the bike was 16±15% on the bike and 35±16% on the treadmill, p=0.013.

Table 11. Comparison of VO2 max and heart rate increase between treadmill and bicycle CPEX testing.

Mean VO_2 max ml/min/kg		p	Mean Increase in heat rate from baseline (%)		p
Bicycle	Treadmill		Bicycle	Treadmill	
13.8 ± 3.2	15.5 ± 4.2	0.03	16.4 ± 15.4	35.3 ± 16	0.01

3.2.6 Discussion

A number of observations can be made from these results. Firstly the mean VO_2 max values for both studies are all low suggesting all patients had poor exercise tolerance. The mean EF was 54±6% on echo, which is at the lower end of normal, bordering on mild LV systolic dysfunction. The LV EF alone cannot really explain the below normal results. A resting LV EF has been shown to not correlate with max VO2 max in patients with underlying IHD. (230) More important was peak LV EF and the LV exercise reserve (change in EF between rest and exercise). (230) The cause for exercise tolerance in this cohort of patients is likely to be multifactorial. These patients had co-existing medical conditions including hypertension, airways disease and ischaemic heart disease, which certainly would reduce exercise tolerance. Perhaps the biggest contributing factor was the fact that these patients had become very deconditioned as a result of the poorly controlled AF. This cohort of patients requiring the pace and ablate strategy are a sicker cohort of AF patients. In the RELAX trial, those patients with AF compared to those in sinus rhythm had a lower peak VO2 in both absolute and relative to age, sex, body-size and exercise mode adjusted predicted values.(231) Both an irregular rhythm (232) and loss of atrial kick to LV filling (233) are recognised to reduce cardiac output in AF patients. The RELAX study demonstrated a lower stroke volume during peak exercise and a steeper Ve/VCO2 slope suggesting pulmonary perfusion may also be impaired in the AF cohort. It has also been shown that in healthy subjects, diastolic parameters including transmitral filling velocities and ratio of early to late filling velocities strongly correlate with VO_2 max. (234) This cohort of patients may have impaired diastolic filling and dysfunction contributing to the lower peak VO_2 max observed. This was demonstrated in the RELAX trial. (231) It is important to note that diastolic function was not directly measured in this study, so this can only be considered a speculative explanation.

The second observation and the reason for this small sub-study was that the CPEX using a treadmill consistently produced higher VO_2 max results when compared to using the bike. This did not reach statistical significance but may relate to the small sample size.

The increase in heart rate achieved on the treadmill was much greater and statistically significant compared to the bike. Numerous studies have demonstrated the finding of an increased VO_2 max using the treadmill, with a mean difference of 7% being reported. (228)

An explanation can be offered using the basic principles of exercise testing. Peak exercise tolerance is defined as “the maximum ability of the cardiovascular system to deliver oxygen to exercising muscles and of the exercising muscle to extract oxygen from the blood”. (235) Therefore exercise is determined by three components, pulmonary gas exchange, cardiovascular performance and skeletal muscle metabolism. Taking this one step further the Fick equation states that oxygen uptake (VO_2) equals cardiac output times the arterial minus mixed venous oxygen content:

$$VO_2 = (\text{Stroke volume} \times \text{Heart rate}) \times (\text{Arterial } O_2 - \text{mixed venous oxygen content})$$

At maximal exercise the same equation states:

$$VO_2max = (SV \times HR) \times (CAO_2max - CVO_2max)$$

The maximum heart rate was lower during bicycle testing in this study and therefore if everything else was equal it would equate to a lower VO_2max. Indeed in other studies the maximal heart rates were found to be consistently lower in maximal bicycle tests compared to treadmill tests, suggesting muscular fatigue occurs before the central CVS system is engaged. (228,236,237) A treadmill also offers an

increased workload due to more muscle groups working against gravity. In health subjects VO_2 max has been shown to correlate with hear rate max (r=0.48). (234)

It is possible that the bigger difference in VO_2 max in this study compared to others is due to the larger difference in max heart rate achieved between the two modalities. In this study heart rate is completely controlled by the PPMs rate response algorithm. The rate response is determined by an accelerometer within the device. This consists of a mounted piezoelectric crystal that responds to movement. The more movement detected (i.e. during exercise) the more the crystal will be stimulated and the greater the paced heart rate becomes. All the patients had a limit of 150bpm, but this was never achieved. The design of the accelerometer is such that activities with more thoracic movement will result in more movement of the crystal and a greater programmed rate response. When on a static bicycle ergometer, the thorax remains relatively still and movement is minimal until higher workloads. Walking on a treadmill creates much more thoracic movement, enhanced by shoulder and arm movement. Therefore this study suggests that in a pacing dependent patient, with the chronotropic response to exercise being governed by the PPM, than a treadmill test will result in a greater max heart rate, compared to a bicycle test. For this reason, the original study design of using a bicycle was altered to using the treadmill instead.

3.2.7 Conclusion

The treadmill CPEX resulted in a higher VO2 max than the bicycle CPEX, which in part could be explained by a larger increase in heart rate observed.

For a pacing dependent patient, the heart rate response is likely to be greater on a treadmill.

Study 3. Any training effect of CPEX testing

3.3. Any training effect of CPEX testing

3.3.1 Introduction

To assess if there performing a CPEX itself improved the following CPEX results due to a training effect rather than a real improvement in patient fitness a small sub-study was conducted with five patients was performed.

3.3.2 Method

On 5 patients CPEX tests were carried out within one week of each other. Both CPEX were done using the treadmill, using the modified Bruce protocol.

3.3.3 Results

The students paired T-test was used to compare the parameters obtained to assess for differences and a Bland Altman analysis was performed on the VO_2 max values obtained.

The mean age of the control population was 67.6± 5.3 years. Two patients were male. From the synopsis in table 12 the two CPEX tests carried at baseline confirm the results are reproducible. Selected cardiopulmonary and haemodynamic variables

demonstrate that there were no significant differences on the basis of a “training effect” or increased familiarity with the exercise equipment. The VO_2 max demonstrated only a 4.9% difference between tests. The results of selected parameters are summarized in table 12.

Table 12. Exercise and haemodynamic parameters on training effect study. N=5.

N=5	CPEX Test 1	CPEX Test 2	% Change	P value
Resting HR (min -1)	62.4±4.8	61.4±3.1	-1.9%	0.67
Resting SBP (mmHg)	130.8±5.8	130.8±6.5	0%	1
Peak SBP	142.8±5.8	140.4±3.8	-1.7%	0.21
Peak HR (min -1)	97±12.2	88.6±13	-8.7%	0.6
RQ	1.13±0.12	1.12±0.14	-0.7%	0.55
VO_2 max (mls/kg/min)	13.36±4.3	14.04±3.6	4.9%	0.4

Using the Bland Altman test with VO_2 max, one can see that all the mean differences in VO_2 max were within 2 standard deviations of the mean difference. (Figure 27)

Figure 27. Bland Altman plot for VO2 max between the two CPEX tests performed.

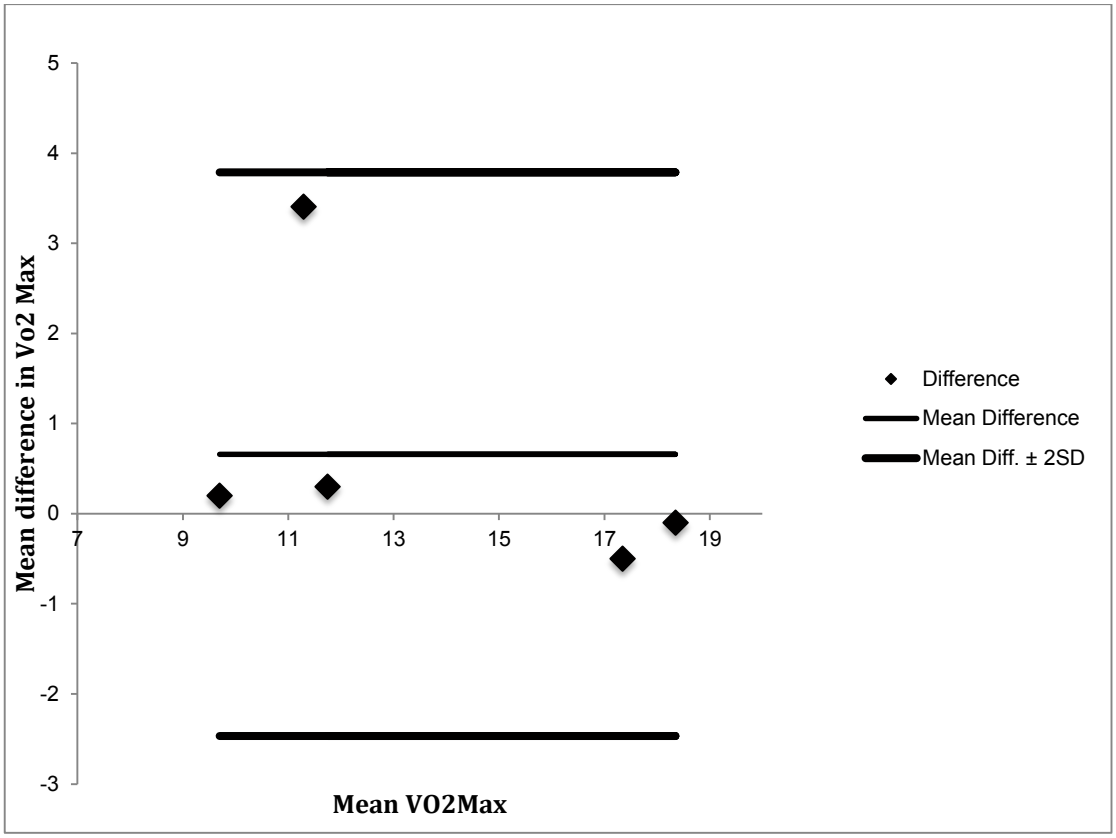

3.3.4 Discussion

There was no apparent training effect demonstrated for the CPEX within the timescale of 1 week. This suggests that any differences in CPEX results between the time points of the study reflect changes in the exercise capacity of the participant. However, a major limitation was that the sample size was small and so the non significant P values are potentially due to this, rather than to any true difference. The sample was only 5 because of economic and logistical constraints.

Study 4. Phantom studies

3.4 Phantom studies

A series of studies were performed using a gel phantom model. Before such studies could take place I had to conduct a methodological study into constructing a gel phantom.

3.4a The Gel Phantom

3.4a.1 Introduction

Tissue equivalent materials are very useful to calibrate and check imaging equipment. They also form a vital part in experimental work in MRI, especially in sequence development. A number of materials can be used including, Vaseline, glycerol, animal hide gels, agarose gels and aqueous mixtures of copper, manganese or nickel ions. (238) None of these materials alone can match the unique T1 or T2 relaxation properties/times found in human tissue. Every tissue within the body has a unique T1 and T2 time, allowing contrast to be generated in the images. Human myocardium has a T1 value ranging from 800 to 1200ms with normal myocardium believed to have T1 varying from 880 to 960ms with most MOLLI variants, and T2 values measured with a range of 48-58ms. (239)

Studies have suggested that a mixture of a paramagnetic ion salt and agar can be used to generate a wide range of T1 and T2 values by manipulating the concentration of the ion and agar. Mitchell et al have shown that agarose gel with the addition of copper sulphate can be used to produce a phantom with tissue equivalent T1 and T2 values. (238)

3.4a.2 Aim

To validate the method described by Mitchell et al in our lab to produce a gel phantom with similar relaxation properties to normal myocardium.

3.4a.3 Methods

Agarose (Sigma chemical corp) at a concentration of 4% weight per volume (w/v) and Copper Sulphate pentahydrate (Cu_2SO_4) at a concentration of 0.1% w/v were made for stock for the experiments. Both dry agarose and copper sulphate were weighed out in plastic receptacles and then separately dissolved in distilled, deionized water. Both solutions were placed on magnetic stirrers to facilitate this process. At room temperature the agarose (4% w/v) takes 5-10 minutes to dissolve. On a hotplate with magnetic stirring, the agarose solution was heated until it turned from cloudy to clear. This signifies the transition from the solid state to molecular solution. This occurs at the solutions boiling point and took approximately 20 minutes. After the transition, the solution was heated for a further 10 minutes to ensure the process was complete. The hot agarose was placed in separate vials containing varying quantities of Cu_2SO_4 solution and distilled/deionized water to produce varying agar concentrations. The results from Mitchell et al were used to

make a prediction to what T1 and T2 values would be produced by altering the concentration of agarose and Cu_2SO4. Six test phantoms were made initially with differing agarose concentrations but the same Cu_2SO_4 concentration. (See table 13)

According to the paper T1 mostly is determined by the copper concentration and T2 depends mostly on the agar concentration.

The vials were vigorously mixed and left to cool at room temperature within the lab.

Once the gel mixture was set, the phantoms were placed in the room containing the MRI scanner to equilibrate with this room temperature.

The phantoms were scanned on a 1.5T MRI scanner (Siemens Avanto) to obtain their true T1 and T2 values.

The T1 was calculated using a spin echo, inversion recovery technique (TE 8.1ms, TR 10000ms) with inversion times of 50, 70, 110, 160, 230, 320, 500, 1500, 3000 and 5000ms. This data was used to generate a T1 recovery curve. The T1 time was extrapolated from this curve as the point when the T1 had recovered 66.66% of its value.

The T2 was calculated using spin echo with a TR of 5000ms and varying TE times of 10, 20, 30, 50, 100, 150 and 200ms. A T2 relaxation curve can be generated and the T2 time is the time to decay to 33.3% of its original value.

Table 13. The constituent parts of the initial six phantoms.

Phantom	T2 aim (ms)	T1 aim (ms)	Phantom volume	Agarose (w/v)	Copper (w/v)	Volume agarose (ml)	Volume copper (ml)	Volume water (mls)
1	40	950	50	2.2	0.0149	27.5	7.5	15.1
2	50	950	50	2	0.0149	25	7.5	17.6
3	60	950	50	1.9	0.0149	23.8	7.5	18.8
4	70	950	50	1.8	0.0149	22.5	7.5	20.1
5	80	950	50	1.7	0.0149	21.3	7.5	21.3
6	90	950	50	1.6	0.0149	20	7.5	22.6

In the first set of phantoms made it was apparent that the gel was not uniform and that there were several discrete layers present where the constituents had separated out. Therefore it was not surprising that the T1 and T2 values were not as predicted (Table 14).

Table 14. Initial six phantoms measured T1 and T2 values compared to predicted value.

Phantom	T2 aim (ms)	T1 aim (ms)	Measured T2 (ms)	Measured T1 (ms)
1	40	950	54.5	777
2	50	950	142	1215
3	60	950	60.22	1001
4	70	950	103	1164
5	80	950	136	1051
6	90	950	101	1176

It was noted that when adding the hot agarose solution to the vials containing copper sulphate/water, the agarose started to solidify on contact due to the temperature difference between the two mediums. To rectify this, the vials containing the copper sulphate/water were preheated in a water bath set to 80^0C. The formation of layers during the setting process was likely the result of gravity during the cooling. To reduce this effect subsequent vials were mixed vigorously on a tube mixer and placed in a fridge to set quicker.

The use of a heated plate was found to be very time consuming in making up the agarose mixture and due to the small size of our plate only a small quantity of agarose could be made. With the desire to make larger phantoms for other studies, it

was decided to experiment with the use of a microwave to heat the solution. The disadvantage of this approach was that the solution had to be stirred manually intermittently throughout the process. It proved very successful at heating large quantities of the agarose solution and was much faster than using the heating plate. The six phantoms were repeated with much better gel consistency with T1 and T2 measurements (see results). Following on from these results a further phantoms were created with varying proportions on constituents (Table 15) to determine the ideal mixture that was similar to myocardium. These were scanned together in the MR scanner as shown in figure 28.

Table 15. The constituent parts of the 19 phantoms.

Phantom	T2 aim (ms)	T1 aim (ms)	Phantom volume	Agarose (w/v)	Copper (w/v)	Volume agarose (ml)	Volume copper (ml)	Volume water (mls)
1	40	950	50	2.2	0.0149	27.5	7.5	15.1
2	50	950	50	2	0.0149	25	7.5	17.6
3	60	950	50	1.9	0.0149	23.8	7.5	18.8
4	70	950	50	1.8	0.0149	22.5	7.5	20.1
5	80	950	50	1.7	0.0149	21.3	7.5	21.3
6	90	950	50	1.6	0.0149	20	7.5	22.6
7	55	800	50	2	0.024	25	12	13
8	55	850	50	2	0.022	25	11	14
9	55	900	50	2	0.02	25	10	15
10	55	950	50	2	0.018	25	9	16

Phantom	T2 aim (ms)	T1 aim (ms)	Phantom volume	Agarose (w/v)	Copper (w/v)	Volume agarose (ml)	Volume copper (ml)	Volume water (mls)
11	55	1000	50	2	0.016	25	8	17
12	55	1050	50	2	0.014	25	7	18
13	55	1100	50	2	0.012	25	6	19
14	55	1250	50	2	0	25	0	25
15	-	-	50	2	0	50	0	0
16	-	-	50	1	0	50	0	0
17	-	-	50	4	0	50	0	0
18	-	-	50	0	0.1	0	50	0
19	-	-	50	0	0	0	0	50

Figure 28. The gel phantoms within the MR scanner.

3.4a.4 Results

Nineteen gel phantoms were scanned and T1 and T2 values measured. A mathematical model derived from Mitchell's paper was used to predict the effect of differing the concentrations of agarose and copper sulphate on T1 and T2. Table 16 gives the predicted values and actual measures for the 19 gel phantoms. For the first 6 phantoms where the agarose concentration was altered and the copper remained the same the mean difference was 4ms± 10 for T2 and 16.5±39 for T1, between the estimated value and the measured values.

Table 16. Predicted and actual measures for 19 phantoms.

Phantom	T2 aim (ms)	T1 aim (ms)	Measured T2 (ms)	Measured T1 (ms)	Difference between actual and predicted T1 (ms)	Difference between actual and predicted T2 (ms)
1a	40	950	49	882	+ 9	- 68
2a	50	950	55	909	+ 5	- 41
3a	60	950	58	926	- 2	- 24
4a	70	950	63	932	- 7	- 18
5a	80	950	68	957	- 12	+ 7
6a	90	950	73	995	- 17	+ 45
7	55	800	52	680	- 3	- 120
8	55	850	57	720	+ 2	- 130
9	55	900	85	855	+ 30	- 45
10	55	950	83	881	+ 28	-69

Phantom	T2 aim (ms)	T1 aim (ms)	Measured T2 (ms)	Measured T1 (ms)	Difference between actual and predicted T1 (ms)	Difference between actual and predicted T2 (ms)
11	55	1000	74	914	+ 19	- 86
12	55	1050	63	1003	+ 8	- 47
13	55	1100	80	1103	+ 25	+ 3
14	55	1250	90	1166	+ 35	- 84
15 (Agarose 1%)	-	-	114	3003	NA	NA
16 (agarose 2%)	-	-	64	2800	NA	NA
17 (agarose 4%)	-	-	30	2180	NA	NA
18 (Copper sulphate 0.1%)	-	-	328	350	NA	NA
19 (Water)	-	-	1791	2938	NA	NA

A Pearson product-moment correlation coefficient was calculated to assess the relationship between the concentration of agarose and the measured T2. There was a negative correlation between the two variables, r = -0.99 (-0.999 to -0.912), n = 6, p <0.01, two tails. Overall there was a very strong negative correlation between agarose concentration and the phantom T2.

A Pearson product-moment correlation coefficient was calculated to assess the relationship between the concentration of agarose and the measured T1. There was a negative correlation between the two variables, r = -0.97 (-0.997 to -0.73), n=6, p=0.002, two tails. Overall there was a very strong negative correlation between agarose concentration and the phantom T1.

A scatter plot summarizes the results in figure 29.

A Pearson product-moment correlation coefficient was calculated to assess the relationship between the concentration of copper and the measured T2.

There was a negative correlation between the two variables, r = -0.66 (-0.93 to 0.08), n=8, p= 0.07 (two tails). Overall there was a strong negative correlation between copper concentration and the T2 of the phantom, but this did not reach statistical significance.

A Pearson product-moment correlation coefficient was calculated to assess the relationship between the concentration of copper and the measured T1. There was a negative correlation between the two variables, r = -0.99 (-0.99 to -0.95), n = 8, p < 0.001. Overall there was a very strong negative correlation between concentration of copper and the measured T1, which was statistically significant. A scatter plot summarizes the results in figure 20.

Figure 29. Scatterplot showing relationship between agarose concentrations and the measured T1 and T2 values in the gel phantom.

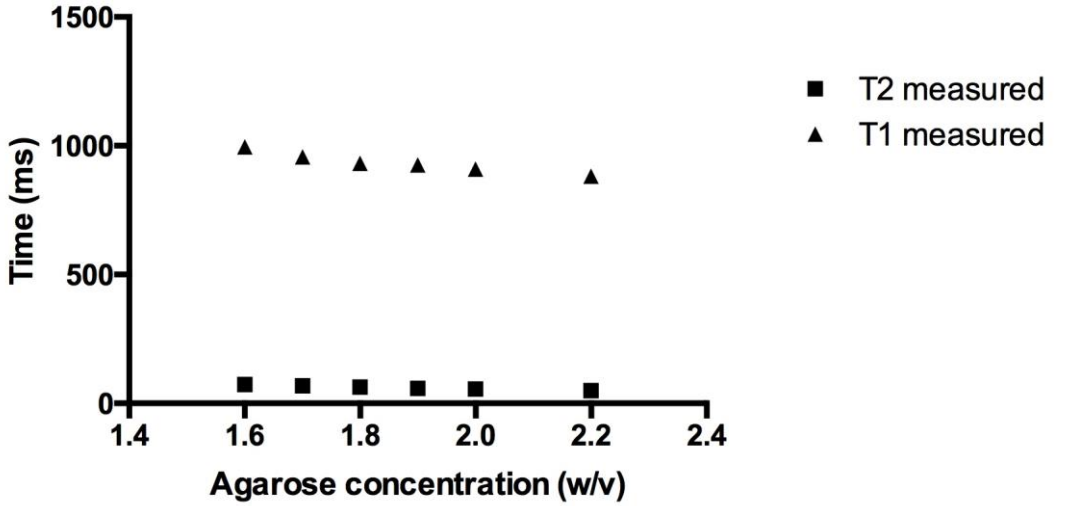

Figure 30. Scatterplot showing relationship between Copper Sulphate concentration and the measured T1 and T2 values in the gel phantom.

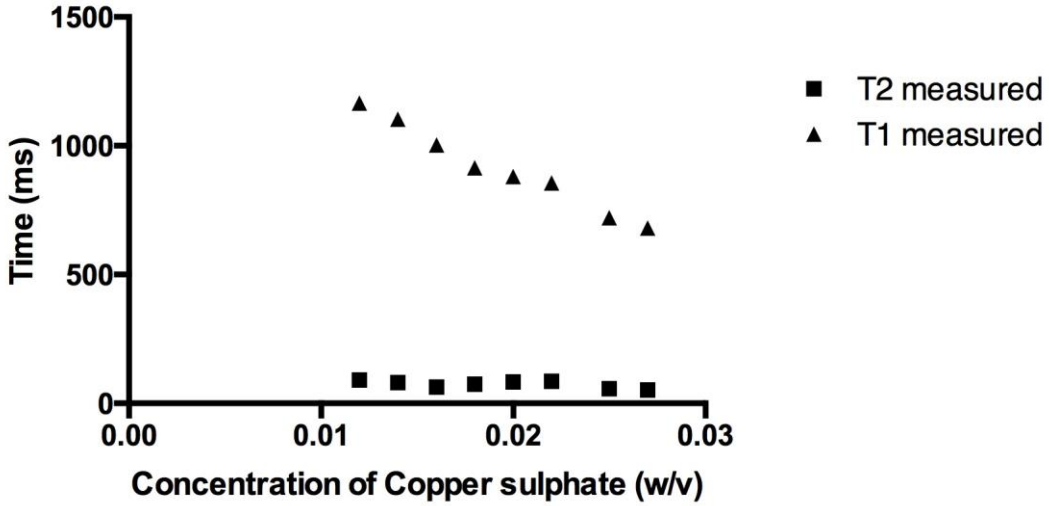

3.4a.5 Discussion

This set of phantoms clearly demonstrated that a tissue equivalent T1 and T2 values (T1 950ms, T2 50ms) could be achieved using the combination of agarose, copper sulphate and deionized water.

From our results it appeared that both components independently affect the T1 and T2 values. Consistent with Mitchell's paper we found that altering the concentration of copper mainly effected the T1 value rather than the T2 value. However in Mitchell's paper it was seen that agarose concentration mainly effected the T2 value rather than the T1 value. We found the opposite in our set of phantoms. Obviously a limitation of this study was that only a limited number of concentrations of the components were used and thus one cannot make firm conclusions regarding the effect on the T1 and T2 values. More phantoms at different concentrations would have to be studied.

The main aim of this study was to validate the method described by Mitchell and it does allow a wide range of T1/T2 values to be obtained. The difficulty in producing a gel phantom that mimics human myocardium is that the range of normal is very tight especially for T2 with a range between 45 and 60 ms. It appears that one has to make a lot of different phantoms using a range of agarose and copper sulphate concentrations to be able to select one that is close to human myocardium.

Study 4b. Effect of Metal Susceptibility artefact on T1 mapping and velocity phase encoding using an agarose phantom model.

3.4b.1 Introduction

Metal susceptibility artefacts from the IPG are seen on the cine images generated in cardiac MR, but in the vast majority of cases this does not prevent a visual assessment of cardiac function. (203)

The presence of a metallic object can create two forms of artefact. The first relates to the magnetic susceptibility of the object. Magnetic susceptibility corresponds to the internal magnetization of a tissue resulting from interactions within an external magnetic field. When two tissues or tissue and object with different magnetic susceptibilities are juxtaposed, local distortions in the magnetic field are created. This creates inhomogeneities in the static magnetic field, resulting in dephasing and frequency shifts of nearby spins. Ferromagnetic metal creates significant magnetic field inhomogeneity, which results in a local signal void and often accompanied by an area of high signal intensity, with distortion of the surrounding area. Signal loss depends on the metal and on the pulse sequence used. The signal loss results from the local field inhomogeneities (T2*) that accelerates transverse relaxation and signal decay, and from magnetic distortion, which alters the precessional frequency shift. When the tissues precessional frequency is shifted, it may result in an absence of spin excitation during the slice selection resulting in loss of a signal, or when the

signal is acquired during the readout gradient the shift will result in a mis-registration of the spatial localization, leading to distortion.

A second artefact is a result of eddy currents set up in conductors by the high frequency RF pulses. These create magnetic counter-fields, which alter the resulting amplitude of the RF pulse across the imaging region, leading to alteration in the spin-echo signals.

T1 mapping is a CMR technique that has been used extensively in research and shows great promise in the clinical setting. It is a method of providing a parametric map whereby each pixel represents a T1 value. The pixel intensity is directly related to the underlying T1 value. T1 maps are generated from a series of images acquired at different times of the T1 recovery curve, following an inversion magnetisation preparation pulse. (240,241) The pulse sequence most commonly used in T1 mapping is the MOLLI sequence. (MOLLI). (224)

Velocity-phase encoding gradient echo imaging (VENC) is an MR technique used for the quantification of blood flow and is widely used in clinical practice. The phase shift that occurs as protons move though a magnetic field allows the direction and velocity of blood flow to be calculated. In CMR this is used to quantify valvular lesions and intra-cardiac shunts.

It is important to determine if T1 mapping and VENC can be performed in presence of an IPG and if so can the results be reliable to make clinical judgments. In order to investigate this we performed a series of MR scans on gel phantom models.

3.4b.2 Methods

2 gel phantoms were studied on a 1.5 Tesla (Magnetom Avanto, Siemens Healthcare Sector, Erlangen, Germany) with a dedicated cardiac 32-element phased-array coil.

3.4b.2.1 Phantom

Two Perspex containers measuring 280x210x110mm were used to mimic the thoracic cavity. In phantom A, the container was filled with the agarose gel solution. In phantom B, an acrylic plastic rig was fitted to allow the placement of a dual chamber PPM (St Jude Medical Verity ADx XL DR) and two 58cm active fixation pacing leads (SJM Tendril MR) (Figure 31).

To mimic human tissue, each container was filled with solution of agarose and copper sulphate (Figure 32). The same method outlined in section 4a.3 was used, but with up-scaled quantities of materials. Multiple small test batches were used to try and calculate the composition that would achieve T1 relaxation properties similar to myocardium.

Figure 31. Phantom B. PPM within container on rig.

Figure 32. Phantom A (right) and B (left) filled with agarose gel.

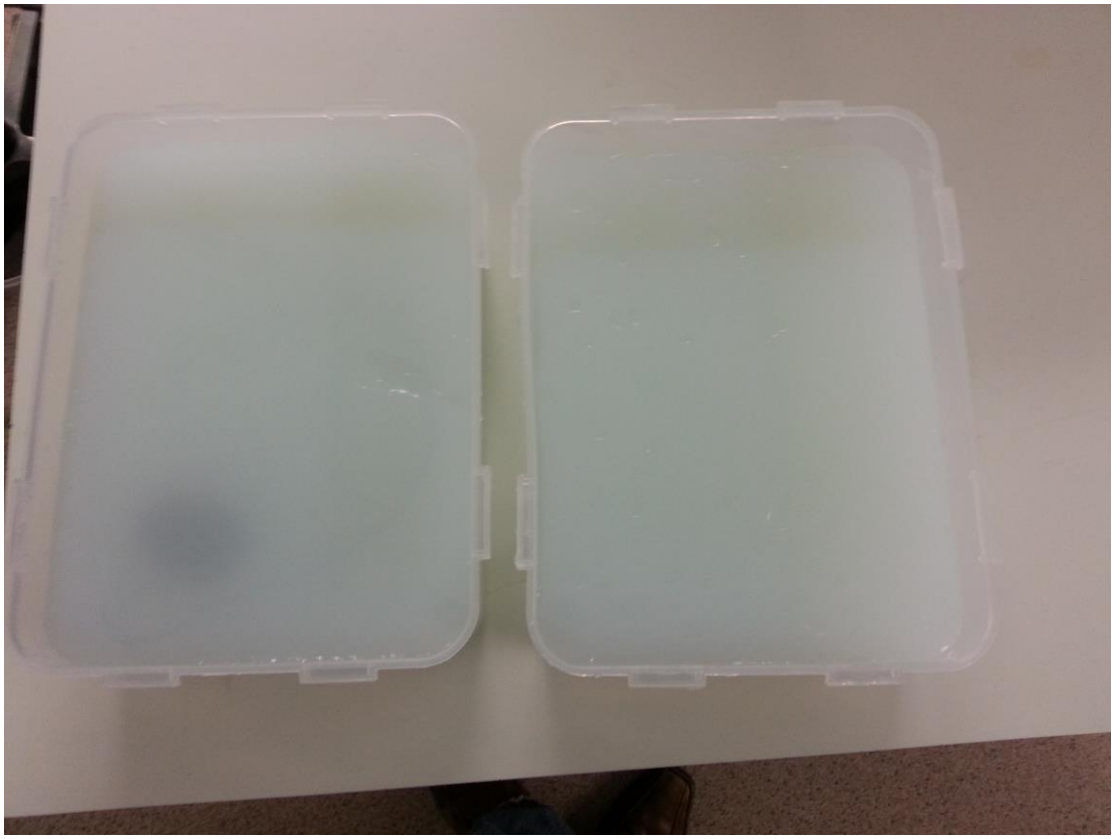

3.4b.2.2 T1 mapping

T1 measurements were made using an ECG triggered single-shot MOLLI sequence as described by Messroghli.(224). Typical parameters were field of view 340×255 mm, matrix 192×138, 8-mm slice thickness, flip angle 35°, parallel imaging factor 2 with 24 reference lines, 6/8 partial Fourier k-space sampling, acquisition time 201 ms for a single image, and initial effective inversion time (TIeff) 100 ms with a TIeff increment of 80 ms. To sample T_1 recovery, serial single-shot diastolic images were acquired every heart beat after 3 nonselective adiabatic inversion pulses (i.e., 3, 3, and 5 images after each inversion pulse, totalling 11 images), with 3 dummy heart beats before the second and third inversion pulses to allow T1 recovery (17 heart beat total acquisition duration).

3.4b.2.3 Velocity phase encoding

Flow was measured in all three orthogonal planes with the imaging plane centred at the magnetic iso-centre. In the axial and sagittal projections, the isocentre was moved 50mm towards and away from the PPM. A one-direction (through-plane) motion-encoded cine gradient echo was applied. Typical parameters were slice thickness 5mm, flip angle 20, TR 29.9, TE 2.18, 192 phase encoding steps over 30 time frames. The Velocity encoding sensitivity (V_{enc}) was 150cm/sec.

3.4b.2.4 Experiments

Eighteen scans were performed on each phantom over a 2-week period. A simulated RR interval of 1000ms was used for all scan sequences.

3.4b.2.5 Analysis

T1 maps were analysed by placing a grid system on the images generated in the three orthogonal planes using OsiriX (©Pixmeo Sarl). An example of the grid used in the coronal plane is shown in figure 33.

The phase-encoded velocity sequences were analysed using CMR42 using regions of interest at differing distances from the PPM.

Figure 33. Grid placed on coronal projection for T1 mapping analysis.

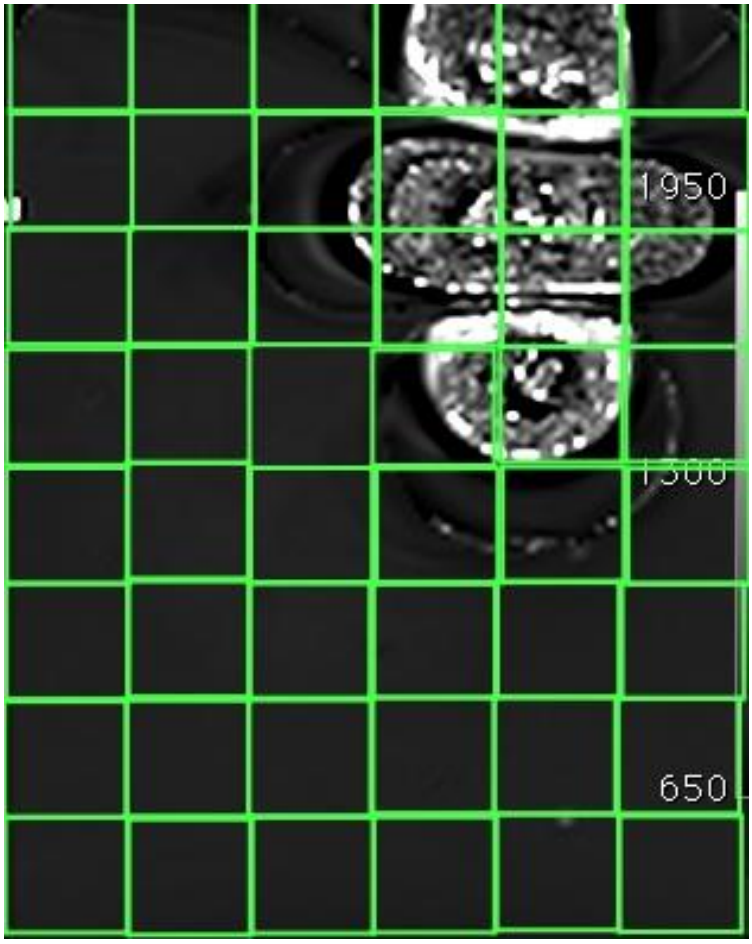

3.4b.3 Results

3.4b.3.1 T1 Mapping

The mean T1 of phantom A (no PPM) for the baseline scan was 844ms ± 21.6 and mean T1 of phantom B (PPM) was 878ms±138 in the coronal plane. A representative localizer and corresponding T1 map of the PPM phantom and a gel only phantom is shown in Figures 34 and 35.

Figure 34. T1 map of the gel only phantom in coronal plane (phantom A).

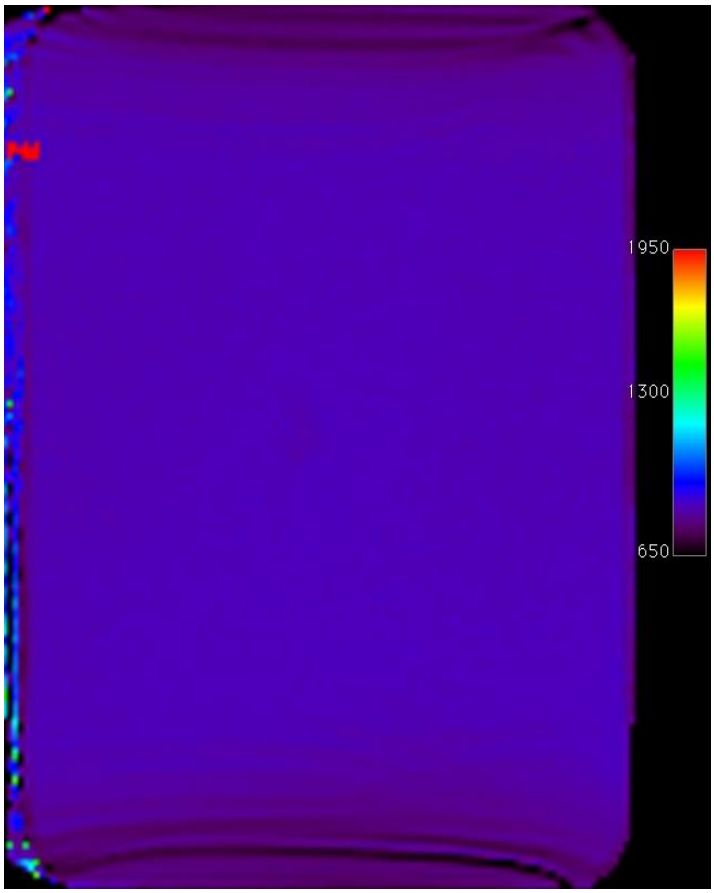

Figure 35. Coronal localiser and corresponding T1 map in the PPM phantom. Marked artefact is observed see spreading out from the centre of the device.

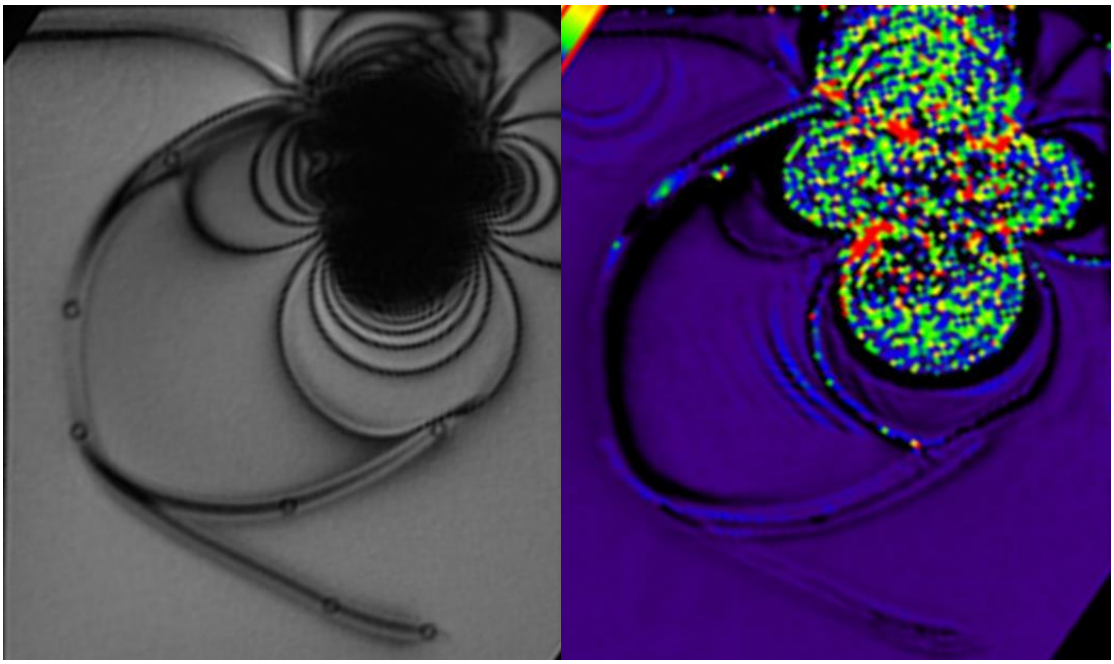

The gel only phantom (A) was relatively homogenous compared to the PPM phantom (B). The values obtained for each sector in the coronal plane grid for 1 scan are shown in figure 36a and b.

Figure 36. T1 values across the two phantom models. The gel only phantom (phantom A) is relatively homogenous with only a small variation in T1 values across the phantom centrally (shaded). In phantom B the heterogeneity introduced by the device can be seen.

834	826	824	820	815	821
922	851	852	851	850	850
847	850	853	854	852	852
849	852	854	857	852	852
845	854	857	858	853	853
846	856	858	858	856	857
847	854	852	851	852	857
815	803	796	793	799	818

742	804	802	1143	1183	813
875	813	775	1103	1284	824
823	815	787	1192	1284	830
823	835	835	973	1182	837
823	841	839	785	761	816
825	837	842	831	822	827
826	833	833	832	834	831
822	826	824	823	829	829

3.4b.3.2 T1 values over time in gel phantom

The scans were performed 18 times over a 2-week period. Figure 37 shows the mean T1 value across the 18 scans. The mean T1 value was 849.9±16ms for the 1st scan and 819.4±9.6ms for the 18th scan. A one way repeated measure of variance was conducted to evaluate the null hypothesis that there is no change in the T1 value of the gel phantom over time. The results of the ANOVA using a multivariate analysis indicated a significant time effect, Wilks lambda = 0.08, $F(17,24) = 167.95$ $p<0.01$ $\eta = 0.99$. Follow up pairwise comparisons using paired student T-tests indicated that no significant differences existed between repeat measures performed on the same day for days 2-6. On day 1 the T1 value for the morning scan, 849.9±16ms and the midday scan, 850.2±21ms were significantly different from the evening scan, 840.7±12ms, $p<0.01$.

Figure 37. T1 time drift. T1 measured over a 2-week period. Every 3 scans represent a single day.

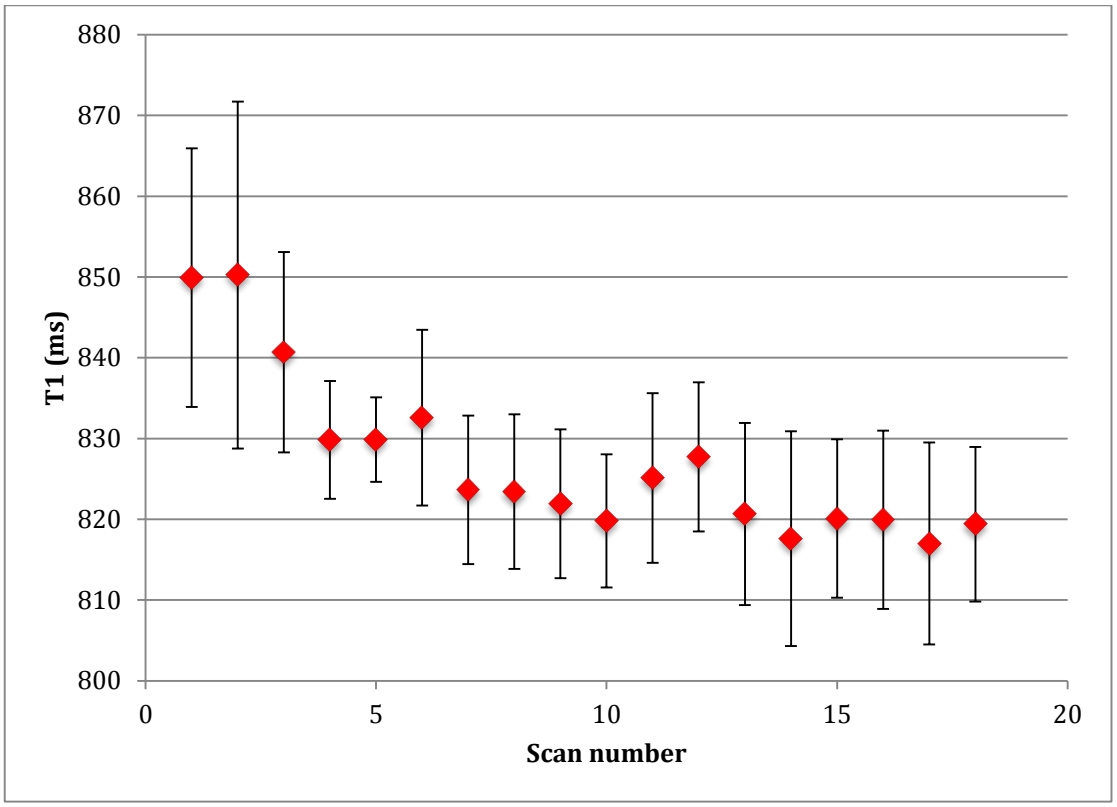

3.4b.3.3 Effect of Pacemaker on T1 mapping

The artefact the PPM generates is clearly visible on the localisers and corresponding T1 maps (Figure 35).

In all three orthogonal planes, regions of interest (ROIs) at increasing distances from the centre of the PPM were used and the corresponding T1 value measured. The measured T1 values against the distance from the PPM in the PPM phantom are shown in figures 38 to 43.

Pearson correlation and linear regression were performed on for each orthogonal plane.

For the coronal position (Figure 38) the measured T1 value had a negative correlation with distance from the PPM r = -0.588, p = <0.01 and the measured T1 could be predicted by the following formula T1= -15.16*Dx from PPM + 1018.74, R^2= 0.345.

For the sagittal position (Figure 39 and 40) the measured T1 value had a negative correlation with distance from the PPM r = -0.589, p = <0.01 and the measured T1 could be predicted by the following formula T1= -11.85*Dx from PPM + 979.9, R^2= 0.347

For the axial position (Figure 41) the measured T1 value had a positive correlation with distance from the PPM r = 0.637, p = <0.01 and the measured T1 could be predicted by the following formula T1= 4.52*Dx from PPM +768.76, R^2= 0.406

On review of the T1 maps it was evident that the axial plane was at the isocentre of the phantom and in a region of artefact, which gave low T1 values. This meant the starting point for the T1 values was low rather than high seen in the other orthogonal planes. The axial plane T1 map was repeated for 3 scans with an axial cut that

crossed the PPM and the results are plotted in figure 42 and 43. Here a high T1 was measured close to the device, with a corresponding reduction In T1 with distance. For this axial projection the measured T1 value had a negative correlation with distance from the PPM r = -0.857, p = <0.01 and the measured T1 could be predicted by the following formula T1= -22.64*Dx from PPM + 1030.9, R^2= 0.734

Figure 38. The relationship between the distance from the PPM and the measured T1 value in the coronal plane, using a scatter plot.

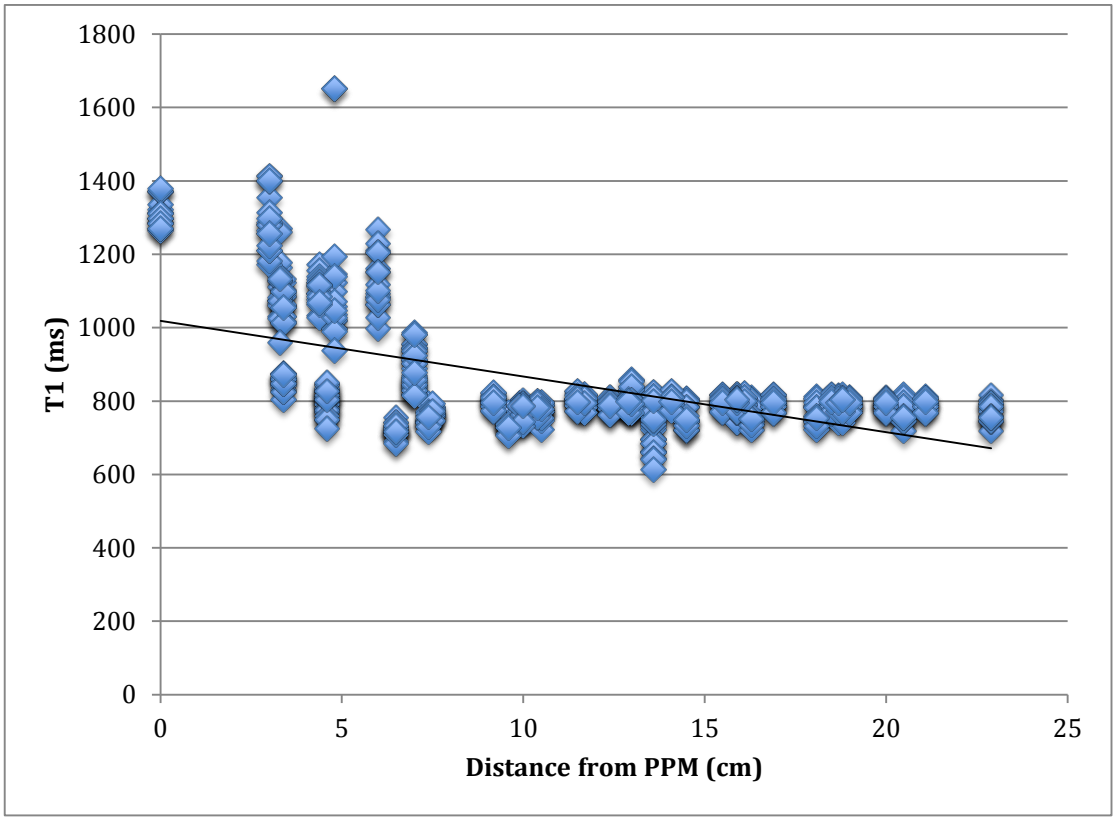

Figure 39. The relationship between the distance from the PPM and the measured T1 value in the sagittal plane, using a scatter plot.

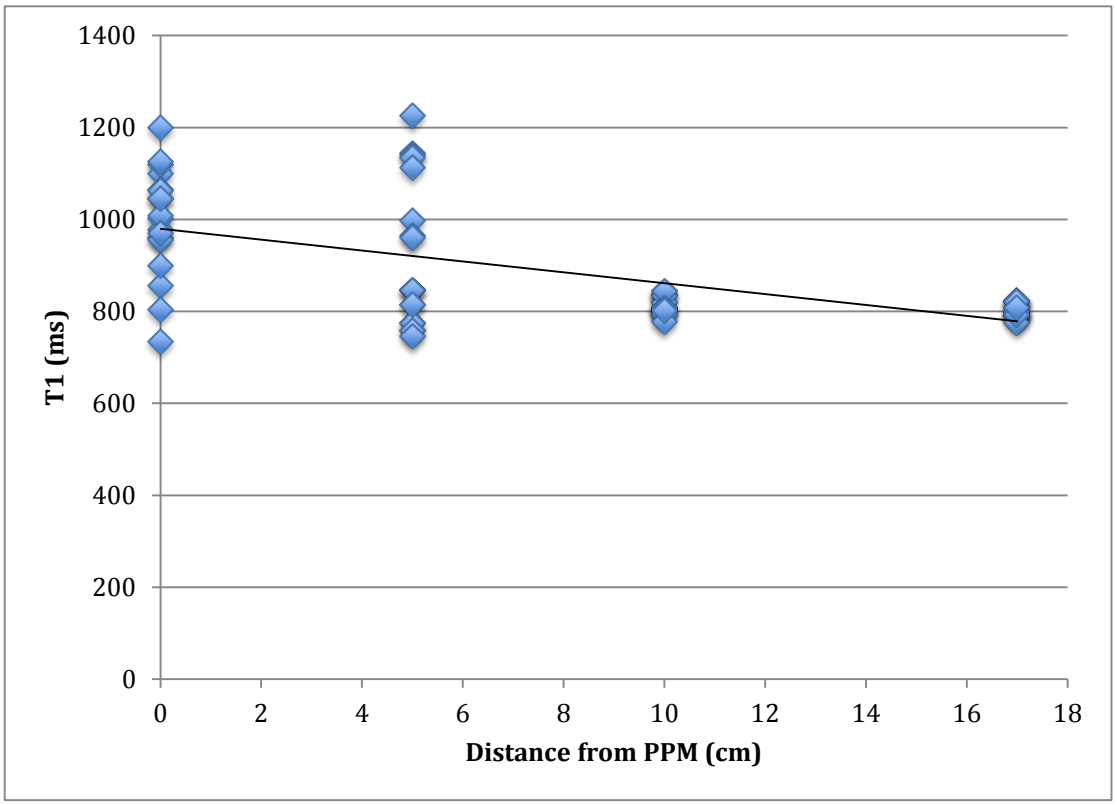

Figure 40. Mean T1 values in PPM phantom compared to gel only phantom in the sagittal plane. The T1 value within the gel phantom remains constant.

At 10 cm from the IPG the effect on T1 is negligible.

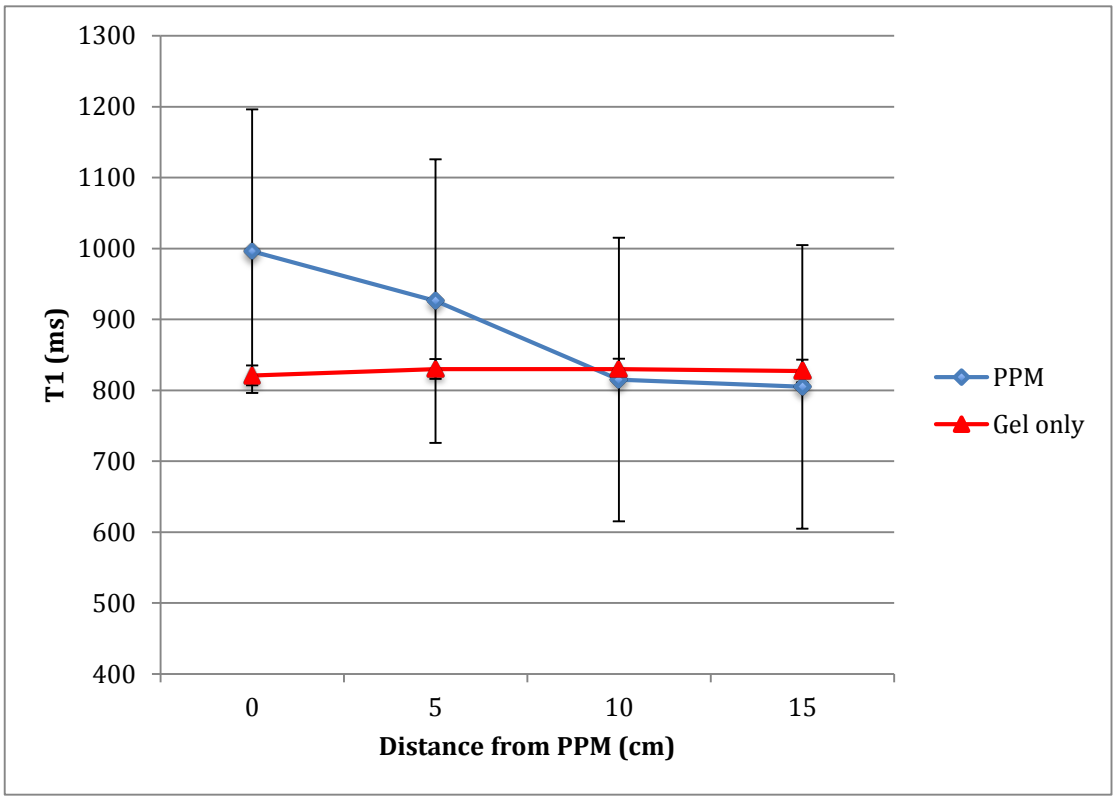

Figure 41. The relationship between the distance from the PPM and the measured value in the axial plane, using a scatter plot.

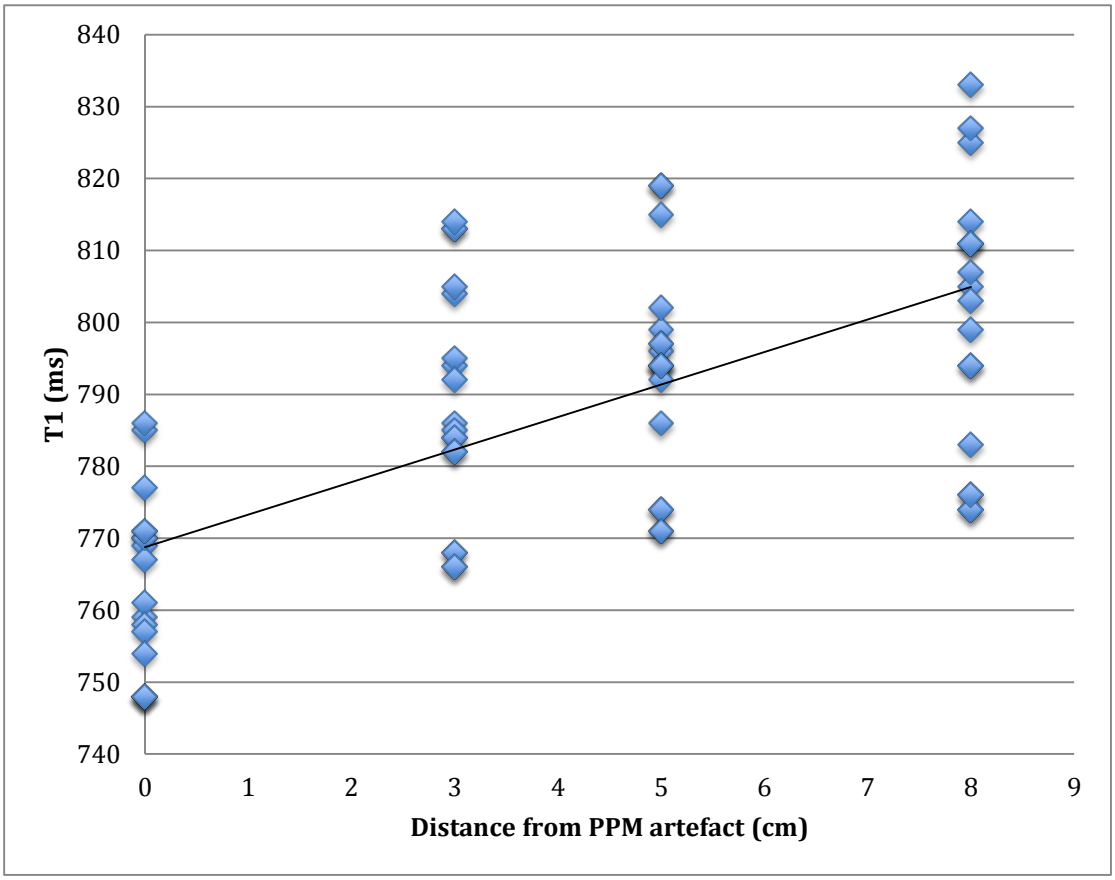

Figure 42. The relationship between the distance from the PPM and the measured T1 value in the axial plane adjusted to cross the PPM, using a scatter plot (see text for explanation)

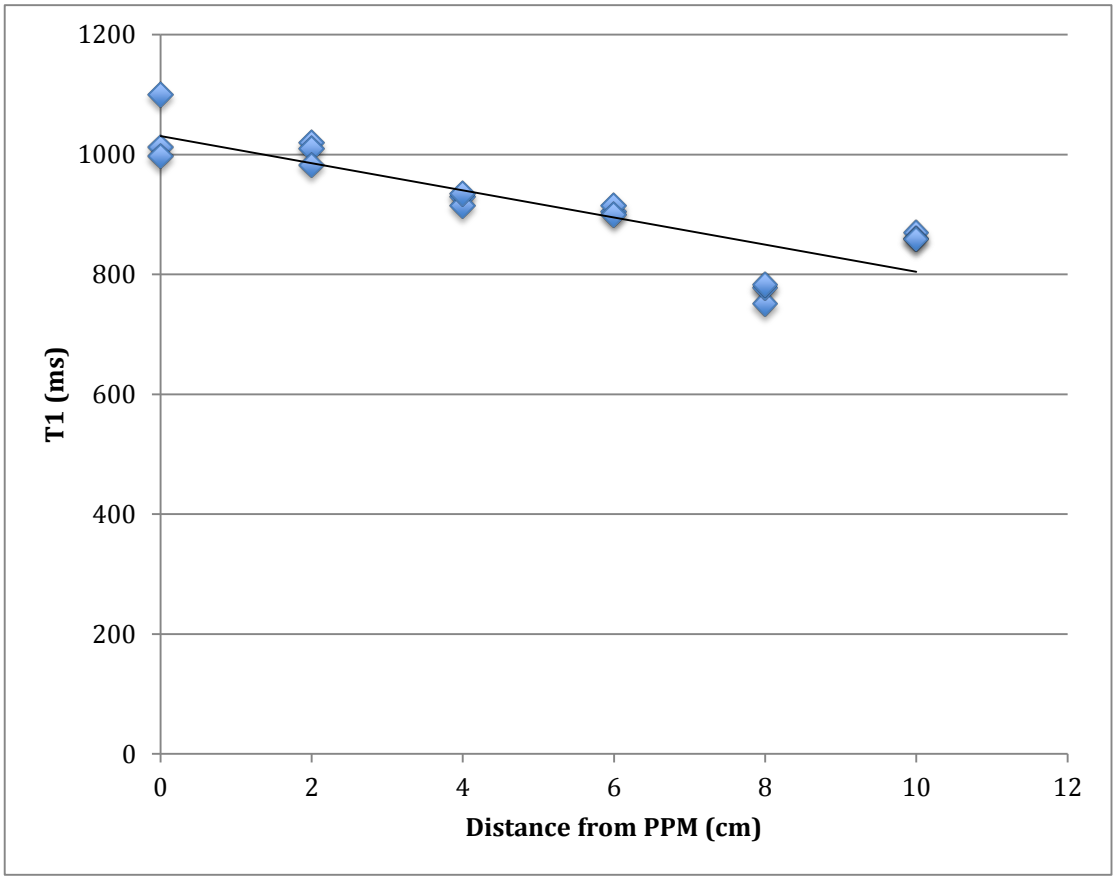

Figure 43. The mean T1 values of PPM phantom compared to gel phantom in axial plane.

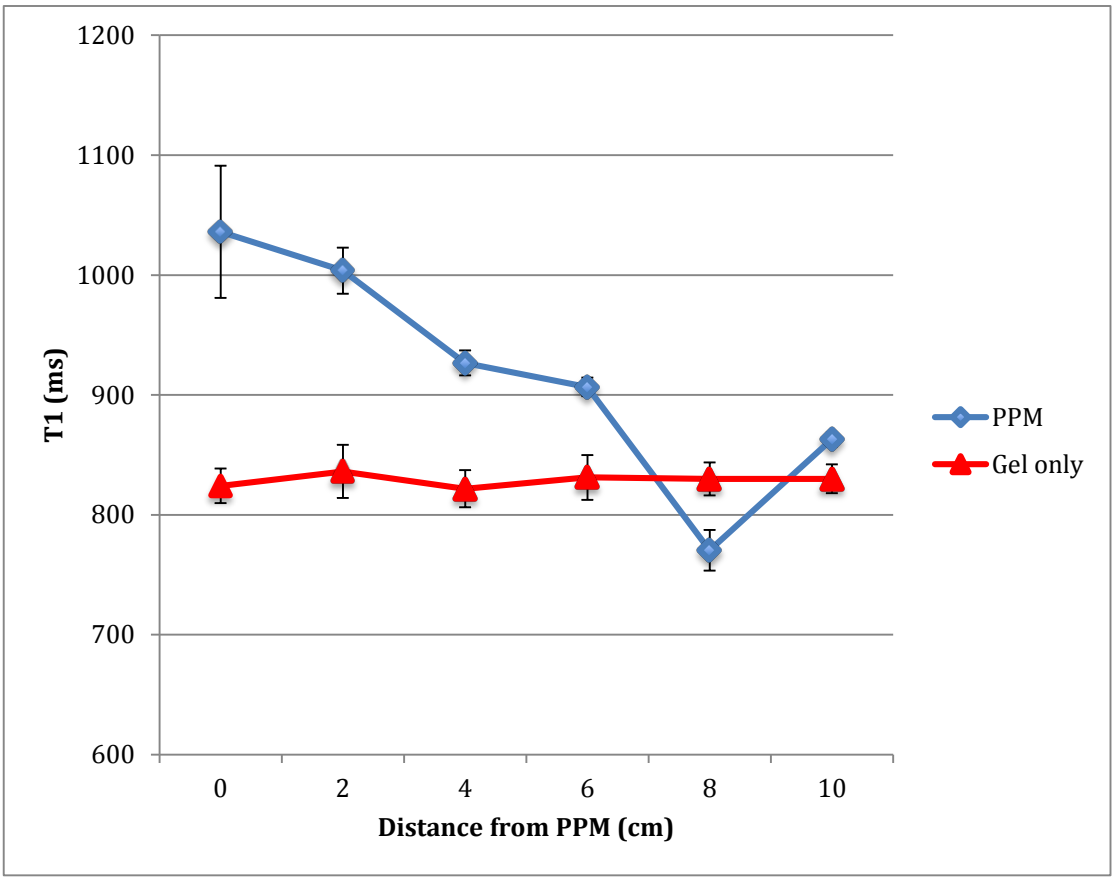

3.4b.3.4 Effect of pacemaker leads on T1 mapping

Whilst the artefact surrounding the PPM was large, only a small artefact was seen around the pacing lead within the phantom. To analyse the effect that the pacing lead would have on the T1 value a grid consisting of 5x5mm squares was placed over one of the pacing lead body and lead tip.

Figure 44. Plot of distance from lead body and mean T1 values in PPM phantom compared to the gel only phantom.

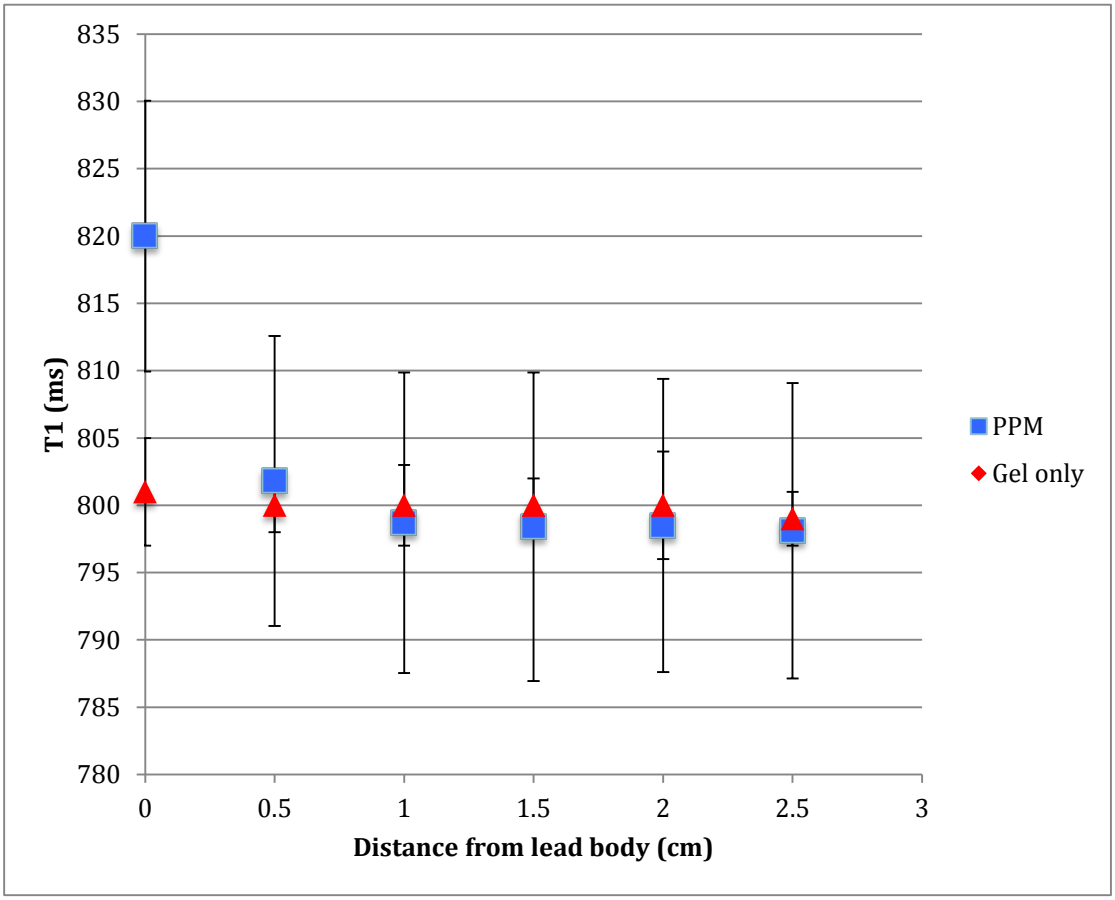

Figure 45. Plot of distance from lead tip and mean T1 values in PPM phantom compared to the gel only phantom.

At 1 cm from lead tip, T1 is not affected.

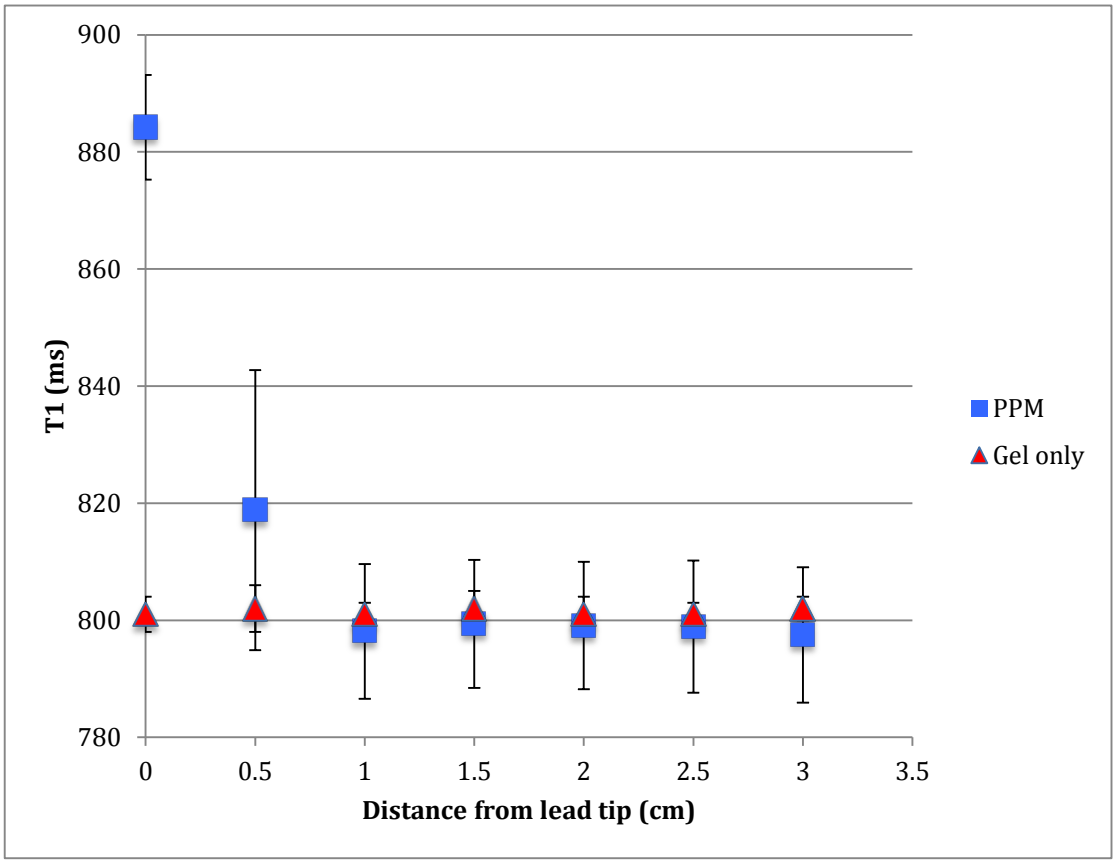

For the lead tip the measured T1 value had a negative correlation with distance from the PPM r = -0.661, p = <0.01 and the measured T1 could be predicted by the following formula T1= -21.35*Dx from PPM + 845.74, R^2= 0.437. At 1cm from the lead tip the mean T1 was 798±11.5 in the PPM phantom compared to 801±2ms in the gel phantom, p = 0.4.

For the lead body position the measured T1 value had a negative correlation with distance from the PPM r = - 0.449, p = <0.01 and the measured T1 could be predicted by the following formula T1= -6.84*Dx from PPM + 811.13, R^2= 0.202. At 1 cm the mean T1 in the PPM phantom was 799±11.2ms compared to 800±3ms in the gel phantom, p = 0.64.

3.4b.3.5 Effect of metal susceptibility artefact on velocity phase encoding

The gel phantom was solid, so any flows measured in the phantom would be related to the inherent phase offset error within the scanner. A clinically relevant phase offset would be considered to be greater than 5 mls.

The mean total flow measured at isocentre was -3.8±0.4mls in the PPM phantom compared to -4±0mls in the gel only phantom, p = 0.08, for the axial projection. In the sagittal projection the means flows measured were 2.4±0.5mls versus 2±0mls, p = 0.04.

The effect of moving the imaging plane was assessed by scanning the phantom with the relative isocentre at 0mm, +50m and -50mm in the sagittal and axial projections. This in effect moved the ROI towards and away the PPM so its effect on the measured flow could be assessed. In the axial plane the mean total flow measured at +50mm was -3.7±0.7mls for the PPM phantom and -3.8±0.4mls for the gel only

phantom, p = 0.79. At -50mm it was -3.8±0.42mls and -3.9±0.32mls respectively, p = 0.33.

In the sagittal projection the mean total flow measured at +50mm was 6.2±0.5mls in the PPM phantom and 6.5±0.51mls, p = 0.135 in the gel phantom. At -50mm it was -9.4±0.7mls and -5.7±0.5mls, p = <0.001.

The flows for the 18 scans in the sagittal projection are shown in figure 46.

Figure 46. Scatterplot showing the effect of moving the isocentre towards and away from the PPM on the flow measured in the phantoms, in the sagittal projection for 18 scans.

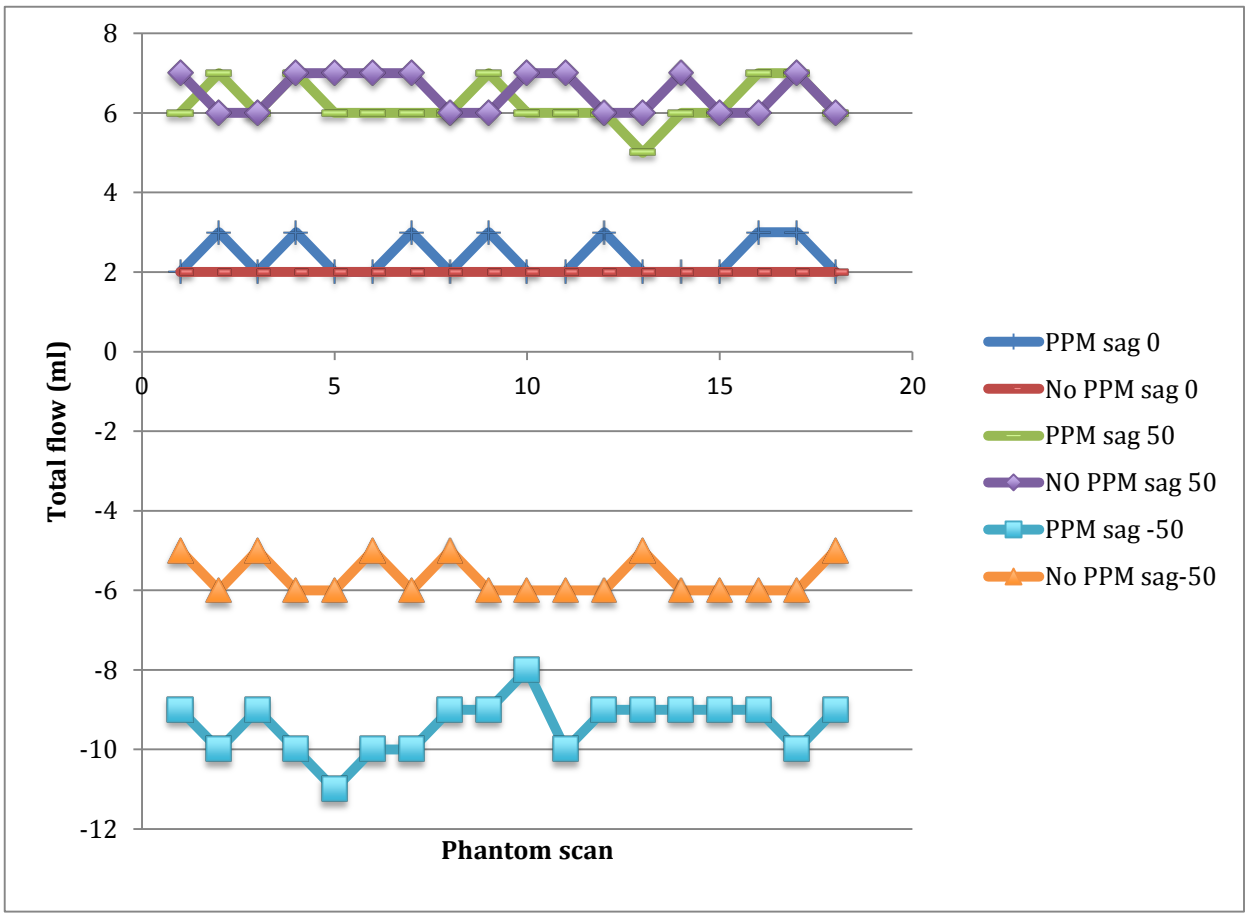

The effect of distance on the measured flow was further assessed by using 4 regions of interest (maximum CMR42 allows) at increasing distance from the PPM. Images at isocentre and +50mm and -50mm offset were used with the same 4 ROIs. Figure 47 shows the relationship between the distance from the PPM and the measured flow in the axial plane. At 2cm from PPM the mean measured flow was -33±1.3mls in the PPM phantom compared with -2±0mls in the gel phantom, p = <0.001. At 4 cm the mean flow measured was -4mls±0 in both the PPM and gel phantoms.

The sagittal plane produced both positive and negative flows depending on whether the isocentre was plus or minus 50mm in both phantoms because the phase ending direction was in the sagittal plane. Therefore a similar distance from the PPM could produce both positive or negative flow depending on if it was 0mm, +50mm or -50mm from isocentre. Figure 48 shows the measured flow for each ROI (1-4) in the sagittal plane at 0, +50 and -50mm. ROI 1 is closest to the PPM and 4 is furthest from the PPM.

Figure 47. The effect of distance from the PPM on the total flow measured in the gel only and PPM phantom in the axial plane.

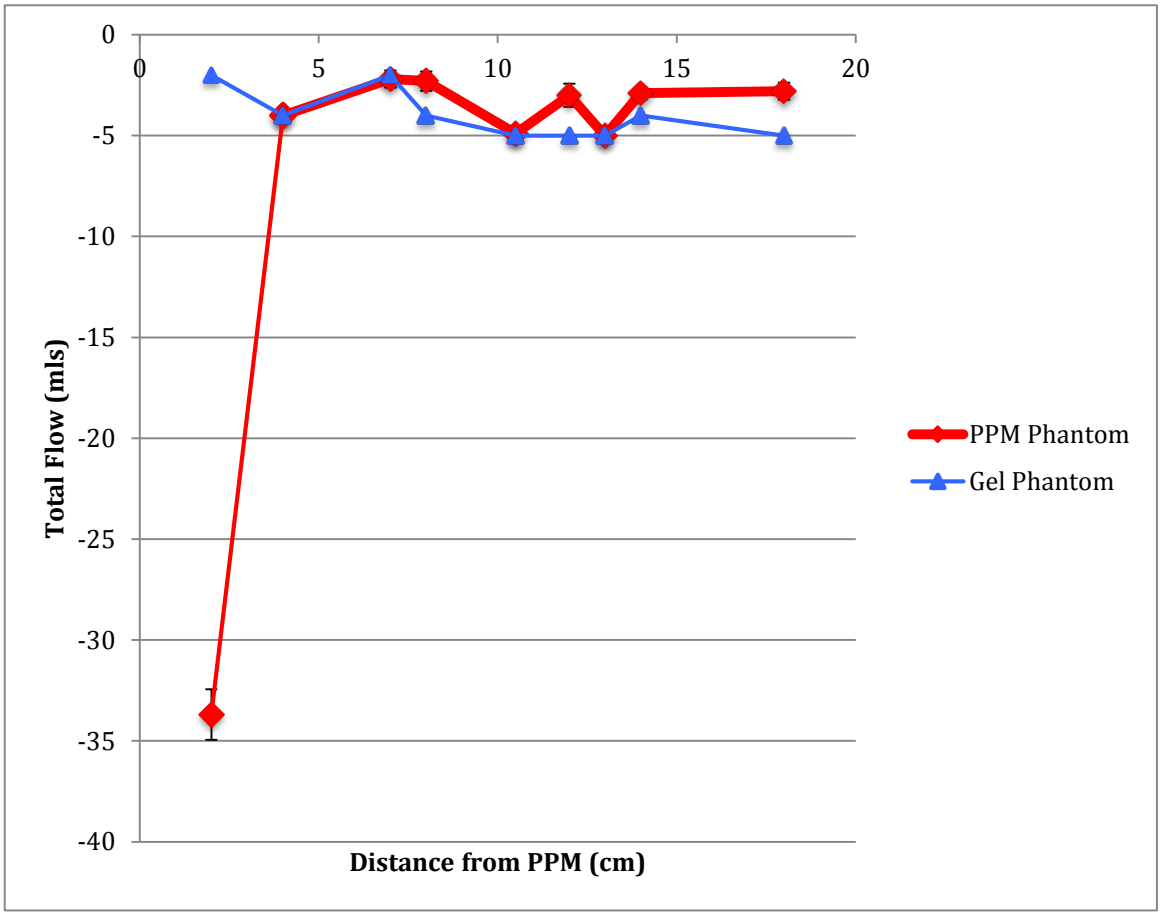

Figure 48. Total flow measured at four regions of interest at different isocentres for both phantoms. ROI closest and ROI 4 furthest from PPM.

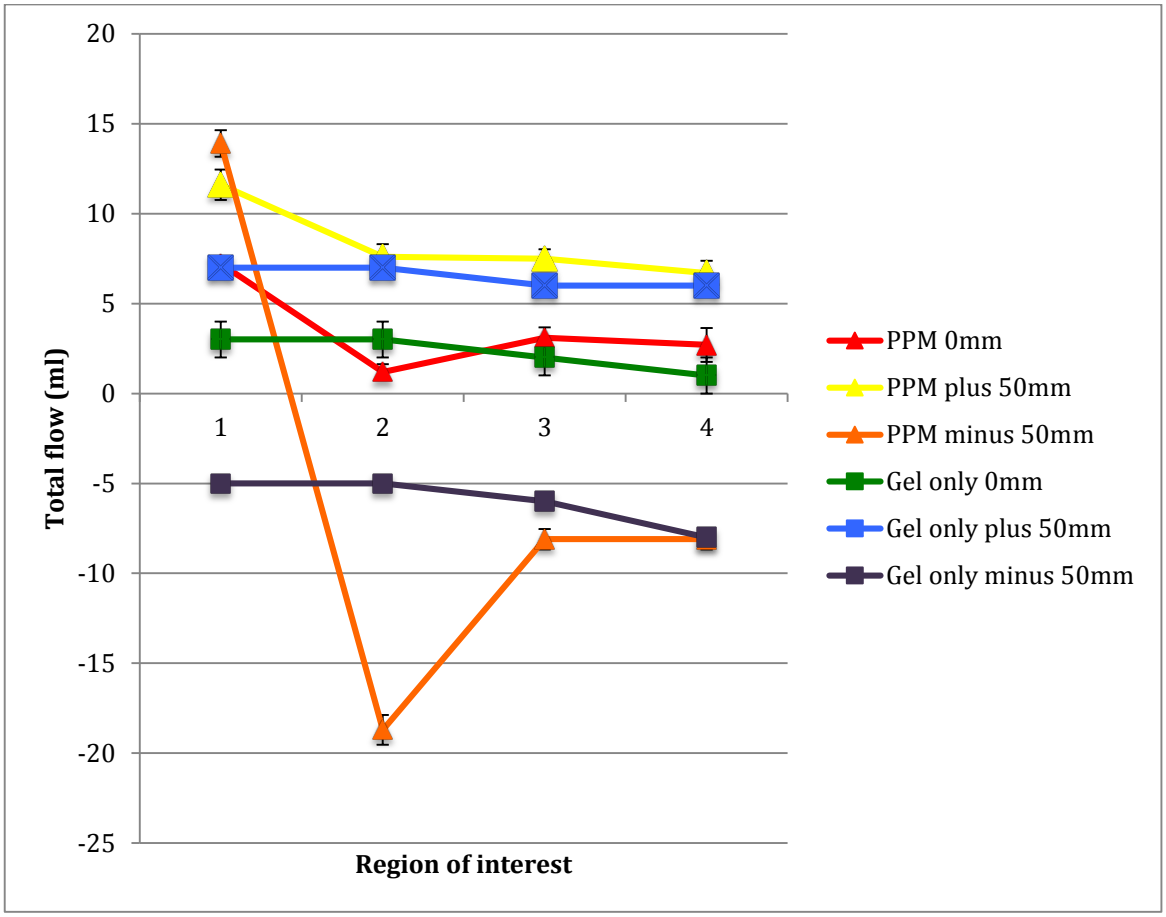

3.4b.4 Discussion

Whilst it was attempted to get a T1 value in the range of normal myocardium (approx 950-1000ms) the mean T1 values of both phantoms were much lower than this. Although the same proportions of agarose, water and copper sulphate were used as in the test sample, which gave a T1 value of 950ms, the test sample was only 30mls. Over 5 litres of solution were required for these phantoms and when up-scaled, the proportions probably differed. The mean T1 value was higher in the PPM phantom due to the presence of the PPM, rather than the inherent property of the agarose/copper sulphate gel. In fact in areas distal to the PPM, the T1 values were actually lower in the PPM phantom. What is clear is that the gel phantom is relatively homogenous, whilst the PPM phantom is heterogeneous. The grid with individual T1 values for each ROI illustrates this (Figure 36).

The value of mean T1 plotted for each scan for the gel only phantom (Figure 37), suggests that the gel phantom changed over the 2-week period. When analysed further it appears that only on day one did the T1 values differ significantly and that if you were to take out the day one results, then the T1 values did not in fact differ significantly within each day nor between subsequent days. On days 2-6, the variability was low suggesting that time of the day and perhaps any temperature changes had minimal impact on the value of T1 measured. The findings on day one are perhaps related to a physical change in the gel, related to when the gel was prepared. The phantoms were prepared the day before the first scan and whilst left overnight to solidify, the gel may not have not fully set for the first scan. If repeating the experiment, I would leave the gels to set for at least 48 hours. A second explanation could relate to the temperature of the phantom. The phantoms were kept in the lab in which they were made and taken to the scanner for the first scan the next day. Following the first scan, the phantoms were kept on a shelf within the

scanner room itself so they had time to aclimatise. Again if repeating the experiment the phantoms would be kept in the scanner room for at least 24 hours.

The T1 maps generated for the PPM phantom clearly show the PPM has an effect on the T1 map generated and the subsequent T1 values. The artefact generated is consistent with other metal susceptibility artefacts, where the metal leads to a magnetic field distortion, which alters the precessional frequency shift. When the tissues precessional frequency is shifted, it may result in an absence of spin excitation during the slice selection resulting in loss of a signal, or when the signal is acquired during the readout gradient the shift will result in a mis-registration of the spatial localization, leading to distortion. On the T1 map, both hyper-intense regions (multiple colours) with high T1 values and areas of hypo- intense (black/signal void) with lower T1 values can be seen. The ROIs drawn were such that they would include both hyper-intense and hypo-intense regions to give the average effect on the T1 value.

There was a moderate negative correlation between the distance from the PPM in both the coronal and sagittal planes. This can be seen visually on the T1 maps generated with the ringing artefact from the PPM decreasing with distance from the PPM. The results generated by the initial analysis of the axial plane illustrate the artefact and subsequent effect on the T1 value is heterogeneous. The T1 maps were generated using the centre of the phantom as reference point so the phantom would be scanned the same every time. By doing this, the axial plane did not cut across the PPM itself but the artefact generated by the PPM. On reviewing the T1 maps it can be seen that this artefact was an area of hypo-intense signal, much lower than the T1 values around it. So for this axial cut it led to there being a positive correlation between the T1 value and distance from the PPM artefact. Following this discovery, the phantom was scanned on 3 more occasions with an axial cut across the PPM itself. When this was done, a strong negative correlation was seen between the T1

value measured and the distance from the PPM. In all 3 planes it is clear that the further the ROI is from the PPM, the T1 value is more likely to represent the underlying tissue rather than the PPM artefact. When compared to the gel only phantom, the T1 values reached similar levels at approximately 12 cm. These results would suggest that in clinical imaging the T1 values for anything within 12 cm of the device are affected by metal susceptibility.

The effect the leads had on the T1 values measured was low in comparison to the PPM. Metal susceptibility artefact relates to the relative size and mass of an object and thus the leads being much smaller than the PPM, the artefact is greatly reduced. The artefact from both the lead tip and lead body extended only a short distance and after approximately 1 cm the T1 values became similar to the rest of the gel phantom. The measured T1 at 1cm was clinically and statistically non-significant between the gel and PPM phantom. This result is consistent with Saki et al, who described artefact of 1cm around pacing leads also. (242) In clinical imaging, it would seem the leads alone would only effect a small area of adjacent myocardium.

The results of the velocity phase encoding analysis shows that the presence of the PPM would influence the measurement of flow by velocity phase encoding. Since this was a static phantom, any positive or negative flow measured was due to phase-offset errors. Phase offset errors occur in the magnetic field under normal circumstances because the magnetic field within the bore is not entirely homogenous, but these are considered insignificant in the clinical setting, during a single patient scan. (243) However concerns have been raised that temporal drift in the baseline offset can occur over a longer period. (243) This is one reason why the ROI should always be placed at the isocentre during clinical scanning. The phase-offset errors were significantly greater in the PPM phantom and the error is related to the proximity of the ROI to the device. The flows measured in the sagittal plane in the gel phantom, illustrates the effect of the phase encoding direction. The change from

a positive to negative flow with the shifting of the isocentre 50mm in either direction, related to the phase encoding direction, not the gel, since the gel has been to shown to be relatively homogenous. This highlights that in clinical practice scans should be done at isocentre with the ROI central. In the sagittal projection using 4 ROIs (Figure 48), it was evident that in the -50mm plane, the effect of the PPM on the flow was greatest. This is because this projection was closer to the actual PPM. It is interesting to note that in ROI 1 and 2 (the 2 closest ROI's to PPM) there was not only a difference in magnitude of the flow measured but also a directional change. This result shows that the PPM can influence both the magnitude and direction of phase-offset errors and that ROIs in close proximity to the PPM will produce erroneous results. The phase encoding direction did not influence the direction of flows in the axial plane, so it allowed the ROI's to be plotted as a distance from the PPM. In this plane, flows are likely to be erroneous within 5 cm of the device.

The effect of the leads on the flows was not assessed because the software used to measure flows made it difficult to produce accurate ROI's small enough. It can be inferred that the effect is likely to be small as seen with the T1 mapping.

3.4b.5 Conclusion

The presence of a PPM generates a significant artefact, which influences both T1 mapping and velocity phase encoding. If the region of interest is located in close proximity to the device then the results are likely to be erroneous. In T1 mapping, regions of interest greater than 10-12cm from this PPM tested and 1cm from these leads will probably reflect the underlying tissue. These findings cannot be generalized to all cases since both the device and leads differ in terms of size and material between products on the market.

Study 5. Image optimization in the presence of an Implantable pulse generator

Study 5. Image optimization in the presence of an IPG.

3.5.1 Introduction

The magnetic field within the scanner is never completely homogenous over the heart in clinical practice. Most tissues create a magnetic field that opposes the applied magnetic filed and are thus diamagnetic. This results in inhomogeneities within the B0 field that can cause local frequency offsets, leading to off-resonance effects. This may result in signal loss or spatial distortion in the image. Medical devices are a source of metal susceptibility artefact and distort the magnetic field. In CMR the sequences most sensitive to magnetic field distortions are the bSSFP sequences, where as turbo spin-echo (TSE) sequences appear less affected.

To determine which image sequences were affected by artefacts and whether the images could be optimized to improve quality, the PPM gel phantom was used. A greater time could be spent on attempting to optimize the images compared to a PPM in-vivo.

3.5.2 Method

The PPM gel phantom was scanned in a 1.5T scanner using the following sequences:

- bSSFP with centre frequencies 0, 25, 50, 75, 100, 125, 150, 175 and 200Hz
- bSSFP with different bandwidths (251, 496, 744, 1488)
- Spoiled gradient (SpGr)
- T1 Black blood turbo spin echo (T1 BB TSE)
- T2 Black blood turbo spin echo (T2 BB TSE)
- Short T1 inversion recovery (STIR)

These were performed in the three orthogonal planes.

3.5.3 Results

This was a qualitative rather than quantitative process. Figure 49 demonstrates the effect of 4 different sequences on the image in an axial plane. Figure 50 demonstrates the effect of altering the local centre frequency on the bSSFP images in the axial plane. A demonstrable effect can be appreciated between the different frequencies.

Figure 51 demonstrates the effect of altering the bandwidth on the bSSFP images in the axial plane.

Figure 49. A) SpGr B) SSFP C) T1 BB TSE D) T2 BB TSE images in the axial projection for the PPM phantom.

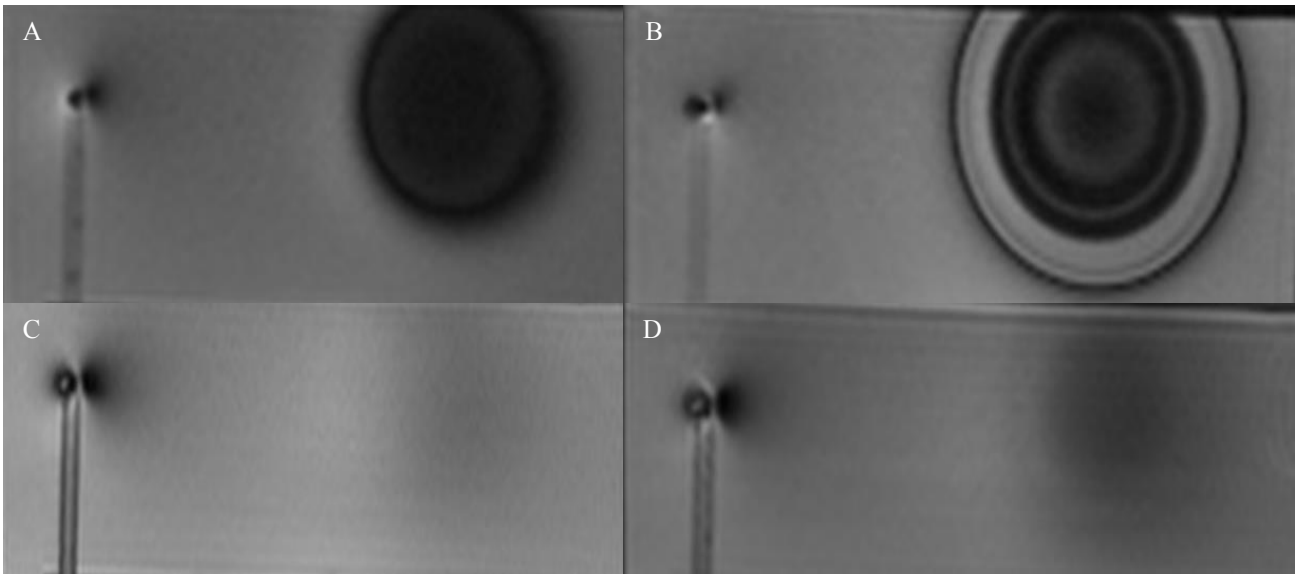

Figure 50. SSFP sequences in the axial projection with the following local centre frequency shifts A) 0Hz B) 25Hz C) 50Hz D) 75Hz E) 100Hz F) 125Hz G) 150Hz F) 175Hz.

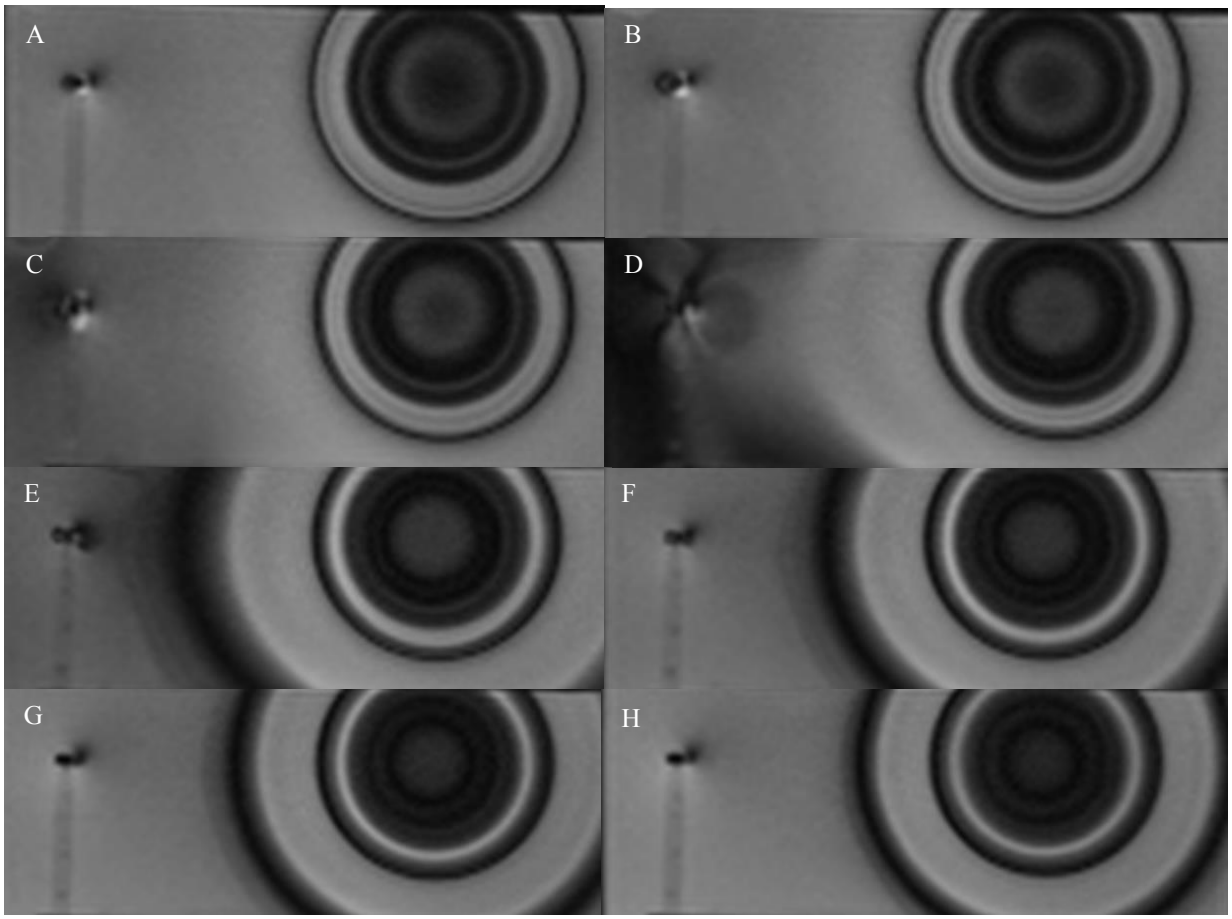

Figure 51. bSSFP in axial plane with the following bandwidths A) 251 B) 496 C) 744 and D) 1488Hz.

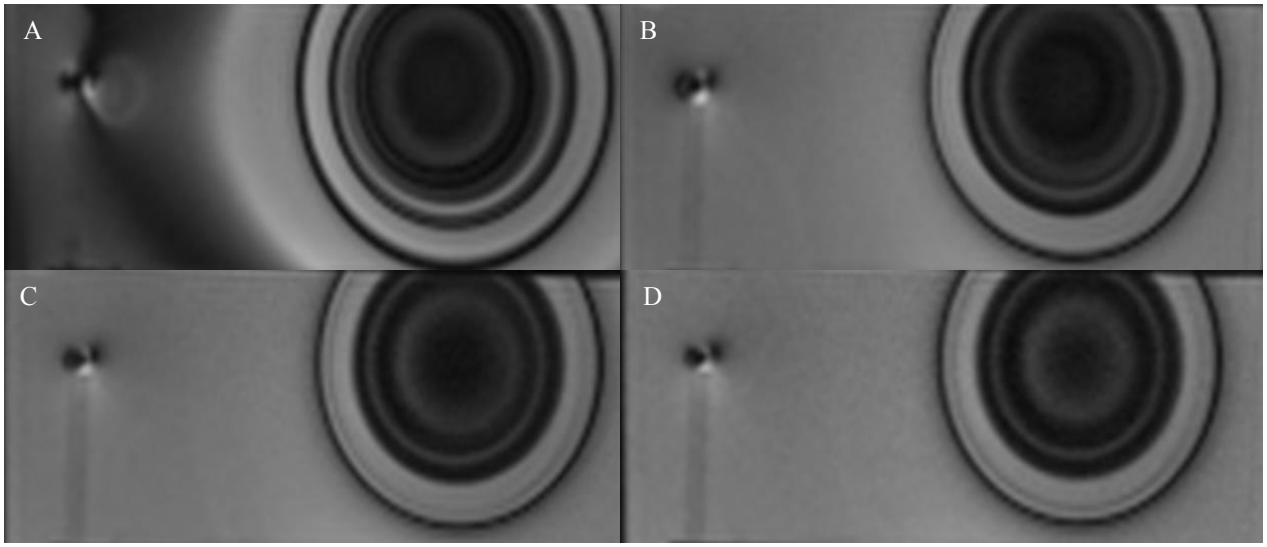

3.5.4 Discussion

Consistent with the literature, bSSFP sequences showed marked signal loss and banding artefacts on the images generated. (244) The inhomogeneity artefacts are quite distinct with SSFP sequences and result in a series of dark bands. The signal response to inhomogeneity is illustrated in figure 52, where the signal remains constant for small frequency offsets, but falls to near zero with a resultant dark band on the corresponding image. This occurs at regularly spaced intervals, with the frequency of the dark bands (no signal) being inversely proportional to the repetition time (TR) of the sequence. Not unsurprisingly the more inhomogeneous the magnetic field the larger signal voids occur within the image. In the case of the PPM the signal voids appear as rings around the device.

SpGr, T1 weighted and T2 images shown in figure 49 clearly demonstrate less artefact. In fact particularly in the T1 weighted image, hardly any artefact from the device or lead is visualized. The short TR used for T1 weighted imaging and the fact it is a spin echo rather than gradient imaging technique make it far less susceptible to metal susceptibility artefact. T1 weighted imaging is however not used for commercial cine imaging.

SpGr images have a lower signal to noise ratio than bSSFP images but because the transverse magnetisation at the end of each TR is spoiled rather than refocused by a gradient as in bSSFP, it is much less sensitive to field inhomogeneities and frequency-offset errors. As can be seen on the phantom, there is a signal void located where the device is, but there are no ring artefacts visible when compared to the corresponding bSSFP image.

The images in figure 50 demonstrate the effect of manipulating the local centre frequency. It is clear that by altering the frequency, the location of the artefacts can

be shifted. However the images clearly demonstrate that the artefact just moves, rather than being removed from the image. The phantom scans also demonstrate that smaller changes in centre frequency shift 25-50Hz should be tried first when scanning patients in-vivo, since these demonstrated much clearer images.

Increasing the bandwidth in bSSFP images has been shown to reduce the dark bands, although at the expense of increased scan time. Phantom scanning using four different bandwidths did demonstrate that the lowest bandwidth had the most artefact across the phantom. However beyond a bandwidth of 496, further increases did not appear to make a noticeable difference. In-vivo scanning requires the scan duration to be as short as possible for patient comfort and scanner throughput. The images in figure 51 suggest that an optimal bandwidth can be achieved, without it being particularly high and so scan times can be kept to the minimum in-vivo.

3.5.5 Conclusions

The phantom scans confirmed that bSSFP imaging is highly affected by metal susceptibility artefact but by manipulating the centre frequency and bandwidth the images can be optimized for an in-vivo setting. The experience gained from the in-vitro experiments was invaluable and carried forward to the in-vivo scans for the MAPS trial.

Figure 52. bSSFP and inhomogeneities in the magnetic field.

A) signal voids are seen at multiples of a frequency offset of ±227Hz B) spherical phantom with homogenous magnetic field C) phantom with left to right gradient with resulting bands at frequency offsets of ±227Hz D) TR made twice as long, doubling the frequency of signal voids. Reproduced with open access permission. (244)

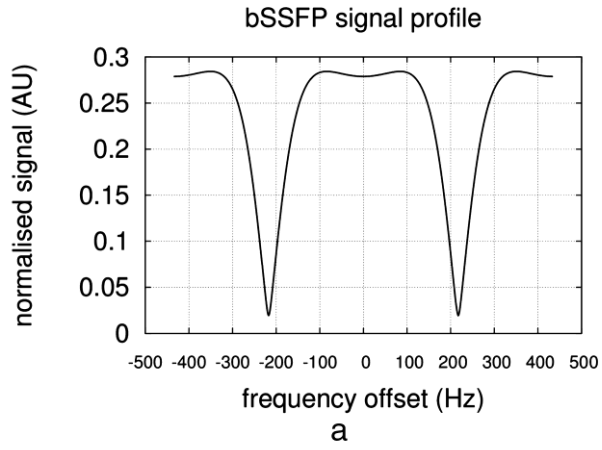

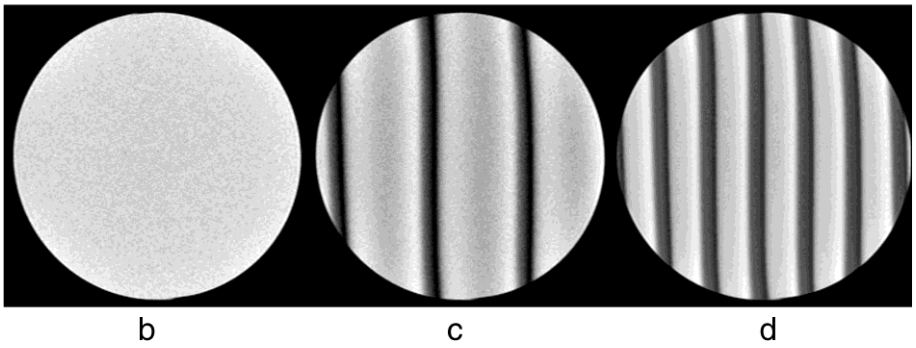

Study 6.Evaluation of left ventricular torsion using cardiac MRI. Validation of tagging and feature tracking.

Study 6. Evaluation of left ventricular torsion using cardiac MRI. Validation of tagging and feature tracking.

3.6.1 Introduction

LV torsion

The assessment of Left ventricular torsion to various cardiovascular disease processes has generated much interest in the last few years. In particular it appears to be more sensitive in detecting pathology before the development of more traditional functional parameters and the development of symptoms. Left ventricular torsion is fundamental to normal LV mechanics. During systole the LV apex rotates anticlockwise (when viewed fro the apex) about its axis to a maximum of about 10 degrees (245) whilst the base also initially rotate anti-clockwise (Clocks) before rotating clockwise. The analogy of wringing out a wet towel is often used. During the diastolic phase the ventricle untwists during iso-volumetric relaxation, releasing the elastic energy stored up. This facilitates rapid diastolic filling.

Torsional deformation is an important measure of cardiac performance that complements standard indices such as EF. It appears very sensitive to changes in endocardial and epicardial contraction, as well as ventricular remodelling. (209)

Torsion has been shown to be altered in a number of pathologies including hypertension (214) and left ventricular hypertrophy (213), even aging (246).

The current gold standard for evaluating torsion is CMR, but a wide variety of techniques exist and as yet the advantages and disadvantages are still to be determined. (209)

Tissue tagging by using SPAMM is widely used (213) and has been reported to have excellent reproducibility for measuring ventricular twist. (215)

The use of image feature tracking software offers an alternative method using standard bSSFP untagged images, (247) offering a potential benefit of shorter scan duration.

Confusion exists in the definition of torsion in the literature, with studies using very different measures making comparisons almost impossible. Twist, length corrected twist, torsional shear angle and shear strain have all been used.

Torsional shear angle is probably the best measure of true torsion currently, but even that can be calculated by several methods. (217,248) The formula by Aelen et al used in many studies offers a simple approximation of the torsional shear angle. (217)

True torsion requires several parameters to be defined and no single commercially available software exists to incorporate all the required steps in an ordered fashion to calculate this. We have developed programs to calculate torsion using CMR derived measures using tagged sequences and standard bSSFP sequences.

The purpose of the study was to compare CMR derived twist and torsion with two differing MR imaging sequences and to validate the software against reference values published in the literature.

Dobutamine was used as inotropic and chronotropic agent to assess whether the software could reliably detect an increase in deformation parameters with increasing heart rate and contractility as the dose increased.

3.6.2 Study Population

This validation study recruited 15 normal volunteers to undergo Cardiac MR.

3.6.3 Hypothesis

The primary hypothesis is that the twist, torsion and strain indices calculated from tagged and SSFP sequences will be comparable with high levels of agreement.

The secondary aims are:

Does dobutamine enhanced cardiac output reflect changes in twist, torsion and strain.

3.6.4 Methods

15 normal healthy volunteers were recruited from members of the public and staff at Wythenshawe hospital. All volunteers went through a screening process and if inclusion and exclusion criteria were met, they were given a detailed patient information sheet (Appendix). Normality was defined as no significant on going medical proabalems. All volunteers gave written informed consent at enrolment. (Appendix)

All scans were performed on a 1.5 Tesla scanner (Avanto, Siemens).

To increase the inotropic and chronotropic response of the heart, an infusion of dobutamine at 7.5mcg/kg/min and 15mcg/kg/min was used. All participants had a scan at baseline, 7.5mcg and 15mcg of dobutamine.

All analysis was done offline. LV volumes were calculated using Argus software (Siemens). Tagging was analysed using Intag as a plugin on OsiriX and feature tracking (TomTec, Diogenes) was used on SSFP sequences. In-house developed software CMR Torsion is an Excel-based macro programmed using Visual Basic that facilitates the calculation and graphical representation of principal strains, twist, torsion and circumferential longitudinal shear from processed tagged short axis slice images and bSSFP cine images obtained by our Siemens 1.5T Avanto CMR scanner. This was further refined to allow data derived from feature tracking software to be processed.

Twist

Rotational data within the InTag and feature tracking raw data files allowed the twist to be calculated. This is given by the formula:

(1) $TWIST_t$ = ROTATION $APEX_t$ – ROTATION $BASE_t$

Normalised Twist

To account for differing sizes of human hearts, the twist can be corrected for the length of the heart. In practical terms this is the distance from the basal short axis and the apical short axis slice in SSFP or tagged images. Basal and apical positions were manually entered into the in-house software to give a value for normalised twist.

$$(1)\ \mathrm{TORSION_t} = \frac{\mathrm{TWIST_t}}{\mathrm{End-diastolic\ distance\ between\ BASE\ SAX\ slice\ and\ APEX\ SAX\ slice}}$$

Circumferential shear angle (Torsion)

The most commonly used formula to derive the circumferential shear angle is that by Aelen. It is as follows:

$$\theta CL = \frac{(\phi apex - \phi base)(r\ apex + r\ base)}{2D}$$

ϕ= average rotation of slice

r = average radius of the cross-section

D= distance between basal and apical slices.

Or more simply:

(1) $\text{CIRCUMFERENTIAL LONGITUDINAL SHEAR}_t = \text{TORSION}_t \times \left\{\frac{\text{BASE RADIUS}_t + \text{APEX RADIUS}_t}{2}\right\}$

Neither data set from Intag or feature tracking software contains the radius of the cross-sectional segments, but CMR Torsion-FT does contain circumferential distance data. The radius can be calculated from the area of a slice using the formula

Area of a circle = πr^2

It is not possible to derive area data from InTag sequences since the contours of the myocardium cannot clearly be delineated. Instead contours were drawn around the epicardium of the closest SSFP sequence of the short axis stack to obtain the cross-sectional area across the cardiac cycle. From this the radius could be derived to calculate the torsion.

CMR Torsion extracts relevant data from the relevant files and carries out the following calculations:

(1) Normalises all time periods to estimated aortic valve closure (AVC) time from the R wave, as a percentage of RR duration. This is done to account for varying heart rates between acquisitions.
(2) Creates a series of time intervals called “Spline Time” and carries out cubic spline interpolation to create a set of isochronal values for each variable entered into the equations above. This is necessary to cater for the different temporal resolutions of cine and tagged images.
(3) Calculates and displays peak rotation, twist, torsion, circumferential longitudinal shear, and corresponding time-to-peak-values expressed as %AVC.
(4) Runs a quality check on resultant data sets to highlight noisy or unexpected curves for further checking by the operator before accepting the final output.

Before the programs can be run, several variables are required to be uploaded and also manually entered. These included:

- Aortic valve closure time for the bSSFP cine images in the 3ch, LVOT and Ao Short axis (Ao SAX) views. (Manual input)
- The R-R interval for the bSSFP cine images in the 3ch, LVOT and Ao SAX views. (Manual input)
- Cross-sectional area throughout the cardiac cycle of the base and apex. ROI export tool on OsiriX used to export data from epicardial contours. (Manual upload)
- Deformational data from Intag or FT. (Manual upload)

3.6.5 Results

The average age of the volunteers was 40.3 ± 16.6 years

8 were female, 7 male.

The average LV EF was 61.6 ± 3% and an end diastolic volume of 155.6 ± 30.2 mls. A second rater also analysed EF and LV volumes and the average was 62.5 ± 3.6 % and 155.6 ± 30.2 mls.

Inter-observer variability is shown by a Bland Altman plot in figure 53.

Figure 53. Bland Altman plot of left ventricular ejection fraction between two raters.

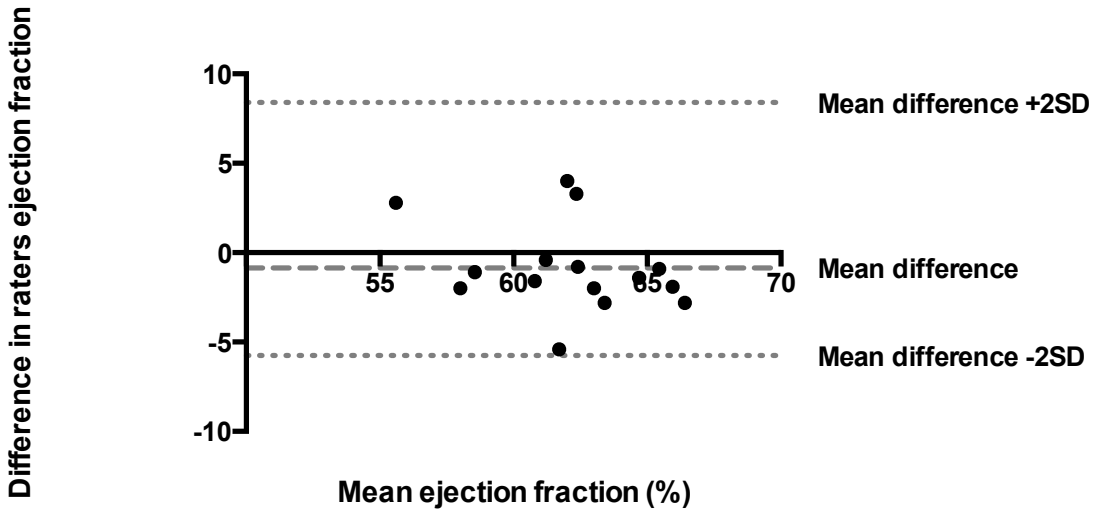

Overall rater agreement was good with the majority of measurements within 2 standards deviations of mean difference.

Effect of dobutamine on strain

Radial and circumferential strain was measured by Intag and FT software, whilst longitudinal strain was measured by FT only. This is because a 4 chamber tagged image was not used (due to time constraints for normal volunteer study). Measurements were at baseline, 7.5mcg and 15mcg dobutamine infusions.

Figures 54, 55 and 56 show the strains measured using FT and figures 57 and 58 show those measured by Intag software.

Figure 54. Longitudinal strain in 4-chamber view at 0, 7.5 and 15mcg dobutamine measured by CMR-FT.

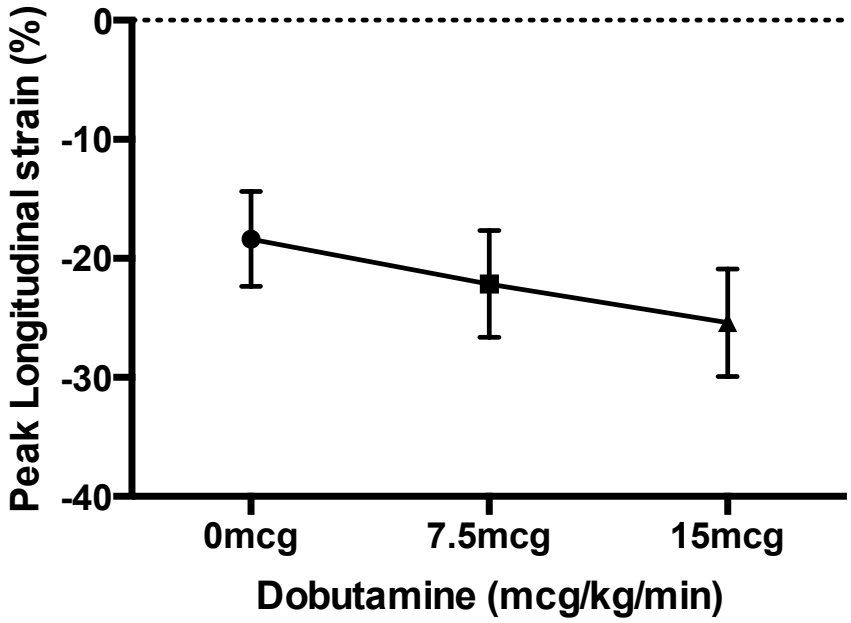

Figure 55. Circumferential strain for the mid-ventricular short axis slice, at 0, 7.5 and 15mcg dobutamine concentrations measured by CMR-FT.

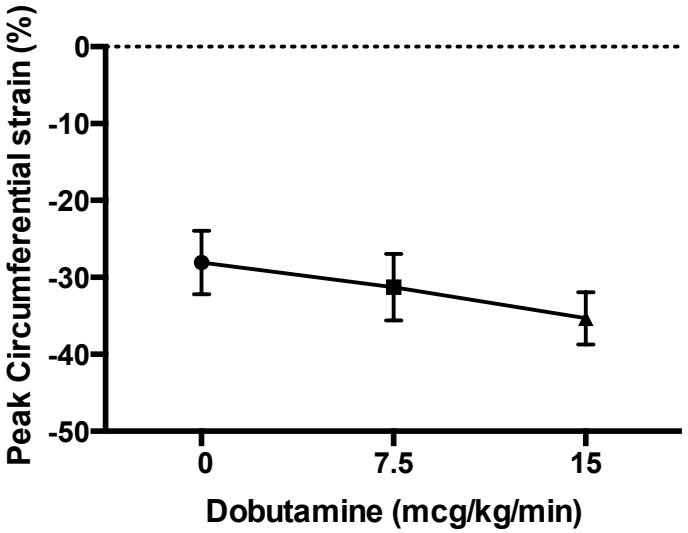

Figure 56. Radial strain in short axis at 0, 7.5 and 15mcg dobutamine concentrations measured by CMR-FT.

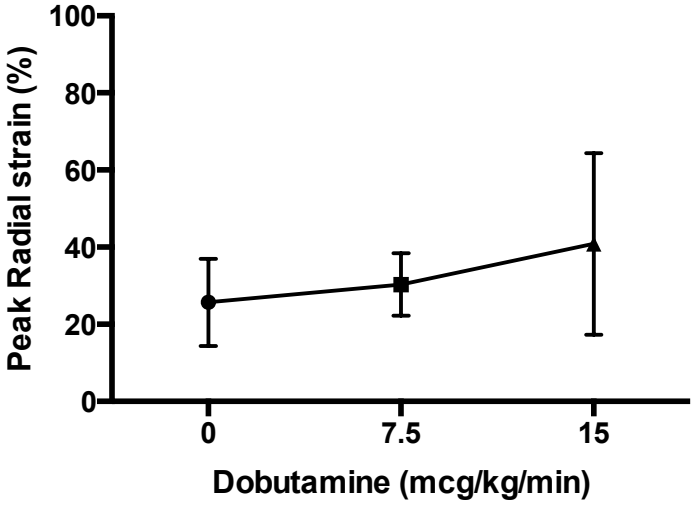

Figure 57. Circumferential strain in short axis at 0, 7.5 and 15 mcg dobutamine concentrations measured by Intag.

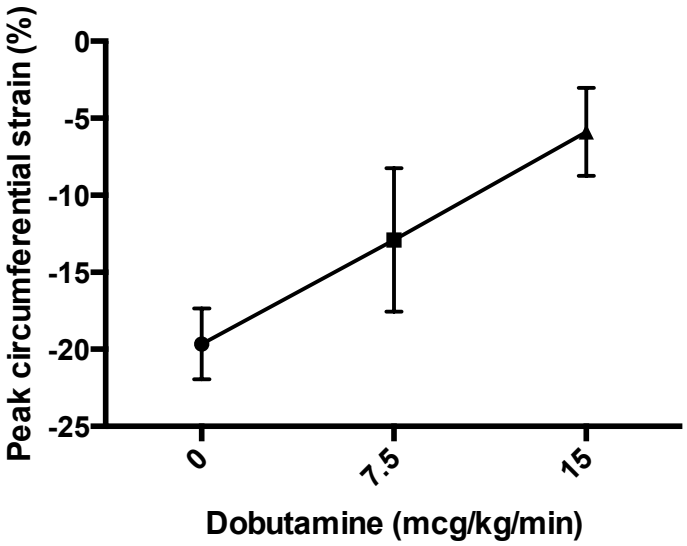

Figure 58. Radial strain in short axis at 0, 7.5 and 15mcg dobutamine concentrations measured by CMR-FT.

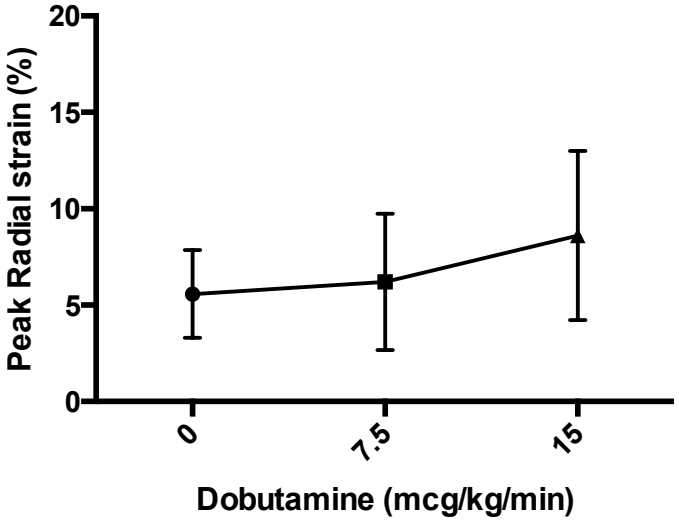

A one-way repeated measures ANOVA was conducted to compare the effect of dobutamine on peak longitudinal strain, circumferential strain and radial strain for CMR-FT. (Table 17)

The data set for Intag derived measures was not complete because the software had difficulty in processing all the values. This meant a repeated measures ANOVA was not possible. A two-tailed paired T test was performed for the baseline and peak dobutamine doses.

Table 17. Strain measured using Intag and CMR-FT.

		Dose of dobutamine (mcg)			ANOVA		T test 0 to 15mcg
		0	7.5	15	F	P	
Peak Longitudinal strain (%)	CMR-FT	-18.4%±4	-22.1%±4.5	-25.4%±4.5	F (1.641, 22.98) = 18.63	p<0.0001	p<0.0001
Peak Circumferential strain (%)	CMR-FT	-28.1±4.1	-31.3±4.3	-35.3±3.4	F(1.75, 24.56) =31.5	p<0.0001.	p<0.0001
	Intag	-19.7±2.3	-12.9±4.7	-5.9±2.9	*		p<0.0001
Peak Radial strain (%)	CMR-FT	25.7±11.3	30.3±8.2	40.9±23.5	F(1.38, 19.34) = 3.8	p=0.055	p=0.04
	Intag	5.6±2.3	6.2±3.5	8.6±4.4	*		p= 0.11

* incomplete data set so ANOVA not performed

A Pearsons r correlation was performed on the strain indices and is shown in table 18.

Table 18. Pearsons correlation on the strain measured with CMR-FT.

		Pearsons correlation		
		n	**r**	**P value**
Peak Longitudinal strain (%)	CMR-FT	45	-0.565	<0.01
Peak Circumferential strain (%)	CMR-FT	45	-0.6	<0.01
	Intag	40	0.847	<0.01
Peak Radial strain (%)	CMR-FT	45	0.375	0.01
	Intag	40	0.343	0.03

The peak longitudinal strain and circumferential strain when measured by CMR-FT showed a strong negative correlation, which was significant. Since strain is a negative value, it means the higher the dose of dobutamine, the more negative the strain value is i.e. a greater strain.

Peak radial strain showed a moderate positive relationship to dose of dobutamine for both CMR-FT and Intag measurements, which was significant.

Peak circumferential strain measured by InTag showed a strong positive relationship, which was significant. Since strain is a negative number, as the dobutamine increased the value of the strain measured by Intag decreased. This is the opposite of what was measured using CMR-FT. Possible reasons for this are explored in the discussion section.

The values obtained for circumferential strain differed between the two methods. A Bland Altman plot was performed for each dose of dobutamine, comparing the values obtained from Intag and CMR-FT. These are shown in figures 59, 60 and 61.

Figure 59. Bland Altman plot of the peak circumferential strain measured by Intag compared to CMR-FT at 0mcg dobutamine.

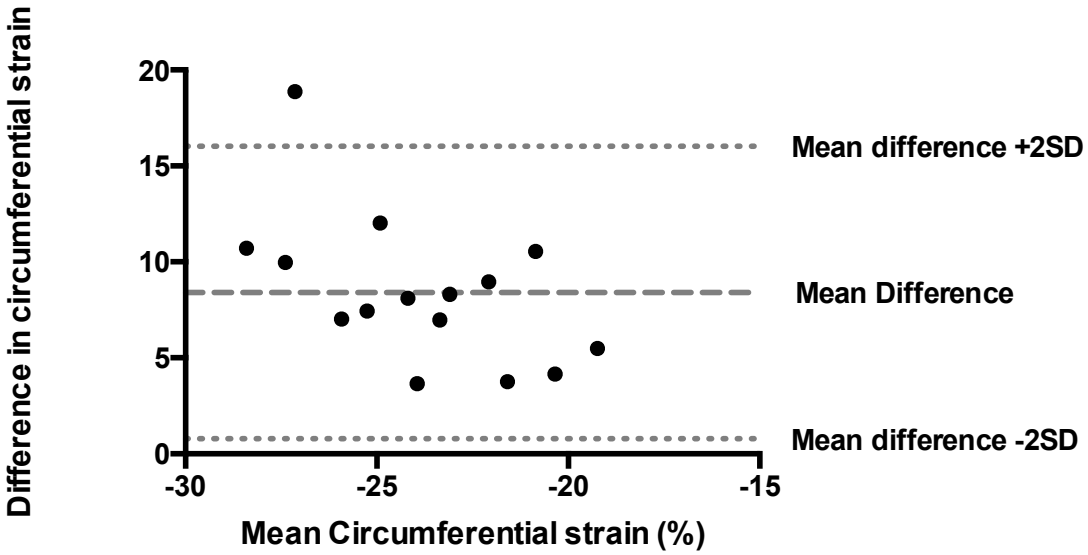

Figure 60. Bland Altman plot of the peak circumferential strain measured by Intag compared to CMR-FT at 7.5mcg dobutamine.

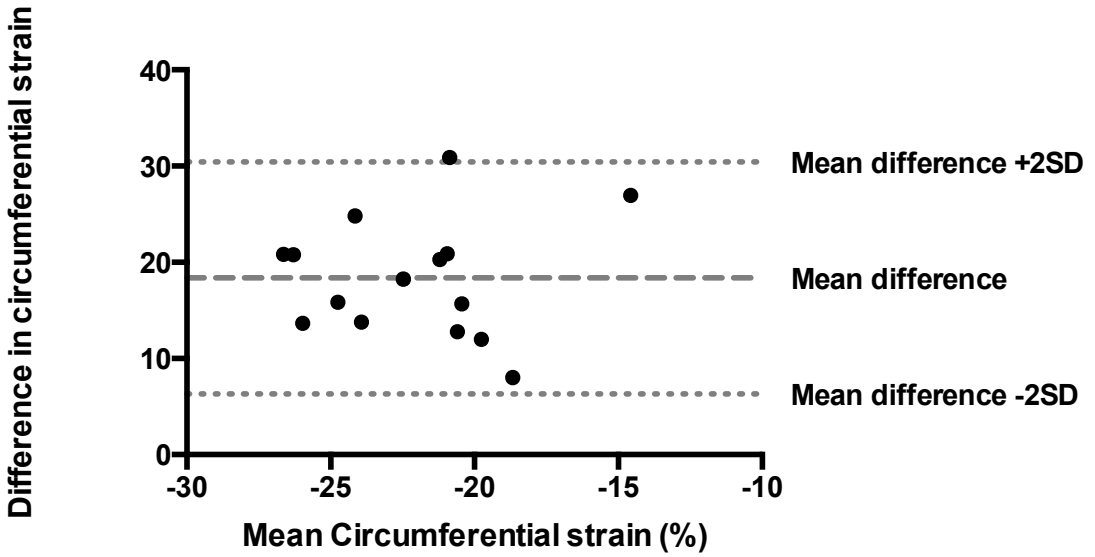

Figure 61. Bland Altman plot of the peak circumferential strain measured by Intag compared to CMR-FT at 15mcg dobutamine.

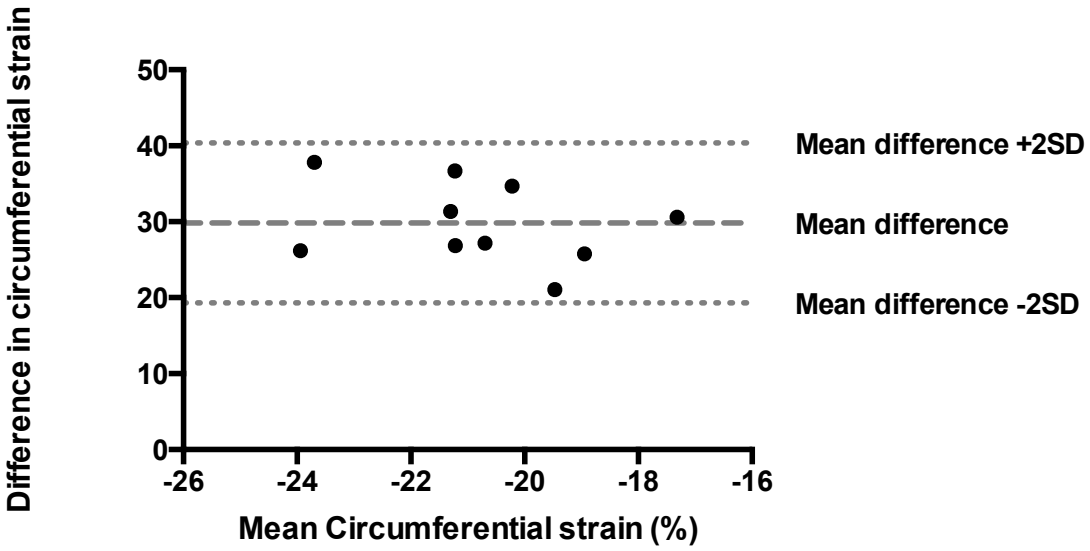

Effect of dobutamine on Twist and Torsion

Using in-house software Twist and Torsion were both calculated from data derived from Intag and CMR-FT.

The effect of increasing dobutamine is illustrated in figures 62-64 a-d.

A one-way repeated measures ANOVA was conducted to compare the effect of dobutamine on Twist and torsion measured. A Pearson correlation was also calculated and shown in table 19.

Figure 62. Effect of increasing dobutamine concentration on twist measured by CMR-FT and Intag.

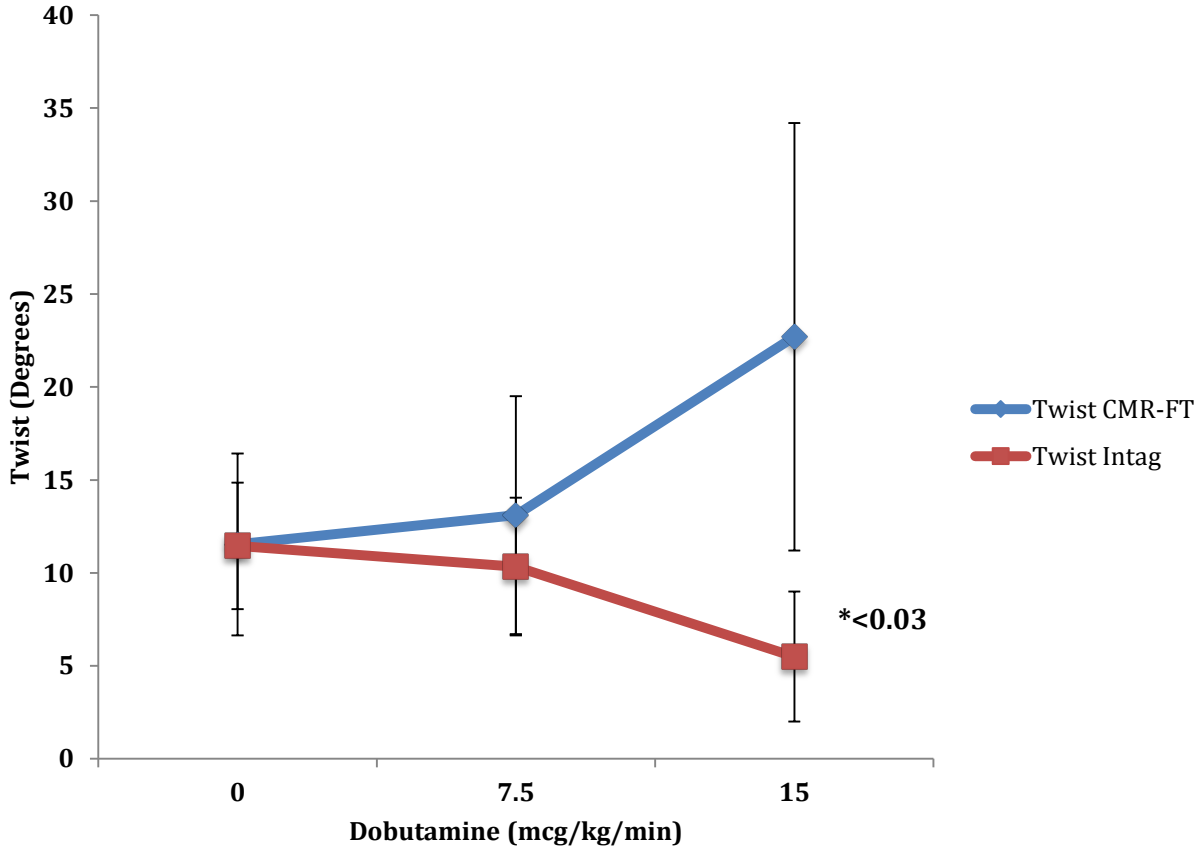

Figure 63. Effect of increasing dobutamine concentration on torsion measured by CMR-FT and Intag

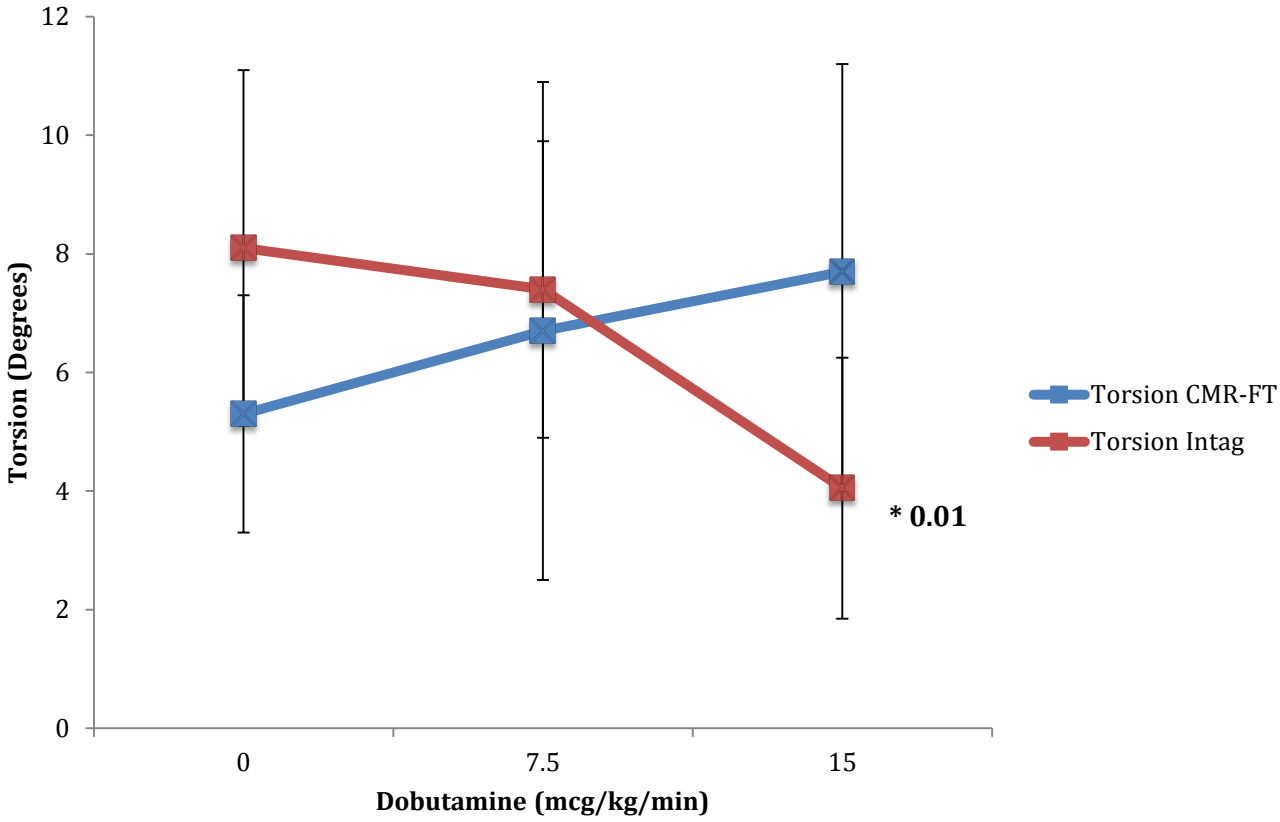

Table 19. Pearsons correlation and ANOVA on the twist and torsion measured .

		Dobutamine (mcg)			ANOVA		Pearson correlation	
		0	7.5	15	F	p	r	p
Twist	CMR-FT	11.53±4.9	13.1±6.4	22.7±11.5	(1.56, 14.02) = 3.4	0.07	0.497	0.001
	Intag	11.45±3.4	10.34±3.7	5.5±3.5	(1.66, 18.26) = 10.42	0.002	-0.563	<0.01
Torsion	CMR-FT	5.3±2	6.7±4.2	7.7±3.5	(1.36, 10.86) = 1.08	0.35	0.288	0.075
	Intag	8.1±3	7.4±2.5	4.05±2.2	(1.68, 11.78) = 7.3	0.01	-0.494	0.002

To determine the variation between the measurements derived from Intag and CMR-FT Bland Altman plots were performed for the twist and torsion at each dobutamine dose. (Figures 66-71)

Figure 64. Bland Altman for Twist at 0mcg dobutamine

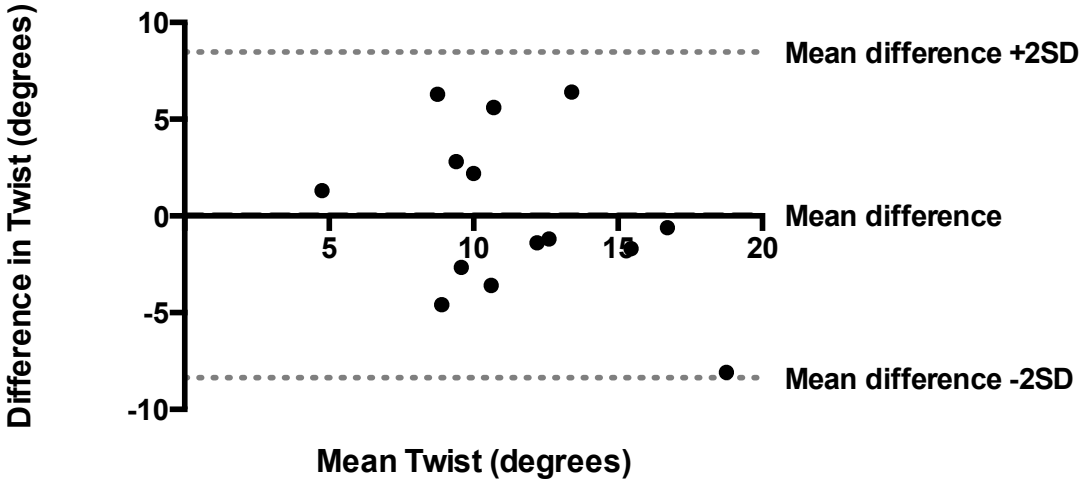

Figure 65. Bland Altman plot for twist at 7.5mcg dobutamine

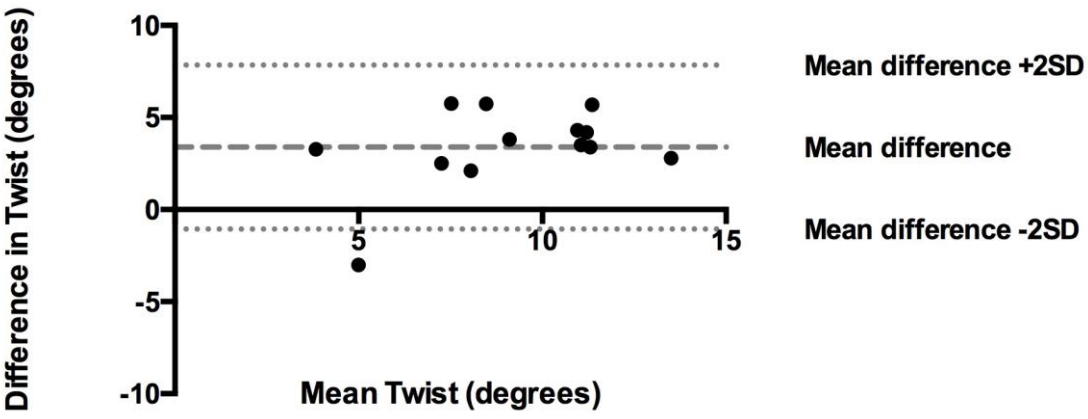

Figure 66. Bland Altman plot for twist at 15mcg dobutamine

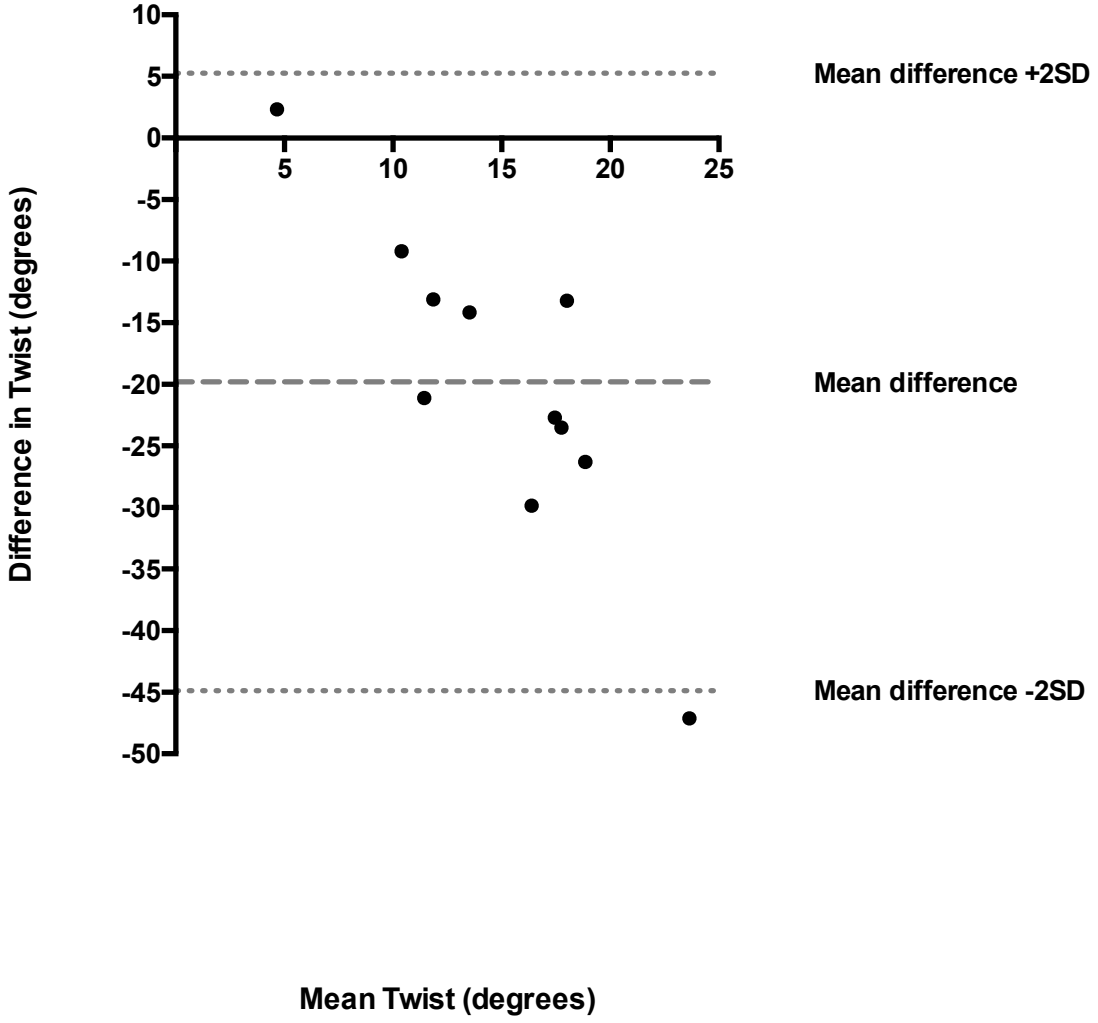

Figure 67. Bland Altman plot for torsion at 0mcg dobutamine

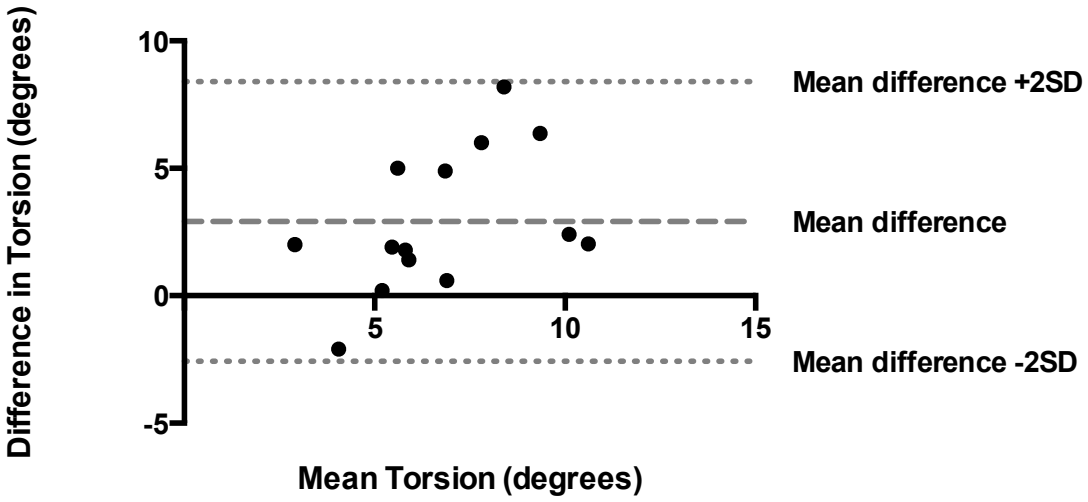

Figure 68. Bland Altman plot for torsion at 7.5mcg dobutamine.

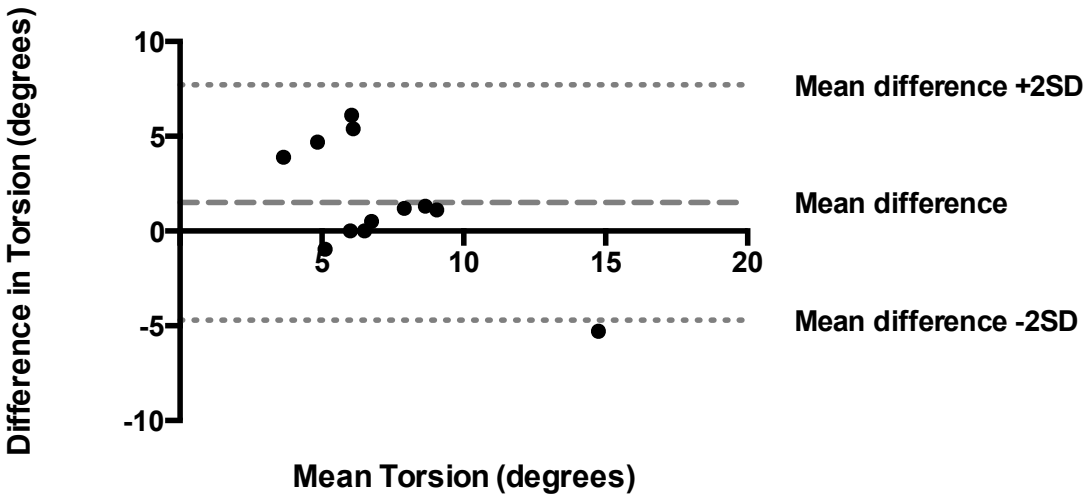

Figure 69. Bland Altman plot for torsion at 15mcg dobutamine.

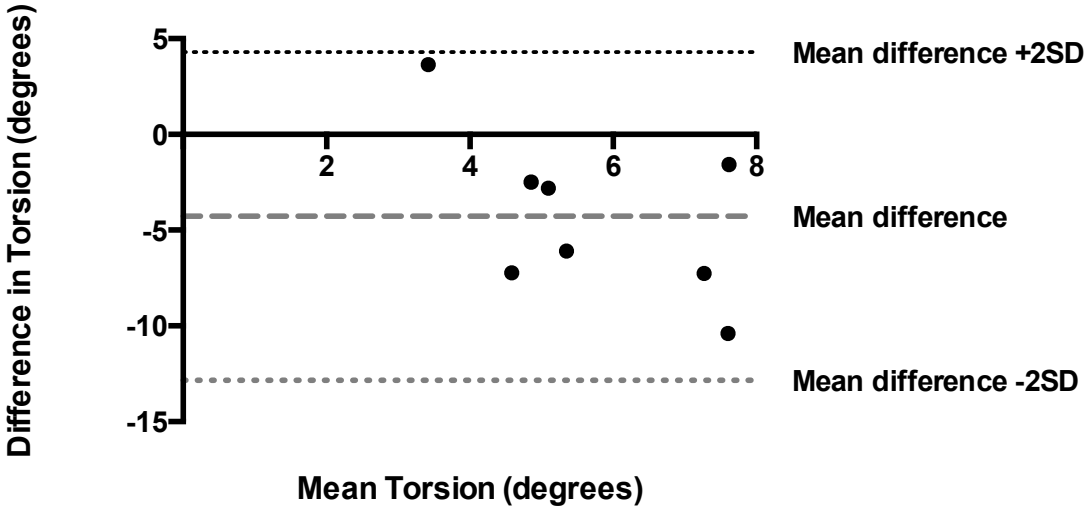

3.6.6 Discussion

This study on 15 healthy volunteers was important to carry out because validation of the two analysis packages was required when used in conjunction with our in-house developed software.

The cohort was seen to have a normal EF 61.6 ± 3% with excellent inter-rater agreement, as illustrated by the Bland-Altman in figure 53.

Dobutamine is a beta agonist acting on alpha-1, beta-1 and (receptors in heart- look up) leading to both a chronotropic and inotropic response. A chronotropic response was observed with a mean HR of 68±9bpm at baseline and 102±20bpm, $p<0.01$.

Subjective visualization of the images showed increased force of contraction with increasing dobutamine concentrations. All 3 strain indices when measured using CMR-FT, showed a dose response relationship with dobutamine. As the dose of dobutamine increased, so did the magnitude of strain measured. A strong correlation was seen with longitudinal and circumferential strain and a moderate correlation with radial strain. Longitudinal and circumferential were negative correlations because strain is a negative number, so the strain becomes more negative with increasing dose, thus the strain is greater.

When measured using InTag, both circumferential and radial strain showed the opposite relationship with increasing dobutamine dose. This appeared to go against what a normal physiological response would be and that observed with CMR-FT. One explanation could be that the construction of tag lines occurs in diastole and that during systole there is a dropout of these lines. With an increased heart rate, it is possible that increased drop out of tag lines means a lot of information of the underlying myocardium is lost. The more drop out, the greater the amount of

information would be lost and therefore the deformation may be recorded as much less than it really is.

Comparison of the two methods for circumferential strain using BA plots showed that as dobutamine increased the mean differences between the plots increased. At baseline, the mean difference between InTag and CMR-FT was 8.4%, which was relatively consistent between the healthy volunteers. The way in which myocardial deformation is calculated using the two methods is different, CMR-FT tracking the endocardial surface where as tagging utilizes information from the myocardium. If there is a consistent difference between the two methods at baseline, if the same applies in a disease process as long as there is not a significant tachycardia then clinically the difference would be acceptable.

Twist and torsion showed a similar dose relationship with dobutamine when comparing measures derived from InTag and CMR-FT. CMR-FT showed a strong positive correlation with increasing dose of dobutamine for twist and a weak positive correlation for torsion, p 0.001 and 0.075 respectively. Intag showed a strong negative correlation fro twist and torsion $p<0.001$ and 0.002 respectively. A possible explanation for this would on similar lines to that given for strain with tag lines disappearing during the more rapid onset of systole. The torsion data derived using InTag may be more susceptible to error than the CMR-FT because data from more programs is required. Whilst the radius is taken directly from the CMR-FT software, the radius has to be extrapolated from contours drawn in OsiriX for the InTag derived torsion used in our in-house software. The level of the SSFP slice used to draw the contour may not be identical to the tagged slice either. These errors would contribute to differences but one would presume these would have a small effect and these alone would not explain the large differences noted.

At baseline there was little difference seen in twist and torsion measured by either method. In fact as the BA plots demonstrate the mean difference was close to 0 for twist with most values clustered around it, with narrow 95% confidence intervals. The mean twist was 11.53±4.9 compared to 11.45±3.4 for CMR-FT and Intag respectively, p = 0.96 (t-test). The mean difference in torsion was only 2.9, with a mean torsion of 5.3±2 compared to 8.1±3, p = 0.002, for CMR-FT and Intag respectively. The value for torsion was greater using InTag than CMR-FT may relate to how the data was processed using the in-house software and the fact that to calculate torsion with InTag required data from OsiriX as well. The data sets generated by the 2 softwares were very different and completely different coded programs were required fro our in-house software. Although the same equations were used, the differing nature of the data may result in a systematic difference in torsion between the 2 methods.

3.6.7 Conclusions

CMR-FT was able to measure strain, twist and torsion, with the expected increase in these indices with dobutamine concentration.

Intag is probably effected by increases in heart rate and becomes less accurate as the RR interval shortens.

At baseline, twist was directly comparable between the 2 methods using the in-house software. Twist may be a more reliable measure currently with this software.

Chapter 4.Septal versus Apical pacing.
Acute Study.

Chapter 4. Septal versus Apical pacing- Acute Study

4.1 Patient Cohort

A total of 50 patients were recruited and implanted with the dual ventricular site PPM. The average age of the patient's was 67.4 ± 8 years, with 60% being male. The demographics, past medical history and medications of the patient cohort are given in tables 20, 21 and 22.

Table 20. Patient cohort enrolled into MAPS trial.

Age (years)		67.4 ± 8
Gender	Male	30
	Female	20
Ethnicity	Caucasian	50
	Other	0
BMI		30.8±5.2
Smoking status	Current	3
	Ex	17
	Never	30

Table 21. Significant past medical history.

Condition		Number
Ischaemic heart disease		5
Hypertension		30
Diabetes	Insulin	0
	Oral medication	7
	Diet controlled	3
Cerebrovascular disease		4
Previous MI		0

Table 22. Medications taken by patients at enrolment.

Drug		Number
Angiotensin converting enzyme Inhibitor		22
Beta-blocker		23
Digoxin		11
Calcium Channel blocker		18
Amiodarone		2
Loop diuretic		14
Statin		20
Aspirin		4
Anticoagulant	Warfarin	44
	Sinthrone	1
	New oral anticoagulant	2

4.2 Baseline exercise capacity

Baseline exercise capacity was assessed for all patients by means of a CPEX test and/or 6MWT. Some patients who were unable to do a CPEX just did the 6MWT. Baseline investigations took place following the AV node ablation, so the patients were dependent on the PPM. Due to logistical constraints it was not possible to perform the 6MWT and CPEX on the same day as well as the CMR scan. The 6MWT took place at pacing clinic ± 1 week of the CMR scan. The CPEX was performed after the CMR scan. Table 23 and 24 give the mean values for these investigations.

Table 23. 6MWT baseline. N=50.

Parameter	
Metres covered (m)	366.5 ± 121
Resting HR (BPM)	64 ± 6
Heart rate max (BPM)	81 ± 15.7
Borg score	13.3 ± 2.1

Table 24. CPEX baseline. N=37.

Parameter	
VO2 Max (ml/kg/min)	18.41 ± 6.3
Anaerobic threshold (L/min)	1.26 ± 0.51
O2 pulse (mls/beat)	17.06 ± 5.2
Resting Heart rate (BPM)	66.2 ± 3.3
Heart rate max (BPM)	104.9 ± 24.3
VE max (L/min)	69.1 ± 26.7
Max Respiratory rate (breaths/min)	33.1 ± 5.65
RQ max	1.08 ± 0.1

4.3 Quality of life

Quality of life was assessed using the SF-36 questionnaire. Prior to the implant and AVN ablation all patients completed the questionnaire. The mean total mental health score was 62 ± 21 and physical health was 52 ± 225, with a mean total score of 58 ± 21. Table 25 gives the full category breakdown.

Table 25. Baseline quality of life using the SF-36 questionnaire.

Category	Out of 100
Physical function	55 ± 29
Role physical	37 ± 39
Body pain	64 ± 28
General health	60 ± 18
Vitality	44 ± 23
Social functioning	70 ± 24
Role emotional	64 ± 40
Mental health (subcategory)	73 ± 21
Total Physical health	52 ± 22
Total Mental health	62 ± 21
Total SF36	**58 ± 21**

4.4 RV Lead positions.

Whilst every attempt was made to place the pacing leads in the optimal position, namely RVOT septum and RV apex, the patient anatomy, lead stability and pacing parameters dictated the final positioning achieved. Using imaging data from fluoroscopy and CMR, I retrospectively determined the location of the right ventricular leads. A grading system was used to determine how optimal each individual lead was and the combination of the lead pair.

4.4.1 Fluoroscopy

As described in the methods, three projections in the catheter lab were used to guide the positioning of the ventricular leads to the RVOT septum and RV apex. Using the classification described in the paper by Mond, (132) the stored fluoroscopic views were analysed and the RV lead positions determined. In the 50 patients, 48 had a successful RVOT placement and 45 a successful true apical lead placement. Out of the 48 RVOT leads 28 were directed to the RVOT septum and 20 directed to the RVOT anterior wall. Table 26 summarises the lead positions based only on fluoroscopy.

Table 26. Lead positions determined by fluoroscopy.

Superior Lead					Inferior lead	
RVOT septum	RVOT anterior wall	High ventricular septum	Mid ventricular septum	Apex	Ventricular septum	Inferior wall
28	20	1	1	45	2	3

N=50

4.4.2 Cardiac MRI

The quality of lead placement was graded with the use four dedicated CMR SpGr cine sequences performed during each scan. SpGr sequences were used because leads were more easily visualized on these views. A 4-chamber view and a RV 2-chamber view were used to grade the apical lead position. A RVOT view and a RV in/out view were used for the RVOT lead position. A grading system of 1 to 3 was used (1 ideal position, 2 reasonable position, 3 not ideal position) for the four views. Figures 72 to 75 demonstrate the grading system in the four views with a corresponding SpGr image with a grade 1 position.

Figure 70. Right ventricular 2-chamber view (RV apical lead position) 1 ideal position, 2 reasonable position, 3 not ideal position.

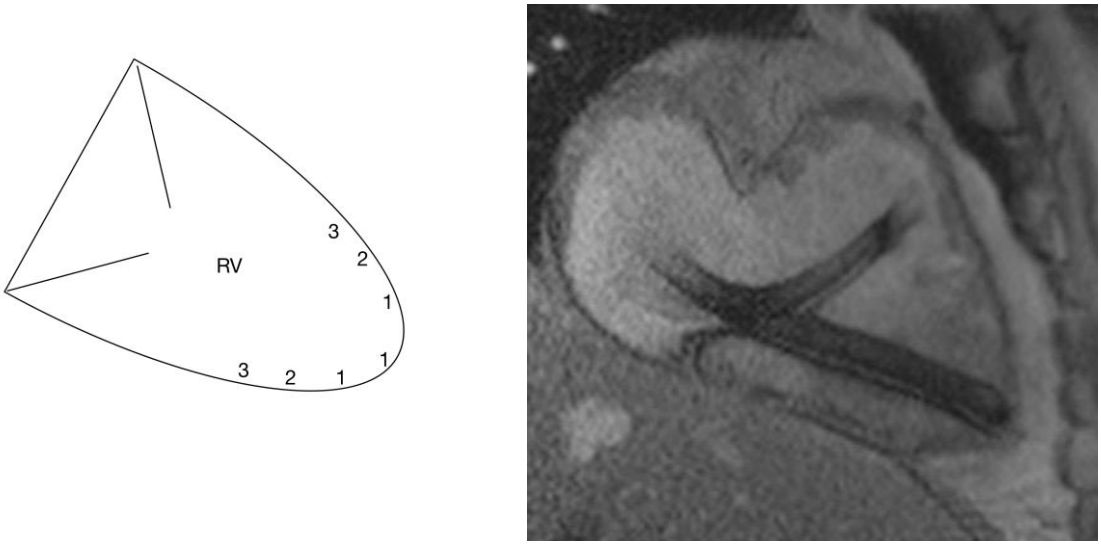

Figure 71. 4-chamber view (RV apical lead position).

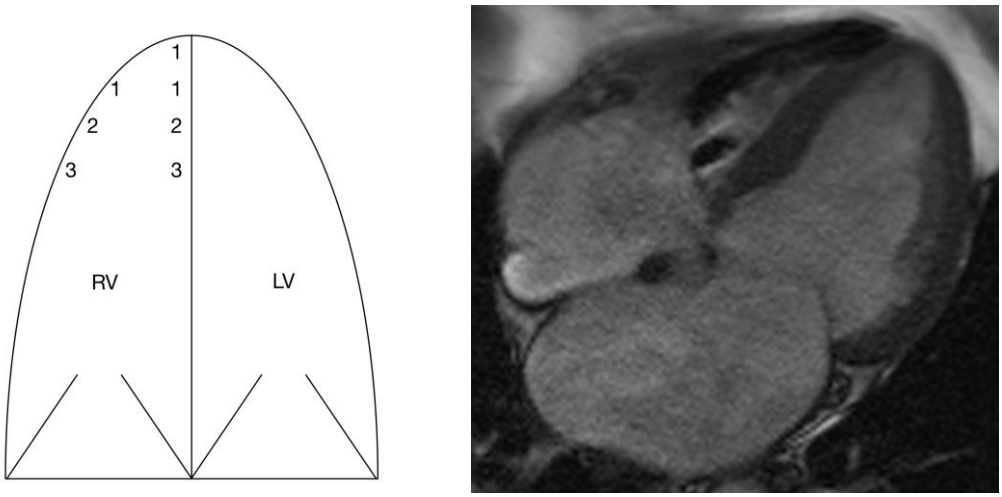

Figure 72. Right ventricular in/out view (RVOT lead position).

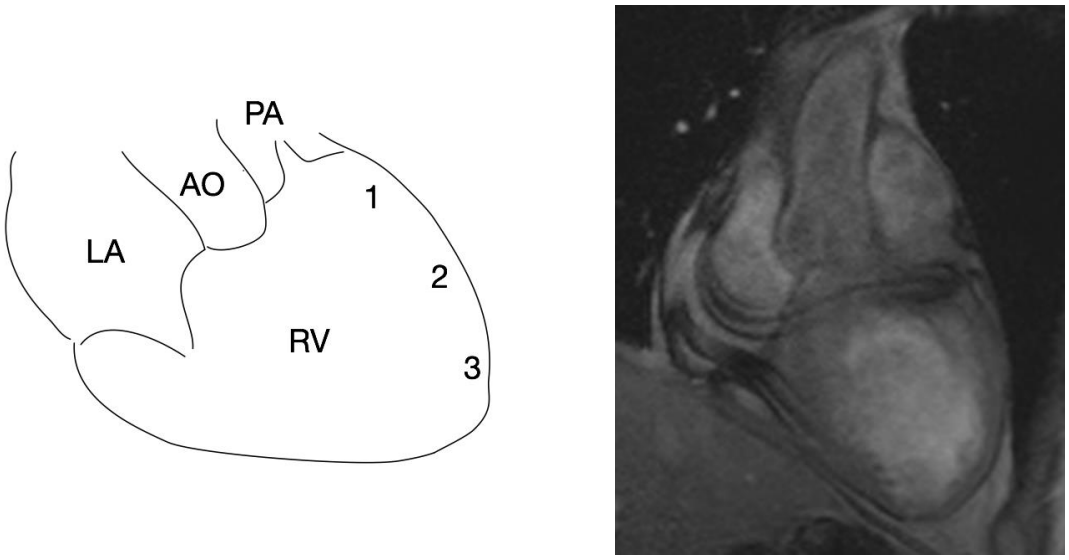

Figure 73. RVOT view (RVOT lead position).

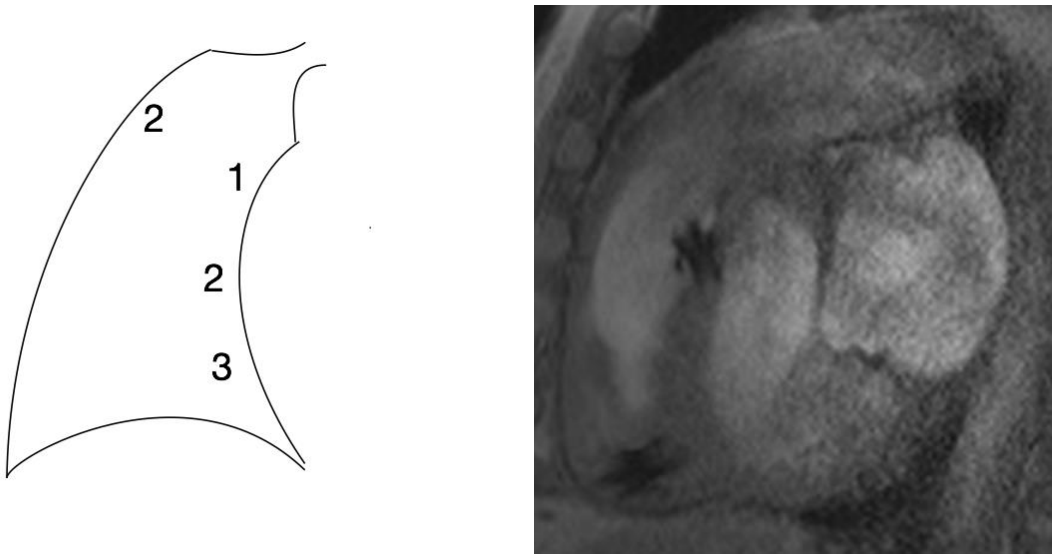

The two scores for each lead were averaged to give a value between 1 and 3. (Table 27). Analysis was performed by myself (MA) on two separate occasions and by a second experienced MR clinician (MS).

A kappa analysis was performed to give both the intra-observer and the inter-observer variability between myself (MA) and another experienced MR clinician (MS) for each of the scores. For the apical lead intra-observer variability was 0.625, inter-observer variability was 0.75. For the RVOT view the intra-observer agreement was 0.674, and inter-observer agreement was 0.614.

Table 27. Grading of RV lead positions by two observers.

SCORE	**APICAL LEAD**			**RVOT lead**		
	Observer 1	Observer 1 (repeat analysis)	Observer 2	Observer 1	Observer 1 (repeat analysis)	Observer 2
1	35	38	38	17	17	21
1.5	8	6	5	19	16	11
2	5	4	6	12	17	18
2.5	1	2	0	1	0	0
3	1	0	1	0	0	0

Because the study was concerned with comparing one pacing position to another, I sought to identify the quality of the pairings of the leads. A composite score was generated, by adding the mean apical score to the mean RVOT score. The lowest score would be 2 for the perfect combination of leads, with a maximum score of 6 for the worst combination of leads.

A score of ≤ 2.5 was considered excellent, > 2.5 and ≤ 4 satisfactory and > 4 unsatisfactory. The distance between the lead tips was also measured on a PA CXR for all patients. The scores and mean distances in each group are shown in table 28. Although the distance is measured in 2D, those leads deemed to be an excellent combination are the furthest apart.

Table 28. Combination of leads.

Lead combination rating by CMR	Number of patients	Distance between leads (cm) on PA CXR
Excellent	25	78.9 ± 22.2
Satisfactory	22	62.2 ± 15.2
Unsatisfactory	3	45.7 ± 5.5

4.5 ECG

The 12 lead ECG was recorded for both lead positions in every patient. The mean QRS duration for the RVOT lead was 141.1 ± 10ms and the apical lead was 150.4 ±9.3ms, p<0.001. The cardiac axis was +4° in the RVOT group and -77° in the apical group, p<0.01.

Using the CMR graded positions; the mean difference in QRS durations was determined for the excellent, satisfactory and unsatisfactory lead combinations. (Table 29)

Table 29. Comparing QRS durations for each lead combination category.

Lead combination rating	RVOT	APICAL	Mean difference between RVOT and Apical QRS	P value
Excellent N=25	141 ± 10.4	150.7 ± 9	9.3	<0.001
Satisfactory N=22	140.3 ± 10	148.6 ± 9	8.3	0.002
Unsatisfactory N=3	145 ± 5	155 ± 8.7	10	0.2

The QRS duration was consistently lower when the RVOT lead was pacing the ventricle. The duration was significantly lower for the excellent and satisfactory categories.

4.5.1 Can the ECG determine lead positions

The direction of the QRS vector was recorded for leads I, II, III, avL, avR and avF, when the ventricle was paced from either lead. Each ECG was analysed and the QRS vector polarity in each of the six leads was determined. The results are shown in table 30.

A negative QRS vector in lead III and AVF had a 100% sensitivity and 100% specificity for an apical lead position.

Table 30. Polarity of QRS complex in apical and RVOT leads.

	APICAL		**RVOT**	
Lead	Positive	Negative	Positive	Negative
I	50	0	19	31
II	1	49	50	0
III	0	50	50	0
AvL	50	0	5	45
AvR	46	4	5	45
AvF	0	50	50	0

The literature suggests that lead I predicts a septal RVOT lead position. (132) The RVOT ECGs were subdivided into an anterior or septal RVOT position using the fluoroscopic views. On fluoroscopy 48 leads were within the RVOT.

Table 31. Lead I in RVOT positions.

	Septal	**Anterior**
Positive in I	8	10
Negative in I	20	10

For leads in the RVOT in this study a negative QRS in lead I has a sensitivity of 0.7 and a specificity of 0.5, with a positive predictive value of 1.43 and a negative predictive value of 0.57.

4.6 Image quality

The presence of image susceptibility artefact was determined in the short axis (SA), horizontal long axis (HLA) and vertical long axis planes (VLA) on cine CMR.

CMR images of patients with a left sided system had more artefact effects on the SA plane of cine CMR compared with those with a right-sided system.

Artefact was determined to be present or absent within each segment of the LV myocardium using a 16 segmental model. Artefact was further graded for each segment using a semi-quantitative approach into 0%, 1-25%, 26-50%, 51-75% and 76 to 100% values.

In the SA plane the basal segments have less artefact than either the mid or apical regions (Figure 76, 77 and 78). Artefact was present in 54% of the basal segments, 69% of the mid segments and 78% of the apical segments. Using the Cochrans Q test, the presence of artefact or no artefact was compared between the SA slices. (Table 32) The artefact between the basal segments and both mid and apical segments was statistically significant.

Table 32. Cochrans Q test.

Basal SA artefact	Mid SA Artefact	Apical SA artefact	Cochrans Q test
54%	69%		<0.001
54%	-	78%	<0.001
-	69%	78%	0.1

Figure 74. Quantification of artefact in the bSSFP short-axis basal slice.

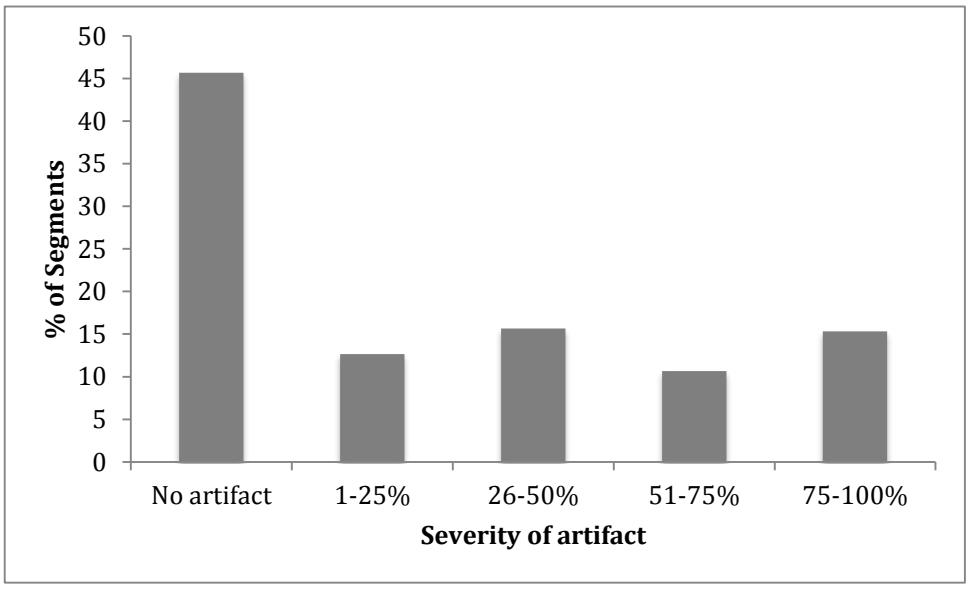

Figure 75. Quantification of artefact in the bSSFP short-axis mid slice.

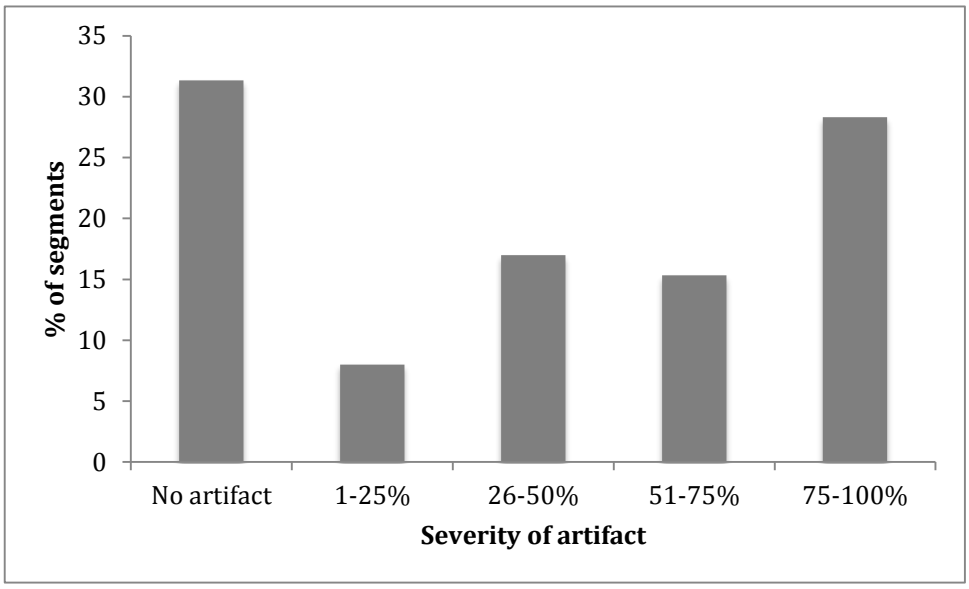

Figure 76. Quantification of artefact in the bSSFP short-axis apical slice.

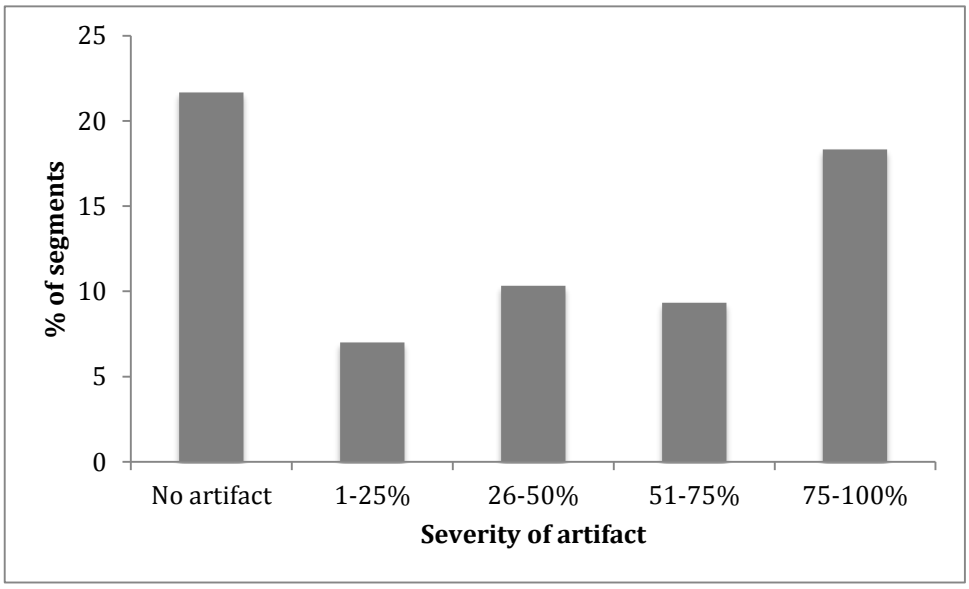

For SSFP cine images at least one segment was affected by artefact in 90% of the MR scans. SpGr cine imaging in the 4-chamber view was performed allowing a comparison between the septal and lateral segments of the two imaging sequences (Figure 79).

The artefact was significantly more pronounced on bSSFP sequences compared to SpGr sequences at basal (53% vs 11.5%, p<0.001), mid (67% vs 31%, p<0.001) and apical regions (65% vs 43%, p=0.001).

Figure 77. Comparison of artefact observed on bSSFP and SpGr sequences in the 4-chamber view at basal, mid and apical levels.

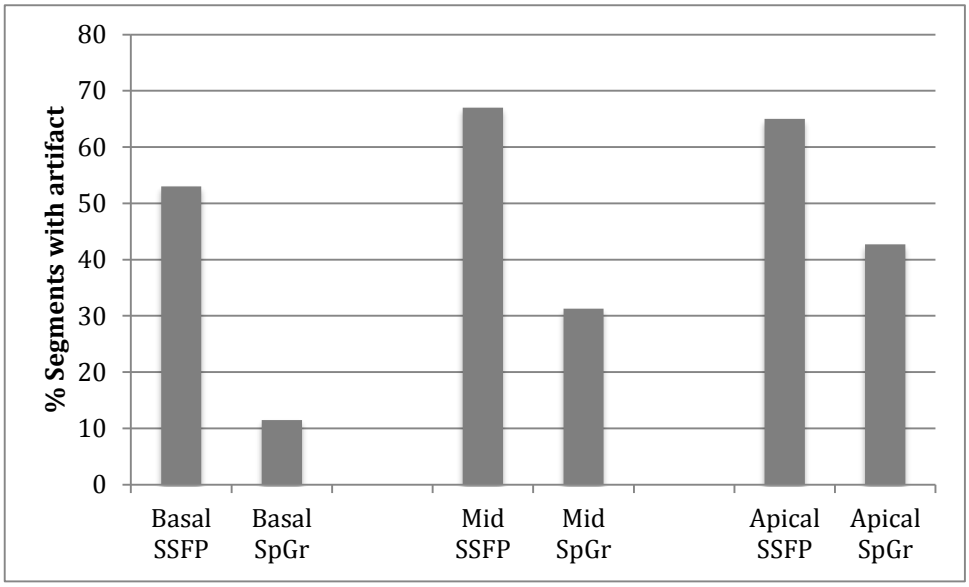

The regions most commonly affected by the metal susceptibility artefact were the anterior and anterior-septal regions within the mid SA plane (Figure 80). In 90% of the MR scans performed, artefact was present in the mid anterior segment using a bSSFP cine sequence. Whilst significant artefacts were observed in many scans, both a qualitative and quantitative assessment of LV function was deemed possible by 2 independent observers applying previously published criteria. (203)

Figure 78. Graph of the 16-segment model of the left ventricle illustrating the distribution of artefact in the bSSFP sequences.

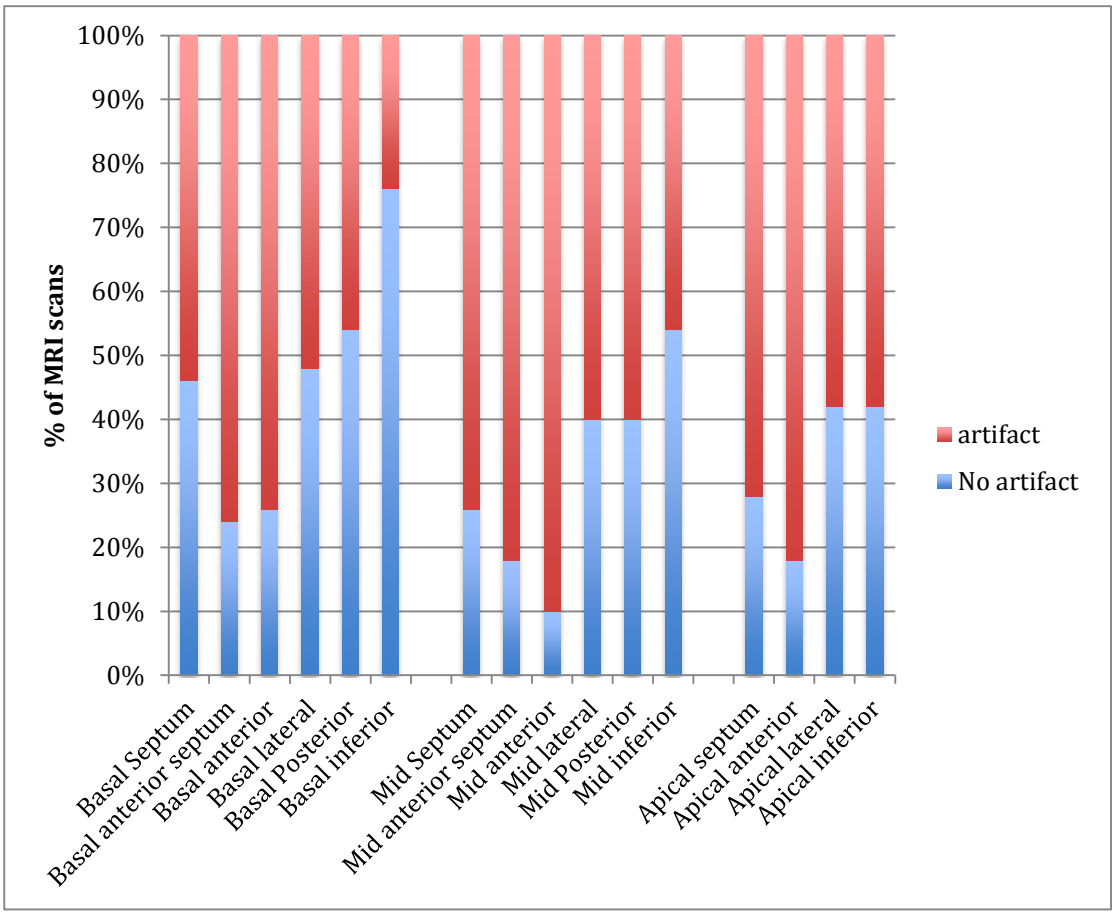

Several different imaging sequences were utilized and the degree of metal susceptibility artefact differed between the modalities as illustrated in figure 81. The relevant distribution of the artefacts was consistent between the modalities. The regions closest to the PPM generator (anterior wall and septum) were affected the most and those regions furthest away (inferior and lateral walls) the least. Using the Cochrans Q test, SpGr and tagging sequences were significantly less affected by metal susceptibility artefact when compared to bSSFP sequences (Table 30). Both T1 and T2 mapping were significantly affected by metal susceptibility artefact from the PPM generator. Late gadolinium imaging was particularly affected in the anterior segment with over 75% of MRI scans performed having artefact in this region.

Table 33. Cochrans Q test between bSSFP and other imaging sequences.

		Septal wall	Anterior wall	Lateral wall	Inferior wall
SSFP	SpGR	<0.001	<0.001	0.08	<0.001
SSFP	LGE	0.275	0.25	0.018	0.07
SSFP	T1mapping	0.083	0.317	1	0.166
SSFP	Tagging	<0.001	<0.001	<0.001	<0.001
SSFP	T2 mapping	0.617	0.013	0.366	1

Figure 79. Comparison of artefact seen in the mid short-axis slice for the different imaging sequences.

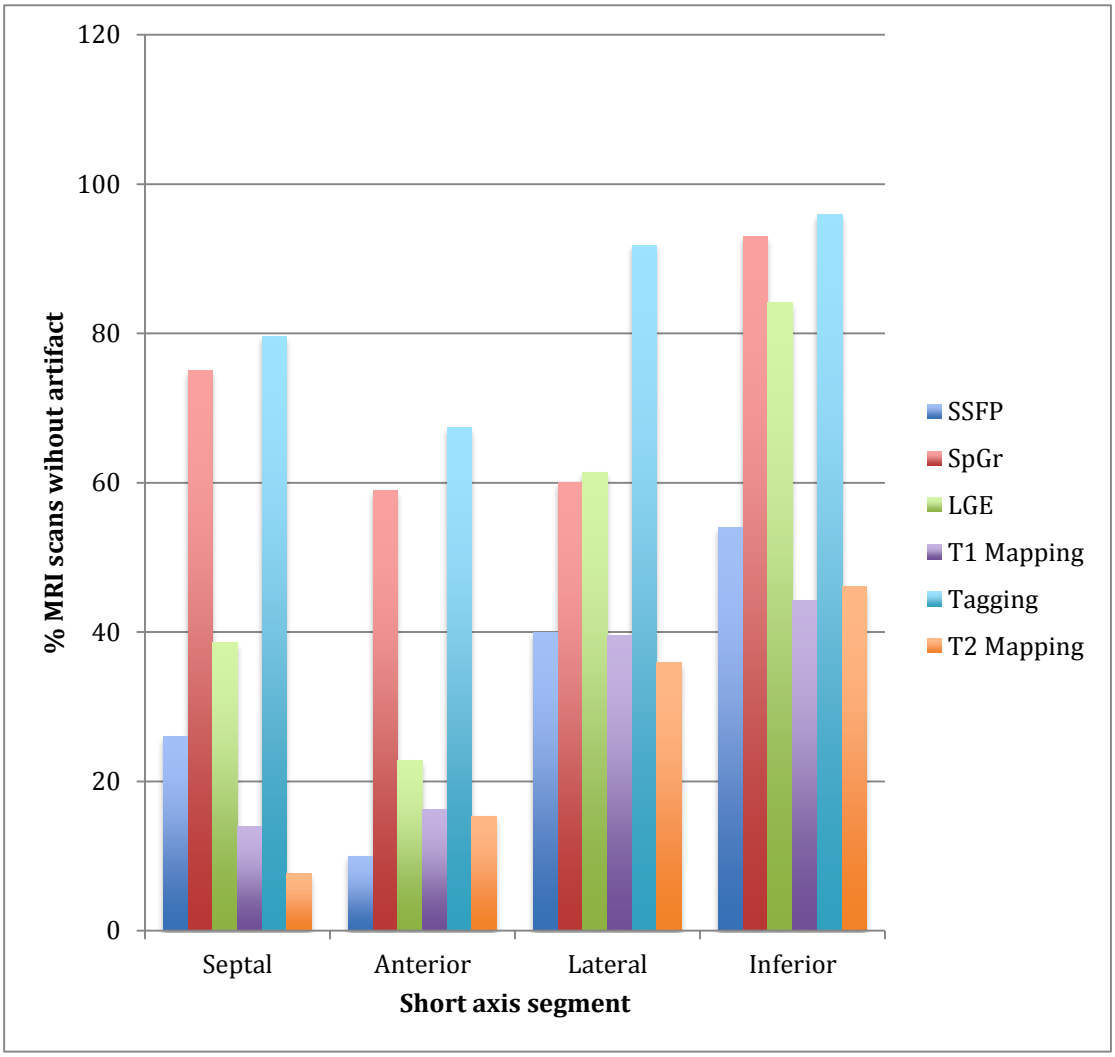

Correlation between artefact and distance from device

The mean distance between the PPM and the Left ventricle was 6.2cm ± 3.3cm, when measured on a PA CXR. This was measured between the most medial edge of the PPM generator and the right heart border of the left ventricle.

There was a negative correlation between the distance of the PPM from the heart and the artefact on the bSSFP MR images, r= -0.561, n=50, p= <0.0001. A scatterplot summarises the results (Figure 82).

The greater the distance from the generator the less artefact is present on the images.

Figure 80. Scatterplot of distance of pacemaker from the left ventricle and the mean artefact on bSSFP images.

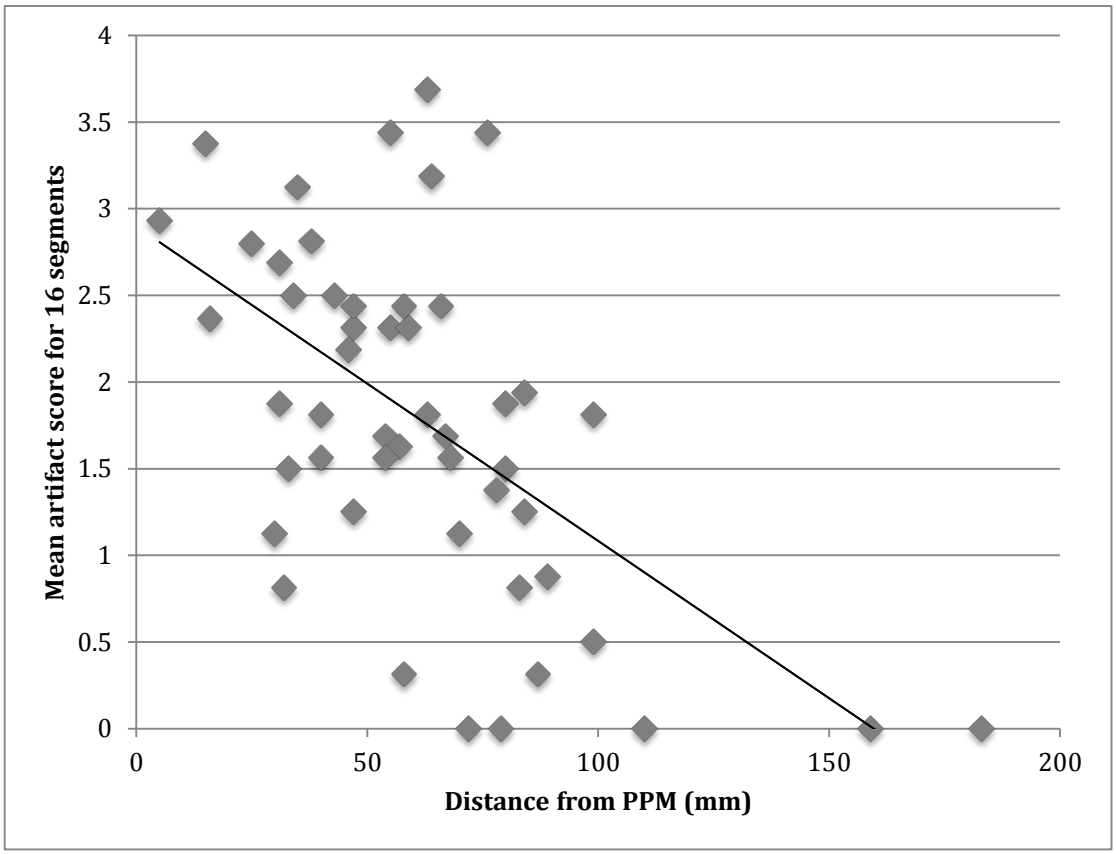

4.7 Acute Safety data

There were no significant adverse events reported during scanning. One patient felt a dragging sensation near to the device during the scan. No loss of capture was seen.

4.7.1 Pacing thresholds, impedance and battery voltage

The mean pacing threshold for the RVOT lead at implant was 0.67± 0.22V and at the 2-week check was 0.73± 0.21V. The mean pacing threshold for the apical lead at implant was 0.71± 0.29V and at the 2-week check was 0.74± 0.26V. The mean pacing impedance for the RVOT lead at implant was 739± 168Ω and at the 2-week check was 655± 251Ω. The mean pacing impedance for the apical lead at implant was 631± 130Ω and at the 2-week check was 616± 81Ω.

The mean battery voltage at implant and at the 2-week check was 3V.

The lead threshold, lead impedance and battery voltage were measured before each CMR scan, at the lead crossover stage mid-way through the scan and after the CMR scan (Table 34).

There was no clinically or statistically significant change in the threshold before and after the CMR scan. The mean difference in the lead threshold before and after the scan was 0.03V, for the RVOT lead, p=0.34 and 0 V for the apical lead, p=1.

The mean difference in impedance before and after the scan was 11Ω, p=0.009 and 4Ω, p=0.003 for the RVOT and apical leads respectively

The mean battery voltage prior to the scan, between and following the scan remained at 2.99±0.03V.

The trial cohort, by virtue of the AVN ablation would be deemed to be high-risk scan patients from a scan safety point of view.(160) This study reported no MR related adverse events in keeping with the results from the ADVISA study using a Medtronic system. (201)

The small increase in pacing capture threshold before and after the 1st MRI scan was neither statistically or clinically significant. Given the pacing dependence of this patient cohort this was very reassuring. Other studies involving scanning of the lumbar spine and brain have also found small increases in pacing thresholds after MR scanning but again these were not clinically significant. (181)

Interestingly the lead impedance was consistently lower following the MR scans for both ventricular leads and this change was statistically significant. The absolute measured differences in impedance were very small (max difference 80Ω) and are perceived as not being clinically significant. The magnetic fields may have led to an alteration in the impedance, but it is also possible that due to the long scan duration the differences reflected normal variations throughout the day.

Table 34. Lead threshold, lead impedance and battery voltage measured during acute study.

Parameter		Pre AVN ablation		CMR scan		
		Implant	2 week check	Prior to baseline scan	At cross-over	End of scan
Lead threshold (Volts)	APICAL	0.71± 0.29V	0.74± 0.26V	0.69±0.17	0.69±0.16	0.69±0.16
	RVOT	0.67± 0.22V	0.73± 0.21V	0.66±0.16	0.66±0.16	0.69±0.27
Lead Impedance (Ohms)	APICAL	631±130Ω	616±81Ω	614±81Ω	612±80Ω	610±80Ω
	RVOT	739±168Ω	655±251Ω	602±117Ω	594±114Ω	591±109Ω
Battery Voltage (Volts)		3V	3V	2.99±0.0V	2.99±0.0V	2.99±0.0V

4.7.2 Specific absorption rate

SAR is a measure of the rate at which energy is absorbed by human tissue when exposed to a radiofrequency electromagnetic field and is defined as the power absorbed per mass of tissue in Watts/Kg (W/Kg). The max SAR permitted for the ST Jude Accent PPM is 4 W/Kg. First level scanning with a max of 4 W/Kg was never exceeded. Figure 83 illustrates the SAR for each of the scan sequences averaged from 10 baseline scans.

Figure 81. Total body SAR measured for each image sequence.

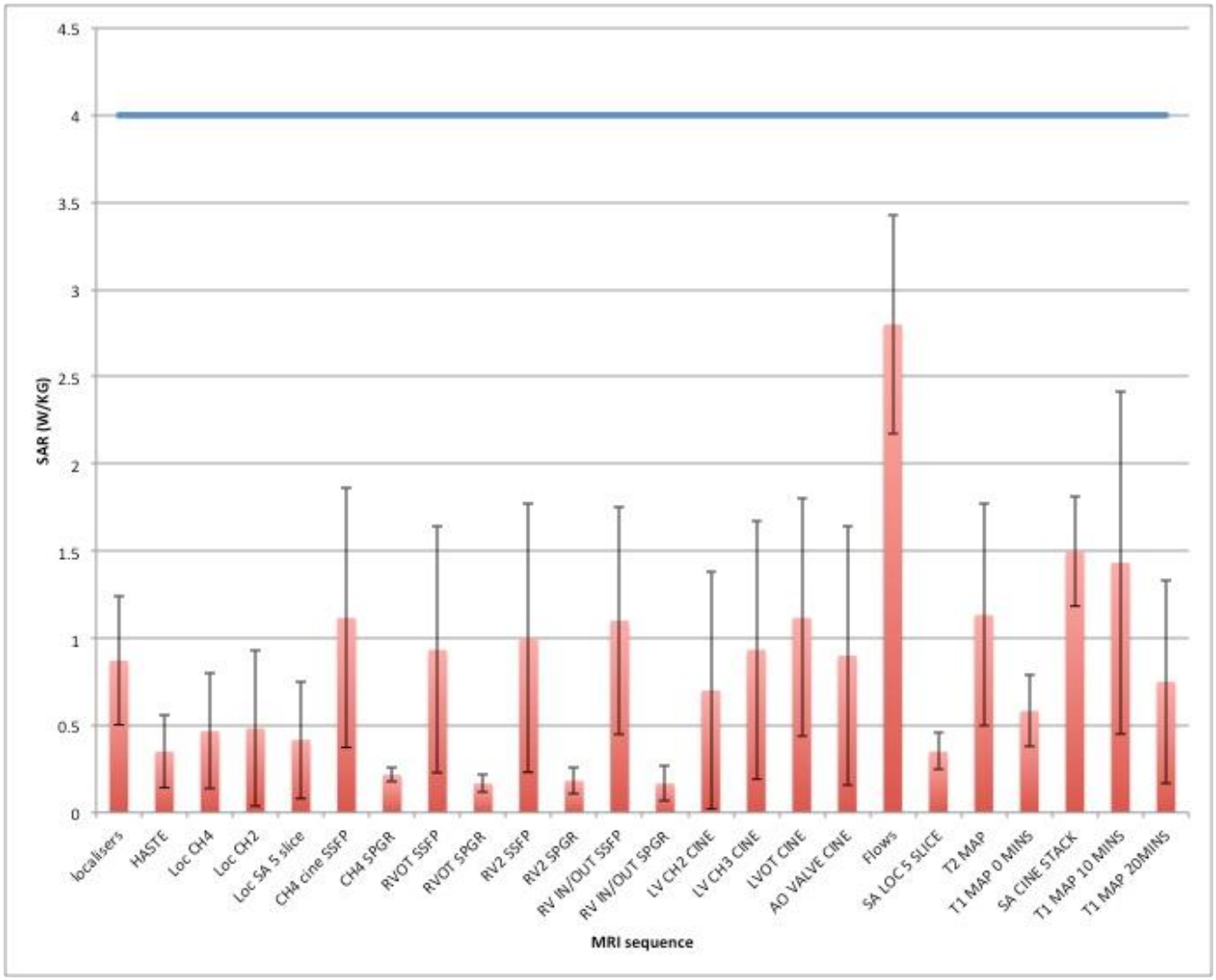

4.8 Effect of acute pacing position on heamodynamics

4.8.1 Blood pressure

The mean arterial blood pressure (MAP) is the product of the cardiac output (CO) and systemic vascular resistance (SVR) plus the central venous pressure (CVP). During the alternative site pacing the SVR and CVP are likely to be constant so acute alterations in the MAP, are potentially the result of a change in the CO. Therefore the MAP may be an indirect measure of changes in the cardiac output in the acute setting.

The MAP for the RVOT lead was 92 ± 20.8mmHG and for the Apical lead this was 90.3 ± 21.1mmHg, p= 0.14

When correcting for lead positioning, for the optimal lead combination the RVOT lead was 92 ± 10mmHg and the apical lead was 90 ± 12mmHg, p= 0.26 n=25. For acceptable lead positions, the RVOT lead was 92 ± 12mmHg and apical 91 ± 12mmhg p= 0.31 n=22. Finally for the worst lead combination the RVOT lead was 90 ± 11mmHg and the apical lead was 89± 21mmHG p= 0.94 n=3.

4.8.2 Aortic and Pulmonary flows

Phase contrast velocity encoding allowed an estimate of aortic and pulmonary flow.

The mean aortic flow was 71.5± 19mls for the RVOT lead and 70.4± 18.1mls for the apical lead, p=0.37. Pulmonary flow was 94.2± 33mls and 91.1± 26.6mls for the RVOT and apical positions respectively, p= 0.08

When correcting for lead positioning, for the optimal lead combination, the aortic flow was 74.6mls ±22.4mls and 73.8 ± 21.8mls for the RVOT and apical positions respectively, p= 0.71. For the pulmonary flow it was 100.5 ± 40.7mls and 96.9± 31mls, p=0.24.

Figure 82. Aortic and pulmonary flows for the RVOT septal and RV apical positions. N=50.

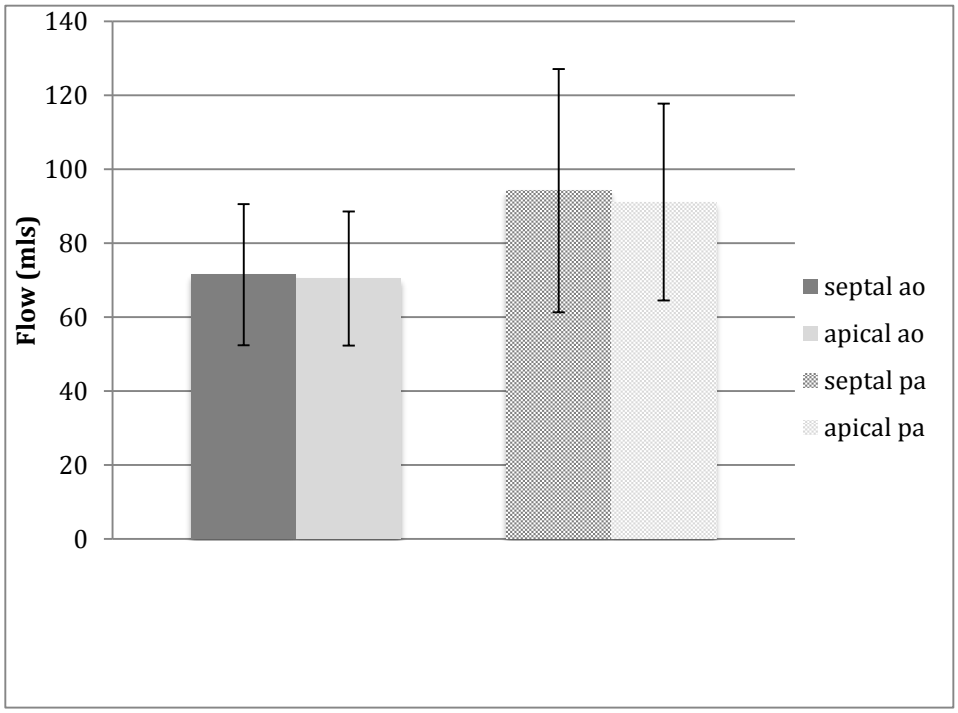

The pulmonary flow was consistently greater than the aortic flow when measured by CMR, with no obvious physiological explanation for this. Indeed one may have expected a lower pulmonary flow if the presence of 2 leads within the ventricle caused any significant tricuspid regurgitation.

The most likely explanation is that the closer proximity of the pulmonary valve to the PPM resulted in a greater phase encoding offset error. Firstly the phantom studies performed illustrated the effect of the PPM on phase encoding errors and subsequent flow. Secondly patients within the study had focused echocardiograms, which included a velocity time integral assessment across the RVOT and the LVOT (Figure 85). The mean velocity time integral (VTI) for the RVOT lead was 21.6 ± 9.9 across the aortic valve and 16 ± 6 across the pulmonary valve, $p < 0.05$. For the apical lead it was 21.8 ± 9.3 versus 14.9 ± 5.4, $p<0.05$. There was no statistical difference between the aortic VTI between the two pacing modes, whilst there was between the pulmonary VTI, $p= 0.7$ and 0.008 respectively. Since the echocardiograms are unaffected by metal susceptibility artefact, the VTI's measured may be a more accurate representation of the flows. Physiologically the difference in VTI measured may represent the presence of tricuspid regurgitation.

Figure 83. Aortic and pulmonary VTI measured by echocardiography for RVOT septal and RV apical positions.

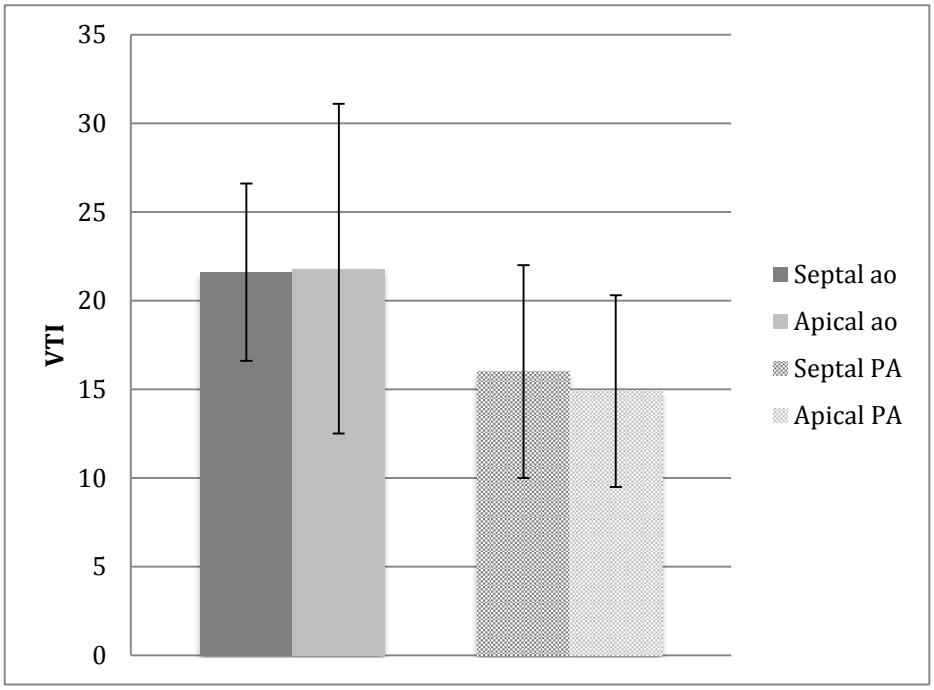

4.8.3 Cardiac dimensions, LV volumes and ejection fraction

Using both CMR tools and Argus Siemens imaging software, the LV dimensions were recorded for each of the pacing sites. These are summarised along with the LV volumes, stroke volume and EF in table 35.

Table 35. Cardiac dimensions, left ventricular volumes and ejection fractions for acute RVOT and RV apical pacing. N=50.

	LA area (cm2)	Diastolic mass (g)	LVIDd (mm)	LVIDs (mm)	Diastolic volume (ml)	Systolic volume (ml)	Stroke volume (ml)	EF (%)
RVOT Septal	41±7.4	158.5± 54	49.5± 6.4	33.2± 7.3	146± 50	63.8± 38.6	82.2± 20.5	58.4± 10.3
Apical	42±7	160.1± 56	50.2± 6.1	33.8± 7.2	146.2± 50	65.5± 37.5	80.6± 21.2	56.9± 8.5
P value	NS	NS	0.14	0.3	0.9	0.05	0.2	0.02

Table 36. Cardiac dimensions, left ventricular volumes and ejection fraction for acute RVOT and RV apical pacing, corrected for optimal lead position combination. N=25.

	LVIDd (mm)	LVIDs (mm)	Diastolic volume(ml)	Systolic volume (ml)	Stroke volume (ml)	EF (%)
RVOT septal	50.8± 6.2	34.5± 7.4	157.8± 56.6	71.9± 48.4	85.9± 18.4	57.3± 10.4
Apical	51.3± 6	35.4± 7.5	158.8± 57.8	73.3± 47.3	85.5± 22.5	56.1± 9.4
P value	0.8	0.4	0.5	0.2	0.8	0.12

Table 37. Cardiac dimensions, left ventricular volumes and ejection fraction for acute RVOT and RV apical pacing, corrected for optimal and acceptable lead position combinations. N=47.

	LVIDd (mm)	LVIDs (mm)	Diastolic volume(ml)	Systolic volume (ml)	Stroke volume (ml)	EF (%)
RVOT Septal	49.5± 6.6	33.2± 7.6	146.6± 51	64± 39.8	82.5± 20.4	58.6± 10.5
Apical	50.2± 6.3	33.8± 7.4	146.8± 51.2	65.6± 38.6	81.1± 21.4	57.1± 8.7
P value	0.15	0.26	0.86	0.08	0.3	0.03

4.8.4 Right Ventricular function

RV function was assessed using TAPSE on CMR and echo. The mean TAPSE was 17.6± 4.4mm for the RVOT position and 16.4± 16.4mm for the apical position, p= 0.05, on CMR. On echocardiography it was 18±8mm and 17±9mm, p=0.05.

4.8.5. Left ventricular Strain

Using CMR-FT software on bSSFP images, the longitudinal, radial and circumferential strain and strain rates were calculated for both lead positions. Global longitudinal strain was also assessed in the 4-chamber view on echocardiography using speckle tracking. The results are given in tables 38 to 44.

Table 38. Longitudinal strain measured by CMR.

	Cardiac view	APICAL	RVOT	P value
Longitudinal strain for all lead pairings (n=50)	4 chamber	-14.9± 4.97	-16.6± 5.04	**0.007**
	2 chamber	-14.8± 4.5	-15.5± 4.75	**0.33**
	3 chamber	-15.2± 6.12	-17.3± 5.8	**0.02**
Optimal lead combination (N=25)	4 chamber	-13.9± 4.6	-15.9± 5.1	**0.01**
	2 chamber	-13.9± 4.4	-15.6± 5.2	**0.08**
	3 chamber	-14.4± 4.6	-17.4± 6.1	**0.015**
Optimal and acceptable lead pairing (N=47)	4 chamber	-14.8± 4.98	-16.5± 5.2	**0.005**
	2 chamber	-14.5± 4.39	-15.6± 4.82	**0.15**
	3 chamber	-14.93± 5.9	-117.2± 5.97	**0.007**

Table 39. Global longitudinal strain measured by speckle tracking on echocardiography.

	Cardiac view	APICAL	RVOT	P value
Longitudinal strain for all lead pairings (n=50)	4 chamber	-10 ± 3.3	-11.5 ± 3.6	**0.0005**

Figure 84. Longitudinal strain measured for apical and RVOT lead. Note strain is a negative value but has been represented as positive for the graph. N=50.

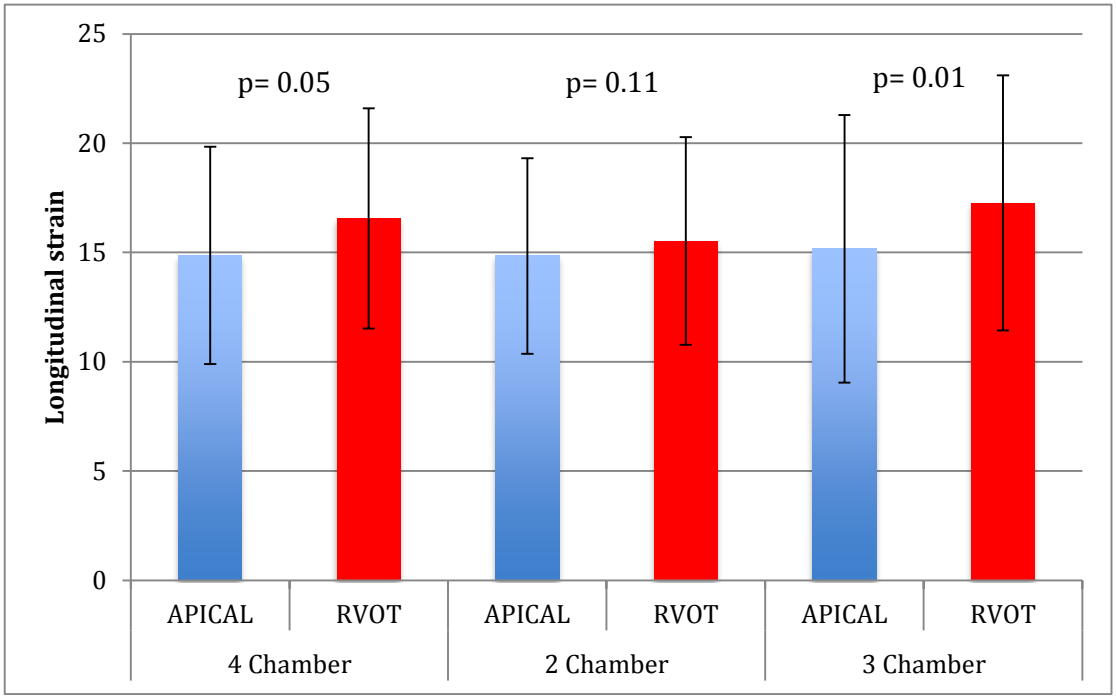

Figure 85. Longitudinal strain measured for apical and RVOT lead in 3 cardiac views, for optimal lead combination. N=25..

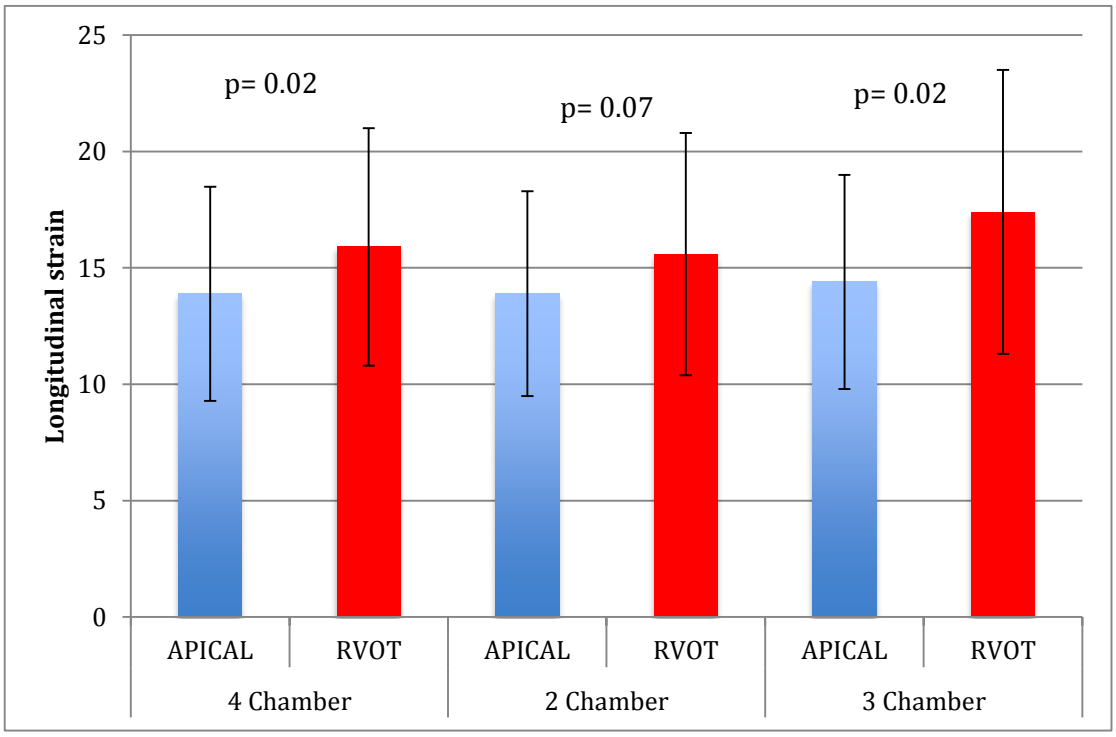

Table 40. Longitudinal strain rate measured on CMR.

	Cardiac view	APICAL	RVOT	P value
All lead parings (n=50)	4 chamber	-1.1± 0.54	-1.2± 0.51	**0.045**
	2 chamber	-0.93± 0.29	-1.003± 0.36	**0.11**
	3 chamber	-1.015± 0.44	-1.19± 0.44	**0.008**
Optimal lead pairings (N=25)	4 chamber	-0.95± 0.4	-1.15± 0.54	**0.016**
	2 chamber	-0.89± 0.29	-0.99± 0.35	**0.07**
	3 chamber	-0.96± 0.34	-1.2± 0.47	**0.016**
Optimal and acceptable lead pairing (N=47)	4 chamber	-1.07± 0.56	-1.2± 0.52	**0.067**
	2 chamber	-0.92± 0.28	-1.01± 0.37	**0.082**
	3 chamber	-1.03± 0.45	-1.2± 0.45	**0.018**

Table 41. Circumferential strain measured on CMR.

		All lead pairings (n=50)			Optimal lead pairing (n=25)			Optimal and acceptable pairing (n=47)		
		APICAL	RVOT	**P value**	APICAL	RVOT	**P value**	APICAL	RVOT	**P value**
Circumferential strain	BASE	-18.4± 4.23	-17.3± 4.01	**0.04**	-17.3± 4.1	-16.7± 4.5	**0.39**	-18.3± 4.4	-17.3± 4.1	**0.05**
	MID	-20.6± 4.1	-19.7± 4.28	**0.13**	-20.8± 4.3	-19.6± 5.05	**0.09**	-20.4± 4.2	-19.7± 4.4	**0.19**
	APEX	-19± 7.8	-19.7± 6.1	**0.45**	-17.8± 6.4	-19.3± 6.5	**0.24**	-19.1± 7.9	-19.7± 6.3	**0.52**

Table 42. Radial strain measured on CMR.

		All lead pairings (n=50)			Optimal lead pairing (n=25)			Optimal and acceptable pairing (n=47)		
		APICAL	RVOT	**P value**	APICAL	RVOT	**P value**	APICAL	RVOT	**P value**
Radial strain	BASE	28.3± 12.4	27.5± 11.3	**0.82**	27.35± 11.7	27.2± 13.5	**0.87**	28.3± 12.8	27.7± 11.63	**0.76**
	MID	34± 14.4	36± 19.9	**0.42**	34.8± 12.5	35± 12	**0.98**	34.2± 14.6	36.8± 20.2	**0.31**
	APEX	17± 8.3	17.8± 8.2	**0.6**	19± 8.9	17.1± 8.4	**0.43**	17.2± 8.4	17.7± 8.4	**0.77**

Table 43. Circumferential strain rate measured on CMR.

		All lead pairings (n =50)			Optimal lead pairing (n=25)			Optimal and acceptable pairing (n=47)		
		APICAL	RVOT	P value	APICAL	RVOT	P value	APICAL	RVOT	P value
Circumferential strain rate	BASE	-1.2± 0.35	-1.1± 0.31	**0.07**	-1.2± 0.35	-1.06± 0.29	**0.04**	-1.21± 0.36	-1.13± 0.32	**0.06**
	MID	-1.31± 0.32	-1.26± 0.31	**0.25**	-1.32± 0.39	-1.24± 0.33	**0.14**	-1.31± 0.33	-1.26± 0.32	**0.21**
	APEX	1.02± 0.41	1.11± 0.46	**0.22**	1.1± 0.4	1.01± 0.35	**0.52**	1.03± 0.41	1.1± 0.45	**0.33**

Table 44. Radial strain rate measured on CMR.

		All lead pairings (n=50)			Optimal lead pairing (n=25)			Optimal and acceptable lead pairing (n=47)		
		APICAL	RVOT	P value	APICAL	RVOT	P value	APICAL	RVOT	P value
Radial strain rate	BASE	1.5± 0.6	1.5± 0.43	**0.93**	1.61± 0.8	1.47± 0.47	**0.52**	1.54± 0.65	1.5± 0.4	**0.99**
	MID	1.59± 0.55	1.62± 0.59	**0.81**	1.6± 0.51	1.59± 0.48	**0.64**	1.61± 0.56	1.64± 0.6	**0.85**
	APEX	-1.25± 0.5	-1.25± 0.45	**0.98**	-1.08± 0.47	-1.15± 0.41	**0.61**	-1.2± 0.58	-1.26± 0.46	**0.94**

4.8.6 Intra-ventricular dyssynchrony

Intra-ventricular dyssynchrony was assessed using two methods a modified Yu index and the maximum opposing wall delay.

The Yu index used a 16 segmental model, by calculating the standard deviation of the time to peak longitudinal strain (T2PLS) and time to peak longitudinal strain rate (T2PLSR). This used long-axis images.

The mean standard deviation for the T2PLS was 167ms for apical pacing and 165ms for RVOT pacing, p= 0.84, n=50. For T2PLSR this was 90.2ms for apical pacing and 88.9ms for RVOT pacing, p=0.81, n=50. When corrected for optimal lead pairing the mean SD for T2PLS was 177ms for apical pacing and 162ms for RVOT pacing, p=0.26, n= 25. When corrected for optimal position the mean SD for T2PLSR was 94 ms for apical pacing and 84ms for septal pacing, p=0.06.

The maximum opposing wall delay is most commonly performed on the septal and lateral walls in the 4-chamber view. The opposing wall delay was calculated for the basal, mid and apical segments. Figure 88 and figure 89 shows the opposing wall delays for all study patients and those corrected for optimal lead positions. A paired t-test was performed and the results are shown below (Table 45).

Table 45. T- Test for max opposing wall delays between septal and lateral walls.

		Base		Mid		Apex	
		Apical	RVOT	Apical	RVOT	Apical	RVOT
All lead pairing	Wall delay (ms)	152± 176	132± 141	178± 168	150± 158	140± 164	107± 121
	P value		0.5		0.4		0.18
Optimal lead pairing	Wall delay (ms)	200± 195	128± 121	236± 191	195± 183	163± 174	98± 108
	P value		0.16		0.5		0.14

Figure 86. Maximum opposing wall delay between the septal and lateral walls at basal, mid and apical ventricular levels. N=50. Error bars are +/- SEM.

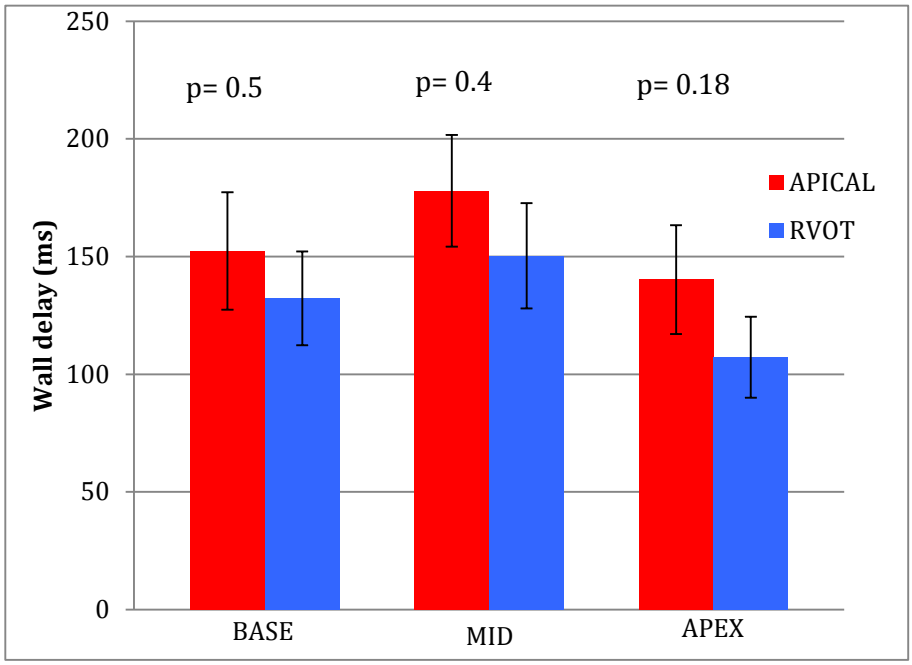

Figure 87. Maximum opposing wall delay between the septal and lateral walls at basal, mid and apical ventricular levels for optimal lead pairings . N=25. Error bars are +/- SEM.

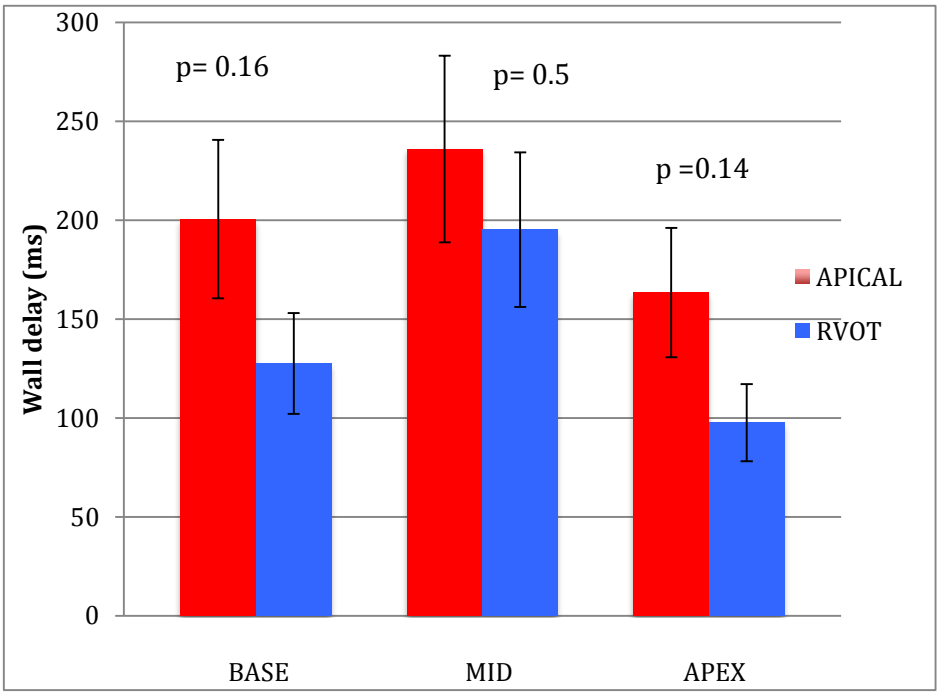

4.8.7. Twist and Torsion

Twist, twist corrected for length and torsion were calculated using data derived from both Intag and CMR-FT. Data for all pacing parings, optimal lead pairing and optimal/acceptable lead pairings are summarised in Table 46. A students paired t-test was used.

Whilst all parameters were greater with RVOT pacing, this did not reach statistical significance for the CMR-FT derived data. However when using Intag derived data, twist, twist corrected for length and torsion were all significantly greater during RVOT pacing.

Table 46. Twist, twist per unit length and torsion calculated using CMR-FT and Intag.

		Twist		Twist per unit length		Torsion	
		CMR-FT	Intag	CMR-FT	Intag	CMR-FT	Intag
All lead pairings	APICAL	9.1± 4.43	6.1± 2.7	0.24± 0.13	0.16± 0.08	5.1± 2.65	4.9± 2.26
	RVOT	9.4± 4	6.8± 2.5	0.31± 0.38	0.19± 0.07	5.48± 3.15	5.7± 2.17
	P value	**0.96**	**0.05**	**0.23**	**0.004**	**0.42**	**0.003**
Optimal lead pairings	APICAL	9.1± 4.71	5.73± 3.1	0.24± 0.13	0.16± 0.1	5.1± 2.6	4.7± 2.7
	RVOT	9.82± 4.9	6.73± 3.3	0.28± 0.28	0.2± 0.09	5.4± 3.9	5.9± 2.8
	P value	**0.8**	**0.06**	**0.44**	**0.01**	**0.75**	**0.009**

		Twist		Twist per unit length		Torsion	
Optimal and acceptable lead pairings	APICAL	9.04± 4.16	6.1± 2.8	0.24± 0.12	0.17± 0.09	5.01± 2.3	4.9± 2.35
	RVOT	9.95± 4.23	6.84± 2.68	0.31± 0.39	0.19± 0.08	5.39± 3.29	5.86± 2.29
	P value	**0.9**	**0.04**	**0.26**	**0.003**	**0.39**	**0.001**

4.9. Discussion

4.9.1 Baseline demographics

The mean age of the study cohort was 68 years old and is in keeping with the literature that 70% of the patients with AF are between 65 and 85 years of age. (249)

The Pace and ablate populations tends to be older with more co-morbidities than the standard AF population whose average age at the time of standard ablative therapy is 55 years. (250) The male preponderance is in keeping with that seen in clinical practice.

The baseline exercise tests and quality of life, revealed that the patients in the study population were physically deconditioned and had a reduced quality of life. This is to be expected given the older age group, presence of co-morbidities and that Pace and Ablate patients are offered this treatment to help with often refractory symptoms.

4.9.2 Right ventricular lead positions

Every attempt was made to place the ventricular leads in the RVOT (in particular the RVOT septum) and the apex with the aid of the three fluoroscopic views described in the methods. Those not placed in the RVOT or apex were due to clinical reasons where the lead stability or pacing parameters were not adequate. Even with the pre-shaped MOND stylet, it was difficult to achieve an RVOT septal position as described by MOND, with only 56% of leads positioned there on review of the images from all implants. True RVOT septal pacing has been described as superior to just RVOT pacing where there is a heterogeneous mix of septal and free wall pacing, (132) but in this study it was not easy to achieve. Since this was a real world study, it was not

felt to be appropriate to expose patients to longer procedure times with increased radiation doses and risk of infection to achieve a true RVOT septal position if it was not obtained within 3 attempts. The lead positions achieved in this study may represent what is achievable in routine clinical practice. Indeed it has been published that in studies comparing outflow tract and apical pacing that only 61% of leads were septal. (114) In fact it has been reported in at least two studies that only a 1/3 of the RVOT leads implanted were actually septal. (251,252)

CMR imaging allowed a further grading of the relative lead positions. The intra and inter-observer agreements were good using a kappa analysis for both the apical and RVOT lead positions. Due to the relatively complex anatomy of the RVOT, a grading system was used to indicate the proximity to true RVOT septal position. A perfect (grade 1) apical position was achieved in 76% of procedures where as a perfect RVOT septal position was seen in 34%. Practically, it is easier to position a lead in the apex compared to the septum. Despite only a small proportion being deemed "perfect", over 72% of the RVOT leads were graded as a good position (score 1-1.5), which is higher than the rating given just on reviewing the fluoroscopic images. This is clearly reassuring but serves to illustrate that there are limitations on a practical level for operators relying just on fluoroscopic images to place the RVOT lead. Intra-operative transoesophageal echocardiography (TOE), in particular 3D TOE would probably offer the most robust real time method of achieving accurate lead position. (253) Achievement of a septal RVOT position with good stability and pacing parameters is perhaps not achievable in all patients.

4.9.3 ECG parameters

Both the QRS duration and the QRS axis were found to be statistically different between the RVOT and apically paced modes.

The RVOT pacing axis was directed inferiorly, whilst that of apical pacing was superiorly directed. The septum and the rest of the ventricle are being activated from opposite positions, so it is not surprising that the summation of depolarisation vectors is found to be significantly different. The work of Molina et al in 2014 also showed this significant difference.

For an RVOT lead position, it was found that an negative QRS in lead I has a sensitivity of 0.7 and a specificity of 0.5, with a positive predictive value of 0.66 and a negative predictive value of 0.57. A number of studies have looked at the QRS morphology. In the study by Balt, septal pacing was significantly more associated with a negative complex in lead I compered to anterior and free wall RVOT pacing. (254) They found that negative complex was not specific for septal pacing, with an iso-electric or negative complex in lead I being 48% sensitive and 74% specific for septal pacing. One study by McGavigan et al had lead I being positive in 54% of septal sites (252) but interesting in a second study by the same group it reported that an iso-electric or negative deflection to be 50% sensitive and 100% specific for septal pacing. (132)

No algorithms have been successfully developed to correlate ECG parameters with lead position. One of the limitations of studies within the literature is that they have relied on fluoroscopic images where clear anatomical landmarks are not necessarily easy to define and as shown in this thesis is there were differences between fluoroscopic and MRI determined positions.

The mean QRS duration for the RVOT lead was on average 10 ms shorter than the apical lead, which suggests the RVOT position confers less electrically dyssynchrony. This finding is consistent with data published by Molina et al last year (113) and other studies. (34,103,255,256)

The biggest difference in electrical dyssynchrony was seen with the combination of true RVOT septal and true apical lead positions. It is possible that this study was able to show a significant difference because the lead positions were characterised by CMR for the analysis. Studies relying just on fluoroscopic images may include RVOT free wall positions, which have been shown to have longer QRS durations than septal or anterior RVOT positions. (254)

4.9.4 Imaging artefacts

Although the Accent PPM and tendril leads are MR conditional they still contain ferromagnetic materials and thus generated metal susceptibility artefact on the MR images. For SSFP cine images at least one segment was affected by artefact in 90% of the MR scans. When compared to SpGr cine images, there was significantly more artefact on SSFP sequences compared to SpGr sequences at basal (53% vs 11.5%, $p<0.001$), mid (67% vs 31%, $p<0.001$) and apical regions (65% vs 43%, $p=0.001$). In Balanced SSFP, the transverse magnetisation originating from several TR's are combined, resulting in greater MR signal amplitudes compared to SpGr. However if there are inhomogeneities within the magnetic field, the transverse magnetisation from different TRs can cancel each other out rather than add together in areas of inhomogeneity. (257) This can create dark bands even in normal phantom models. (244) In the presence of an IPG, there is significant inhomogeneity resulting in increased artefact.

The regions most commonly affected by the metal susceptibility artefact were the anterior and anterior-septal regions within the mid SA plane (Figure 80). In 90% of the MR scans performed, artefact was present in the mid anterior segment on SSFP sequences. This finding is similar to that reported by Sasaki et al. (202) Whilst significant artefacts were observed in many scans, both a qualitative and quantitative assessment of LV function was deemed possible by 2 independent observers in all patients. This is in keeping with the findings of the ADVISA sub study of image quality, where only 5% of total scans were not deemed to give diagnostic quality images of the LV. (203)

Certain imaging sequences were more adversely affected than others. In particular LGE imaging, T1 and T2 mapping showed significant artefacts. LGE uses an inversion recovery sequences with a longer echo time (TE) than gradient echo and spin echo, thus is associated with greater magnetic susceptibility artefacts. (202) T1 mapping used the MOLLI sequence and this is based on an inversion recovery sequence and uses a bSSFP readout. Multiple inversions are used to acquire information at different inversion times. This sequence by virtue of multiple inversion times and using SSFP is going to make it susceptible to metal susceptibility artefacts. Given the degree of artefact seen in this study, it is unlikely that T1 or T2 mapping with have much clinical use in the patients with an IPG.

The main determinant of artefact was the distance of the device from the heart with a negative correlation between the distance of the PPM from the heart and the artefact on the SSFP MR images, $r= -0.561$, $n=50$, $p= <0.0001$. These in-vivo results are consistent with the in-vitro data from the phantom studies previously discussed. The inverse relationship between artefact size and distance from the IPG was reported also by Sasaki et al. (202)

4.9.5 Safety data

The manufacture of MR conditional devices was born out of the original safety concerns of scanning standard devices. (160) Apart from the major Medtronic trials, there is a paucity of safety data with regards to the other manufacturers. (159,201) There were no adverse events during the 50 CMR scans performed for the acute study. The study scan times were in excess of 90 minutes and thus much longer than in clinical practice. Despite this, there was no clinically or statistically significant change in the threshold before and after the CMR scan. The mean differences in threshold before and after the scan was 0.03V, p=0.34 for the RVOT lead and 0V, p=1 for the apical lead. There was a statistical significant difference for lead impedance before and after the scan, but the maximum difference was only 11Ω for the RVOT lead, which is clinically insignificant. Lead impedances show great variance throughout the day and are affected by multiple factors including body fluid status, concomitant drugs, particular antiarrhythmics and even different foods. (258)

This study clearly demonstrated the safety of prolonged CMR scanning of the St Jude Accent PPM.

4.9.6 Haemodynamics

There were several ways the acute study attempted to measure the impact of pacing site on cardiac haemodynamics. The MAP was calculated using peripherally measured blood pressure (two measurement s and average taken) and was essentially the same between pacing modes 92mmHg vs 90mmHg, for RVOT and apical pacing respectively. The use of non-continuous monitoring of blood pressure is a major limitation but even those studies where invasive measures were used to calculate the MAP have not shown a statistical significant difference between the two pacing sites. (119,124) The use of an automated pressure cuff within the MR scanner was used to measure the BP during the scans for each pacing mode. It is very possible that the time the BP was taken during the scan session influenced the measurement. The scans were of long duration so the normal circadian cycle of BP may contribute to the lack of significant differences seen. It is also possible that the patient's level of stress during the scan may impact the measured BP. It was observed that some patients were very stressed at the beginning of the scan but became more relaxed as the scan went on, as they became used to being within the scanner. For some patients, the opposite was observed and they became progressively more stressed.

The flow of blood across the aortic and pulmonary valves is an indirect measure of cardiac output from the left and right ventricle. When corrected for the optimal lead combination, both aortic and pulmonary flows were greater in the RVOT position when measured by CMR, but these were neither clinically or statistically significant different. A striking observation was that the pulmonary flow was consistently greater than the aortic flow when measured by CMR, with no obvious physiological explanation for this. Indeed one may have expected a pulmonary flow lower than that

of the aorta, if the presence of 2 leads within the ventricle caused any significant tricuspid regurgitation. The most likely explanation for this observation is that there is a greater phase encoding offset error caused by the pulmonary valve being in closer proximity to the PPM. Indeed the phantom studies performed illustrated the effect of the PPM on phase encoding errors and subsequent flow. The closer the ROIs to the PPM, the greater the phase offset error. Secondly the echo data showed the opposite flow pattern with the LVOT flow greater than the pulmonary flow, which perhaps represents the presence of tricuspid regurgitation. Since ultrasound is not affected by metal susceptibility, the assumption would be that the observed differences seen with CMR were the result of a phase offset error. This has very important clinical implications since it would suggest that flow assessments cannot be done accurately in the presence of a PPM.

The LVOT flow was not significantly different between the pacing positions when measured by echocardiography. This is consistent with some studies (34,119) but not with others. (100,124)

A greater stroke volume and EF was measured for the RVOT lead compared to the apical lead on CMR. The difference in stroke volume was 1.6mls and the EF 1.5%. The difference in EF was statistically significant with a P value of 0.02, but this is not a clinically significant difference. It is within the noise level that would be found in echocardiography. At baseline in the crossover study by Mera et al, the high septal position gave an EF of 57% versus an apical position of 53% measured by nuclear ventriculography. (126) Victor published 2 studies with a crossover design. The first was RVOT vs RVA pacing and no difference in EF was observed acutely. (259) The second was high RV septum vs RVA and this interestingly showed for those with an EF > 45%, there was no difference between the two pacing sites but for those with a reduced EF of < 45% there was a significant difference on echocardiography. (129) In the MAPS study cohort the mean EF was >55% at baseline and thus one

explanation for the small difference in EF seen between the pacing sites is that with a normal EF, acute alterations in ventricular activation do not result in large haemodynamic changes. In those with a normal EF, it is likely to take time for pacing induced ventricular remodelling to take place. Consistent with this would be the findings of Tse et al using a parallel study design.(102) It was only after 18 months that the RVA group showed a decreased LV function compared to the RVS group.

4.9.7 Right ventricular function

RV function was assessed using TAPSE on CMR and echo. The mean TAPSE was 17.6 ± 4.4mm for the RVOT position and 16.4 ± 16.4mm for the apical position, p= 0.05, on CMR. This is comparable to that measured by echocardiography with 18 ± 8mm and 17 ± 9mm, for RVOT and RVA positions respectively p=0.05. The majority of studies in the literature focus only on the LV functional parameters rather than the RV which is the ventricle being paced. Whilst statistically significant, the difference in TAPSE is small and not clinically significant.

4.9.8 Deformational measures of left ventricle- Strain, twist, torsion

Myocardial strain, twist and torsion provide complementary information to standard pump function indices. They are more direct measures of the mechanical processes occurring during both contraction and relaxation. (209,260–262) This perhaps makes them more sensitive to change in left ventricular performance at an earlier stage of pathologies affecting the heart.

Global longitudinal strain was greater for RVOT pacing than apical pacing in all 3 long axis orientations, measured by CMR feature tracking. This was statistically significant for both 3-chamber (-14.9 vs -7.2, p=0.007) and 4-chamber views (-14.8 vs -16.5, p= 0.001). Echocardiography also showed a significant difference in 4-chamber longitudinal strain between pacing positions (-10 vs -11.5, p= 0.0005). These findings are consistent with the recent sub-study of Protect Pace(131), which showed a global longitudinal strain of -13.9 ± 4.1 for RVA and -15.5 ± 4.6 for the high RV septal position, p= 0.02. Global longitudinal strain (GLS) is a more subtle measure of myocardial dysfunction and it was observed in the Protect Pace sub study that whilst RVA pacing altered the GLS, it was not always accompanied by a change in the EF. (263) This finding is similar to the MAPS acute study where the difference in EF between the pacing positions was small.

Circumferential and radial strain did not appear significantly different between the pacing modes, which was a finding of Protect-Pace also. As discussed by Saito et al, both radial and circumferential parameters are far less reproducible measures and difficult to measure. (263) One problem is that it is much more difficult to accurately define the base, mid and apex.

The twisting motion of the heart is a characteristic of normal cardiac function. Twist accounts for rotational deformation at both the base and apex, so is perhaps a better measure of global rotational performance than circumferential and radial strain. Global twist was found to be greater for RVOT pacing when measured by both Intag and CMR-FT, compared to RVA pacing. Only the measurements by Intag were statistically different (6.1° vs 6.8°, p=0.05). The CMR-FT derived measures were larger than the Intag derived measures. The methods are fundamentally different. The generation of the tagged and Cine SSFP images is very different, the information encoded in the data is different and the post-processing software used also differs between the methods. Therefore it is difficult to directly compare the two

measures of rotational deformation. It is however reassuring that both methods showed RVOT pacing had a greater twist. It should be pointed out that although the phantom studies performed as part of the validation work showed that tagging appeared to become unreliable at elevated heart rates, at baseline the results were comparable. All scan were performed with a heart rate at 60bpm (paced) and therefore it seemed reasonable to use both CMR-FT and InTag for analysis.

Delgado et al showed acute RVA pacing impaired LV twist significantly compared from 12.4±□37° to 9.7±2.6°, P=□0.001 on echocardiography. (58) Inoue et al also found a significant difference between RV apical pacing and RVS septal pacing in favour of the RV septal position (7±3° vs 14±5°, p <0.05) using speckle tracking echocardiography. Interestingly the rate of untwisting of the ventricle was also found to be significantly different, suggesting that both systolic and diastolic components are influenced by the pacing site. (264)

Torsion is perhaps the best measure of myocardial performance since it encompasses both rotational and longitudinal deformation. Torsion was greater in the RVOT paced group compared to the apical group using both Intag and CMR-FT derived indices. However only the InTag results showed a significant difference between the groups 4.9± 2.26° vs 5.7± 2.17° p= 0.003.

4.9.9 Dyssynchrony

Much of the work in pacing and particular the heart failure population has focussed on measures of myocardial dyssynchrony. As previously described in chapter 1, there are numerous measures with no consensus to a gold standard. A modified Yu index was used to calculate the standard deviation for both the T2PLS and T2PLSR. When uncorrected for all lead combinations, there was no significant difference between the two pacing sites. However when corrected for the optimal lead combination, the mean SD for the T2PLS showed a difference of 15ms in favour of the RVOT position (p=0.26) and 10ms for T2PLSR (p=0.06). The maximum wall delay for corrected lead combinations was 163±174ms and 98±108ms for apical and RVOT positions respectively but this did not reach statistical significance, p=0.14.

Both measures, whilst not reaching statistical significance demonstrated a trend towards the RVOT position producing less dyssynchrony than the apical position. It is likely that a significant difference would have been found if there were more patients with the optimal lead position. This finding illustrates a point that has been made by Mond et al that a reason why many studies have not demonstrated any differences between RVOT and apical pacing is that lead placement is very heterogeneous, particularly in the RVOT. (132)

Inoue et al demonstrated more greater dyssynchrony in the RVA group with multiple measures from echocardiography, including a basal septum to lateral wall delay, SD of the time to peak systolic velocity, a radial dyssynchrony index and the SD of time to peak longitudinal strain. (264) Not all studies have demonstrated this, Ng et al found RVS pacing was associated with more dyssynchrony, but this can be part explained by the fact the RVS positioning was noted to be very heterogeneous. (72)

Chapter 5

Septal versus Apical pacing

Medium term study

5.1 Septal versus apical pacing- medium term study.

Provisional data from the mid-point of the study is described here. Fourteen patients had a CMR scan nine months after the first scan. Eight were paced from the apex and six the RVOT septum.

5.2 Safety data

It is normal with lead maturation that clinical parameters change over time. For example it would only be considered clinically significant if the lead threshold doubled, over a 9-month period. In fact in this study both the lead and battery parameters over the 9-month period did not show any clinically significant alterations. The mean battery voltage decreased by only 0.02V from 2.98 to 2.96V, which one would be expect in any clinical setting for a bradycardia device. Similar to the 1st CMR scan, the changes in pacing parameters before, at the crossover point and after the 2nd scan were not clinically significant. The parameters are illustrated in table 47.

Table 47. Safety data over 9 months. N=18.

		CMR 1 (0 months)			CMR 2 (9 months)		
		Before scan	Cross-over	After scan	Before scan	Cross-over	After scan
Threshold (V)	APICAL lead	0.68±0.16	0.68±0.17	0.75±0.35	0.83±0.62	0.86±0.6	0.86±0.6
		0.74±0.18	0.75±0.17	0.76±0.16	0.81±0.28	0.82±0.32	0.82±0.33
	RVOT lead						
Impedance (Ω)	Apical	555±112	551±110	552±110	538±161	548±194	564±257
	RVOT	594±69	592±70	597±70	571±74	569±73	573±75
Battery voltage (V)		2.98	2.98	2.98	2.96	2.96	2.96
Battery lifespan (years)		8.2±1.1		8.2±1.1	7.4±1.4		7.4±1.4

5.2 Quality of life SF36

The SF36 questionnaire was used at the 9-month interval. Table 48 gives the scores for each category. The total physical health score was 58 ± 25 and mental health score was 65 ± 25.

Table 48. Summary of QOL scores at 9 month interval. N=18.

Category	Score out of 100
Physical function	55 ± 30
Role physical	66 ± 43
Body pain	60 ± 32
General health	60 ± 18
Vitality	50 ± 23
Social functioning	78 ± 28
Role emotional	67 ± 43
Mental health (subcategory)	73 ± 26
Total Physical health	58 ± 25
Total Mental health	65 ± 25
Total SF36	**64 ± 27**

Figure 90 shows the SF36 scores at 0 and 9 months. The physical health score went from 42.9 to 58.4, p = 0.003, the mental health score went from 56.1 to 65.5, p = 0.02, and the overall SF36 score went from 50.4 to 63.6, p = 0.006. The quality of life scores increased across all categories.

Figure 88. SF36 scores for 0 and 9 months following the AV node ablation.

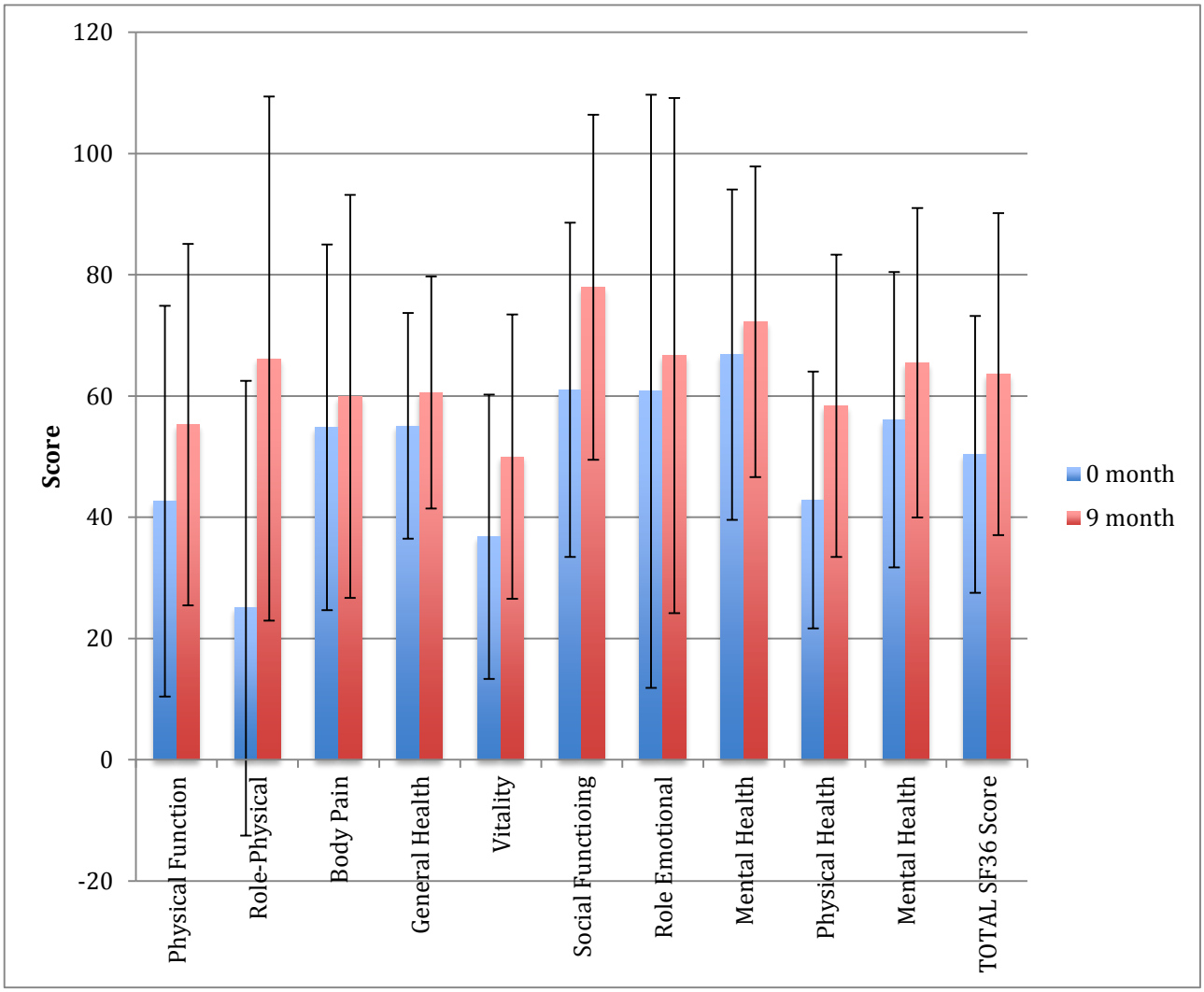

5.4 Exercise capacity

Exercise capacity was assessed at 0 and 9 months with a formal CPEX performed on the treadmill and the 6MWT. On CPEX testing the mean VO2 max rose from 16.1 to 17ml/kg/min, p = 0.13. The mean distance covered on the 6MWT rose from 367m to 391m, p = 0.04.

Figure 89. Exercise capacity assessed by CPEX at 0 and 9 months.

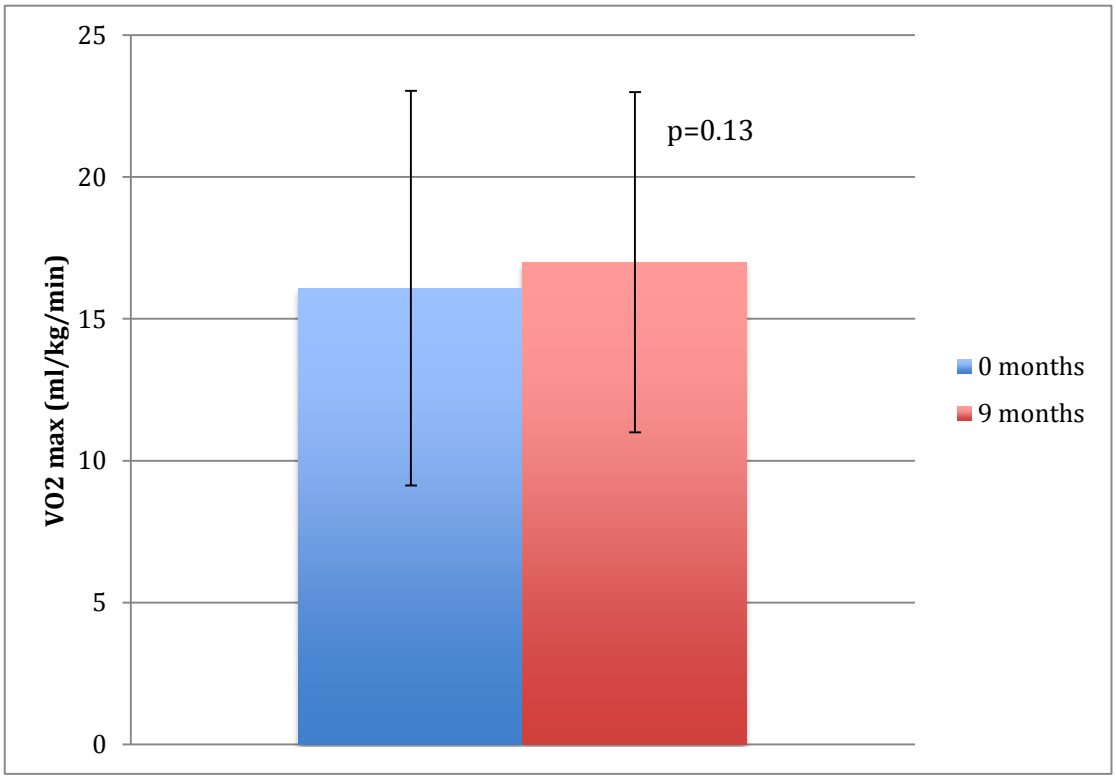

5.5 Left ventricular function

Measures of left ventricular performance were measured as described in the acute study for both pacing modes at 9 months. LV volumes, EF, longitudinal strain, twist and torsion were calculated and the results are summarized, along with the baseline data in tables 49 and 50. A students paired T test was used to determine the statistical significance of the differences between RVOT and apical pacing sites.

Table 49. LV heamodynamics at 0 and 9 months for RVOT and apical pacing.

		MAP (mmHg)	AO flow (ml)	PA flow (ml)	TAPSE (mm)	EDV (ml)	ESV (ml)	SV (ml)	EF (%)	Longitudinal strain in 4 chamber	Twist (°)	Torsion (°)	Wall delay 4 ch mid. (ms)
APICAL	0M	92±8	73±24	89±32	16±4	134±49	56±20	78±32	58±7	-15±4.5	7.6±2.3	5.2±2.6	178±168
	9M	94±11	74±22	92±31	15±5	136±57	55±23	81±34	59.6±8.3	-16.4±3.9	8.1±3.1	6.1±3	170±155
RVOT	0M	94±10	80±18	112±20	15±4	136±50	52±33	84±19	61.7±10	-20±4	10.4±5.3	7.5±5.7	150±158
	9M	97±12	82±21	111±23	15±4	137±49	49±36	88±22	64.2±11.8	-20.7±5.2	11.2±5	8.4±5.5	156±130

Table 50. Differences between baseline and 9 month haemodynamics.

Difference between apical and RVOT lead	Map (mmHg)	AO flow (ml)	PA flow (ml)	TAPSE (mm)	EDV (ml)	ESV (ml)	SV (ml)	EF (%)	Longitudinal strain in 4 chamber	Twist (°)	Torsion (°)	Wall delay 4 Ch mid segment
0 months	2	7	23	-1	2	-4	6	3.7	5	2.8	2.3	28
9 months	3	8	19	0	1	-6	7	4.8	4.3	3.1	2.3	14
P value at 0 months	NS	NS	<0.01	NS	NS	NS	NS	0.05	0.03	0.14	0.1	0.4
P value at 9 months	NS	NS	<0.01	NS	NS	0.1	0.08	0.03	0.05	0.12	0.09	0.53

5.6 Discussion

14 patients reached the mid point of the study and were analysed for this thesis. Importantly there were no clinically significant changes in pacing parameters for each of the CMR scans. Despite having two CMR scans neither the lead nor the battery parameters would be considered to be different from that of a patient with no scans.

The SF36 results clearly show that patient's quality of life significantly improved after 9-months of 100% ventricular pacing. This is keeping with other studies of patients with AF following an AVN ablation. (18,265,266) These patients are generally very symptomatic, with physical and psychological ailments, often as a result of palpitations or side effects from their medication. Finding an improvement in all quality of life parameters is thus very reassuring from a clinical perspective in this study. Quality of life parameters were not compared between the pacing modes since the numbers at this stage of the study was very small at the time of analysis.

The exercise tolerance increased over the 9-month period, which again is consistent with the findings of Wood et al who performed a meta-analysis of data in 2000. (18) The 6MWT reached statistical significance, whilst the CPEX did not, with only a small rise in VO_2max. Whilst the peak exercise capacity did not significantly increase, the significant difference found in the 6MWT should represent an increased ability of the patients to perform their activities of daily living. This would certainly be in keeping with the findings of the improved quality of life scores.

Each patient acted as his or her own control, allowing a direct comparison of RVOT versus apical pacing at baseline and at the 9-month point. A comparison was not made between the two leads over the 9-month period since the numbers in each group were small. At baseline, there was a trend across all the measures of left ventricular performance that RVOT was superior to apical pacing. Both the EF and longitudinal strain were statistically

significant and discussed fully in the acute pacing chapter. At the 9-month interval a similar trend was observed. When compared to baseline the measures of ventricular performance were seen to be greater including longitudinal strain and EF. This result would be in keeping with that found after 6 months of pacing by Molina et al. They found the EF increased from 57 to 58% and 52 to 55% for the RV septal and RV apical groups respectively after a period of 6 months. (113) Interestingly it was not until 1 year that the septal and apical groups diverged, with the septal EF increasing further to 61% and the apical group falling slightly to 54%. Unlike this study, I found that the EDV of the apical group increased rather than decreased, implying dilation of the ventricle and potentially negative remodelling was occurring. It is likely that LV remodelling will occur over a longer period than the 9-month crossover point of this study. Indeed studies by Hillock and Mond, and Tse et al suggest changes may occur after 12-18 months. (267,268) It is possible that at 9 months there was not enough time for significant remodelling to have occurred. In the Protect pace study there was a longer 2 year follow up and a small decrease in LV systolic function was observed for both RVOT and RVOT/high septal groups, suggesting that there was no significant difference between the sites. (269) However a sub analysis showed there was a significant difference in global longitudinal strain and dyssynchrony, both in favour of the RVOT/high septal position. (263) In keeping with Protect pace, I also found that longitudinal strain was greater in the RVOT group than the apical group at both baseline and 9 months. It can be hypothesized that the superior longitudinal strain for the RVOT group is the result of electrical activation of the heart that is more analogous to the normal physiological activation of the myocardium via the His-purkinje system.

Twist and torsion were greater in the RVOT group at baseline and at the 9-month point, but neither achieved statistically significance. This in part is likely due to the small number patients at the crossover point available for analysis for this thesis. Likewise the intra-ventricular dyssynchrony, as determined by the maximum opposing wall delay in the 4

chamber view at mid-level, was less for the RVOT lead at both baseline and at the 9 month crossover, but not statistically significant.

The alternate pacing positions do lead to differing activation patterns of the myocardium, which is clearly demonstrated by the opposite cardiac axis on the surface ECG. Animal models have suggested that pacing lead positions alter myocyte fibre shortening, relaxation and strain at a regional level. (49,50) This may provide a mechanistic explanation to why the differences in longitudinal strain, twist, torsion and dyssynchrony were observed between the pacing sites.

Whilst differences of LV myocardial performance have been demonstrated by this study, these do not appear to be clinically significant over the 9-month time course. There has been a great deal of debate over how long it takes remodelling to occur during pacing. Certainly the percentage of pacing will have an effect, and one explanation for the heterogeneity of results in this field is that this differs between studies. The Protect-pace study used those with high degree AV block, so the percentage of pacing was high. There appeared to be minimal differences in LV remodelling between the two groups, although as discussed the RVS strain was superior over the two year period. It is perhaps of no great surprise that despite using CMR, a more robust measure of LV volumetrics, that significant differences were not seen over the time course of the study reported. The results of the full cohort of patients at the 9 and 18-month intervals may expand on these findings.

Chapter 6.

Conclusions and future directions

6. Conclusions and future directions

6.1 Conclusions

There are a number of conclusions that can be drawn from this body of work undertaken as part of the MAPS trial. Firstly, cardiac imaging of those patients with IPG's is likely to become an increasing requirement in modern day cardiology and this study demonstrates a good safety profile for scanning this device in the MR environment when set scanning protocols are adhered to. There is not an inconsiderable amount of metal susceptibility artefact that is generated and this is both affected by the distance of the IPG from the heart and MR sequence employed. Determining myocardial function can be performed reliably, but tissue characterization is problematic in those areas where artefact is observed. Both the phantom and clinical studies suggested that flows measurements were subject to phase offset errors and this related to the distance of the IPG from the region of interest. Therefore valve analysis should be performed with extra caution. Sequence optimization is important in an IPG patient, and simple measures such as using spoiled gradient instead of SSFP sequences, or altering the centre frequency can be employed to good effect.

Whilst scanning MR conditional devices is safe, this study illustrates that due to artefact limitations, not all clinical questions can be answered and that other imaging modalities may have to be considered.

With regards to the AF cohort, the trial confirms that the Pace and ablate strategy can lead to both improved myocardial performance and functional status, with an increase in EF and

QOL both demonstrated. Regardless of the pacing site, both RVOT and RVA groups showed improvements in functional status and exercise capacity.

The position of the leads in the correct location has been greatly debated in the literature and it has been speculated that the heterogeneity of positions within the RVOT and RVS has contributed to inconclusive results when compared to the apical position. In this study, the use of dedicated fluoroscopy views, combined with the pre-shaped Mond stylet, only conferred a 56% of successful RVOT implantation if fluoroscopy alone was used to determine position. When reviewed using dedicated MR images, the successful RVOT implantation rate was 72%. In the Protect pace trial only 66% of leads were on the high RVS/low RVOT, so this study was comparable. My study serves to illustrate that in clinical practice true RVOT septal positions may often be difficult.

At baseline the RVOT site was seen to be superior to the apical, in terms of a higher EF, greater longitudinal strain, twist and torsion, and less dyssynchrony, especially when corrected for optimal lead position. The EF was statistically different but a 1% difference has minimal clinical significance. It remains to be seen if over a longer period of time, more clinically significance differences arise. Certainly mechanistic differences between the two pacing sites were observed.

Although it is perhaps disappointing that clinical differences were not observed the study does suggest that there is no reason why the RVOT position should not be chosen in preference if it can be achieved in a timely fashion with good pacing parameters.

6.2 Future directions

Clearly the follow up of this cohort of patients over the 18-month period will shed more light on the question of RV lead placement. In fact, despite 100% V pacing 18 months may not be long enough to determine any significant clinical differences (if they do exist) and so the hope would be to follow up this cohort for an extended period say 5 years.

Biomarker analysis of the entire cohort of patients will be very interesting to see if markers of myocardial dysfunction such as troponin and BNP, or markers of fibrosis such as MMP are altered as a direct result of pacing. The literature suggests pacing is not good for the heart and increasing the risk of heart failure. Despite the huge number of patients with cardiac devices there are not large numbers of them developing clinical heart failure. The use of biomarkers may help to predict those patients that may go on to develop heart failure and perhaps select patients for an upgrade to a biventricular device.

Imaging of patients with IPGs is in its infancy and further work is required to determine what image sequences can be used in the clinical setting. Certainly the issue over whether velocity phase encoding can be used will be important to resolve since it is used frequently in valvular assessments.

So far there are no biventricular cardiac devices on the market that are MR conditional and it is perhaps here where the future lies. There is already a huge body of work that uses CMR

prior to the implantation to determine scar distribution and burden that may influence LV lead placement and whether a defibrillator should be placed. The use of CMR in this cohort may provide further information regarding LV remodelling and perhaps more importantly assist in optimizing the device in non-responders.

The block-HF trial suggested that individuals with a reduced LV function and high degree AV block that CRT was superior to RV only pacing. The RV group was heterogeneous in lead position and it would be worthwhile doing a trial of RVOT septal versus CRT in this group using CMR.

Appendix

Appendix

Borg Scale of perceived exertion

The rating of perceived exertion (RPE) scale measures feelings of effort and/or fatigue experienced during both aerobic and anaerobic exertion. The perception of physical exertion is a subjective experience and reflects the interaction between physical and psychological elements. During exertion many physiological changes occur, including changes in ventilation, oxygen uptake, cellular metabolism and substrate utilisation. As ventilation increases so does perceived exertion.

The RPE was developed by the Swedish psychologist Gunnar Borg as was originally graded 6-20. Each grade is roughly meant to correspond to how the heart rate increases if you multiply it by a factor of 10. For example at grade 6, the expected heart rate is 60bpm; at grade 10 it is 100bpm. The scale is valid in that it generally evidences a linear relation with both heart rate and oxygen uptake during aerobic exercise. The scale can be simplified to an 11-point version.

<table>
<tr><td>Rating 0-20</td><td>Description</td><td>Rating 1-10</td></tr>
<tr><td>6</td><td>No exertion at all</td><td>0</td></tr>
<tr><td>7</td><td rowspan="2">Extremely light</td><td rowspan="2">0.5</td></tr>
<tr><td>8</td></tr>
<tr><td>9</td><td>Very light</td><td>1</td></tr>
<tr><td>10</td><td rowspan="3">light</td><td rowspan="3">2</td></tr>
<tr><td>11</td></tr>
<tr><td>12</td></tr>
</table>

13	Somewhat hard	3
14		4
15	Hard (heavy)	5
16		6
17	Very hard	7
18		8
19	Extremely hard	9
20	Maximal exertion	10

(270)

Worksheet for 6MWT

Study No:

Visit No:

	Start	Finish
Heart rate (bpm)		
Blood Pressure (mmHg)		
RPE		
Metres covered		

Health Survey for Pacemaker Study Patients (SF36)

Study number:
Patient Identification Number for this study:

Todays Date:_____

This survey asks for your views about your health. This information will help keep track of how you feel and how well you are able to do your usual activities.

Please answer these questions by putting a Cross in the box.
Please select only one choice for each item.

1- In general, would you say your health is:

□ 1. Excellent □ 2. Very good □ 3. Good □ 4. Fair □ 5. Poor

2- Compared to ONE YEAR AGO, how would you rate your health in general NOW?

□ 1. MUCH BETTER than one year ago.

□ 2. Somewhat BETTER now than one year ago.

□ 3. About the SAME as one year ago.

□ 4. Somewhat WORSE now than one year ago.

□ 5. MUCH WORSE now than one year ago.

3- The following items are about activities you might do during a typical day. **Does your health now limit you** in these activities? If so, how much?

Activities	**1. Yes, Limited A Lot**	**2. Yes, Limited A Little**	**3. No, Not Limited At All**
a) **Vigorous activities,** such as running, lifting heavy objects, participating in strenuous sports?	□ 1. Yes, limited a lot	□ 2. Yes, limited a little	□ 3. No, not limited at all
b) **Moderate activities,** such as moving a table, pushing a vacuum cleaner, bowling, or playing golf?	□ 1. Yes, limited a lot	□ 2. Yes, limited a little	□ 3. No, not limited at all
c) Lifting or carrying groceries?	□ 1. Yes, limited a lot	□ 2. Yes, limited a little	□ 3. No, not limited at all
d) Climbing **several flights** of stairs?	□ 1. Yes, limited a lot	□ 2. Yes, limited a little	□ 3. No, not limited at all
e) Climbing **one** flight of stairs?	□ 1. Yes, limited a lot	□ 2. Yes, limited a little	□ 3. No, not limited at all
f) Bending, kneeing or stooping?	□ 1. Yes, limited a lot	□ 2. Yes, limited a little	□ 3. No, not limited at all
g) Walking **more than a mile**?	□ 1. Yes, limited a lot	□ 2. Yes, limited a little	□ 3. No, not limited at all
h) Walking **several** blocks?	□ 1. Yes, limited a lot	□ 2. Yes, limited a little	□ 3. No, not limited at all
i) Walking **one** block?	□ 1. Yes, limited a lot	□ 2. Yes, limited a little	□ 3. No, not limited at all
j) Bathing or dressing yourself?	□ 1. Yes, limited a lot	□ 2. Yes, limited a little	□ 3. No, not limited at all

4- During the **past 4 weeks**, have you had any of the following problems with your work or other regular activities *as a result of your physical health*?

	Yes	No
a) Cut down on the **amount of time** you spent on work or other activities?	□ 1. yes	□ 2. No
b) **Accomplished less** than you would like?	□ 1. yes	□ 2. No
c) Were limited in the **kind** of work or other activities?	□ 1. yes	□ 2. No
d) Had **difficulty** performing the work or other activities (for example it took extra effort)?	□ 1. yes	□ 2. No

5- During the **past 4 weeks**, have you had any of the following problems with your work or other regular daily activities **as a result of any emotional problems** (such as feeling depressed or anxious)?

	Yes	No
a) Cut down on the **amount of time** you spent on work or other activities?	□ 1. yes	□ 2. No
b) **Accomplished less** than you would like?	□ 1. yes	□ 2. No
c) Didn't do work or other activities as **carefully** as usual?	□ 1. yes	□ 2. No

6. During the **past 4 weeks**, to what extent has your physical health or emotional problems interfered with your normal social activities with family, friends, neighbors, or groups?

□ 1. Not at all □ 2. Slightly □ 3. Moderately □ 4. Quite a bit □ 5. Extremely

7. How much **bodily pain** have you had during the **past 4 weeks**?

□ 1. None □ 2. Very mild □ 3. Mild □ 4. Moderate □ 5. Severe □ 6. Very severe

8. During the **past 4 weeks**, how much did **pain** interfere with your normal work (including both work outside the home and housework)?

□ 1. Not at all □ 2. A little bit □ 3. Moderately □ 4. Quite a bit □ 5. Extremely

9. These questions are about how you feel and how things have been with you **during the past 4 weeks**. For each question, please give the one answer that comes closest to the way you have been feeling. How much of the time during the **past 4 week** …

	1. All of the time	2. Most of the time	3. A good bit of the time	4. Some of the time	5. A little of the time	6. None of the time
a) Did you feel full of pep?	□ 1. All of the time	□ 2. Most of the time	□ 3. A good bit of the time	□ 4. Some of the time	□ 5. A little of the time	□ 6. None of the time
b) Have you been a very nervous person?	□ 1. All of the time	□ 2. Most of the time	□ 3. A good bit of the time	□ 4. Some of the time	□ 5. A little of the time	□ 6. None of the time
c) Have you felt so down in the dumps that nothing could cheer you up?	□ 1. All of the time	□ 2. Most of the time	□ 3. A good bit of the time	□ 4. Some of the time	□ 5. A little of the time	□ 6. None of the time
d) Have you felt calm and peaceful?	□ 1. All of the time	□ 2. Most of the time	□ 3. A good bit of the time	□ 4. Some of the time	□ 5. A little of the time	□ 6. None of the time
e) Did you have a lot of energy?	□ 1. All of the time	□ 2. Most of the time	□ 3. A good bit of the time	□ 4. Some of the time	□ 5. A little of the time	□ 6. None of the time
f) Have you felt downhearted and blue?	□ 1. All of the time	□ 2. Most of the time	□ 3. A good bit of the time	□ 4. Some of the time	□ 5. A little of the time	□ 6. None of the time
g) Do you feel worn out?	□ 1. All of the time	□ 2. Most of the time	□ 3. A good bit of the time	□ 4. Some of the time	□ 5. A little of the time	□ 6. None of the time
h) Have you been a happy person?	□ 1. All of the time	□ 2. Most of the time	□ 3. A good bit of the time	□ 4. Some of the time	□ 5. A little of the time	□ 6. None of the time
i) Did you feel tired?	□ 1. All of the time	□ 2. Most of the time	□ 3. A good bit of the time	□ 4. Some of the time	□ 5. A little of the time	□ 6. None of the time

10. During the **past 4 weeks**, how much of the time has your **physical health or emotional problems** interfered with your social activities (like visiting with friends, relatives, etc.)?

□ 1. All of the time

□ 2. Most of the time.

□ 3. Some of the time

□ 4. A little of the time.

□ 5. None of the time.

11. How TRUE or FALSE is **each** of the following statements for you?

	1. Definitely true	2. Mostly true	3. Don't know	4. Mostly false	5. Definitely false
a) I seem to get sick a little easier than other people?	□ 1. Definitely true	□ 2. Mostly true	□ 3. Don't know	□ 4. Mostly false	□ 5. Definitely false
b) I am as healthy as anybody I know?	□ 1. Definitely true	□ 2. Mostly true	□ 3. Don't know	□ 4. Mostly false	□ 5. Definitely false
c) I expect my health to get worse?	□ 1. Definitely true	□ 2. Mostly true	□ 3. Don't know	□ 4. Mostly false	□ 5. Definitely false
d) My health is excellent?	□ 1. Definitely true	□ 2. Mostly true	□ 3. Don't know	□ 4. Mostly false	□ 5. Definitely false

Thank you!

Radiation dose risk assessment by medical physics

Research Study Dose and Risk assessment

Short Name	MRI Pacemaker Study
Full title	Determining the difference between RVOT and Apical pacing using cardiac MR
Local ref number	NA
Main site:	Wythenshawe Hospital, University Hospital of South Manchester NHS Foundation Trust
Additional sites:	None

Dose and risk information for Part B Section 3 of IRAS form

A Radioactive materials

Radionuclide procedures are not being performed as part of this study. This section of the IRAS form should not be completed.

B Other ionizing radiation

Procedure	No. of procedures	No. of standard care	Estimated Procedure dose
Chest X-ray	1	1	Effective dose of 0.02 mSv
Fluoroscopy during pacemaker in-plant	1	1	Effective dose of 1.7 mSv

C Combined dose and risk assessment

Dose and risk assessment
The total effective dose involved in the study (based on average sized patients) is estimated as 1.8 mSv, all of which could be considered standard care. This dose estimate is based on local audit data at the University of South Manchester NHS Foundation Trust indicating mean dose area product for a pacemaker implant of 8 Gy cm^2. This is below the national dose reference level of 11 Gy cm^2 as recommended by the Health Protection Agency. This level of dose is equivalent to less than a year of natural background radiation. For a participant in normal health, there would be an extra risk of cancer induction due to exposure to radiation. For a 30-40 year old adult, the estimated lifetime risk of fatal cancer associated with the total study dose is 1 in 11,000 (using fatal risk coefficient 5.0 x 10^{-5} per mSv ICRP103). This level of dose places this study in Category IIb (ICRP 62) considered to involve an intermediate level of risk and requiring an moderate level of societal benefit.

Other IRMER issues

Dose constraints	Not required as all procedures are part of standard clinical care
Patient Information sheet:	IRMER requires that the risk associated with exposures associated with research studies are explained to the participants. The following statement is suggested for insertion into the PIS: *Positioning of all pacemakers is monitored by X-ray imaging. The radiation dose associated with this procedure is less that you will receive from a year of*

	naturally occurring background radiation. You are not expected to be exposed to a higher radiation dose than normal because you are having this model of pacemaker.

Lead MPE

Prepared by:	Anne Walker (Mrs)
Post	Consultant Medical Physicist
Professional registration	CS02359
Organisation	North Western Medical Physics
Address	Christie Hospital NHS Trust Wilmslow Road Withington Manchester
Postcode	M20 4BX
Telephone/fax:	0161 446 3544/3545
E-mail:	anne.walker@physics.cr.man.ac.uk

Appendix: ICRP 62 "Radiological Protection in Biomedical Research" Annals of the ICRP 22 (3) 1991
Categories of risk and corresponding required levels of benefit

Category and Level of risk	Total risk of detrimental radiation effect	Corresponding effective dose range (adults) (mSv)	Level of social benefit required
I Trivial	$\sim 10^{-6}$ or less	<0.1	Minor
IIa Minor	$\sim 10^{-5}$	0.1-1	Intermediate
IIb Intermediate	$\sim 10^{-4}$	1-10	Moderate
III Moderate	$\sim 10^{-3}$ or more	>10	Substantial

NHS
National Research Ethics Service
NRES Committee North West - Greater Manchester South
Northwest Centre for Research Ethics Committees
3rd Floor - Barlow House
4 Minshull Street
Manchester
M1 3DZ

Telephone: 0161 625 7820

16 November 2011

Dr Mark Ainslie, Cardiology SPR
Wythenshawe Hospital
Southmoor Road
Manchester
M23 9LT

Dear Dr Ainslie

Study title: **Determining the acute effects of Right ventricular septal (RVS) vs RV apical (RVA) pacing- a cross over design using Cardiac Magnetic Resonance Imaging.**

REC reference: **11/NW/0699**

Thank you for your letter of 25 October 2011, responding to the Committee's request for further information on the above research and submitting revised documentation. The further information has been considered on behalf of the Committee by the Chair.

Confirmation of ethical opinion

On behalf of the Committee, I am pleased to confirm a favourable ethical opinion for the above research on the basis described in the application form, protocol and supporting documentation as revised, **subject to** the conditions specified below.

Ethical review of research sites

NHS sites

The favourable opinion applies to all NHS sites taking part in the study, subject to management permission being obtained from the NHS/HSC R&D office prior to the start of the study (see "Conditions of the favourable opinion" below)..

Conditions of the favourable opinion

The favourable opinion is subject to the following conditions being met prior to the start of the study.

Management permission or approval must be obtained from each host organisation prior to the start of the study at the site concerned.

Management permission ("R&D approval") should be sought from all NHS organisations involved in the study in accordance with NHS research governance arrangements. Guidance on applying for NHS permission for research is available in the Integrated Research Application System or at http://www.rdforum.nhs.uk.

Where a NHS organisation's role in the study is limited to identifying and referring potential participants to research sites ("participant identification centre"), guidance should be sought from the R&D office on the information it requires to give permission for this activity.

Statement of compliance

The Committee is constituted in accordance with the Governance Arrangements for Research Ethics Committees (July 2001) and complies fully with the Standard Operating Procedures for Research Ethics Committees in the UK.

After ethical review

Reporting requirements

The attached document *"After ethical review – guidance for researchers"* gives detailed guidance on reporting requirements for studies with a favourable opinion, including:

- Notifying substantial amendments
- Adding new sites and investigators
- Notification of serious breaches of the protocol
- Progress and safety reports
- Notifying the end of the study

The NRES website also provides guidance on these topics, which is updated in the light of changes in reporting requirements or procedures.

Feedback

You are invited to give your view of the service that you have received from the National Research Ethics Service and the application procedure. If you wish to make your views known please use the feedback form available on the website.

Further information is available at National Research Ethics Service website > After Review

11/NW/0699	**Please quote this number on all correspondence**

With the Committee's best wishes for the success of this project

Yours sincerely

pp **Dr Ann Wakefield**
Chair

Email: elaine.hutchings@northwest.nhs.uk

Enclosure: "After ethical review – guidance for researchers"

Copy to: *Louise Fletcher, R&D*
University Hospital of South Manchester

Consent form

University Hospital of South Manchester NHS
NHS Foundation Trust

Study number:
Patient Identification Number for this study:

CONSENT FORM

Effect of septal vs apical pacing- a comparative study using Cardiac MRI

Name of Lead Researchers: Mark Ainslie, Ben Brown, Matthias Schmitt, Neil Davidson

Please initial boxes

1. I confirm that I have read and understood the information sheet for the above study and have had the opportunity to ask questions and these have been answered satisfactorily. ☐
2. I understand that my participation is voluntary and that I am free to withdraw at any time without giving any reason, without my medical care or legal rights being affected. ☐
3. I understand that relevant sections of my medical notes and data collected during the study may be looked at by responsible individuals from regulatory authorities or from the UHSM Trust, where it is relevant to my taking part in this research. I give permission for these individuals to have access to my records. ☐
4. I agree to my GP being informed of my participation in the study ☐
5. I agree to take part in the above study. ☐

_____	_____	_____
Name of Patient	Date	Signature
_____	_____	_____
Person Taking Consent (if different from Researcher)	Date	Signature
_____	_____	_____
Researcher	Date	Signature

When completed, 1 for patient; 1 for researcher site file; 1 (original to be kept in medical notes

Patient information sheet

University Hospital of South Manchester NHS

NHS Foundation Trust

PATIENT INFORMATION SHEET

Determining the best method of pacing using Cardiac Magnetic Resonance Imaging

You are being invited to take part in a research study carried out here at Wythenshawe hospital. Before you decide to take part it is important for you to understand why the research is being done and what it will involve.

Please read the following information carefully and discuss it with others if you wish. Ask us if there is anything that is not clear, or if you would like more information. Take time to decide whether or not you wish to take part.

Why is the study being carried out?

It is still not clear where the best position to put the pacemaker lead is within the heart.

This study aims to look at this question by using cardiac MRI (Cardiovascular Magnetic Resonance Imaging). Standard pacemakers cannot go through an MRI scan, but as part of this study you will receive a new type of pacemaker that allows this type of scan.

Why have I been chosen?

You have Atrial Fibrillation (AF) and as part of your treatment you require a procedure called an AV node ablation. The AV node receives electrical signals from the top of the heart and transfers it to the bottom of the heart. Ablation (which is destroying the tissue so the signal cannot be transmitted) of the AV node can treat your AF. Before having the AV node ablation you will have a pacemaker implanted. This study looks at the pacemaker you will have as part of this treatment.

Do I have to take part?

Your participation is entirely voluntary and declining to take part will not alter your care.

If you do decide to take part you will be asked to sign a consent form. If you decide to take part you are free to withdraw at any time, without any changes to your subsequent care. The study will not affect any private medical insurance that you may have.

What will happen to me if I take part?

The Study is going to last 2 years, starting from the time you first have the pacemaker implanted.

Rather than having a pacemaker with one lead going into the heart, in this study you will be fitted with a pacemaker that has two leads. Each lead will be in a different position in the heart, but only one lead will be working at any one time. During the course of the study, we will change which lead your heart uses, to see if this changes the way your heart pumps. This will help us determine whether one position is better than the other. It may be that both are the same. Changing which lead you are using does not involve any operation or

procedure – it is simply reprogrammed in a very similar way to how you would normally have a pacemaker check. Having the extra pacemaker lead will add about 10 minutes onto the length of the pacemaker insertion.

We will assess the effect of the two different positions on how well your heart is functioning by doing Cardiac MRI scans. Cardiac MRI is a relatively new imaging technique. It uses a strong magnetic field to build up pictures based on differences in the water content of various body tissues. MRI scanning is extremely safe; indeed, it is described by the National Institute for Health and Clinical Excellence (NICE) as “one of the safest medical procedures currently available”. It does not involve x-rays (i.e. it does not use ionising radiation).

Wythenshawe Hospital carries out hundreds of these scans every year. The scanner is doughnut-shaped. You will be asked to lie still on a comfortable bed and the bed will move into the scanner. The scan will last for approximately 40 minutes. At times during the scan, you may be asked to hold your breath for up to 10-15 seconds. It is not painful. Before the scan we will put a needle into a vein in your arm and during the scan you will receive some dye called gadolinium contrast through this needle. Gadolinium contrast is used routinely in clinical cardiac MRI scanning. You will have 3 of these cardiac MRI scans during the 2 years and all will coincide with appointments that you would routinely have following a pacemaker. Therefore no extra visits are required.

Before your pacemaker is fitted you will also have an echocardiogram (also called an echo, an ultrasound test of the heart), a fitness test, a blood test and you will be asked to complete a short “quality of life questionnaire”. These will be done every 6 months following the pacemaker and AV node ablation and coincide with your pacemaker checks and/or doctor appointments. Therefore you will not have to have extra visits.

An echocardiogram involves having a probe with gel on it being placed on the chest. It is a very safe procedure but can occasionally cause mild discomfort when pressing on the chest wall. It takes about 20 minutes to do.

The fitness test involves cycling on an exercise bike while breathing through a mouthpiece. This measures your heart and lung function and can tell how fit you are. It is safe and takes about 30 minutes.

We will be taking a blood sample when you come for the visits. About 5mls of blood (less than a tablespoonsful) is required to fill one sample tube. The blood will be used to measure chemical substances in your blood called "biomarkers". These are measures of your body's function and we want to know whether they change throughout the study. The blood sample will be stored until we have lots of patients' samples so we can run all the tests together. The samples are stored on site in a secure laboratory and are anonymised.

Finally, a questionnaire regarding your general wellbeing will be used to see how you are. This will take about 15 minutes to complete and is the same each time you come. This will allow us to see if anything has changed over the 2 year period.

A complete timeline of the study is attached at the back as an appendix.

What are the possible disadvantages and risks of taking part?

As we are implanting two leads rather than one lead there is a small increase in the risk of a lead becoming loose. However, as there are two leads and both will have been fully tested, the second lead can be used instead of the loose lead, without you needing to have another procedure to reposition the lead. In the unlikely event of a lead becoming loose, however, we would not be able to include you in the remainder of the study.

Positioning of all pacemakers is monitored by X-ray imaging. The radiation dose associated with this procedure is less than the amount that you receive from a year of naturally-occurring background radiation. You are not expected to be exposed to a higher radiation dose than normal by having this MRI-safe pacemaker.

Cardiac MRI scanning is considered to be a safe procedure provided you do not have any contraindications to the procedure (i.e. reasons that would prohibit you from having a scan). All patients will be carefully screened and if there is a reason you could not have a cardiac MRI then you will not be allowed to take part in the study. Some people who are claustrophobic do not like being in the scanner, although the bore of the scanner (the 'hole' in the 'doughnut') is wide and you will be able to talk with the person taking the pictures (the radiographer) throughout. As such more than 98% of patients tolerate it.

Some aspects of the scanning procedure can potentially be associated with the following disadvantages and risks:

- Putting a needle into a vein in your arm – this can be mildly painful and can, on occasion, cause a bruise.
- Gadolinium contrast – Gadolinium is very well tolerated. Allergic reaction occurs in less than 1 in 3000 patients, with symptoms such as nausea and a transient skin rash.

Having MRI scans and exercise tests will make your visits to Wythenshawe longer but they will not increase the number of visits you have to make.

What are the possible benefits of taking part?

By taking part in this study you will have the most modern pacemaker that allows you to have MRI scans in the future (standard pacemakers are not allowed in MRI machines). This could be for something completely unrelated to the heart, eg if you needed an MRI scan of your knee. You will be more closely observed than if you had not taken part in the study and thus potential problems may be discovered much sooner.

The results of this research may improve the knowledge and care of patients like yourself in the future.

What if there is a problem?

If you have a concern about any aspect of this study, you should ask to speak to one of the researchers who will do their best to answer your questions. Our contact number is 0161 291 4940. If you remain unhappy and wish to complain formally, you can do this by contacting the Patient Liaison Service at Wythenshawe Hospital. The contact number for the Patient Liaison service is 0161 291 5600 and the email address is pls@uhsm.nhs.uk.

In the event that something does go wrong and you are harmed during the research and this is due to someone's negligence then you may have grounds for a legal action for compensation against University Hospital of South Manchester NHS Trust but you may have to pay your legal costs. The normal National Health Service complaints mechanisms will still be available to you.

Who has reviewed the study?

The study has been reviewed by NRES committee North West- Greater Manchester South.

The study has also been reviewed by the Pacing Manufacturer and has gone through their Scientific review panel.

What happens when the research study stops?

Once the study is complete, you will continue to be followed-up routinely as part of your normal ongoing care.

Will my taking part in this study be kept confidential?

At the beginning of the study you will be given a study identification number. All the information collected will be recorded using this number. Your name and address or other information will not be passed on to any third party. No information that could identify you as an individual would ever be published. The data will be stored securely on a computer and the study will be compliant with the Data Protection Act 1998. The data will ordinarily be accessible only to the research team but may be open to regulatory authorities and the Trust Research and Development Department for audit purposes if necessary. With your consent we will inform your GP of your participation in the study.

Who is organising and funding the research?

The research is being organised by the Pacing and Cardiac MRI teams at Wythenshawe Hospital. The study is being funded by the Cardiology department with support from St Jude Medical Limited, the manufacturer of the pacemaker. There is no financial incentive for the hospital or doctor for recruiting into the study. Being part of the study will not affect the standard of care you receive from the NHS in any way.

What will happen to the results of the research study?

The results will be used to form conclusions about the best position to put a pacemaker lead and we aim to publish these in leading journals.

The study is part of an educational project and will form part of a thesis at the University of Manchester.

The Academic supervisor for this is Dr Neil Davidson, Clinical Director of Cardiology at Wythenshawe Hospital and Honorary Senior Lecturer at the University of Manchester. His contact number is via his secretary 0161 291 2390.

Contact for further information

If you have any questions please contact Dr Mark Ainslie the Principal investigator, direct line 0161 291 4640.

We would like to thank you for taking time to read this information sheet

and potentially participating in the study

Kind Regards

Dr Mark Ainslie	*Cardiology Registrar*
Dr Ben Brown	*Cardiology Consultant*
Dr Matthias Schmitt	*Cardiology Consultant*
Dr Neil Davidson	*Cardiology Consultant*

University Hospital of South Manchester NHS
NHS Foundation Trust

***Pt invite*. Effect of Septal vs Apical pacing- a comparative study using cardiac MRI**

Dear Sir/ Madam,

We are running a research study at Wythenshawe Hospital and we would like to invite you to take part. The study is being jointly run by the cardiac pacing and cardiac imaging teams.

We are testing to see how best a pacemaker can be used to maintain the heart's health. Different areas of the heart can be paced and we are trying to determine the best position for the pacemaker leads to help to improve care for patients in the future.

The study involves Cardiac MRI scans. Enclosed is a comprehensive information sheet describing the background to the study and explaining what taking part would involve.

If, having read the information sheet, you are willing to take part, please could you complete page 2 of this letter. If you have any questions, please contact Dr Mark Ainslie on 0161 291 4640.

When you sign the form, Dr Ainslie will speak to you to discuss the details of taking part and answer any questions.

You will also have a further opportunity to discuss things when you attend for your pacemaker and we will ask you to sign a consent form.

If, having read the information sheet, you would rather not take part in the study, we would fully understand and your decision will not affect your care now or in the future in any way.

Many thanks for taking the time to consider the study

Kind regards

Dr Mark Ainslie — Cardiology Registrar

Dr Ben Brown, Dr Matthias Schmitt, Dr Neil Davidson — Cardiology Consultants

Effect of Septal vs Apical pacing- a comparative study using cardiac MRI

I am willing to consider taking part in the above study as described in the information sheet and letter.

Name: _____

Signature: _____

University Hospital of South Manchester NHS
NHS Foundation Trust

GP Sheet

Effect of Septal vs Apical pacing- a comparative study using cardiac MRI

RE:Dear Dr

Your patient has given consent to take part in the above trial that is taking place in the Cardiology Department at Wythenshawe Hospital.

This trial is running from 1st December 2011. Your patient with Atrial Fibrillation has had a pacemaker fitted, after which they will undergo an AV node ablation as part of their "pace and ablate" treatment. This pacemaker is MRI-compatible so they can undergo MRI imaging without risk to their pacemaker. The pacemaker has 2 ventricular leads, one sited at the septum, the other at the apex.

The trial involves pacing the heart from the 2 different ventricular sites at differing times, in order to determine which is the superior site for preserving cardiac function.

The study takes place over 2 years, and your patient will undergo a series of echoes, exercise tests, quality of life questionnaires and 3 cardiac MRI scans. Blood tests will also be taken for measuring biomarkers such as brain natriuretic peptide (BNP). Please find enclosed the timeline for patients in the study.

This study should not have any effect on treatments for co-existing conditions. The study does not involve any new medications. The study is forming part of an MD project at The University of Manchester and we hope to publish the results.

If you have any questions regarding the trial please do not hesitate to contact us.

Yours Sincerely

Dr Mark Ainslie, Dr Ben Brown, Dr Matthias Schmitt, Dr Neil Davidson
Contact: Principal investigator and Cardiology SpR Mark Ainslie markainslie@nhs.net, direct line 0161 2914640

MAPS protocol

IMPORTANT – REMAIN AT NORMAL SAR LEVEL

1. Orthogonal localisers
2. HASTE axial
3. Localisers- CH4, CH2, SA 5 slice stack
4. CH4 cine (SpGR and SSFP)
5. RVOT cine (SpGR and SSFP)
6. Dedicated RV2 view (SpGR and SSFP)
7. Dedicated RV inflow/outflow (SpGR and SSFP)
8. LV CH2 Cine
9. LV CH3 cine
10. LVOT cine
11. AO valve cine
12. PA flow **x3** VENC 150 to start
13. AO flow **x3 (check BP)**
14. SA localisers (5 slice) LV stack
15. T2 mapping (T2 SSFP Mid SA repeated at T2 prep times: 0, 25, 45, 65ms
16. T2 map – Mid SA
17. T1 mapping **pre contrast** (MOLLI capture cycle NC and CC)
    a. Mid SA
    b. 4Ch
18. Tagging
    a. 4ch
    b. basal
    c. mid
    d. apical
19. 0.2mmol/kg **Dotarem** – ie: 0.4mls per kg (up to 40mls max)
20. SA cine stack (SSFP sequences, 8mm slice thickness, no inter-slice gap)
21. T1 mapping **10 MINS post contrast** (MOLLI capture cycle NC and CC)
    a. Mid SA
    b. 4Ch
22. TI scout
23. LGE – SA stack only

24. T1 mapping **20 MINS post contrast** (MOLLI capture cycle NC and CC)
    a. Mid SA
    b. 4Ch
25. Pt leaves scanner and pacemaker is reprogrammed to alternate lead

26. Orthogonal Localisers
27. HASTE axial
28. Localisers- ch4, ch2, SA 5 slice stack
29. CH4 cine (SpGR and SSFP)
30. RVOT cine
31. Dedicated RV2 view
32. CH2 cine
33. CH3 cine
34. LVOT cine
35. AO valve cine
36. PA flow **x3** VENC 150 to start
37. AO flow **x3 (check BP)**
38. SA localisers (5 slices) LV stack
39. Tagging 4ch
    a. 4ch
    b. basal
    c. mid
    d. apical
40. SA cine stack

Protocol for effect of metal susceptibility artefact on T1 mapping and velocity phase encoding

Scans am/noon/pm wed/thurs/fri for 2 weeks

1. **Othogonal localisers**
2. **Velocity phase encoding Venc 150 cm/s**
    a. **Axial 0mm, +50mm, -50mm**
    b. **Saggital- 0mm, 50mm, -50mm**
    c. **Coronal- 0mm**
3. **T1 mapping**
    a. **MOLLI sequence,**
        i. **TI 50 to 1000ms, slice thickness 8mm**

Evaluation of left ventricular torsion using cardiac MRI. Validation of tagging and feature tracking.

CMR protocol

- Orthogonal localizer
- Haste
- Localisers – CH4, CH2, SA 5 slice stack
- CH4 cine
- LV CH2 cine
- LV CH3 cine
- LVOT cine
- Aortic Valve cine
- Short axis LV stack
- Tagging (4 ch, basal, mid, apical)
- SA cine stack SSFP- 8mm slices, no gap.
- Medium dose dobutamine
    - 4 chamber
    - SA basal
    - SA mid
    - SA apex
    - Tagging (basal and apical)

Inclusion and exclusion criteria

Inclusion Criteria
Patients aged 18 to 85 years old
Able to consent for study
Exclusion Criteria
Patients with an implantable pulse generator
Patients with a myocardial infarction within three months prior to enrolment
Patients that received a bypass within three months prior to enrolment
Patients that have had a valve replacement within three months prior to enrolment or a mechanical right heart valve.
Patients where a right ventricular lead cannot be placed e.g. complex congenital heart disease
Patients with hypertrophic cardiomyopathy
Patients with acute coronary syndrome, unstable angina, severe mitral regurgitation and/or haemodynamically significant aortic stenosis
Terminal conditions with a life expectancy less than 12 months
Participation in any other study that would confound the results of this study
Psychological or emotional problems that may interfere with the volunteer's ability to provide full consent or fully understand the purposes of the study
Pregnant patients
Contraindications for using MRI e.g. neurosurgical clips or claustrophobia
Contraindications for using dobutamine
Chronic illness that requires regular medication

References

1. Kirchhof P, Auricchio A, Bax J, Crijns H, Camm J, Diener H-C, et al. Outcome parameters for trials in atrial fibrillation: executive summary. Eur Heart J [Internet]. 2007 Nov;28(22):2803–17.
2. Psaty BM, Manolio TA, Kuller LH, Kronmal RA, Cushman M, Fried LP, et al. Incidence of and Risk Factors for Atrial Fibrillation in Older Adults. Circ [Internet]. 1997 Oct 7;96 (7):2455–61.
3. Miyasaka Y, Barnes ME, Gersh BJ, Cha SS, Bailey KR, Abhayaratna WP, et al. Secular trends in incidence of atrial fibrillation in Olmsted County, Minnesota, 1980 to 2000, and implications on the projections for future prevalence. Circulation [Internet]. 2006 Jul 11;114(2):119–25.
4. Roger VL, Go AS, Lloyd-Jones DM, Benjamin EJ, Berry JD, Borden WB, et al. Heart disease and stroke statistics--2012 update: a report from the American Heart Association. Circulation [Internet]. 2012 Jan 3;125(1):e2–220.
5. Anter E, Jessup M, Callans DJ. Atrial fibrillation and heart failure: treatment considerations for a dual epidemic. Circulation [Internet]. 2009 May 12;119(18):2516–25.
6. Benjamin EJ, Wolf P a., D'Agostino RB, Silbershatz H, Kannel WB, Levy D. Impact of Atrial Fibrillation on the Risk of Death : The Framingham Heart Study. Circulation [Internet]. 1998 Sep 8;98(10):946–52.
7. Miyasaka Y, Barnes ME, Bailey KR, Cha SS, Gersh BJ, Seward JB, et al. Mortality trends in patients diagnosed with first atrial fibrillation: a 21-year community-based study. J Am Coll Cardiol [Internet]. 2007 Mar 6;49(9):986–92.
8. Haïssaguerre M, Jaïs P, Shah DC, Takahashi a, Hocini M, Quiniou G, et al. Spontaneous initiation of atrial fibrillation by ectopic beats originating in the pulmonary veins. N Engl J Med [Internet]. 1998 Sep 3;339(10):659–66.
9. Brundel BJJM, Henning RH, Kampinga HH, Van Gelder IC, Crijns HJGM. Molecular mechanisms of remodeling in human atrial fibrillation. Cardiovasc Res [Internet]. 2002 May;54(2):315–24.
10. Camm a J, Lip GYH, De Caterina R, Savelieva I, Atar D, Hohnloser SH, et al. 2012 focused update of the ESC Guidelines for the management of atrial fibrillation: an update of the 2010 ESC Guidelines for the management of atrial fibrillation. Developed with the special contribution of the European Heart Rhythm Association. Eur Heart J [Internet]. 2012 Nov;33(21):2719–47.
11. Lip GYH, Frison L, Halperin JL, Lane D a. Identifying patients at high risk for stroke despite anticoagulation: a comparison of contemporary stroke risk stratification schemes in an anticoagulated atrial fibrillation cohort. Stroke [Internet]. 2010 Dec;41(12):2731–8.
12. AFFIRM. AFFIRM trial: a comparison of rate control and rhythm control in patients with atrial fibrillation. N Engl J Med [Internet]. 2002;347(23):1825–33.
13. Van Gelder IC, Hagens VE, Bosker HA, Kingma JH, Kamp O, Kingma T, et al. A comparison of rate control and rhythm control in patients with recurrent persistent atrial fibrillation. N Engl J Med [Internet]. 2002;347(23):1834–40.
14. Camm a J. Safety considerations in the pharmacological management of atrial fibrillation. Int J Cardiol [Internet]. 2008 Jul 21;127(3):299–306.

15. Oral H. Pulmonary Vein Isolation for Paroxysmal and Persistent Atrial Fibrillation. Circulation [Internet]. 2002 Feb 4;105(9):1077–81.

16. Pappone C, Augello G, Sala S, Gugliotta F, Vicedomini G, Gulletta S, et al. A randomized trial of circumferential pulmonary vein ablation versus antiarrhythmic drug therapy in paroxysmal atrial fibrillation: the APAF Study. J Am Coll Cardiol [Internet]. 2006 Dec 5;48(11):2340–7.

17. Jaïs P, Cauchemez B, Macle L, Daoud E, Khairy P, Subbiah R, et al. Catheter ablation versus antiarrhythmic drugs for atrial fibrillation: the A4 study. Circulation [Internet]. 2008 Dec 9;118(24):2498–505.

18. Wood M a., Brown-Mahoney C, Kay GN, Ellenbogen K a. Clinical Outcomes After Ablation and Pacing Therapy for Atrial Fibrillation : A Meta-Analysis. Circulation [Internet]. 2000 Mar 14;101(10):1138–44.

19. Connolly S, Kerr C, Gent M, RS R, Ysuf S, AM G, et al. EFFECTS OF PHYSIOLOGIC PACING VERSUS VENTRICULAR PACING ON THE RISK OF STROKE AND DEATH DUE TO CARDIOVASCULAR CAUSES. N Engl J Med [Internet]. 2000;342(19):1385–91.

20. Lamas G a, Lee KL, Sweeney MO, Silverman R, Leon A, Yee R, et al. Ventricular pacing or dual-chamber pacing for sinus-node dysfunction. N Engl J Med [Internet]. 2002;346(24):1854–62.

21. Andersen HR, Nielsen JC, Thomsen PE, Thuesen L, Mortensen PT, Vesterlund T, et al. Long-term follow-up of patients from a randomised trial of atrial versus ventricular pacing for sick-sinus syndrome. Lancet [Internet]. 1997 Oct 25;350(9086):1210–6.

22. Healey JS, Toff WD, Lamas G a, Andersen HR, Thorpe KE, Ellenbogen K a, et al. Cardiovascular outcomes with atrial-based pacing compared with ventricular pacing: meta-analysis of randomized trials, using individual patient data. Circulation [Internet]. 2006 Jul 4;114(1):11–7.

23. Wilkoff B, Cook J, Epstein A, Greene L, Hallstrom A, Kutalek S, et al. Dual-Chamber Pacing or Ventricular Backup Pacing in Patients With an Implantable Defibrillator. The Dual Chamber and VVI Implantable Defibrillator (DAVID) Trial. JAMA [Internet]. 2002;288(24):3115–23.

24. Sweeney MO, Bank AJ, Nsah E, Koullick M, Zeng QC, Hettrick D, et al. Minimizing ventricular pacing to reduce atrial fibrillation in sinus-node disease. N Engl J Med [Internet]. 2007 Sep 6;357(10):1000–8.

25. Knight BP, Gersh BJ, Carlson MD, Friedman P a, McNamara RL, Strickberger SA, et al. Role of permanent pacing to prevent atrial fibrillation: science advisory from the American Heart Association Council on Clinical Cardiology (Subcommittee on Electrocardiography and Arrhythmias) and the Quality of Care and Outcomes Research Interdisciplin. Circulation [Internet]. 2005 Jan 18;111(2):240–3.

26. Israel CW, Hohnloser SH. Pacing to prevent atrial fibrillation. J Cardiovasc Electrophysiol [Internet]. 2003 Sep;14(9 Suppl):S20–6.

27. Saksena S, Prakash A, Ziegler P, Hummel JD, Friedman P, Plumb VJ, et al. Improved suppression of recurrent atrial fibrillation with dual-site right atrial pacing and antiarrhythmic drug therapy. J Am Coll Cardiol [Internet]. 2002 Sep 18;40(6):1140–50; discussion 1151–2.

28. Brignole M, Auricchio A, Baron-Esquivias G, Bordachar P, Boriani G, Breithardt O-A, et al. 2013 ESC Guidelines on cardiac pacing and cardiac resynchronization therapy: The Task Force on cardiac pacing and resynchronization therapy of the European Society of Cardiology (ESC). Developed in collaboration with the European Heart Rhythm Association . Eur Heart J [Internet]. 2013 Jun 24;

29. Epstein AE, DiMarco JP, Ellenbogen K a, Estes N a M, Freedman R a, Gettes LS, et al. ACC/AHA/HRS 2008 Guidelines for Device-Based Therapy of Cardiac Rhythm Abnormalities: a report of the American College of Cardiology/American Heart Association Task Force on Practice Guidelines (Writing Committee to Revise the ACC/AHA/NASPE 2002 Guideline. J Am Coll Cardiol [Internet]. 2008 May 27;51(21):e1–62.

30. Ector H, Vardas P. Current use of pacemakers, implantable cardioverter defibrillators, and resynchronization devices: data from the registry of the European Heart Rhythm Association. Eur Hear J Suppl [Internet]. 2007 Dec 1;9(Suppl I):I44–9.

31. Tops LF, Schalij MJ, Holman ER, van Erven L, van der Wall EE, Bax JJ. Right ventricular pacing can induce ventricular dyssynchrony in patients with atrial fibrillation after atrioventricular node ablation. J Am Coll Cardiol [Internet]. 2006 Oct 17;48(8):1642–8.

32. Hayes DL, Furman S. Cardiac pacing: how it started, where we are, where we are going. J Cardiovasc Electrophysiol [Internet]. 2004 May;15(5):619–27.

33. Rajappan K. Permanent pacemaker implantation technique: part I: arrhythmias. Heart [Internet]. 2009 Mar;95(3):259–64.

34. Victor F, Leclercq C, Mabo P, Pavin D, Deviller A, Place C, et al. Optimal right ventricular pacing site in chronically implanted patients: A prospective randomized crossover comparison of apical and outflow tract pacing. J Am Coll Cardiol [Internet]. 1999;33(2):311–6.

35. Moss A, Zareba W, Hall W, Klein H, Wilber D, Cannom D, et al. Prophylactic implantation of a defibrillator in patients with myocardial infarction and reduced ejection fraction. N Engl J Med [Internet]. 2002;346(12):877–83.

36. Steinberg JS, Fischer A, Wang P, Schuger C, Daubert J, McNitt S, et al. The clinical implications of cumulative right ventricular pacing in the multicenter automatic defibrillator trial II. J Cardiovasc Electrophysiol [Internet]. 2005 Apr;16(4):359–65.

37. Sweeney MO, Hellkamp AS, Ellenbogen K a, Greenspon AJ, Freedman R a, Lee KL, et al. Adverse effect of ventricular pacing on heart failure and atrial fibrillation among patients with normal baseline QRS duration in a clinical trial of pacemaker therapy for sinus node dysfunction. Circulation [Internet]. 2003 Jun 17;107(23):2932–7.

38. Prinzen F, Peschar M. Relation Between the Pacing Induced Sequence of Activation and Left Ventricular Pump function in animals. Pacing Clin Electrophysiol [Internet]. 2002;25(4):484–98.

39. Myerburg RJ, Nilsson K, Gelband H. Physiology of Canine Intraventricular Conduction and Endocardial Excitation. Circ Res [Internet]. 1972 Feb 1;30(2):217–43.

40. Lister J, Klotz D, Jomain S. Effect of pacemaker site on cardiac output and ventricular activation in dogs with complete heart block. Am J Cardiol. 1964;14:494–503.

41. Wyman BT, Hunter WC, Prinzen FW, McVeigh ER. Mapping propagation of mechanical activation in the paced heart with MRI tagging. Am J Physiol [Internet]. 1999 Mar;276(3 Pt 2):H881–91.

42. Prinzen FW, Van Oosterhout MF, Vanagt WY, Storm C, Reneman RS. Optimization of ventricular function by improving the activation sequence during ventricular pacing. Pacing Clin Electrophysiol [Internet]. 1998 Nov;21(11 Pt 2):2256–60.

43. Karpawich P, Justice C, Cavitt D, Chang C. Developmental sequelae of fixed-rate ventricular pacing in the immature canine heart:an electrophysiologic hemodynamic, and histopathologic evaluation. Am Heart J. 1990;119(5):1077–83.

44. Karpawich PP, Gates J, Stokes KB. Septal His-Purkinje ventricular pacing in canines: a new endocardial electrode approach. Pacing Clin Electrophysiol [Internet]. 1992

Nov;15(11 Pt 2):2011–5.

45. Rosenqvist M, Bergfeldt L, Haga Y, Rydén J, Rydén L, Owall a. The effect of ventricular activation sequence on cardiac performance during pacing. Pacing Clin Electrophysiol [Internet]. 1996 Sep;19(9):1279–86.

46. Scherlag B. A technique for ventricular pacing from the His bundle of the intact heart. J Appl Physiol [Internet]. 1967;22(3):584–7.

47. Grover M, Glantz S a. Endocardial pacing site affects left ventricular end-diastolic volume and performance in the intact anesthetized dog. Circ Res [Internet]. 1983 Jul;53(1):72–85.

48. Buchalter M, Rademakers FE, Weiss J, Rogers W, Weisfeldt M, Shapiro E. Rotational deformation of the canine left ventricle measured by magnetic resonance tagging: effects of catecholamines, ischaemia, and pacing. Cardiovasc Res [Internet]. 1994;28:629–35.

49. Prinzen FW, Hunter WC, Wyman BT, McVeigh ER. Mapping of regional myocardial strain and work during ventricular pacing: experimental study using magnetic resonance imaging tagging. J Am Coll Cardiol [Internet]. 1999 May;33(6):1735–42.

50. Prinzen FW, Augustijn CH, Arts T, Allessie M a, Reneman RS. Redistribution of myocardial fiber strain and blood flow by asynchronous activation. Am J Physiol [Internet]. 1990 Aug;259(2 Pt 2):H300–8.

51. Badke FR, Boinay P, Covell JW. Effects of ventricular pacing on regional left ventricular performance in the dog. Am J Physiol [Internet]. 1980 Jun;238(6):H858–67.

52. Delhaas T, Arts T, Prinzen FW, Reneman RS. Regional fibre stress-fibre strain area as an estimate of regional blood flow and oxygen demand in the canine heart. J Physiol [Internet]. 1994 Jun 15;477 (Pt 3(1994):481–96.

53. Samet P, Castillo C, Bernstein W. hemodynamic consequences of sequential atrioventricular pacing. Am J Cardiol. 1968;21(February):207–12.

54. Daggett WM, Bianco J a., Powell WJ, Austen WG. Relative Contributions of the Atrial Systole-Ventricular Systole Interval and of Patterns of Ventricular Activation to Ventricular Function during Electrical Pacing of the Dog Heart. Circ Res [Internet]. 1970 Jul 1;27(1):69–79.

55. van Oosterhout MFM, Prinzen FW, Arts T, Schreuder JJ, Vanagt WYR, Cleutjens JPM, et al. Asynchronous Electrical Activation Induces Asymmetrical Hypertrophy of the Left Ventricular Wall. Circulation [Internet]. 1998 Aug 11;98(6):588–95.

56. Miyazawa K, Shirato K, Haneda T, Honna T, Arai T. Effects of varying pacemaker sites on left ventricular performance. Tohoku J Exp Med [Internet]. 1976;120(4):301–8.

57. Tyers G. Comparison of the effect on cardiac function of single-site and simultaneous mutiple-site ventricualr stiumlation after A-V block. J Thorac Cardiovasc Surg. 1970;59(2):211–7.

58. Delgado V, Tops LF, Trines S a, Zeppenfeld K, Marsan NA, Bertini M, et al. Acute effects of right ventricular apical pacing on left ventricular synchrony and mechanics. Circ Arrhythm Electrophysiol [Internet]. 2009 Apr;2(2):135–45.

59. Liu W-H, Chen M-C, Chen Y-L, Guo B-F, Pan K-L, Yang C-H, et al. Right ventricular apical pacing acutely impairs left ventricular function and induces mechanical dyssynchrony in patients with sick sinus syndrome: a real-time three-dimensional echocardiographic study. J Am Soc Echocardiogr [Internet]. 2008 Mar;21(3):224–9.

60. Nahlawi M, Waligora M, Spies SM, Bonow RO, Kadish AH, Goldberger JJ. Left

ventricular function during and after right ventricular pacing. J Am Coll Cardiol [Internet]. 2004 Nov 2;44(9):1883–8.

61. Bank AJ, Kaufman CL, Burns K V, Parah JS, Johnson L, Kelly AS, et al. Intramural dyssynchrony and response to cardiac resynchronization therapy in patients with and without previous right ventricular pacing. Eur J Heart Fail [Internet]. 2010 Dec;12(12):1317–24.

62. Carlsson M, Ugander M, Mose H, Buhre T, Arheden H, Carlsson M, et al. Atrioventricular plane displacement is the major contributor to left ventricular pumping in healthy adults , athletes , and patients with dilated cardiomyopathy. Am J Physiol Hear Circ Physio. 2007;292:1452–9.

63. Leclercq C, Gras D, Le Helloco a, Nicol L, Mabo P, Daubert C. Hemodynamic importance of preserving the normal sequence of ventricular activation in permanent cardiac pacing. Am Heart J [Internet]. 1995 Jun;129(6):1133–41.

64. Pastore G, Noventa F, Piovesana P, Cazzin R, Aggio S, Verlato R, et al. Left ventricular dyssynchrony resulting from right ventricular apical pacing: relevance of baseline assessment. Pacing Clin Electrophysiol [Internet]. 2008 Nov;31(11):1456–62.

65. Tops LF, Schalij MJ, Bax JJ. The effects of right ventricular apical pacing on ventricular function and dyssynchrony implications for therapy. J Am Coll Cardiol [Internet]. American College of Cardiology Foundation; 2009 Aug 25;54(9):764–76.

66. Sweeney MO, Hellkamp AS. Heart failure during cardiac pacing. Circulation [Internet]. 2006 May 2;113(17):2082–8.

67. Chen L, Hodge D, Jahangir A, Ozcan C, Trusty J, Friedman P, et al. Preserved left ventricular ejection fraction following atrioventricular junction ablation and pacing for atrial fibrillation. J Cardiovasc Electrophysiol [Internet]. 2008 Jan;19(1):19–27.

68. Zhang X-H, Chen H, Siu C-W, Yiu K-H, Chan W-S, Lee KL, et al. New-onset heart failure after permanent right ventricular apical pacing in patients with acquired high-grade atrioventricular block and normal left ventricular function. J Cardiovasc Electrophysiol [Internet]. 2008 Feb;19(2):136–41.

69. Tops LF, Suffoletto MS, Bleeker GB, Boersma E, van der Wall EE, Gorcsan J, et al. Speckle-tracking radial strain reveals left ventricular dyssynchrony in patients with permanent right ventricular pacing. J Am Coll Cardiol [Internet]. 2007 Sep 18;50(12):1180–8.

70. Thambo J-B, Bordachar P, Garrigue S, Lafitte S, Sanders P, Reuter S, et al. Detrimental ventricular remodeling in patients with congenital complete heart block and chronic right ventricular apical pacing. Circulation [Internet]. 2004 Dec 21;110(25):3766–72.

71. Fang F, Chan JY-S, Yip GW-K, Xie J-M, Zhang Q, Fung JW-H, et al. Prevalence and determinants of left ventricular systolic dyssynchrony in patients with normal ejection fraction received right ventricular apical pacing: a real-time three-dimensional echocardiographic study. Eur J Echocardiogr [Internet]. 2010 Mar;11(2):109–18.

72. Ng ACT, Allman C, Vidaic J, Tie H, Hopkins AP, Leung DY. Long-term impact of right ventricular septal versus apical pacing on left ventricular synchrony and function in patients with second- or third-degree heart block. Am J Cardiol [Internet]. Elsevier Inc.; 2009 Apr 15;103(8):1096–101.

73. Bank AJ, Gage RM, Burns K V. Right ventricular pacing, mechanical dyssynchrony, and heart failure. J Cardiovasc Transl Res [Internet]. 2012 Apr;5(2):219–31.

74. Burns K V, Kaufman CL, Kelly AS, Parah JS, Dengel DR, Bank AJ. Torsion and dyssynchrony differences between chronically paced and non-paced heart failure

patients. J Card Fail [Internet]. 2011 Jun;17(6):495–502.

75. Tse HF, Lau CP. Long-term effect of right ventricular pacing on myocardial perfusion and function. J Am Coll Cardiol [Internet]. 1997 Mar 15;29(4):744–9.

76. Karpawich PP, Rabah R, Haas JE. Altered cardiac histology following apical right ventricular pacing in patients with congenital atrioventricular block. Pacing Clin Electrophysiol [Internet]. 1999 Sep;22(9):1372–7.

77. Abraham WT, Hayes DL. Cardiac resynchronization therapy for heart failure. Circulation [Internet]. 2003 Nov 25;108(21):2596–603.

78. Hayes JJ, Sharma AD, Love JC, Herre JM, Leonen AO, Kudenchuk PJ, et al. Abnormal Conduction Increases Risk of Adverse Outcomes From Right Ventricular Pacing. J Am Coll Cardiol [Internet]. 2006;48(8):1628–33.

79. SCHNEIDER JF, THOMAS H. EMERSON J, KREGER BE, McNAMARA PM, KANNEL WB. Newly Acquired Left Bundle-Branch Block: The Framingham Study. Ann Intern Med [Internet]. 1979 Mar 1;90(3):303–10.

80. Bader H, Garrigue S, Lafitte S, Reuter S, Jaïs P, Haïssaguerre M, et al. Intra-left ventricular electromechanical asynchrony. J Am Coll Cardiol [Internet]. 2004 Jan;43(2):248–56.

81. Marsan NA, Breithardt O a, Delgado V, Bertini M, Tops LF. Predicting response to CRT. The value of two- and three-dimensional echocardiography. Europace [Internet]. 2008 Nov;10 Suppl 3:iii73–9.

82. Kindermann M, Hennen B, Jung J, Geisel J, Böhm M, Fröhlig G. Biventricular versus conventional right ventricular stimulation for patients with standard pacing indication and left ventricular dysfunction: the Homburg Biventricular Pacing Evaluation (HOBIPACE). J Am Coll Cardiol [Internet]. 2006 May 16;47(10):1927–37.

83. Curtis AB, Worley SJ, Adamson PB, Chung ES, Niazi I, Sherfesee L, et al. Biventricular pacing for atrioventricular block and systolic dysfunction. N Engl J Med [Internet]. 2013 Apr 25;368(17):1585–93.

84. Yu C-M, Chan JY-S, Zhang Q, Omar R, Yip GW-K, Hussin A, et al. Biventricular pacing in patients with bradycardia and normal ejection fraction. N Engl J Med [Internet]. 2009 Dec 26;361(22):2123–34.

85. Chan JY-S, Fang F, Zhang Q, Fung JW-H, Razali O, Azlan H, et al. Biventricular pacing is superior to right ventricular pacing in bradycardia patients with preserved systolic function: 2-year results of the PACE trial. Eur Heart J [Internet]. 2011 Oct;32(20):2533–40.

86. Doshi RN, Daoud EG, Fellows C, Turk K, Duran A, Hamdan MH, et al. Left ventricular-based cardiac stimulation post AV nodal ablation evaluation (the PAVE study). J Cardiovasc Electrophysiol [Internet]. 2005 Nov;16(11):1160–5.

87. Leclercq C. Comparative effects of permanent biventricular and right-univentricular pacing in heart failure patients with chronic atrial fibrillation. Eur Heart J [Internet]. 2002 Nov 15;23(22):1780–7.

88. Brignole M, Gammage M, Puggioni E, Alboni P, Raviele a, Sutton R, et al. Comparative assessment of right, left, and biventricular pacing in patients with permanent atrial fibrillation. Eur Heart J [Internet]. 2005 Apr;26(7):712–22.

89. Brignole M, Botto G, Mont L, Iacopino S, Marchi G De, Oddone D, et al. Cardiac resynchronization therapy in patients undergoing atrioventricular junction ablation for permanent atrial fibrillation : a randomized trial. Eur Heart J. 2011;32(19):2420–9.

90. Stockburger M, Gómez-Doblas JJ, Lamas G, Alzueta J, Fernández-Lozano I, Cobo E, et al. Preventing ventricular dysfunction in pacemaker patients without advanced

heart failure: results from a multicentre international randomized trial (PREVENT-HF). Eur J Heart Fail [Internet]. 2011 Jun;13(6):633–41.

91. Kronborg MB, Mortensen PT, Gerdes JC, Jensen HK, Nielsen JC. His and para-His pacing in AV block: feasibility and electrocardiographic findings. J Interv Card Electrophysiol [Internet]. 2011 Sep;31(3):255–62.

92. Catanzariti D, Maines M, Cemin C, Broso G, Marotta T, Vergara G. Permanent direct his bundle pacing does not induce ventricular dyssynchrony unlike conventional right ventricular apical pacing. An intrapatient acute comparison study. J Interv Card Electrophysiol [Internet]. 2006 Aug;16(2):81–92.

93. Zanon F, Bacchiega E, Rampin L, Aggio S, Baracca E, Pastore G, et al. Direct His bundle pacing preserves coronary perfusion compared with right ventricular apical pacing: a prospective, cross-over mid-term study. Europace [Internet]. 2008 May;10(5):580–7.

94. Deshmukh P, Casavant DA, Romanyshyn M, Anderson K. Permanent direct His-bundle pacing. a novel approach in cardaic pacing. Circ J. 2000;

95. Occhetta E, Bortnik M, Magnani A, Francalacci G, Piccinino C, Plebani L, et al. Prevention of ventricular desynchronization by permanent para-Hisian pacing after atrioventricular node ablation in chronic atrial fibrillation: a crossover, blinded, randomized study versus apical right ventricular pacing. J Am Coll Cardiol [Internet]. 2006 May 16;47(10):1938–45.

96. Res JCJ, Bokern MJJ a, de Cock CC, van Loenhout T, Bronzwaer PN a, Spierenburg H a M. The BRIGHT study: bifocal right ventricular resynchronization therapy: a randomized study. Europace [Internet]. 2007 Oct;9(10):857–61.

97. Albouaini K, Alkarmi a, Mudawi T, Gammage MD, Wright DJ. Selective site right ventricular pacing. Heart [Internet]. 2009 Dec;95(24):2030–9.

98. Barin ES, Jones SM, Ward DE, Camm a J, Nathan a W. The right ventricular outflow tract as an alternative permanent pacing site: long-term follow-up. Pacing Clin Electrophysiol [Internet]. 1991 Jan;14(1):3–6.

99. Yamano T, Kubo T, Takarada S, Ishibashi K, Komukai K, Tanimoto T, et al. Advantage of right ventricular outflow tract pacing on cardiac function and coronary circulation in comparison with right ventricular apex pacing. J Am Soc Echocardiogr [Internet]. 2010 Nov;23(11):1177–82.

100. Giudici MC, Thornburg G a, Buck DL, Coyne EP, Walton MC, Paul DL, et al. Comparison of right ventricular outflow tract and apical lead permanent pacing on cardiac output. Am J Cardiol [Internet]. 1997 Jan 15;79(2):209–12.

101. Leong DP, Mitchell A-M, Salna I, Brooks AG, Sharma G, Lim HS, et al. Long-term mechanical consequences of permanent right ventricular pacing: effect of pacing site. J Cardiovasc Electrophysiol [Internet]. 2010 Oct;21(10):1120–6.

102. Tse HF, Yu C, Wong KK, Tsang V, Leung YL, Ho WY, et al. Functional abnormalities in patients with permanent right ventricular pacing: the effect of sites of electrical stimulation. J Am Coll Cardiol [Internet]. 2002 Oct 16;40(8):1451–8.

103. Stambler BS, Ellenbogen K a., Zhang X, Porter TR, Xie F, Malik R, et al. Right Ventricular Outflow Versus Apical Pacing in Pacemaker Patients with Congestive Heart Failure and Atrial Fibrillation. J Cardiovasc Electrophysiol [Internet]. 2003 Nov;14(11):1180–6.

104. Dabrowska-Kugacka A, Lewicka-Nowak E, Tybura S, Wilczek R, Staniewicz J, Zagozdzon P, et al. Survival analysis in patients with preserved left ventricular function and standard indications for permanent cardiac pacing randomized to right ventricular apical or septal outflow tract pacing. Circ J [Internet]. 2009

Oct;73(10):1812–9.

105. Vanerio G, Vidal JL, Fernández Banizi P, Banina Aguerre D, Viana P, Tejada J. Medium- and long-term survival after pacemaker implant: Improved survival with right ventricular outflow tract pacing. J Interv Card Electrophysiol [Internet]. 2008 Apr;21(3):195–201.
106. Burri H, Sunthorn H, Dorsaz P-A, Viera I, Shah D. Thresholds and complications with right ventricular septal pacing compared to apical pacing. Pacing Clin Electrophysiol [Internet]. 2007 Jan;30 Suppl 1(January):S75–8.
107. Yu C-C, Liu Y-B, Lin M-S, Wang J-Y, Lin J-L, Lin L-C. Septal pacing preserving better left ventricular mechanical performance and contractile synchronism than apical pacing in patients implanted with an atrioventricular sequential dual chamber pacemaker. Int J Cardiol [Internet]. 2007 May 16;118(1):97–106.
108. Inoue K, Okayama H, Nishimura K, Saito M, Yoshii T, Hiasa G, et al. Right Ventricular Septal Pacing Preserves Global Left Ventricular Longitudinal Function in Comparison With Apical Pacing. Circ J [Internet]. 2011;75(7):1609–15.
109. Schwaab B, Fröhlig G, Alexander C, Kindermann M, Hellwig N, Schwerdt H, et al. Influence of right ventricular stimulation site on left ventricular function in atrial synchronous ventricular pacing. J Am Coll Cardiol [Internet]. 1999 Mar;33(2):317–23.
110. Cano O, Osca J, Sancho-Tello M-J, Sánchez JM, Ortiz V, Castro JE, et al. Comparison of effectiveness of right ventricular septal pacing versus right ventricular apical pacing. Am J Cardiol [Internet]. Elsevier Inc.; 2010 May 15;105(10):1426–32.
111. Cho G-Y, Kim M-J, Park J-H, Kim H-S, Youn HJ, Kim K-H, et al. Comparison of ventricular dyssynchrony according to the position of right ventricular pacing electrode: a multi-center prospective echocardiographic study. J Cardiovasc Ultrasound [Internet]. 2011 Mar;19(1):15–20.
112. Kypta A, Steinwender C, Kammler J, Leisch F, Hofmann R. Long-term outcomes in patients with atrioventricular block undergoing septal ventricular lead implantation compared with standard apical pacing. Europace [Internet]. 2008 May;10(5):574–9.
113. Molina L, Sutton R, Gandoy W, Reyes N, Lara S, Limón F, et al. Medium-term effects of septal and apical pacing in pacemaker-dependent patients: a double-blind prospective randomized study. Pacing Clin Electrophysiol [Internet]. 2014 Feb;37(2):207–14.
114. Francis J, Jayesh B, Ashishkumar M, Faizal A, Mond H. Editorial Right Ventricular Septal Pacing : Has it come of age ? Indian Pacing Electrophysiol J. 2010;10(2):69–71.
115. Buckingham T a, Candinas R, Schläpfer J, Aebischer N, Jeanrenaud X, Landolt J, et al. Acute hemodynamic effects of atrioventricular pacing at differing sites in the right ventricle individually and simultaneously. Pacing Clin Electrophysiol [Internet]. 1997 Apr;20(4 Pt 1):909–15.
116. Bellenger NG, Burgess MI, Ray SG, Lahiri a, Coats a J, Cleland JG, et al. Comparison of left ventricular ejection fraction and volumes in heart failure by echocardiography, radionuclide ventriculography and cardiovascular magnetic resonance; are they interchangeable? Eur Heart J [Internet]. 2000 Aug;21(16):1387–96.
117. Rajappan K, Bellenger NG, Anderson L, Pennell DJ. The role of cardiovascular magnetic resonance in heart failure. Eur J Heart Fail [Internet]. 2000 Oct;2(3):241–52.
118. Reicheck N GD. Atlas of Cardiovascular Imaging. In: Krmaer C HG, editor. Atlas of Cardiovascular Imaging. 1st ed. Saunders; 2010. p. 33.
119. Benchimol a., Liggett MS. Cardiac Hemodynamics During Stimulation of the Right

Atrium, Right Ventricle, and Left Ventricle in Normal and Abnormal Hearts. Circulation [Internet]. 1966 Jun 1;33(6):933–44.

120. Barold SS, linhart j, Hildner F, Samet P. Comparison the Right of Endocardial Tracts of Pacing of Outflow and Inflow tracts of the right ventricle. Am J Cardiol. 1969;23(May):697–701.
121. Cowell R, Morris-Thurgood J, Ilsley C, Paul V. Septal short atrioventricular delay pacing: additional hemodynamic improvements in heart failure. Pacing Clin Electrophysiol [Internet]. 1994 Nov;17(11 Pt 2):1980–3.
122. Karpawich PP, Mital S. Comparative left ventricular function following atrial, septal, and apical single chamber heart pacing in the young. Pacing Clin Electrophysiol [Internet]. 1997 Aug;20(8 Pt 1):1983–8.
123. Buckingham T a, Candinas R, Attenhofer C, Van Hoeven H, Hug R, Hess O, et al. Systolic and diastolic function with alternate and combined site pacing in the right ventricle. Pacing Clin Electrophysiol [Internet]. 1998 May;21(5):1077–84.
124. de Cock CC, Meyer a, Kamp O, Visser C a. Hemodynamic benefits of right ventricular outflow tract pacing: comparison with right ventricular apex pacing. Pacing Clin Electrophysiol [Internet]. 1998 Mar;21(3):536–41.
125. Alboni P, Scarfò S, Fucà G, Mele D, Dinelli M, Paparella N. Short-term hemodynamic effects of DDD pacing from ventricular apex, right ventricular outflow tract and proximal septum. G Ital Cardiol. 1998;28(3):237–41.
126. Mera F, DeLurgio DB, Patterson RE, Merlino JD, Wade ME, León a R. A comparison of ventricular function during high right ventricular septal and apical pacing after his-bundle ablation for refractory atrial fibrillation. Pacing Clin Electrophysiol [Internet]. 1999 Aug;22(8):1234–9.
127. Kolettis TM, Kyriakides ZS, Tsiapras D, Popov T, Paraskevaides I, Kremastinos D. During Short-term Right Ventricular Outflow Tract Compared to Apical Pacing *. Chest. 2000;117:60–4.
128. Deshmukh PM, Romanyshyn M. Direct His-bundle pacing: present and future. Pacing Clin Electrophysiol [Internet]. 2004 Jun;27(6 Pt 2):862–70.
129. Victor F, Mabo P, Mansour H, Pavin D, Kabalu G, de Place C, et al. A randomized comparison of permanent septal versus apical right ventricular pacing: short-term results. J Cardiovasc Electrophysiol [Internet]. 2006 Mar;17(3):238–42.
130. ten Cate TJF, Scheffer MG, Sutherland GR, Verzijlbergen JF, van Hemel NM. Right ventricular outflow and apical pacing comparably worsen the echocardiographic normal left ventricle. Eur J Echocardiogr [Internet]. 2008 Sep;9(5):672–7.
131. Kaye GC, Linker NJ, Marwick TH, Pollock L, Graham L, Pouliot E, et al. Effect of right ventricular pacing lead site on left ventricular function in patients with high-grade atrioventricular block: results of the Protect-Pace study. Eur Heart J [Internet]. 2015 Apr 7;36(14):856–62.
132. Mond HG, Hillock RJ, Stevenson IH, McGavigan AD. The right ventricular outflow tract: the road to septal pacing. Pacing Clin Electrophysiol [Internet]. 2007 May;30(4):482–91.
133. Giudici MC, Karpawich PP. Alternative site pacing: it's time to define terms. Pacing Clin Electrophysiol [Internet]. 1999 Apr;22(4 Pt 1):551–3.
134. Lieberman R, Grenz D, Mond HG, Gammage MD. Selective site pacing: defining and reaching the selected site. Pacing Clin Electrophysiol [Internet]. 2004 Jun;27(6 Pt 2):883–6.
135. Kvitting J, Wigström L, Strotmann J, Sutherland G. How accurate is visual

assessment of synchronicity in myocardial motion? An In vitro study with computer-simulated regional delay in myocardial motion: clinical implications for rest and stress echocardiography studies. J Am Soc Echocardiogr. 1999;12(9):698–705.

136. Chung ES, Leon AR, Tavazzi L, Sun J-P, Nihoyannopoulos P, Merlino J, et al. Results of the Predictors of Response to CRT (PROSPECT) trial. Circulation [Internet]. 2008 May 20;117(20):2608–16.

137. Gabriel R, Bakshi T, Scott A, Christiansen J, Patel H, Wong S, et al. Reliability of echocardiographic indices of dyssynchrony. Echocardiogrpahy [Internet]. 2007;24(1):40–6.

138. Cazeau S, Bordachar P, Jauvert G, Lazarus S, Alonso M, Mugica J, et al. Echocardiographic modeling of cardiac dyssynchrony before and during multisite stimulation: a prospective study. Pacing Clin Electrophysiol [Internet]. 2003;26(January):137–43.

139. Pitzalis MV, Iacoviello M, Romito R, Massari F, Rizzon B, Luzzi G, et al. Cardiac resynchronization therapy tailored by echocardiographic evaluation of ventricular asynchrony. J Am Coll Cardiol. 2002;40(9):1615–22.

140. Yu C-M, Fung W-H, Lin H, Zhang Q, Sanderson JE, Lau C-P. Predictors of left ventricular reverse remodeling after cardiac resynchronization therapy for heart failure secondary to idiopathic dilated or ischemic cardiomyopathy. Am J Cardiol [Internet]. 2003 Mar;91(6):684–8.

141. Marcus GM, Rose E, Viloria EM, Schafer J, De Marco T, Saxon L a, et al. Septal to posterior wall motion delay fails to predict reverse remodeling or clinical improvement in patients undergoing cardiac resynchronization therapy. J Am Coll Cardiol [Internet]. 2005 Dec 20;46(12):2208–14.

142. Antonini C, Rivaben F, D. B. Posterior wall motion to aortic valve closure delay: A new sipmle M-mode/PW Doppler index of intraventricualr asynchrony. Eur J Echocardiogr. 2005;Dec(6):S1–193.

143. Bax JJ, Molhoek SG, Marwick TH, Erven L Van, Voogd PJ, Somer S, et al. Usefulness of Myocardial Tissue Doppler Echocardiography to Evaluate Left Ventricular Dyssynchrony Before and After Biventricular Pacing in. Am J Cardiol. 2003;91(02):94–7.

144. Yu C-M, Zhang Q, Fung JW-H, Chan HC-K, Chan Y-S, Yip GW-K, et al. A novel tool to assess systolic asynchrony and identify responders of cardiac resynchronization therapy by tissue synchronization imaging. J Am Coll Cardiol [Internet]. 2005 Mar 1;45(5):677–84.

145. Marwick TH. Measurement of strain and strain rate by echocardiography: ready for prime time? J Am Coll Cardiol [Internet]. 2006 Apr 4;47(7):1313–27.

146. Dai M, Lu J, Qian D-J, Cai J-F, Liu X-Y, Wu X-Q, et al. Assessment of left ventricular dyssynchrony and cardiac function in patients with different pacing modes using real-time three-dimensional echocardiography: Comparison with tissue Doppler imaging. Exp Ther Med [Internet]. 2013 Nov;6(5):1213–9.

147. Burgess MI, Jenkins C, Chan J, Marwick TH. Measurement of left ventricular dyssynchrony in patients with ischaemic cardiomyopathy: a comparison of real-time three- dimensional and tissue Doppler echocardiography. Heart. 2007;93:1191–7.

148. Fauchier L, Marie O, Casset-senon D, Babuty D, Cosnay P, Fauchier JP. Interventricular and Intraventricular Dyssynchrony in Idiopathic Dilated Cardiomyopathy A Prognostic Study With Fourier Phase Analysis of Radionuclide Angioscintigraphy. J Am Coll Cardiol. 2002;40(11):2022–30.

149. Grothues F, Smith GC, Moon JCC, Bellenger NG, Collins P, Klein HU, et al.

Comparison of interstudy reproducibility of cardiovascular magnetic resonance with two-dimensional echocardiography in normal subjects and in patients with heart failure or left ventricular hypertrophy. Am J Cardiol [Internet]. 2002 Jul 1;90(1):29–34.

150. Marta CS, Ledesma-Carbayo M, Bajo A, Perez-David E, Santos A, Desco M. Respiratory gated SPAMM sequence for magnetic resonance cardiac tagging. Comput Cardiol [Internet]. 2006;33:61–4.

151. Osman NF, Kerwin WS, Mcveigh ER, Prince JL. Cardiac Motion Tracking Using CINE Harmonic Phase (HARP) Magnetic Resonance Imaging. Magn Reson Med. 1999;42:1048–60.

152. Rutz A, Manka R, Kozerke S. dyssynchrony in patients with left bundle branch block and patients after myocardial infarction: integration of mechanics and viability by cardiac magnetic resonance. Eur Hear … [Internet]. 2009;30:2117–27.

153. Leclercq C, Faris O, Tunin R, Johnson J. Systolic improvement and mechanical resynchronization does not require electrical synchrony in the dilated failing heart with left bundle-branch block. Circulation [Internet]. 2002;106:1760–3.

154. Westenberg JJM, Lamb HJ, van der Geest RJ, Bleeker GB, Holman ER, Schalij MJ, et al. Assessment of left ventricular dyssynchrony in patients with conduction delay and idiopathic dilated cardiomyopathy: head-to-head comparison between tissue doppler imaging and velocity-encoded magnetic resonance imaging. J Am Coll Cardiol [Internet]. 2006 May 16;47(10):2042–8.

155. Marsan NA, Westenberg JJM, Ypenburg C, van Bommel RJ, Roes S, Delgado V, et al. Magnetic resonance imaging and response to cardiac resynchronization therapy: relative merits of left ventricular dyssynchrony and scar tissue. Eur Heart J [Internet]. 2009 Oct;30(19):2360–7.

156. Chalil S, Stegemann B, Muhyaldeen S, Khadjooi K, Smith RE a, Jordan PJ, et al. Intraventricular dyssynchrony predicts mortality and morbidity after cardiac resynchronization therapy: a study using cardiovascular magnetic resonance tissue synchronization imaging. J Am Coll Cardiol [Internet]. 2007 Jul 17;50(3):243–52.

157. Hor KN, Baumann R, Pedrizzetti G, Tonti G, Gottliebson WM, Taylor M, et al. Magnetic resonance derived myocardial strain assessment using feature tracking. J Vis Exp [Internet]. 2011 Jan;(48):1–6.

158. Onishi T, Saha SK, Ludwig DR, Onishi T, Marek JJ, Cavalcante JL, et al. Feature tracking measurement of dyssynchrony from cardiovascular magnetic resonance cine acquisitions : comparison with echocardiographic speckle tracking. J Cardiovasc Magn Reson [Internet]. Journal of Cardiovascular Magnetic Resonance; 2013;15(95):1–8.

159. Sutton R, Kanal E, Wilkoff BL, al. B et. Safety of magnetic resonance imaging of patients with a new medtronic EnRhythm MRI Surescan pacing system: Clinical Study Design. Trials. 2008;(9):68.

160. Ainslie M, Miller C, Brown B, Schmitt M. Cardiac MRI of patients with implanted electrical cardiac devices. Heart [Internet]. 2013 Jul 19;1–7.

161. Bruder O, Wagner A, Lombardi M, Schwitter J, van Rossum A, Pilz G, et al. European cardiovascular magnetic resonance (EuroCMR) registry -- multi national results from 57 centers in 15 countries. J Cardiovasc Magn Reson [Internet]. 2013 Jan 18;15(1):9.

162. Antony R, Daghem M, McCann GP, Daghem S, Moon J, Pennell DJ, et al. Cardiovascular magnetic resonance activity in the United Kingdom: a survey on behalf of the British Society of Cardiovascular Magnetic Resonance. J Cardiovasc Magn Reson [Internet]. 2011/10/08 ed. 2011;13:57.

163. Cunningham D, Whittaker T. Cardiac Rhythm Management UK National Clinical Audit

Report. 2011.

164. Kalin R, Stanton MS. Current Clinical issues for MRI scanning of pacemaker and defibrillator patients. PACE. 2005;28:2878–91.

165. Gimbel JR, Bailey SM, Tchou PJ, Ruggieri PM, Wilkoff BL. Strategies for the safe magnetic resonance imaging of pacemaker-dependent patients. Pacing Clin Electrophysiol. 2005/10/14 ed. 2005;28(10):1041–6.

166. Gimbel JR. Unexpected asystole during 3T magnetic resonance imaging of a pacemaker-dependent patient with a “modern” pacemaker. Europace [Internet]. 2009 Sep;11(9):1241–2.

167. Luechinger R, Schwitter J. Safety in MRI. In: Schwitter J, Abdel-Aty H, editors. CMR update. J. Schwitter; 2008. p. 28–41.

168. Pohost GM, Blackwell GG, Shellock FG. Safety of Patients with Medical Devices during Application of Magnetic Resonance Methods. Ann N Y Acad Sci [Internet]. Blackwell Publishing Ltd; 1992;649(1):302–12.

169. Gimbel JR, Kanal E. Can patients with implantable pacemakers safely undergo magnetic resonance imaging? J Am Coll Cardiol. J Am Coll Cardiol. 2004 Apr 7;43(7):1325-7.; 2004;43(7):1325–7.

170. Shellock FG, Crues J V. MR Safety and the American College of Radiology White Paper. Am J Roentgenol [Internet]. 2002;178(6):1349–52.

171. Pinski SL, Trohman RG. Interference in implanted cardiac devices, part II. Pacing Clin Electrophysiol. 2002;25(10):1496–509.

172. Niehaus M, Tebbenjohanns J. Electromagnetic interference in patients with implanted pacemakers or cardioverter-defibrillators. Heart [Internet]. 2001 Oct;86(3):246–8.

173. Erlebacher JA, Cahill PT, Pannizzo F, Knowles RJ. Effect of magnetic resonance imaging on DDD pacemakers. Am J Cardiol. 1986;57(6):437–40.

174. Hayes DL, Vlietstra RE. Pacemaker malfunction. Ann Intern Med. 1993;119(8):828–35.

175. Pavlicek W, Geisinger M, Castle L, Borkowski GP, Meaney TF, Bream BL, et al. The effects of nuclear magnetic resonance on patients with cardiac pacemakers. Radiology [Internet]. 1983;147(1):149–53.

176. Fetter J, Aram G, Holmes Jr. DR, Gray JE, Hayes DL. The effects of nuclear magnetic resonance imagers on external and implantable pulse generators. Pacing Clin Electrophysiol. 1984;7(4):720–7.

177. Nazarian S, Halperin HR. How to perform magnetic resonance imaging on patients with implantable cardiac arrhythmia devices. Hear Rhythm. 2009/01/06 ed. 2009;6(1):138–43.

178. Roguin A, Zviman MM, Meininger GR, Rodrigues ER, Dickfeld TM, Bluemke D a, et al. Modern pacemaker and implantable cardioverter/defibrillator systems can be magnetic resonance imaging safe: in vitro and in vivo assessment of safety and function at 1.5 T. Circulation [Internet]. 2004 Aug 3;110(5):475–82.

179. Tandri H, Zviman MM, Wedan SR, Lloyd T, Berger RD, Halperin H. Determinants of gradient field-induced current in a pacemaker lead system in a magnetic resonance imaging environment. Hear Rhythm. 2008/03/04 ed. 2008;5(3):462–8.

180. Achenbach S, Moshage W, Diem B, Bieberle T, Schibgilla V, Bachmann K. Effects of magnetic resonance imaging on cardiac pacemakers and electrodes. Am Heart J [Internet]. 1997 Sep;134(3):467–73.

181. Wilkoff BL, Bello D, Taborsky M, Vymazal J, Kanal E, Heuer H, et al. Magnetic resonance imaging in patients with a pacemaker system designed for the magnetic

resonance environment. Heart Rhythm [Internet]. Elsevier Inc.; 2011 Jan;8(1):65–73.

182. Bottomley P a, Redington RW, Edelstein W a, Schenck JF. Estimating radiofrequency power deposition in body NMR imaging. Magn Reson Med [Internet]. 1985 Aug;2(4):336–49.

183. Chou CK, Bassen H, Osepchuk J, Balzano Q, Petersen R, Meltz M, et al. Radio Frequency Electromagnetic Exposure : Tutorial Review on Experimental Dosimetry. Bioelectromagnetics. 1996;17:195–208.

184. Cline H, Mallozzi R, Li Z, McKinnon G, Barber W. Radiofrequency power deposition utilizing thermal imaging. Magn Reson Med [Internet]. 2004 Jun;51(6):1129–37.

185. Bottomley PA, Edelstein WA. Power deposition in whole body NMR imaging. Med Phys. 1981. p. 510–2.

186. Luechinger R, Zeijlemaker V a, Pedersen EM, Mortensen P, Falk E, Duru F, et al. In vivo heating of pacemaker leads during magnetic resonance imaging. Eur Heart J [Internet]. 2005 Feb;26(4):376–83; discussion 325–7.

187. Sommer T, Naehle CP, Yang A, Zeijlemaker V, Hackenbroch M, Schmiedel A, et al. Strategy for safe performance of extrathoracic magnetic resonance imaging at 1.5 tesla in the presence of cardiac pacemakers in non-pacemaker-dependent patients: a prospective study with 115 examinations. Circulation [Internet]. 2006 Oct 19;114(12):1285–92.

188. Shellock FG, Tkach J a., Ruggieri PM, Masaryk TJ. Cardiac Pacemakers, Icds, And Loop Recorder: Evaluation Of Translational Attraction Using Conventional (“Long-bore”) And “Short-bore” 1.5- And 3.0-Tesla Mr Systems. J Cardiovasc Magn Reson [Internet]. 2003 Mar 25;5(2):387–97.

189. Levine GN, Gomes AS, Arai AE, Bluemke D a, Flamm SD, Kanal E, et al. Safety of magnetic resonance imaging in patients with cardiovascular devices: an American Heart Association scientific statement from the Committee on Diagnostic and Interventional Cardiac Catheterization, Council on Clinical Cardiology, and the Council o. Circulation [Internet]. 2007 Dec 11;116(24):2878–91.

190. Luechinger R, Duru F, Zeijlemaker VA, Scheidegger MB, Boesiger P, Candinas R. Pacemaker reed switch behavior in 0.5, 1.5, and 3.0 Tesla magnetic resonance imaging units: are reed switches always closed in strong magnetic fields? Pacing Clin Electrophysiol. 2002;25(10):1419–23.

191. Lauck G, von Smekal A, Wolke S, Seelos KC, Jung W, Manz M, et al. Effects of nuclear magnetic resonance imaging on cardiac pacemakers. Pacing Clin Electrophysiol. 1995;18(8):1549–55.

192. Mollerus M, Albin G, Lipinski M, Lucca J. Ectopy in Patients with Permanent Pacemakers and Implantable Cardioverter-Defibrillators Undergoing an MRI Scan. Pacing Clin Electrophysiol [Internet]. Blackwell Publishing Inc; 2009;32(6):772–8.

193. Martin ET, Coman JA, Shellock FG, Pulling CC, Fair R, Jenkins K. Magnetic resonance imaging and cardiac pacemaker safety at 1.5-Tesla. J Am Coll Cardiol. 2004;43(7):1315–24.

194. Roguin A, Schwitter J, Vahlhaus C, Lombardi M, Brugada J, Vardas P, et al. Magnetic resonance imaging in individuals with cardiovascular implantable electronic devices†. Europace [Internet]. 2008;10(3):336–46.

195. Irnich W, Irnich B, Bartsch C, Stertmann WA, Gufler H, Weiler G. Do we need pacemakers resistant to magnetic resonance imaging? Europace [Internet]. 2005 Jul;7(4):353–65.

196. Bovenschulte H, Schlüter-Brust K, Liebig T, Erdmann E, Eysel P, Zobel C. MRI in patients with pacemakers: overview and procedural management. Dtsch Arztebl Int

[Internet]. 2012 May;109(15):270–5.

197. Nazarian S, Hansford R, Roguin A, Goldsher D, Zviman MM. A Prospective Evaluation of a Protocol for Magnetic Resonance. Ann Intern Med. 2011;155:415–24.

198. Junttila MJ, Fishman JE, Lopera G a, Pattany PM, Velazquez DL, Williams AR, et al. Safety of serial MRI in patients with implantable cardioverter defibrillators. Heart [Internet]. 2011 Nov;97(22):1852–6.

199. Russo RJ. Determining the risks of clinically indicated nonthoracic magnetic resonance imaging at 1.5 T for patients with pacemakers and implantable cardioverter-defibrillators: Rationale and design of the MagnaSafe Registry. Am Heart J [Internet]. Mosby, Inc.; 2013 Mar;165(3):266–72.

200. Russo RJ et al. Determining the Risks of Magnetic Resonance Imaging at 1.5 Tesla for Patients with Pacamakers and Implantable Cardioverter Defibrillators (The Magnasafe Registry). Am Hear Assoc Sci Sess. 2012;126:A11726.

201. Rod Gimbel J, Bello D, Schmitt M, Merkely B, Schwitter J, Hayes DL, et al. Randomized trial of pacemaker and lead system for safe scanning at 1.5 Tesla. Heart Rhythm [Internet]. 2013 Jan 17;

202. Sasaki T, Hansford R, Zviman MM, Kolandaivelu A, Bluemke DA, Berger RD, et al. Quantitative Assessment of Artifacts on Cardiac Magnetic Resonance Imaging of Patients With Pacemakers and Implantable Cardioverter-Defibrillators / Clinical Perspective. Circ Cardiovasc Imaging [Internet]. 2011;4(6):662–70.

203. Schwitter J, Kanal E, Schmitt M, Anselme F, Albert T, Hayes DL, et al. Impact of the Advisa MRI™ Pacing System on the diagnostic quality of cardiac MR images and contraction patterns of cardiac muscle during scans: Advisa MRI randomized clinical multicenter study results. Heart Rhythm [Internet]. 2013 Feb 19;

204. Rajappan K. Permanent pacemaker implantation technique: part II. Heart [Internet]. 2009 Feb;95(4):334–42.

205. McHorney CA, Ware Jr. JE, Lu JF, Sherbourne CD. The MOS 36-item Short-Form Health Survey (SF-36): III. Tests of data quality, scaling assumptions, and reliability across diverse patient groups. Med Care. 1994;32(1):40–66.

206. Deaton C, Kimble LP, Veledar E, Hartigan P, Boden WE, O'Rourke R a, et al. The synergistic effect of heart disease and diabetes on self-management, symptoms, and health status. Heart Lung [Internet]. 2006;35(5):315–23.

207. Palumbo MV, Wu G, Shaner-McRae H, Rambur B, McIntosh B. Tai Chi for older nurses: a workplace wellness pilot study. Appl Nurs Res [Internet]. Elsevier Inc.; 2012 Feb;25(1):54–9.

208. Arts T, Prinzen FW, Delhaas T, Milles JR, Rossi AC, Clarysse P. Mapping displacement and deformation of the heart with local sine-wave modeling. IEEE Trans Med Imaging [Internet]. 2010 May;29(5):1114–23.

209. Young A a, Cowan BR. Evaluation of left ventricular torsion by cardiovascular magnetic resonance. J Cardiovasc Magn Reson. 2012 Jan;14:49.

210. Young a. a., Imai H, Chang CN, Axel L. Two-dimensional left ventricular deformation during systole using magnetic resonance imaging with spatial modulation of magnetization [published erratum appears in Circulation 1994 Sep;90(3):1584]. Circulation [Internet]. 1994 Feb 1;89(2):740–52.

211. Ingels NB, Hansen DE, Daughters GT, Stinson EB, Alderman EL, Miller DC. Relation between longitudinal, circumferential, and oblique shortening and torsional deformation in the left ventricle of the transplanted human heart. Circ Res [Internet]. 1989 May 1;64(5):915–27.

212. Ashikaga H, Criscione JC, Omens JH, Covell JW, Ingels NB. Transmural left ventricular mechanics underlying torsional recoil during relaxation. Am J Physiol Heart Circ Physiol [Internet]. 2004 Feb;286(2):H640–7.

213. Young a. a., Kramer CM, Ferrari V a., Axel L, Reichek N. Three-dimensional left ventricular deformation in hypertrophic cardiomyopathy. Circulation [Internet]. 1994 Aug 1;90(2):854–67.

214. Nagel E. Cardiac rotation and relaxation in patients with aortic valve stenosis. Eur Heart J [Internet]. 2000 Apr 1;21(7):582–9.

215. Lorenz CH, Pastorek J, JM B. Delineation of normal human left ventricular twist throughout systole by tagged cine magnetic resonance imaging. J Cardiovasc Magn Reson. 2000;2(2):97–108.

216. Sorger JM, Wyman BT, Ph D, Faris OP, William C, Mcveigh ER. NIH Public Access. 2008;5(4):521–30.

217. Aelen F, Arts T, Sanders DGM, Thelissen G, Prinzen FW, Muijtjens AMM, et al. F. W. Prinzeng and R. S. RenemanEj. J Biomech. 1997;30(3):207–12.

218. Zakeri SA, Panayotova R, Borg AN, Miller CA, Schmitt M. Cardiovascular Magnetic Resonance Validation of Fractional Changes in Annulo-Apical Angles and Tricuspid Annular Plane Systolic Excursion for Rapid Assessment of Right Ventricular Systolic Function. J Magn Reson Imaging. 2014;40:133–9.

219. Yu C-M, Gorcsan J, Bleeker GB, Zhang Q, Schalij MJ, Suffoletto MS, et al. Usefulness of tissue Doppler velocity and strain dyssynchrony for predicting left ventricular reverse remodeling response after cardiac resynchronization therapy. Am J Cardiol [Internet]. 2007 Oct 15;100(8):1263–70.

220. Mewton N, Liu CY, Croisille P, Bluemke D, Lima J a C. Assessment of myocardial fibrosis with cardiovascular magnetic resonance. J Am Coll Cardiol [Internet]. 2011 Feb 22;57(8):891–903.

221. Iles L, Pfluger H, Phrommintikul A, Cherayath J, Aksit P, Gupta SN, et al. Evaluation of diffuse myocardial fibrosis in heart failure with cardiac magnetic resonance contrast-enhanced T1 mapping. J Am Coll Cardiol [Internet]. 2008 Nov 4;52(19):1574–80.

222. Conrad CH, Brooks WW, Hayes JA, Sen S, Robinson KG, Bing OHL. Myocardial Fibrosis and Stiffness With Hypertrophy and Heart Failure in the Spontaneously Hypertensive Rat. Circ [Internet]. 1995 Jan 1;91 (1):161–70.

223. Simonetti OP, Kim RJ, Fieno DS, Hillenbrand HB, Wu E, Bundy JM, et al. Cardiac Imaging Technique for the Visualization of Myocardial Infarction 1. Radiology. 2001;218(9):215–23.

224. Messroghli DR, Radjenovic A, Kozerke S, Higgins DM, Sivananthan MU, Ridgway JP. Modified Look-Locker inversion recovery (MOLLI) for high-resolution T1 mapping of the heart. Magn Reson Med [Internet]. 2004 Jul;52(1):141–6.

225. Lotz J, Meier C, Leppert A, Galanski M. Measurement with Imaging : Basic Facts and Implementation 1. 2002;651–71.

226. Kondo C, Caputo GR, Semelka R, Foster E, Shimakawa a, Higgins CB. Right and left ventricular stroke volume measurements with velocity-encoded cine MR imaging: in vitro and in vivo validation. AJR Am J Roentgenol [Internet]. 1991 Jul;157(1):9–16.

227. Hoeper MM, Tongers J, Leppert a, Baus S, Maier R, Lotz J. Evaluation of right ventricular performance with a right ventricular ejection fraction thermodilution catheter and MRI in patients with pulmonary hypertension. Chest [Internet]. 2001 Aug;120(2):502–7.

228. McKay G a, Banister EW. A comparison of maximum oxygen uptake determination by bicycle ergometry at various pedaling frequencies and by treadmill running at various speeds. Eur J Appl Physiol Occup Physiol [Internet]. 1976 Aug 12;35(3):191–200.

229. Issues S, Test MW, Equipment R, Preparation P. American Thoracic Society ATS Statement : Guidelines for the Six-Minute Walk Test. 2002;166:111–7.

230. Ehsani a a, Biello D, Seals DR, Austin MB, Schultz J. The effect of left ventricular systolic function on maximal aerobic exercise capacity in asymptomatic patients with coronary artery disease. Circulation. 1984;70:552–60.

231. Zakeri R, Borlaug BA, McNulty SE, Mohammed SF, Lewis GD, Semigran MJ, et al. Impact of atrial fibrillation on exercise capacity in heart failure with preserved ejection fraction a relax trial ancillary study. Circ Hear Fail. 2014;7(1):123–30.

232. Clark DM, Plumb VJ, Epstein AE, Kay GN. Hemodynamic effects of an irregular sequence of ventricular cycle lengths during atrial fibrillation. J Am Coll Cardiol. 1997;30(4):1039–45.

233. Kristensson BE, Arnman K, Rydén L. The haemodynamic importance of atrioventricular synchrony and rate increase at rest and during exercise. Eur Heart J [Internet]. 1985 Sep;6(9):773–8.

234. Vanoverschelde JJ, Essamri B, Vanbutsele R, D'Hondt A, Cosyns JR, Detry JR, et al. Contribution of left ventricular diastolic function to exercise capacity in normal subjects. J Appl Physiol. 1993;74:2225–33.

235. Dennis C. Rehabilitation of patients with coronary artery disease. In: Braunwald E, editor. Heart disease, a textbook of cardiovascular medicine. 4th ed. 1992. p. 1382.

236. Hermansen L, Saltin B. Oxygen uptake during maximal treadmill and bicycle exercise. J Appl Physiol. 1969;26(1):31–7.

237. Hermansen L, Ekblom B, Saltin B. Cardiac output during submaxiaml and maximal treadmill and bicycle exercise. J Appl Physiol. 1970;29(1):82–6.

238. Mitchell MD, Kundel HL, Joseph PM, Axel L. AGAROSE AS A TISSUE EQUIVALENT PHANTOM MATERIAL for NMR IMAGING. Magn Reson Imaging. 1986;4:263–6.

239. Dabir D, Child N, Kalra A, Rogers T, Gebker R, Jabbour A, et al. Reference values for healthy human myocardium using a T1 mapping methodology: results from the International T1 Multicenter cardiovascular magnetic resonance study. J Cardiovasc Magn Reson [Internet]. 2014 Jan;16(1):69.

240. Moon JC, Messroghli DR, Kellman P, Piechnik SK, Robson MD, Ugander M, et al. Myocardial T1 mapping and extracellular volume quantification: a Society for Cardiovascular Magnetic Resonance (SCMR) and CMR Working Group of the European Society of Cardiology consensus statement. J Cardiovasc Magn Reson [Internet]. 2013 Jan;15(1):92.

241. Kellman P, Hansen MS. T1-mapping in the heart: accuracy and precision. J Cardiovasc Magn Reson [Internet]. 2014 Jan 4;16(1):2.

242. Sasaki T, Hansford R, Zviman MM, Kolandaivelu A, Bluemke D a, Berger RD, et al. Quantitative assessment of artifacts on cardiac magnetic resonance imaging of patients with pacemakers and implantable cardioverter-defibrillators. Circ Cardiovasc Imaging [Internet]. 2011 Nov;4(6):662–70.

243. Gatehouse PD, Rolf MP, Bloch KM, Graves MJ, Kilner PJ, Firmin DN, et al. A multi-center inter-manufacturer study of the temporal stability of phase-contrast velocity mapping background offset errors. J Cardiovasc Magn Reson [Internet]. 2012 Jan;14(1):72.

244. Ferreira PF, Gatehouse PD, Mohiaddin RH, Firmin DN. Cardiovascular magnetic

resonance artefacts. J Cardiovasc Magn Reson [Internet]. 2013 Jan;15(1):41.

245. Lorenz CH, Pastorek JS, Bundy JM. Delineation of normal human left ventricular twist throughout systole by tagged cine magnetic resonance imaging. J Cardiovasc Magn Reson [Internet]. 2000 Jan;2(2):97–108.

246. Lumens J, Delhaas T, Arts T, Cowan BR, Young AA. Impaired subendocardial contractile myofiber function in asymptomatic aged humans , as detected using MRI. Am J Physiol Hear Circ Physio. 2006;291:1573–9.

247. Schuster A, Kutty S, Padiyath A, Parish V, Gribben P, Danford D a, et al. Cardiovascular magnetic resonance myocardial feature tracking detects quantitative wall motion during dobutamine stress. J Cardiovasc Magn Reson [Internet]. 2011 Jan;13(1):58.

248. Rüssel IK, Götte MJW. New insights in LV torsion for the selection of cardiac resynchronisation therapy candidates. Neth Heart J [Internet]. 2011 Sep;19(9):386–91.

249. Kistler PM, Sanders P, Fynn SP, Stevenson IH, Spence SJ, Vohra JK, et al. Electrophysiologic and electroanatomic changes in the human atrium associated with age. J Am Coll Cardiol [Internet]. 2004 Jul 7;44(1):109–16.

250. Wann LS, Curtis AB, January CT, Ellenbogen K a, Lowe JE, Estes N a M, et al. 2011 ACCF/AHA/HRS focused update on the management of patients with atrial fibrillation (Updating the 2006 Guideline): a report of the American College of Cardiology Foundation/American Heart Association Task Force on Practice Guidelines. Heart Rhythm [Internet]. 2011 Jan;8(1):157–76.

251. Balt JC, Hemel NM Van, Wellens HJJ, Voogt WG De. Radiological and electrocardiographic characterization of right ventricular outflow tract pacing. 2010;1739–44.

252. McGavigan AD, Kurt C, Hillock R, Stevenson I, Mond H. Right Ventricular Outflow Tract Pacing : Radiographic and Electrocardiographic Correlates of Lead Position. Pacing Clin Electrophysiol. 2006;29(October):1063–8.

253. Gao CH, Zhang H, Cui JY, Zou DZ. Real-time three-dimensional echocardiographic determination of right ventricular outflow tract high septal pacing sites. Eur Heart J Cardiovasc Imaging. 2012;13(1):104–8.

254. Balt JC, Van Hemel NM, Wellens HJJ, De Voogt WG. Radiological and electrocardiographic characterization of right ventricular outflow tract pacing. Europace. 2010;12(12):1739–44.

255. Lieberman R, Padeletti L, Schreuder J, Jackson K, Michelucci A, Colella A, et al. Ventricular pacing lead location alters systemic hemodynamics and left ventricular function in patients with and without reduced ejection fraction. J Am Coll Cardiol [Internet]. 2006 Oct 17;48(8):1634–41.

256. Hillock R, Stevenson I, Mond H. The Right Ventricular Outflow Tract : A Comparative Study of Septal , Anterior Wall , and Free Wall Pacing. Pacing Clin Electrophysiol. 2007;30(August):942–7.

257. Ridgway JP. Cardiovascular magnetic resonance physics for clinicians: part I. J Cardiovasc Magn Reson [Internet]. 2010 Jan;12(1):71.

258. Hayes D, Friedman P. Cardiac Pacing, Defibrillation and Resynchronization. 2nd ed. Wiley Blackwell; 2008. 1-623. p.

259. Victor F, Leclercq C, Mabo P, Pavin D, Deviller A, de Place C, et al. Optimal right ventricular pacing site in chronically implanted patients. J Am Coll Cardiol [Internet]. 1999 Feb;33(2):311–6.

260. Beladan CC, Calin A, Rosca M, Ginghina C, Popescu B a. Left ventricular twist dynamics: principles and applications. Heart [Internet]. 2013 May 9;1–10.

261. Rüssel IK, Götte MJW, Bronzwaer JG, Knaapen P, Paulus WJ, van Rossum AC. Left ventricular torsion: an expanding role in the analysis of myocardial dysfunction. JACC Cardiovasc Imaging [Internet]. 2009 May;2(5):648–55.

262. Saito M, Kaye G, Negishi K, Linker N, Gammage M, Kosmala W, et al. Dyssynchrony, contraction efficiency and regional function with apical and non-apical RV pacing. Heart [Internet]. 2015 Feb 9;1–9.

263. Saito M, Kaye G, Negishi K, Linker N, Gammage M, Kosmala W, et al. Dyssynchrony, contraction efficiency and regional function with apical and non-apical RV pacing. Heart. 2015 Feb;1–9.

264. Inoue K, Okayama H, Nishimura K, Ogimoto A, Ohtsuka T, Saito M, et al. Right ventricular pacing from the septum avoids the acute exacerbation in left ventricular dyssynchrony and torsional behavior seen with pacing from the apex. J Am Soc Echocardiogr [Internet]. 2010 Feb;23(2):195–200.

265. Brignole M, Gianfranchi L, Menozzi C, Alboni P, Musso G, Bongiorni MG, et al. Prospective , randomized study of atrioventricular ablation and mode-switching , dual chamber pacemaker implantation versus medical therapy in drug-resistant paroxysmal atrial fibrillation The PAF study. Europace. 1999;1:15–9.

266. Brignole M, Menozzi C, Gianfranchi L, Musso G, Mureddu R, Bottoni N, et al. Assessment of Atrioventricular Junction Ablation and VVIR Pacemaker Versus Pharmacological Treatment in Patients With Heart Failure and Chronic Atrial Fibrillation. Circulation. 1998;98:953–61.

267. Tse H, Yu C, Wong K, Tsang V, Leung YL, Ho WY, et al. Functional Abnormalities in Patients With Permanent Right Ventricular Pacing The Effect of Sites of Electrical Stimulation. Am J Cardiol [Internet]. 2002;40(8):1451–8.

268. Hillock RJ, Mond HG. Pacing the right ventricular outflow tract septum: time to embrace the future. Europace [Internet]. 2011 Aug 15;14(1):28–35.

269. Kaye GC, Linker NJ, Marwick TH, Pollock L, Graham L, Pouliot E, et al. Effect of right ventricular pacing lead site on left ventricular function in patients with high-grade atrioventricular block: results of the Protect-Pace study. Eur Heart J [Internet]. 2014 Sep 4;14–7.

270. Borg G. Borg's Perceived Exertion and Pain Scales [Internet]. Human Kinetics; 1998.